Scuola Dottorale in Geologia dell'Ambiente e delle Risorse

Sezione Geologia delle Risorse Naturali

XXVI CICLO

Application of quantitative hydrogeological methodologies in northern sector of Vulsini

Dottorando: Stefano Viaroli _____

Relatore: Dott. Roberto Mazza _____

INDEX

Extended abstract

English

Introduction

Perythirrenic volcanic aquifers of Central Italy are important resources for the local water supply. The optimal management of this resource is closely related to the knowledge of groundwater hydrological dynamics. The increasing urbanization, industrialization and agricultural withdrawals lead to several management problems such as the depletion of groundwater and deterioration of water quality. Data about pronounced decreasing in springs discharge and in piezometric levels were described in these aquifers during the last twenty years (Capelli et al. 2005). A detailed hydrogeological survey was performed in umbrian sector of Vulsini Mounts to evaluate the quantitative conservation of the drinking resource in compared to previous works (Pagano et al. 2000, Capelli et al 2005). Several authors focused their attention on natural contamination problems of volcanic aquifers exploited for water supply. Most of studies concern water quality lowering by fluorine and arsenic occurrence due to geogenic contamination. On the contrary shallow aquifers water quality is often affected by anthropogenic activities, i.e. common contamination is due to nitrate in agricultural territory or heavy metal pollution close to industrial areas.
Arpa Umbria detected anomalous concentrations of aluminum and iron in volcanic aquifer of the area near Orvieto in January 2010. Analyzed samples did not fulfil guidelines for water human consumption (98/83/EC implemented in Italy with D. Lgs 31/2001), then the authorities forbid the use of public water for drinking use.Al and Fe occur as colloids according to detected pH (6,5-7,5) and oxidizing Eh conditions. Another study area, characterized by similar volcanological and hydrogeological features and by the same colloids contamination in groundwater, was searched to understand similarities in the causes and processes of natural contamination of shallow aquifers near Orvieto. The second monitoring area was detected on the NE flank of Roccamonfina Volcano (Campania Region, Central Italy).

Hydrogeological survey of Vulsini Volcanic District

A new hydrogeological survey was performed during the summer of 2013 in the umbrian sector of Vulsini Volcanic District to improve the hydrogeological knowledge of this area. Water table elevation data and springs discharge rates about the basal volcanic aquifer were collect in order to realize a new hydrogeological map. Two hydrogeological basins were detected; they are separated by a NW-SE dynamic groundwater divide characterized by water table elevation decreasing south-eastward from 460 m a.s.l. (near Castel Giorgio Town) to 420 m a.s.l. (near Torre S.SeveroTown). The first basin corresponds to the south-western area of umbrian Vulsini and it belongs to Bolsena Lake hydrogeological basin. The second detected hydrogeological basin belongs to Paglia River basin; its southern limit corresponds to the dynamic groundwater divide whereas the other boundaries correspond to the outcropping limit of volcanic deposits. The main groundwater flow direction is north-eastward towards the base of volcanic slope where several springs,

characterized by different discharge rate up to more than 100 L/s, were detected. The comparison of data collected in 2011 and in 2013 hydrogeological surveys, evidences only minor differences in water table elevation (Δ = ±2 m). No significant variations of water table morphology were detected, and then the two hydrogeological basins are constantly recharged by the same basin.

Hydrogeological survey of Roccamonfina Volcanic Complex

A hydrogeological survey was performed during the summer of 2012 to examine the non - homogeneous hydrogeological setting of this system. This survey focuses especially on the eastern slope of Roccamonfina volcanic edifice, on Riardo and Presenzano Plains. Springs and streams discharge, the water table elevation in wells and piezometers were measured during this survey. Several volcanic aquifers were distinguished: a regional volcanic aquifer and several shallow aquifers. The elaborated hydrogeological map shows some differences from previous works (Capelli et al. 1999, Allocca et al. 2007) especially in Roccamonfina volcano area. These differences are related to a different hydrogeological conceptual model of Roccamonfina. According to Capelli et al. (1999) the volcano edifice hosts only one aquifer and the authors realized the water table surface map correlating the elevation of several springs on the east slope of Roccamonfina to piezometric data measured in wells placed in surrounding plains. During the hydrogeological survey several springs detected on the east flank of Roccamonfina were related to shallow aquifers. In fact volcanic deposits outcropping in east slope of Roccamonfina volcano are characterized by different permeability. These difference could determinate the development of shallow aquifers characterized by scarce water yield and by variable flow rate during the hydrological year on Roccamonfina slope. It’s very difficult distinguish the limits of these basins due to the temporary nature of aquifer and to lack of boreholes in which measure groundwater level.

Geochemical characterization

A detailed monitoring site was detected in each study area: Rocca Ripesena promontory near Orvieto Town in Vulsini area and Rianale Stream Valley on Roccamonfina Volcano. A weekly monitoring was performed from March to July 2013. During this monitoring data about discharge rate and chemical – physical parameters (electrical conductivity, pH, temperature and Eh) of several springs were collected. Four aliquots of water were collected from each motoring point for chemical analyses.

Analyzed water samples are characterized by low mineralization and by an intermediate alkali – bicarbonate to alkali earth – bicarbonate facies. The constant Na/K ratio detected in all samples confirms the absence of water mixing between studied volcanic aquifers and other external aquifers. No significant variations in major ions concentration occurred during the monitoring whereas ICPMS data about metal concentrations reveal a great variability in aluminum and iron concentrations in time. Shallow aquifers are characterized by high concentrations in Al and Fe in unfiltered samples collected in both study areas. A linear relationship correlates Al and Fe concentration, then the enrichment in these two elements depending to the same natural process. In fact aluminum and iron are not

available as ion form according to neutral pH and oxidant Eh values as detected in field, so their presence in water depends only by colloids concentration. Barium and manganese show a similar behavior like aluminum and iron due to be adsorbed on colloids surfaces. A direct relationship was detected between rainfall and colloids concentration, it can be distinguish a first rainy period in which high concentrations of Fe and Al were detected and a second period characterized by lesser rainy events in which colloids concentration quickly decrease.

(Principal Component Analysis (PCA) has been elaborated on the whole database to point out the relationship between the water parameters and their chemical behavior in studied water systems. Chemical variables (analyzed parameters) governed by the same geochemical processes fall within the same factor. In the study areas the same processes were distinguished: the first factor explains the enrichment of ions in solution (EC, HCO_3^-, Cl^-, NO_3^-, SO_4^{2-}, Na^+, K^+, Mg^{2+}, Ca^{2+}, Sr e V) related to chemical alteration of rocks whereas the second factor explains a physical colloids mobilization(Al, Ba, Fe e Mn) which occurs independently from water mineralization).

Pedological analyses

A weathered pyroclastic flow belonging to Teano pyroclastic formation (Giordano 1996) was identified in Rianale Stream Valley on Roccamonfina Volcano. A significant discharge of water rich in colloids was detected through this saturated deposit during the monitoring. Therefore pedological and mineralogical analyses were performed in order to improve the knowledge of this volcanic formation. Sixteen samples were collected from the detected weathered profile. Four analyses were performed for each sample: H_2O pH, NaF pH, particle size distribution and organic carbon concentration. The results show neutral pH values in water as expected in a volcanic deposit and alkaline pH values (about 8,5) in NaF, derived from the high concentration of short-range order minerals or free aluminum (oxyhydroxide forms) in soils. Organic carbon concentration quickly decreases downward so we can exclude a significant role of organic matter in colloids mobilization in the studied system. Particle size distribution analyses were realized on earth fine fraction (φ <2mm). The results show a progressive increase in silt and clay fractions downward to the base of the pyroclastic flow. XRD analyses were realized in order to characterize the mineralogical composition of soil layers distinguish on primary (Mica, sanidine and plagioclase) and weathered minerals (Halloysite).

Another sampling site was detected in the recharge area of monitored shallow springs in Rocca Ripesena near Orvieto. Ten samples were collected from a weathered pyroclastic deposit outcrop. These samples were process and analyzed using the same methodologies as well as the Roccamonfina ones. The results are characterized by low variability. This low variability can be related to human activities that can have altered the entirety of soil structure, or to an intense weathering affecting the pyroclastic deposits up to a depth greater than about two meters (sampled thickness)

Conclusions

All detected natural-contaminate springs, both in Orvieto area and on Roccamonfina Volcano, were referred to an unconsolidated weathered pyroclastic aquifer constituted by deposits emplaced in a similar period (about 330 ka) and characterized by intense weathering. Furthermore study areas show a fundamental difference for water management: the basal aquifer in Orvieto district is characterized by a higher vulnerability than Roccamonfina one. The intermediate aquitard near Orvieto is constituted by lava characterized by variable (from low to average) permeability and irregular distribution in the whole area. On the contrary about 100 meters of low permeability pyroclastic flow deposits protect the basal aquifer from the shallow contamination on Roccamonfina Volcano. Identification background values of Al and Fe in shallow volcanic aquifers is fundamental for environmental management in order to discriminate natural processes from human pollution. Un-isolated drilling or wells could increase vulnerability of deep resource; therefore shallow aquifers should be isolated from the basal one through a correct cementation of borehole.

Italiano

Introduzione

Gli acquiferi vulcanici peritirrenici dell'Italia centrale costituiscono delle risorse molto importanti per l'approvigionamento idrico della popolazione. Una gestione accurata della risorsa prevede la conoscenza delle dinamiche che influenzano la falda. L'aumento della pressione antropica (fabbisogno idrico a uso sanitario, agricolo e industriale) ha portato l'insorgenza di diversi problemi sulla conservazione delle qualità e della quantità della falda potabile.

Nell'ultimo ventennio sono stati evidenziati negli acquiferi vulcanici peritirrenici fenomeni di marcata riduzione delle portate sorgive e di progressivo abbattimento dei livelli piezometrici (Capelli et al. 2005). Per questo motivo tramite un dettagliato rilevamento idrogeologico è stato possibile aggiornare le conoscenze geologiche e idrogeologiche del settore umbro dei monti Vulsini, area oggetto del presente studio, valutandone lo stato quantitativo di conservazione della falda potabile rispetto ai lavori esistenti (Pagano et al. 2000, Capelli et al. 2005).Diversi autori hanno focalizzato la loro attenzione su problemi di contaminazione degli acquiferi vulcanici profondi utilizzati come riserva potabile. La maggior parte di questi studi tratta la presenza e le dinamiche di contaminazione da fluoro e arsenico a causa della natura delle rocce vulcaniche che costituiscono l'acquifero. Al contrario la qualità degli acquiferi superficiali è spesso messa a rischio dalle attività umane come ad esempio contaminazioni da nitrati nelle aree agricole o inquinamento da metalli pesanti nelle aree industriali.

Nel Gennaio 2010 alcune analisi compiute dall'ARPA Umbria sulle acque dell'acquifero Vulsini captate a scopo potabile nei pressi di Orvieto, misero in evidenza concentrazioni di ferro e alluminio superiori ai limiti di legge previsti per il consumo umano (98/83/EC implemented in Italy with D. Lgs 31/2001); per questo motivo le autorità proibirono l'uso

dell'acqua comunale per circa un mese. L'alluminio e il ferro misurati nelle acque si trovano come colloidi poiché a valori di pH neutri e condizioni di Eh ossidanti come quelli misurati in campo questi elementi non solo in soluzione. Una seconda area di studio caratterizzata dalle stesse caratteristiche vulcanologiche e idrogeologiche e dalla stessa contaminazione da colloidi è stata individuata sul fianco nord orientale del Vulcano Roccamonfina. Lo studio parallelo di queste due aree permette di evidenziare quelle che sono le cause comuni della contaminazione osservata.

Rilevamento idrogeologico del Distretto Vulcanico Vulsino

Un nuovo rilevamento idrogeologico è stato svolto nell'estate del 2013 nel settore umbro dei monti Vulsini per definire in dettaglio il modello idrogeologico concettuale dell'area. Sono stati raccolti dati sull'ubicazione e la portata di sorgenti e sulla quota piezometrica della falda vulcanica basale; questi dati sono stati poi utilizzati per la realizzazione di una carta idrogeologica. Dall'andamento della piezometria si possono distinguere due bacini idrogeologici, separati da uno spartiacque dinamico ad andamento nord ovest- sud est con quote, di saturazione comprese tra 460 m s.l.m. nei pressi di Castel Giorgio e 420 m s.l.m. vicino a Torre S. Severo. Il primo bacino idrogeologico corrisponde al settore sud occidentale dell'area di studio e fa parte del bacino idrogeologico del Lago di Bolsena. Il secondo bacino fa parte del bacino del Fiume Paglia, il limite meridionale corrisponde allo spartiacque dinamico mentre i restanti limiti corrispondono al limite di affioramento delle vulcaniti vulsine. Il deflusso principale della falda è verso nord est verso il fronte delle vulcaniti alla base delle quali si trovano numerose sorgenti caratterizzate da portate fino a 100 L/s. Dal confronto tra i dati raccolti nel 2011 e nel 2013, si evidenziano solo piccole differenze sulle quote della falda basale ($\Delta = \pm 2$ m) mantenendo pressoché costante la posizione dello spartiacque dinamico. Durante il rilevamento sono state individuate numerose sorgenti e pozzi poco profondi alimentati da circolazioni superficiali. Questi acquiferi sono stati rinvenuti su tutta l'area di studio in maniera discontinua dovuto alla mancanza di un acquicludo sufficientemente continuo. Per questo motivo non è stato possibile realizzare una carta piezometrica di questi acquiferi.

Rilevamento idrogeologico del Complesso Vulcanico di Roccamonfina

Durante l'estate 2012 è stato svolto un rilevamento idrogeologico sul versante orientale del Vulcano Roccamonfina e sulle limitrofe piane di Riardo e Presenzano per definire le caratteristiche di questo sistema complesso e non omogeneo. Durante il rilevamento sono stati raccolti dati sulla portata di sorgenti e corsi d'acqua e misure di livelli piezometrici all'interno di pozzi e piezometri. Dai risultati ottenuti sono stati distinti diversi acquiferi vulcanici: un acquifero principale e alcuni piccoli acquiferi superficiali. Nella zona del vulcano Roccamonfina si riscontrano sostanziali differenze tra il modello concettuale di riferimento proposto da precedenti lavori (Capelli et al. 1999, Allocca et al. 2007) e la carta idrogeologica prodotta in questo studio. Queste differenze sono legate a un diverso modello concettuale dell'assetto idrogeologico del Roccamonfina: infatti, gli autori (Capelli et al. 1999, Allocca et al. 2007) correlavano le sorgenti individuate sul versante del vulcano all'acquifero basale, mentre dai dati raccolti durante la campagna di misure 2012

è emerso come queste manifestazioni sorgive siano da associare alla presenza di acquiferi superficiali caratterizzati da scarsa produttività e limitata estensione.

Caratterizzazione geochimica

In ogni area di studio è stato individuato un sito di monitoraggio idrogeologico e geochimico: il promontorio di Rocca Ripesena vicino a Orvieto sui Vulsini e la Valle del Torrente Rianale sul Vulcano Roccamonfina. Il monitoraggio settimanale, realizzato da Marzo a Luglio 2013, prevedeva la raccolta di dati sulla portata delle sorgenti studiate, la raccolta di dati chimico-fisici (conducibilità elettrica, pH, temperatura ed Eh) e di campioni d'acqua per le analisi di laboratorio. Le acque analizzate sono poco mineralizzate e classificate alle facies intermedia bicarbonato alcalina e bicarbonato alcalina – terrosa. Dall'analisi del rapporto tra Na/K si evidenzia come gli acquiferi in esame siano di natura vulcanica, escludendo quindi apporti da sistemi idrogeologici esterni. Durante il periodo di monitoraggio non emergono grandi variazioni delle concentrazioni dei principali ioni in soluzione a conferma che l'acquifero monitorato non ha apporti esterni. Osservando le concentrazioni dei metalli analizzati tramite ICPMS si nota come alluminio e ferro presentino invece grande variabilità nel tempo e a seconda della filtrazione utilizzata sul campione. I campioni d'acqua non filtrati raccolti durante i primi campionamenti presentano concentrazioni molto elevate di alluminio e ferro, mentre questi valori diminuiscono rapidamente nella seconda parte del monitoraggio. La variabilità nel tempo delle concentrazioni di questi elementi può essere collegata alla frequenza e all'intensità di eventi piovosi che sono la causa della mobilizzazione. Fe e Al risultano strettamente correlati indice di un medesimo meccanismo di mobilizzazione e la loro concentrazione è legata a quella dei colloidi in sospensione dal momento che entrambi gli elementi non si trovano in soluzione alle condizioni di pH - Eh misurate in situ. Altri elementi come il Bario e il Manganese presentano il medesimo trend di Fe e Al anche se con concentrazioni nettamente più basse; questa correlazione può essere spiegata tramite l'affinità di questi elementi ad essere adsorbiti e trasportati sulla superficie dei colloidi.
Tramite l'analisi delle componenti principali (PCA) estrapolate dai dati geochimici raccolti è stato possibile individuare due processi che condizionano il chimismo delle acque: la prima componente (circa il 55% della varianza totale) è caratterizzata da alta correlazione tra EC, HCO_3^-, Cl^-, NO_3^-, SO_4^{2-}, Na^+, K^+, Mg^{2+}, Ca^{2+}, Sr e V mentre la seconda componente (oltre il 20% della varianza totale) è caratterizzata da alti valori di correlazione di Al, Ba, Fe e Mn e inversamente correlata alla temperatura. Gli elementi identificati nella prima componente corrispondono agli elementi in soluzione in acqua derivanti dall'interazione acqua – roccia

Analisi pedologiche

Dopo aver approfondito lo studio geochimico delle aree di monitoraggio, l'attenzione si è spostata verso l'individuazione della sorgente della contaminazione. All'interno della valle del Torrente Rianale è stato individuato un affioramento di una colata piroclastica facente parte delle Piroclastiti di Teano (Giordano 1996) attraverso la quale fuoriusciva diffusamente acqua di colore bianco, molto torbida come osservato nelle sorgenti monitorate; per questo motivo sono state condotte analisi pedologiche e mineralogiche

volte a caratterizzare questo tipo di deposito. Sono stati raccolti sedici campioni da un profilo di suolo. Per ogni campione sono state svolte quattro analisi: pH in acqua, pH in fluoruro di sodio, tessitura e contenuto di carbonio organico. I valori di pH in acqua di tutti i campioni rientrano nel range di pH neutri caratteristici di questi depositi. I valori di pH in NaF sono invece più alti (circa 8,5); questi valori indicano la presenza di minerali a scarso ordine cristallino come idrossidi di alluminio o ferro. L'analisi delle concentrazioni del carbonio organico s'individua una rapida diminuzione con la profondità fino a raggiungere livelli in cui si trovano solo tracce di carbonio organico. Viste le modeste concentrazioni, possiamo ipotizzare che la sostanza organica svolga un ruolo notevolmente secondario nella mobilizzazione dei colloidi all'interno del sistema studiato. L'analisi granulometrica eseguita sul setacciato <2mm dei campioni evidenzia un graduale aumento della frazione fine scendendo lungo la sezione analizzata fino ad arrivare a un livello particolarmente argillificato corrispondente alla base del flusso piroclastico. Questo aumento della frazione fine è sia legato in parte alla natura stessa della colata ma soprattutto all'alterazione della parte basale del deposito, la porzione più soggetta alla saturazione. Dall'analisi diffrattometrica dei campioni si identificano alcuni minerali primari caratteristici di questi depositi vulcanici come Miche, Sanidino e Plagioclasi e minerali secondari come l'Halloysite legata all'alterazione di alluminosilicati. Un secondo sito di campionamento è stato individuato sopra l'altopiano di Rocca Ripesena vicino Orvieto a monte delle sorgenti monitorate. Sono stati raccolti dieci campioni di materiale piroclastico pedogenizzato lungo una sezione di 2 metri di spessore (suolo). Questi campioni sono stati trattati e analizzati seguendo le stesse metodologie utilizzate per i campioni di Roccamonfina, ma i risultati ottenuti non sono significativi vista la scarsa variabilità dei dati ottenuti. Questa scarsa variabilità nei primi due metri può essere ricondotta ad attività antropiche legate all'agricoltura che possono aver intaccato l'integrità del deposito o alla presenza di un un'alterazione spinta anche a diversi metri di profondità dal piano campagna.

Conclusioni

I bacini di ricarica delle sorgenti contaminate, individuate sia a Orvieto sia a Roccamonfina, sono costituiti da prodotti piroclastici sciolti di età simile (circa 330 mila anni) e caratterizzati da intensa alterazione. In ottica gestionale sussistono delle importanti differenze tra il dominio vulsino e quello di Roccamonfina: dalla ricostruzione dell'assetto geologico e idrogeologico della falda basale potabile delle due aree è emerso un rischio di contaminazione maggiore nella zona vulsina dove l'acquicludo intermedio che separa la falda potabile basale dagli acquiferi superficiali contaminati è costituito da colate di lave discontinue arealmente e caratterizzate da una permeabilità secondaria variabile. Al contrario a Roccamonfina i due acquiferi sono separati da circa 100 metri di depositi di flusso piroclastico a bassa permeabilità. La ricerca mette in evidenza come lo studio dettagliato degli acquiferi permetta l'individuazione di elevati valori di fondo di alluminio e ferro che caratterizzano gli acquiferi vulcanici superficiali, permettendo di discriminare tra eventi di contaminazione naturale legata alla natura stessa dell'acquifero, rispetto a fenomeni di inquinamento umano. La mobilizzazione dei collodi osservata durante il monitoraggio risulta fortemente influenzata dalla variabilità delle precipitazioni che innescano il fenomeno. A seguito di queste osservazioni risulta fondamentale in ottica di

salvaguardia della risorsa potabile la corretta realizzazione di captazioni evitando che queste diventino vie privilegiate di mixing tra acque superficiali e la falda basale.

1. Introduction

Perythirrenic volcanic aquifers of Central Italy are important resources for the local water supply. The optimal management of this resource is closely linked to the knowledge of the hydrological dynamics. The increasing urbanization, industrialization and agricultural withdrawals lead to several management problems such as the depletion of groundwater and deterioration of water quality.

Several authors focused their attention on contamination problems of deep volcanic aquifers used for water supply and characterized by a long residence time. Most of water quality studies of volcanic aquifers deal with fluorine (Cordeiro et al. 2012, Ducciand Sellerino 2012) and with arsenic occurrence in water (Casentini et al. 2010, Baiocchi et al. 2011, Preziosi et al. 2010). Usually in deep aquifers contamination is due to geogenic contaminants on the contrary shallow a aquifers water quality is often affected by anthropogenic activities, i.e. common contamination is due nitrate in agricultural areas or heavy metal pollution close to industrial areas. Water mixing among deep and shallow aquifers could further deteriorate water quality status with different contaminants (Celico 1988, Custodio and Llamas.2005).

High concentration in aluminum was detected in and drinking groundwater resource during the monitoring on quality of waters made by ARPA UMBRIA (regional agency for environmental protection of Umbria Region) in January 2010. Analyzed samples did not fulfil guidelines for water human consumption (European Council Directive 98/83/EC implemented in Italy with D. Lgs 31/2001 and then reported in the. Decrete Law number 152 published on 3rd April 2006, Attachment n°2, Part n°3).In the Orvieto District on 9th January 2010 the ordinance n.674 forbid the use of public water for drinking use due to aluminum and iron concentration exceeding 200 µg/L (the allowed maximum concentration) to the population (about 20000 people).Only 16 days later, on 25th January, residents in Orvieto were allowed to use drinking water. Another similar episode occurred between 26th February and 9th March 2010. The cause of water quality deterioration was a mixing between shallow aquifers characterized by high colloid concentration and the deeper resource.

Shallow aquifers in hydrogeological studies are often overlooked due to their low productivity but this research will be focus on the quantification and on the chemical characteristics of these aquifers that are a possible source of contamination for the main groundwater resources. This study was carried out using a multi-disciplinary approach to give a complete overview about colloidal contamination of shallow volcanic aquifers. Regional Hydrogeological surveys were integrated with geochemical analyses and study of variability in chemical composition of monitoring springs. Then pedological survey and mineralogical analyses were carried out to determinate the possible source of colloidal contamination. For better understand mobilization dynamics of solids producing turbidity the same phenomena in a different area has been investigated.

The new monitoring area should be a similar volcanologic district and a similar hydrogeological setting characterized by overlying aquifers. The new area will be also characterized by the development of a similar colloids contamination in groundwater. Regional extended approach to colloid generation in volcanic district allows comparisons

between characteristics and behavior of two different systems in order to identify the common origins and related parameters of this kind of contamination.
The second monitoring area was identify in the Rianale Stream Valley, on the NE flank of Roccamonfina Volcano (Campania Region, Central Italy), after a detailed research along all perityrrenic volcanic domains.
Colloids mobilization was usually debated in chemical research or in agronomic studies (Gray and McLaren 2005, Laegdsmand et al. 2007, Galvez et al. 2008, Sequaris et al. 2013, Deepagoda et al. 2011) with a detail focus on the top soil layers behavior in relationship to the plants growing. At present time the processes related to colloids contamination have been not clearly described. Weathered volcanic formations have been suspected to produce colloids according to available data (ARPA Umbria 2013). The aim of the present study is to investigate in detail the processes involved in colloids mobilization. The integration of hydrogeological prospections with geochemical and pedological surveys has been necessary for carrying out the investigation of studied areas.

2. Vulsini Volcanic District

2.1. Geological Evolution

The Vulsini Volcanic District (hereafter VVD), covers an area of about 2000 km^2between Tuscany and Latium; it developed around 600-100 ka, in the same time interval of the other volcanoes belonging to the Quaternary Roman Volcanic Province (Gillot et al. 1991, Nappi et al. 1995, Peccerillo 2005). In fact, at about 600 ka volcanism seems to begun in central – northern Latium and southern Tuscany at Vulsini, Sabatini and Colli albani (Fornaseri 1985, Cioni et al.1993, Santi 1990, Conticelli and Peccerillo 1992, Barberi et al. 1994).

VVD has been subdivided into four volcanic complexes on the basis of temporal and spatial distribution of eruptive activity: Paleobolsena, Bolsena, Latera and Montefiascone (Nappi et al. 1991). The volcanic complexes display similar eruptive styles, characterized by ignimbrite-forming events preceded and followed by effusive and strombolian activities, usually taking place along peripheral circum-calderic fault system (Capaccioni et al. 2012)

The sedimentary substratum was defined through deep geothermal exploration data and trough outcrops at the edge of the VDD. It can be divided into the following formations (Bertini et al. 1971, Barberi et al. 1984, Buonasorte et al. 1987, 1991):

- Allochthonous flysch formations belonging to the Liguridi units; they are composed by shales, siltstones and marls with subordinate sandstones, limestone and ophiolitic units ranging from Lower Cretaceous to Paleocene;
- Limestone, marls, marly arenaceous formations and shales of the Tuscan sequences ranging from Upper Triassic to Eocene–Oligocene;
- Limestone, marls and anhydrites representing the Upper Triassic–Oligocene Umbrian series.
- Plio – Pleistocene post – orogenic deposits (Neoautochtonous) composed by marine clay, sand and conglomerate sediments of to brackish environment.

During Late Piacenzian the whole VVD area was emerged. Pleistocene marine sediments outcrop only in the easternmost margin of Vulsini corresponding to the Chiani – Tevere Basin (Barberi et al. 1994).In the eastern sector of VVD the top of the carbonate basement deepens toward NE, as suggested by the Bouger gravity anomalies according to Toro (1978), Amodio et al. (1987), Nappi et al (1991), Barberi et al (1994) and Di Filippo et al (1999). On the contrary in the western VVD area the structural setting of the sedimentary substratum underneath the Latera Caldera seems to be the result of a series of collapses following each Latera ignimbrite – forming eruption (Nappi et al. 1995).

VVD started its activity about 600 ka ago (Paleobolsena volcanic complex)(Santi1990, Nappi et al. 1995). Nowadays information about size and configuration of Paleobolsena is conjectural because the deposits belonging this activity are mostly buried by younger rocks and/or masked by Bolsena Lake (Nappi et al. 1998) The oldest outcropping products can be attributed to Civitella d'Agliano Formation (Nenfro auct., 505 ka) a Plinian-type activity corresponding to the largest ignimbrite-forming eruptions of the whole District (Aurisicchio et al. 1992; Nappi et al., 1995.). The Palaeobolsena caldera is probably

located in the northern sector of the present Bolsena Lake (Nappi et al. 1994) and it can be referred to collapses occurred after the eruption of these deposits (Nappi et al. 1991). After the Palaeobolsena eruptions the activity shifted towards the east (Bolsena and Montefiascone complexes) and west (Latera complex).The Bolsena Volcanic Complex mainly developed in the northern and eastern sectors of the VVD. Pyroclastic and minor effusive eruptions took place until about 330 ka when the “Orvieto Bagnoregio Ignimbrite” (Varekamp 1980, Nappi et al. 1982, Faraone and Stroppa 1988, Nappi et al. 1991, Nappi et al. 1994) was erupted. This ignimbrite represents the climax of Bolsena volcanic complex, it has an original areal distribution of about 200 km^2 and a total inferred volume of about 2-3 km^3 (Nappi et al. 1995).The Volcanic activity in the NE Vulsini decreased after the “Orvieto Bagnoregio Ignimbrite” eruption, moderate effusive events are recorded from about 330 ka to 250 ka and a renewed explosive activity took place at the end of this time interval (Nappi et al. 1995).Whereas after the Orvieto Bagnoregio Ignimbrite eruption, an increase in frequency of pyroclastic and lavas formations occurred in the S and SE VVD area (Montefiascone Volcanic complex).

The Latera Volcanic Complex developed in the western part of the district between 300–100 ka. Plinian and pyroclastic flow-forming explosive eruptions that created a strato - volcano truncated by a polygenetic collapse caldera in its central area, dominated its activity. The final activity from was characterized by strombolian, hydromagmatic and effusive eruption styles in intra- and circum-caldera centers (Nappi et al. 1969, Sparks 1975, Metzeltin and Vezzoli 1983, Vezzoli et al. 1987, Palladino and Valentine 1995, Palladino and Agosta 1997, Palladino and Simei 2005).

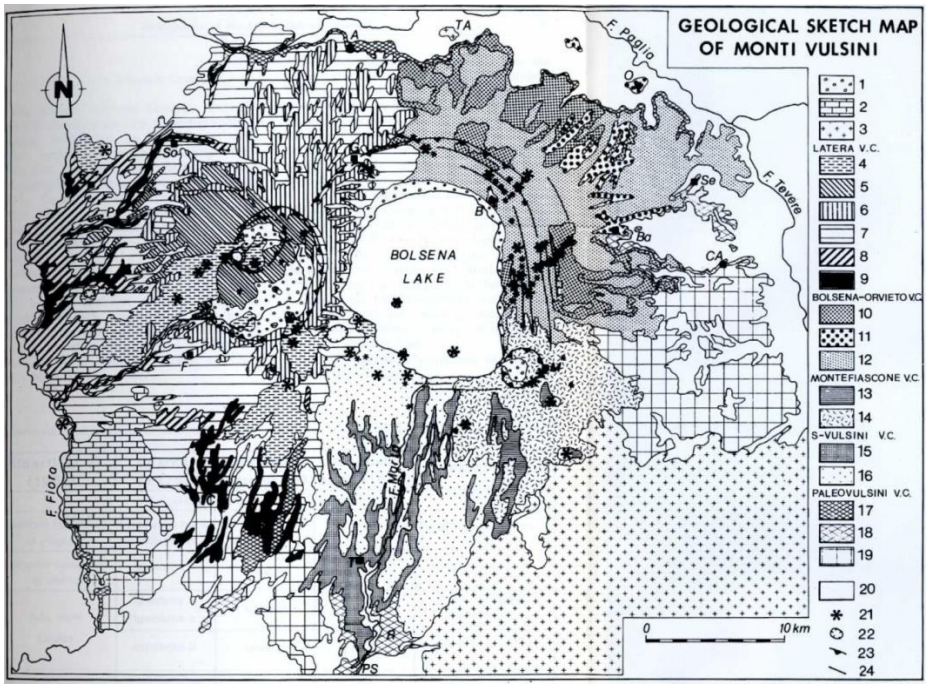

Figure 1Geological sketch map of VVD. 1) Quaternary sedimentary deposits; 2) Travertine; 3) Torre Alfina and Vico Volcanic Complex products; 4) Products of final effusive and strombolian activity; 5) Pitigliano Formation; 6) Onano Formation, Poggio Pinzo Tuff member; 7) Onano Formation, Grotte di Castro Formation and Sorano Formation; 8) Sovana Formation; 9) Canino Formation and Farnese Formation; 10) Lava flows of Bolsena – Orvieto Volcanic Complex; 11) Bolsena – Bagnoregio Ignimbrite; 12) Pyroclastic succession of Bolsena – Orvieto Volcanic Complex; 13) Lava flows of Montefiascone Volcanic Complex; 14) Pyroclastic succession of Montefiascone Volcanic Complex; 15) Lava flows of Southern Vulsini Volcanic Complex; 16) Pyroclastic succession of Southern Vulsini Volcanic Complex; 17) Lava flows of Paleo – Vulsini Volcanic Complex; 18) Basal Ignimbrite; 19) Pyroclastic and volcano – sedimentary successions; 20) Sedimentary substratum; 21) Scoria cones; 22) Craters; 23) Caldera rims; 24) Faults and fractures (Vezzoli et al.1987)

2.2. Geological settings

The research activities in this study initially focused on defining the relationship between the sedimentary basement and the volcanic deposits the lithological description of sedimentary and volcanic formations were detected from the most recent and detailed Geological maps at 1:10000 scale (Di Matteo and Dragoni 2006).

The volcanic deposits outcropping in the Umbrian sector of Vulsini Mounts were emplaced during the activity defined as Bolsena Volcanic Complex. These products overlay a sedimentary basement consisting primarily in Plio - Pleistocene marine clay and sand outcropping in the NE sector of the study area. These sediments were deposed in unconformity over Allochthonous deposits of the Liguridi Units. Flysch deposits outcrop only in a limited NW sector of the study area near Castel Viscardo Town.

The morphology map of the pre-volcanic basement was realized through the interpretation of geophysical and stratigraphical data. Electric tomography maps were collected from CMP (Compagnia Mediterranea Prosepzioni) archive and from minor geological reports. Location of several vertical electric soundings (VES) and information about thickness of high electrical resistivity deposits are represented on these maps Fig 2.

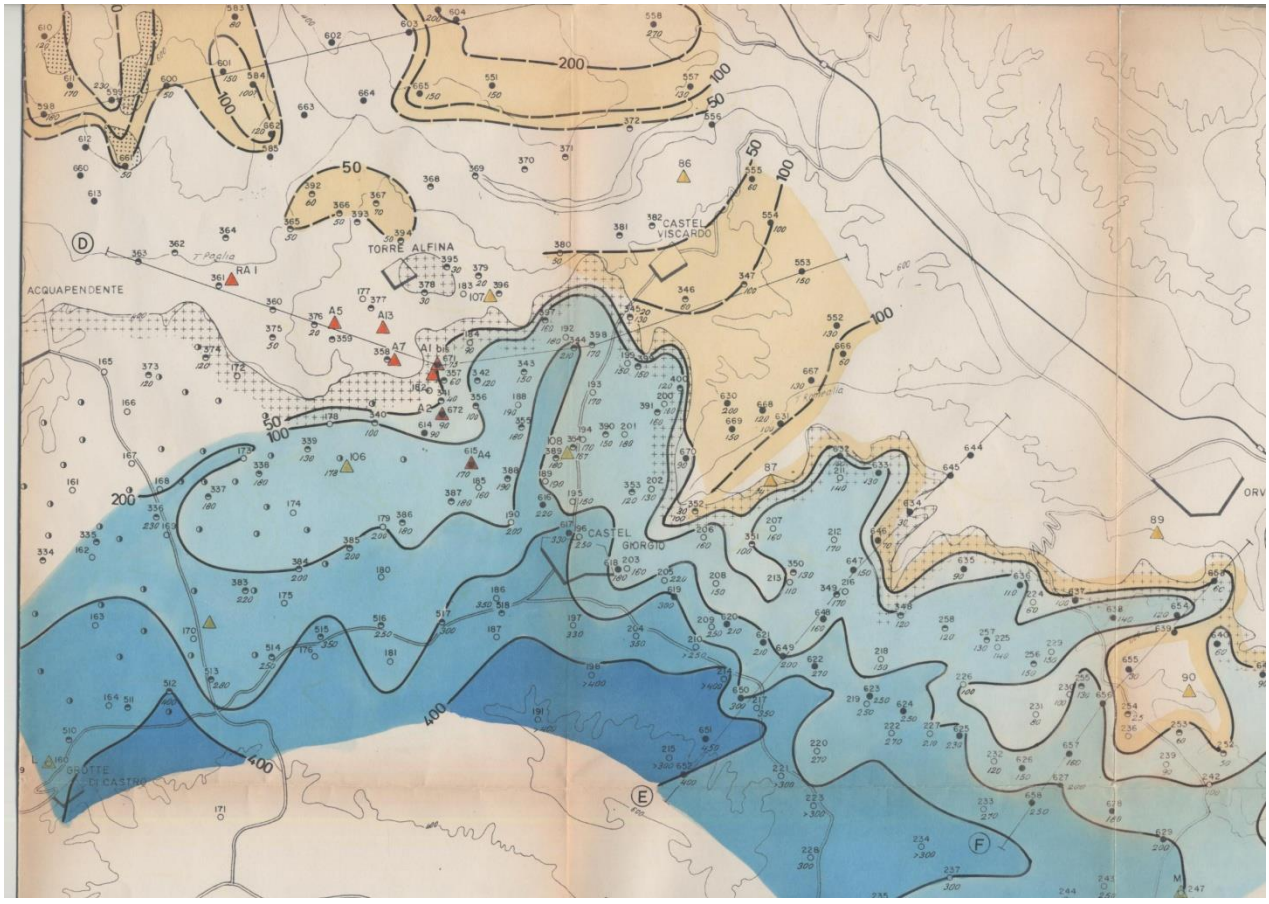

Figure 2 VES locations (CMP Archive)

These deposits are interpreted as volcanic units, characterized by a higher resistivity than clayey formations of the sedimentary substratum. All VES data and boreholes stratigraphies were collected in a database and later spatialized and elaborated through a

GIS system. These data were integrated with the elevation of the outcrops of the substratum to reconstruct the isopaches of volcanic deposits. Then the map of the sedimentary basement morphology was realized subtracting the calculated thickness of volcanic deposits to the topography.

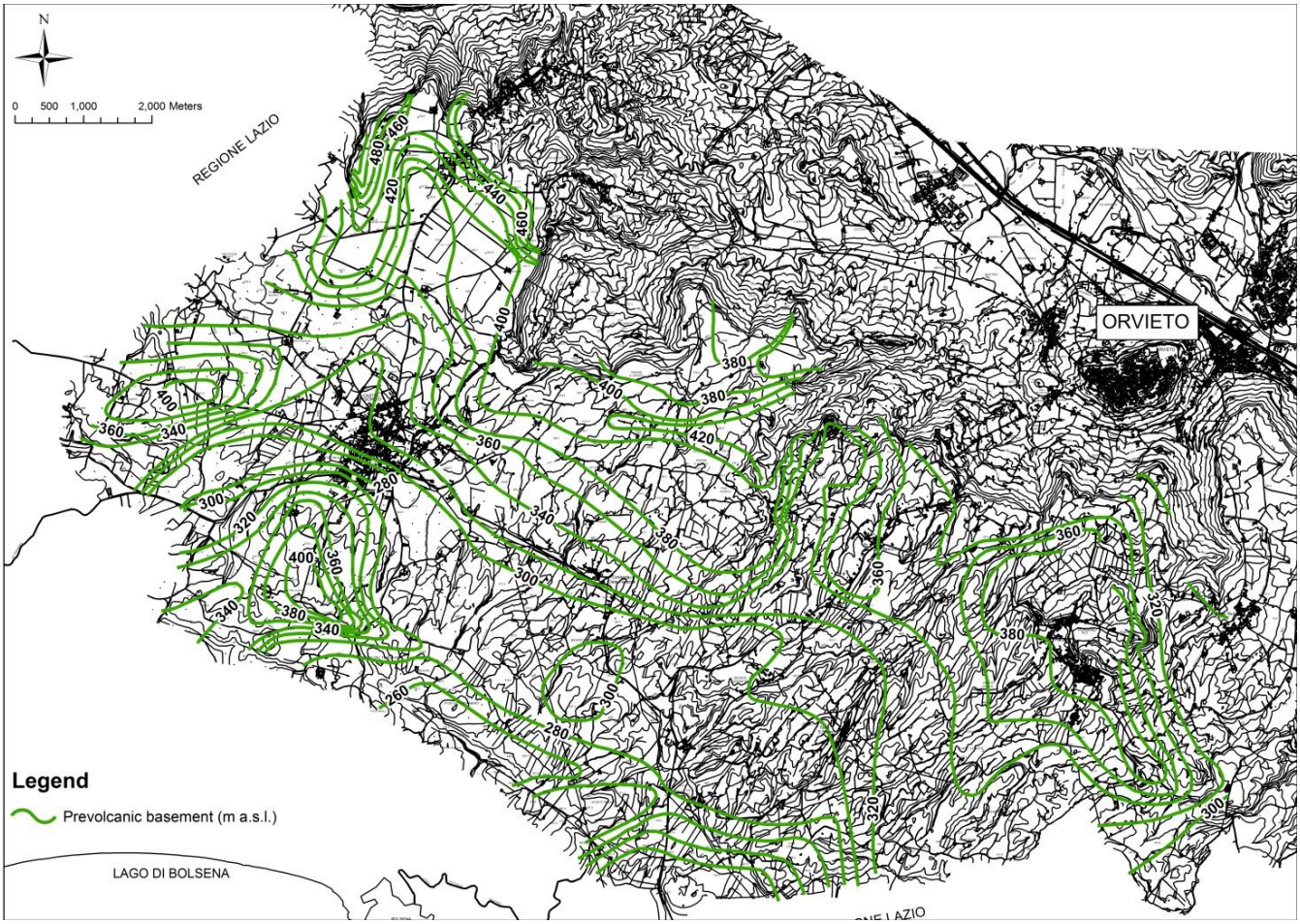

Figure 3 Prevolcanic basement elevation

The outcropping deposits were divided in synthems, formations and units as follow:

Allochthnous Unit

- **Santa Fiora Formation**: grey marly limestone, sandstone with calcareous cement, calcarenite and multi colored clays (Lower Cretaceous)

Chiani – Tevere Synthem

- **Lithofacies ALVa**: yellow sand and silty sand with variable grain size. They are well thickened or lithified. These sands are intercalated with conglomerate layers, composed by rounded carbonate clasts within a silty-sand matrix. (Lower Pleistocene)
- **Lithofacies ALVb**: gray silty clay or marly clay. (Lower Pleistocene)
- **Lithofacies ALVc**: yellow clayey silt and yellow silty clay occasionally with gray-blue shades. (Lower Pleistocene)

Sugano Synthem

- **Tione Formation**: pyroclastic succession (ti) composed by lower pumice levels, scoria layers and thin levels of yellow tuff. Reworked structures are sometimes visible. A discontinuous aphyric lava flow (ti1) lies at the base of this formation. Whereas a leucite lava flow (ti2) with a porphyria structure was emplaced on the top of Tione formation.

Orvieto Synthem

Canonica – Torre S. Severo Subsynthem

- **Corsica Formation**: pyroclastic succession composed by alternation of decimeter tuff strata and thick layers of sorting pumice and scoria lapilli tuff. There are some lava interpose with the pyroclastic deposits:
    - (co1) Tephrytic lava flows with aphyric texture were emplaced in the lower pyroclastic succession.
    - (co2) Porphyritic lava flows with millimetric to centimetric leucite crystals were emplaced in the uppermost formation
- **Orvieto – Bagnoregio Ignimbrite (ig):** it's composed by a basal plinian fall deposit and a main ignimbrite deposit. The latter is made up of a ground surge, a near vent lithic breccia deposits, a series of thin and highly dispersed pumice flow units (lowermost unit) and a thick pyroclastic flow (uppermost unit) (Nappi 94)

Montalfina – Castel Giorgio Subsynthem

- **Podere Sambuco Formation:** succession of layered tuff and pumice – scoria lapilli tuff (ps).Some lava flows and scoria layers are inter - bedded with this formation:
    - Case Perazza lava and scoria layers: four leucititic to tephritic -phonolitic lava with porphyric structure (cp1)were emplaced in the lowermost formation, interpose with decimetric or metric tuff – breccia deposits (cp)
    - Castel Giorgio lava: (cg): leucititic to tephritic -phonolitic lava with a weakly porphyric structure
    - Poggio del Torrone lava and scoria layers: Leucititic to tepritic -phonolitic lava (pt1), lie in the uppermost formation; they are interpose with varicolored scoria with rock fragments and layered lapilli (pt). These deposits are relate to Poggio del Torrone, Poggio Pocatrabbio and Monte Panaro vents.

Holocene deposits

- Debris deposits (Holocene): loose and unconsolidated sediments deposited at the base of the slope of volcanic plateau. These deposits often derived from collapse or landslide of Vulsini volcanic deposits.
- Colluvium – eluvium (b2) (Holocene): unconsolidated fine sediments deriving from the erosion of pyroclastic deposits on the volcanic plateau. These deposits can have a thickness from a few meters up to 15 meters.
- Travertine (tr) (Holocene): porous lithified travertine with a lot of cavities

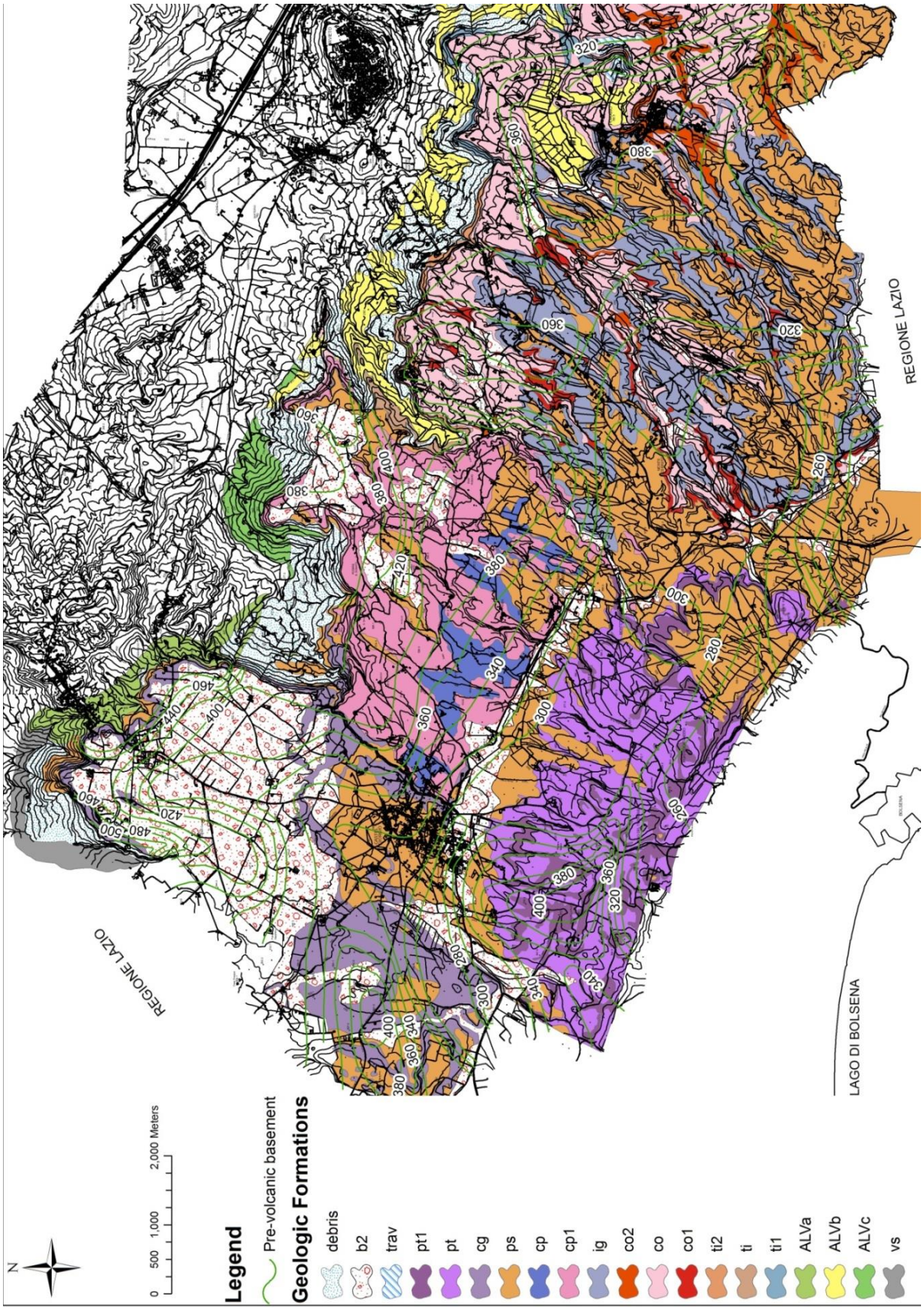

Figure 4 Geological map of Umbrian sector of VVD. Legend: Allochtonous Units (vs); marine sand, silt and clay (ALVa, ALVb, ALVc) Chiani –Tevere Syntem; Tione Formation: pyroclastic (ti) and lava (ti1, ti2) deposits; Corsica Formation: pyroclastic layered deposits (co) and interpose lava flow (co1 e co2); Orvieto Ignimbrite (ig); Podere Sambuco Formation: pyroclastic layered deposits (ps); Poggio del Torrone lava and scoria layers (pt, pt1); Castel Giorgio lava (cg); Case Perazza lava (cp, cp1); Travertine (trav);Colluvium (b2); debris deposits (debris).

The geological settings of the study area were pointed out through three geological cross sections. These cross sections were realize using geological and geophysical data coming from several database

- Ispra 464/84 Archive (2012),
- Geotecna Geological firm (2011),
- Laboratory of Hydrogeology, Roma Tre University (2013)

The first cross section (F) (Fig 4) starts from Poggio del Torrone and ends at Castel Giorgio airport with N-S direction. It focus on Montalfina – Castel Giorgio subsynthem; distinguish between Casa Pedrazza lava flows (cp1) and the uppermost Castel Giorgio lava (cg). These lava are intrabedded in the pyroclastic deposits (ps). Products from Poggio del Torrone vent (pt and pt1) lie over the previous deposits as it can see in the southern part of the profile. Two eluvium deposits are identified near Castel Giorgio town and near the Castel Giorgio airport with a thickness about 15 meters.

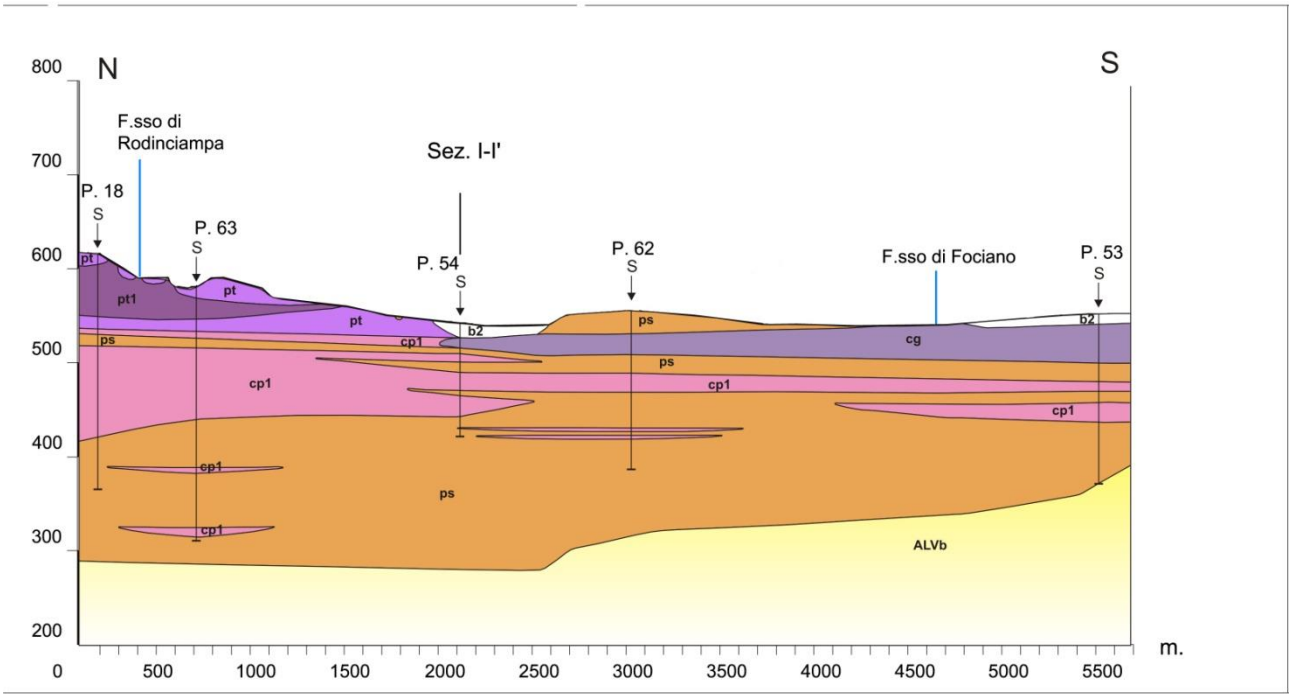

Figure 5 Geological cross section F (modified from ATI4 and Sii 2011)

The second geological cross section (G) (Fig 5) starts near Monte Panaro and ends at Villanuova Town with SW – NE direction. In this cross section the relationship between the Sugano Synthem, Canonica – San Severo Subsynthem and Montalfina – Castel Giorgio Subsynthem is point out. In effect according to the stratigraphic succession previously described volcanic units of Sugano Synthem overlie the sedimentary basement that deepens southward consequently to the collapse of Bolsena Caldera. Then Canonica – San Severo Subsynthem deposits were emplaced largely on preexisting volcanic deposits and minor directly on pre – volcanic basement. This subsynthem is characterized by an alternation of pyroclastic deposits, at least three main lava flows and the finale eruption of Orvieto Ignimbrite. Later, when volcanic activity shift westward, Montalfina – Castel Giorgio

subsynthem deposits filled the preexisted morphology covering Canonica – Torre San Severo subsystem deposits.

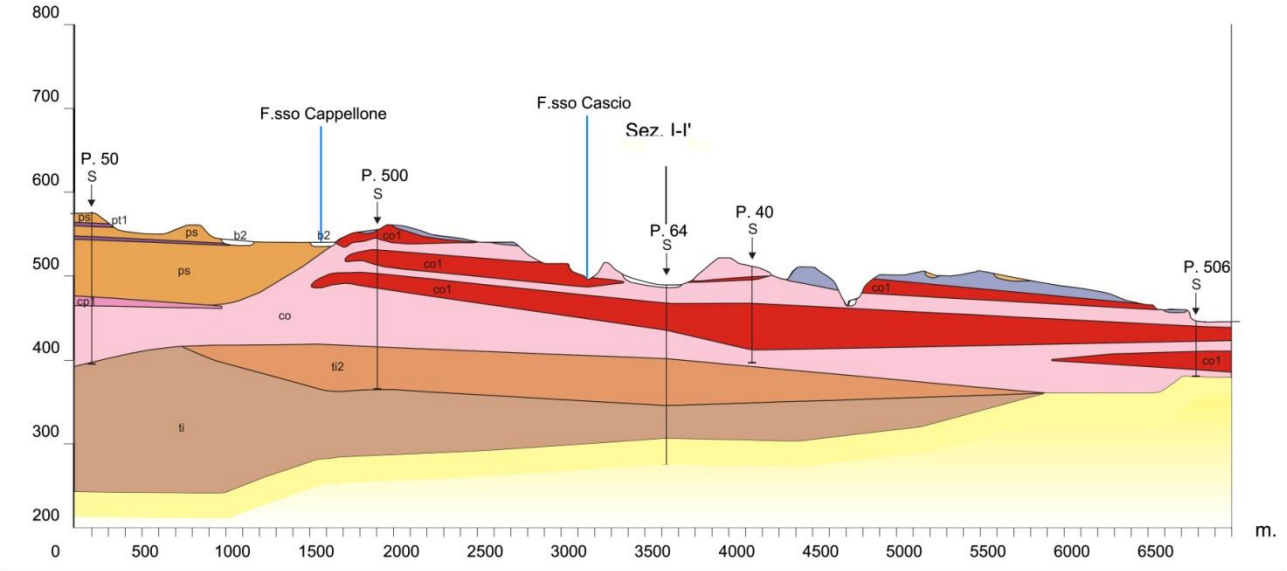

Figure 6 Geological cross section G (modified from ATI4 and Sii 2011)

The cross section I (Fig 6) has a NW – SE direction and focus on the lateral relationship between the Montalfina – CastelGiorgio subsynthem, in the western sector of the study area and the older volcanic units of Sugano Synthem and Canonica Tore San Severo subsynthem. Corsica Formation deposits (co) were detected lying over the sedimentary substratum In P65 borehole whereas about 3000 meters far from it this formation was detected in the first 100 meters under ground level in P64 borehole. The correlation between these two stratigraphies has a still uncertain geometry related to the western flank of the Canonica – Torre San Severo deposits that limited the later volcanic phases.

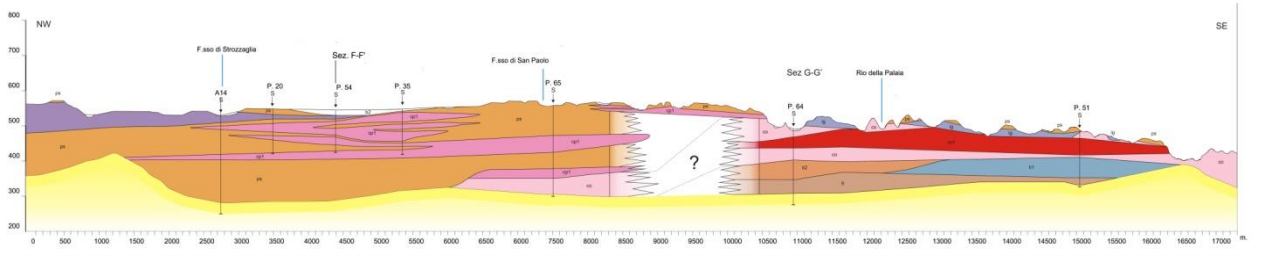

Figure 7 Geological cross section I (modified from ATI4 and Sii 2011)

2.3. Hydrogeological settings

The basal aquifer of volcanic formations is considered a strategic resource in Umbria since many years. The first hydrogeological studies carried out in this area date back to the 80's. Then in the 90's Regione Umbria commissioned a complete work (Piano Lotti) in the NE sector of VVD to identify suitable hydraulic supply areas. Pagano et al (2000) analyzed the entire hydrogeological basin of Bolsena Lake. In their hydrogeological model (Fig 8A) the northern edge of the studied basin passed through Castel Giorgio Town, where a high load in water table elevation map was detected. The same hydrogeological pattern was taken up later by Capelli et al. (2005). Indeed the authors identified a groundwater divide coming from Castel Giorgio Town to Bagnoregio Town, that separates Marta Basin (basin n°14) from NE Vulsini basin (basin n°13) (Fig 8B), later revised by Di Matteo et al (2010) too.

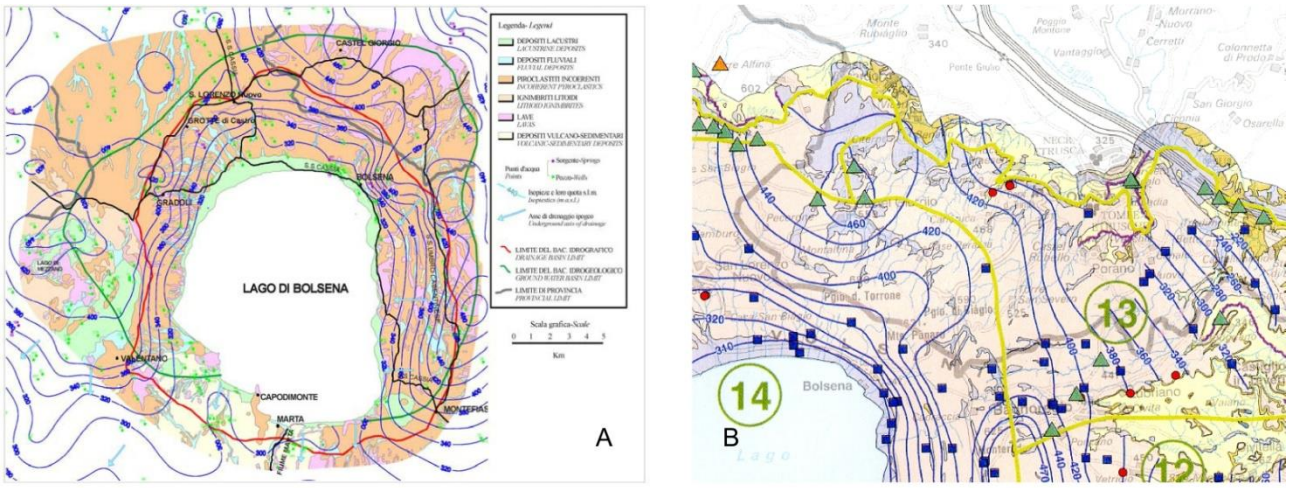

Figure 8 A) Hydrogeological map realized by Pagano et al. (2000); B) Hydrogeological map realized by Capelli et al. (2005)

In this work previous geological and geophysical data were integrated to a new piezometric survey carried out in 2002 to realize a detailed hydrogeological conceptual model. Water table elevation data show the same anomaly level under Castel Giorgio as detected by previous works. In this area water table elevation reaches at about 460 m a.s.l.; this unexpected piezometric load could not be related neither to a structural high of sedimentary basement neither by the rising of deeper fluids according to water chemical data (ARPA Umbria 2013).

In these works the groundwater divide of the NE Vulsini hydrogeological basin (n°13 in Fig 8B) is close to volcanic slope in direction of Paglia Valley, it defines a not extended basin probably insufficient to recharge the very productive springs of Sugano and Tione characterized by a mean discharge of about 150 L/s.

Hydrogeological characterization of the Umbrian sector of VVD has been carried out through geological analysis based on the previously described geological setting and in-field hydrogeological survey. The volcanic and sedimentary units outcropping in this area were included in five hydrogeological complexes. Each hydrogeological complex is composed by geological formations characterized by similar hydrogeological properties like permeability, capacities for infiltration and storage.

The defined hydrogeological complexes (Fig. 9) are as follows (modified from Capelli et al. 2005):

(Post volcanic units)

Eluvium complex: the products forming this complex derived from the weathering of pyroclastic units. This complex is characterized by an average to low primary permeability due to abundant silty – clayey matrix. It has a variable thickness from few meters up to 15 – 20 near Castel Giorgio Town where it hosts a superficial aquifer

(Volcanic units)

Pyroclastic complex: pyroclastic deposits composing this hydrogeological complex consist of alternating tuff, lapilli, pumice and minor volcanic ash characterized by a variable primary porosity due to its heterogeneity. In fact the presence of fine grain size levels reduces the vertical permeability of this complex. This hydrogeological complex has a thickness of several tens of meters and it hosts the main aquifer of volcanic units. Some low permeability deposits can support minor superficial aquifers

Lava complex: lava flows forming this complex are intrabedded in the pyroclastic deposits and are characterized by variable thickness from 10 meters up to 60 meters. Lava are characterized by an average or high secondary hydraulic conductivity.

Ignimbritic complex: this complex corresponds to the Orvieto – Bagnoregio Ignimbrite Formation. This formation is composed of pumice flow units, breccia deposits and pyroclastic flow deposits as previously described. This complex is characterized both by primary and secondary porosity.

(Pre volcanic units)

Pre volcanic complex: this complex corresponds to the pre volcanic sedimentary units; it is composed of sand, silt and clay marine deposits and allochthonous units. This complex it is characterized by notability low hydraulic conductivity and constitutes the basal regional aquiclude of the volcanic aquifer.

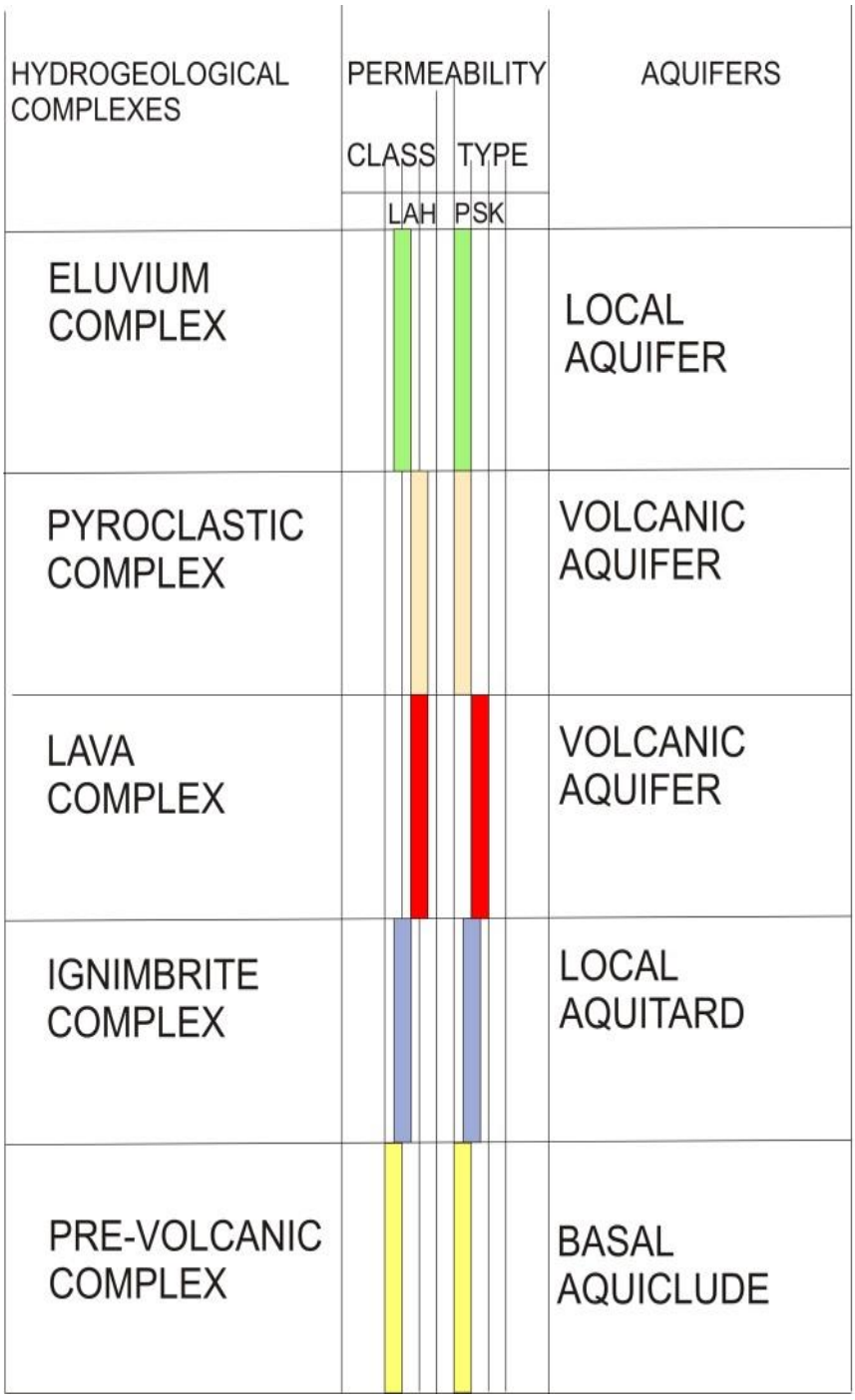

Figure 9 Summary of hydrogeological complexes. Classes of permeability: L (low), A (average) and H (high). Types of permeability: P (primary), S (secondary) and K (karst)

Waters of volcanic aquifers are characterized by low mineralization (less than 300 mg/L), electric conductivity usually less than 500 μS/cm and neutral pH values (7 – 7.5) (Frondini et al. 2013).Hydrogeochemical facies of groundwater is alkali – earth bicarbonate (Chiodini et al. 1982) and chemical composition of all volcanic aquifers is similar, with only minor differences related to rock – water interaction processes and residence time of water in volcanic deposits. In fact water of the basal aquifer is characterized by higher concentration in Na, Li, F, As and Si (Frondini et al. 2013).

3. Hydrogeological survey of Vulsini Volcanic District

A new hydrogeological survey was performed during the summer of 2013 in the Umbrian sector of VVD to improve the hydrogeological knowledge of this area.

As seen in the previous paragraph there are some uncertainties on the reliability of the previous works probably due to incorrect correlation of water table elevation. Alternation of pyroclastic deposits, characterized by different hydraulic conductivity, and lava flows allows the formation of superficial aquifers. The presence of these aquifers could alter the in situ measurements of water table elevation and chemical – physical analysis. In fact detected values could be the result of mixing of water from deep and shallow aquifer.

This mixing process could take place on a large scale due to variability of thickness or the absence of the intermediate aquitard. In fact, as already described, intermediate aquitard is made up by lava flows characterized by an irregular pattern related to the paleo-morphology. Therefore in some areas the lack of these deposits doesn't allow the distinction of aquifers. Other preferential mixing zones are located at the front of volcanic plateau. In fact outcropping lava show evidences of detensioning fractures that increase the permeability of these deposits. Sometimes boreholes could be a possible area where water mixing occurred. Incorrect cementing of well doesn't isolate the shallow and the basal aquifer so water could percolate through the fractured zone outside well casing to underlying aquifer.

3.1. Materials and Methods

Wells with known technics information were measured during the survey due to the hydrogeological heterogeneities of this area. All surveyed points were detected from LINQ (2013) database (Hydrogeological Laboratory of Roma Tre University) and ATI4 and Sii (2011) database in which boreholes characteristics were reported. Only deep wells, draining the basal aquifer, were selected among all available data. Chemical analyses are another essential guideline to distinguish wells referring to different aquifers. Bibliographic chemical data (ATI4 and Sii, 2011) were collected in order to characterize some boreholes in the study area. Water table was detected in 18 boreholes, and its elevation was defined in meters above sea level (m a.s.l.) using traditional gauges and sonic meter water level gauge. The survey points for measurement of groundwater were private wells and drinking supply wells drilled into the volcanic deposits; the depth was variable from about 60 meters to more than 200 meters, and all measurements were performed under static conditions. Data about 40 springs were collected during the survey. For each point were reported information about elevation of spring outlet, about discharge rate and chemical – physical analysis. At first the elevation of springs outlet was an essential parameter to distinguish springs related to basal aquifer or to shallow one. Discharge rate measurements were realized using volumetric method in localized spring characterized by a flow rate less than 1 L/s. Flow measurements of diffuse or in high discharge rate springs were performed using a SEBA Hydrometrie M1 mini current meter and by analyzing the flow velocity along every discharge section (velocity area distribution of International Standards 2007).

The location of every survey point was obtained using a GPS, while the elevation of every point was determined from detailed geographic cartography resource (CTR – Carta Tecnica Regionale 1:10.000). The topographic reference is the same used by other authors to allow comparison among results. Water table elevation map was realized using experimental data and minor bibliographic references. The map was first hand-drawn using triangulation method with 10 meters of contour interval, in order to produce a detailed reconstruction, then it was digitalized and elaborated in a GIS system. It is possible evaluate some features of basal aquifer starting from realized hydrogeological map. At first a triangulated irregular networks (TIN) were created from linear shapefile representing water table elevation (m a.s.l.) and pre-volcanic deposits elevation (m a.s.l.). Then a subtraction of these two layers generates a new surface showing the thickness of saturated zone. The depth of groundwater can be calculated subtracting water table elevation TIN to Digital elevation model (DEM) of the study area

3.2. Results

Hydrogeological data collected during the survey were analyzed in order to delete anomalous data did not referred to the basal aquifer. According to ATI4 and Sii (2011) molar ratio between Lithium and Rubidium is a significant marker between deep and shallow aquifers. In fact molar ratio value between these two metals, belonging to the alkali metal group, is close to 1 in rainfall waters. Therefore shallow aquifers, defined by rapid discharge with little water – rock ion exchange, show values of molar Li/Rb nearby 1. Whereas samples of water of basal aquifer are characterized by higher molar Li/Rb values due to relative enrichment of Lithium. This different concentration of Lithium in water could be relate to long time storage in volcanic reservoir or to the leaching of marine clays lying under VVD deposits. Therefore these analyses, where available, could identify the measured aquifer The hydrogeological map (Fig 9) depicts a clear reconstruction of two hydrogeological basins separate by a dynamic groundwater divide. It has NW-SE direction and its water table elevation decrease south-eastward from 460 m a.s.l. (near Castel Giorgio Town) to 420 m a.s.l. (near Torre S. Severo Town).The first basin corresponds to the south-western area of Umbrian VVD and it belongs to Bolsena Lake hydrogeological basin. The second detected hydrogeological basin belongs to Paglia River basin. The southern boundary of this basin corresponds to the dynamic groundwater divide whereas the other boundaries are marked by the outcropping limit of volcanic deposits. The main groundwater flow direction is north-eastward towards the base of volcanic slope. This sector of VVD is the recharge area of several springs characterized by different discharge rate, from 1 L/s up to more than 100 L/s. The most productive springs are used for drinkable water supply (Sugano 1 Spring, Sugano 2 Spring and Capita Spring) or bottling of mineral water (Tione Spring).It’s important monitor the morphology of dynamic groundwater divide and its variations in time in order to preserve water reservoir since these springs are important resources for population.
The comparison of data collected in 2011 and in 2013 hydrogeological surveys, evidences only minor differences in water table elevation ($\Delta = \pm 2$ m). No significant variations of water table morphology were detected then the two hydrogeological basins maintain the same recharge areas.

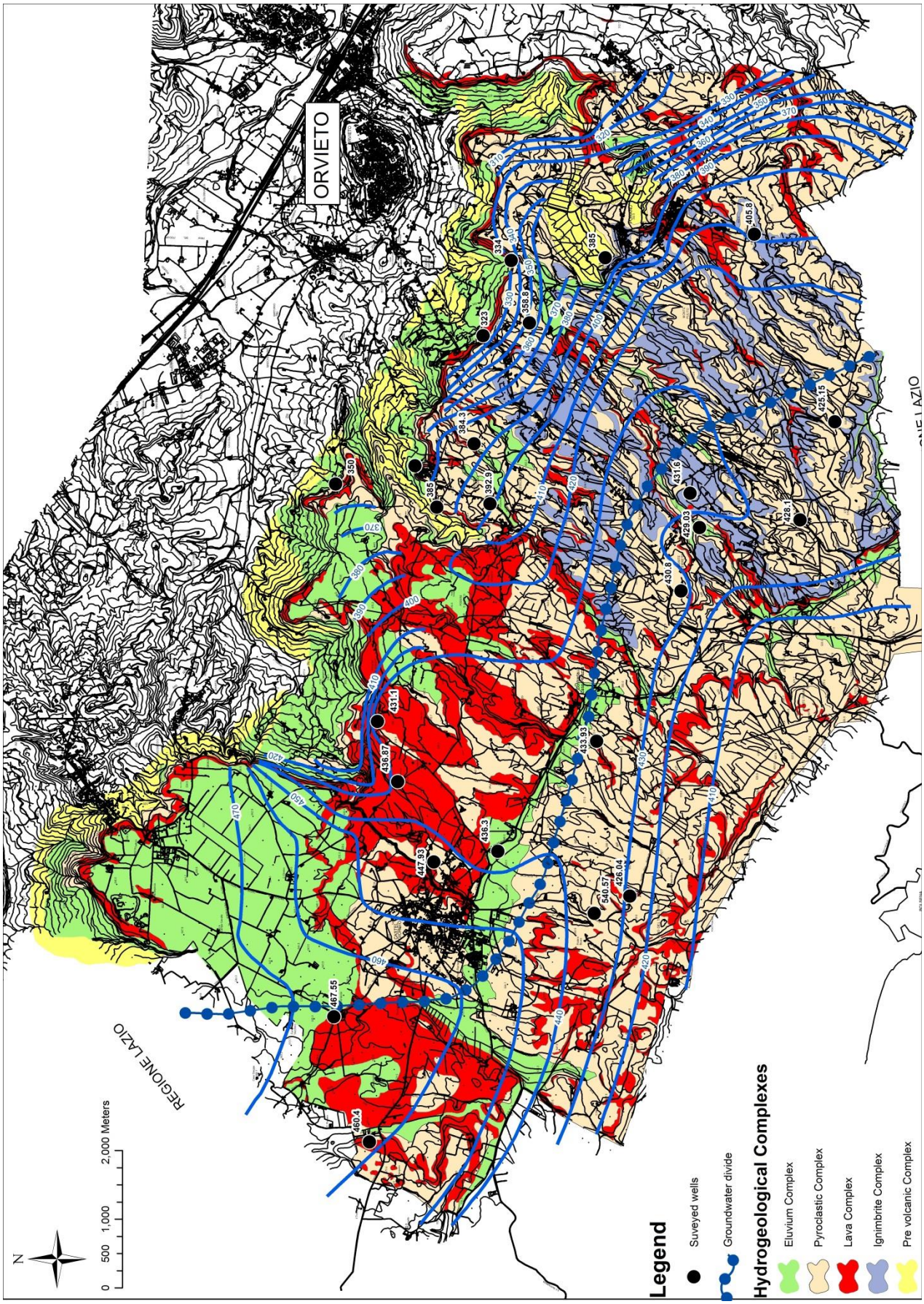

Figure 10 Hydrogeological map of Umbrian area of VVD (2013)

Groundwater thickness was calculated in a GIS system. The aquifer thickness reaches southward up to 200 meters due to the steep deepening of basal aquiclude (Fig 11); whereas it decreases up to few meters close to the springs on volcanic slope. Some anomalies were caused by the presence of morphological high of sedimentary deposits as can be seen south of Castel Giorgio Town.

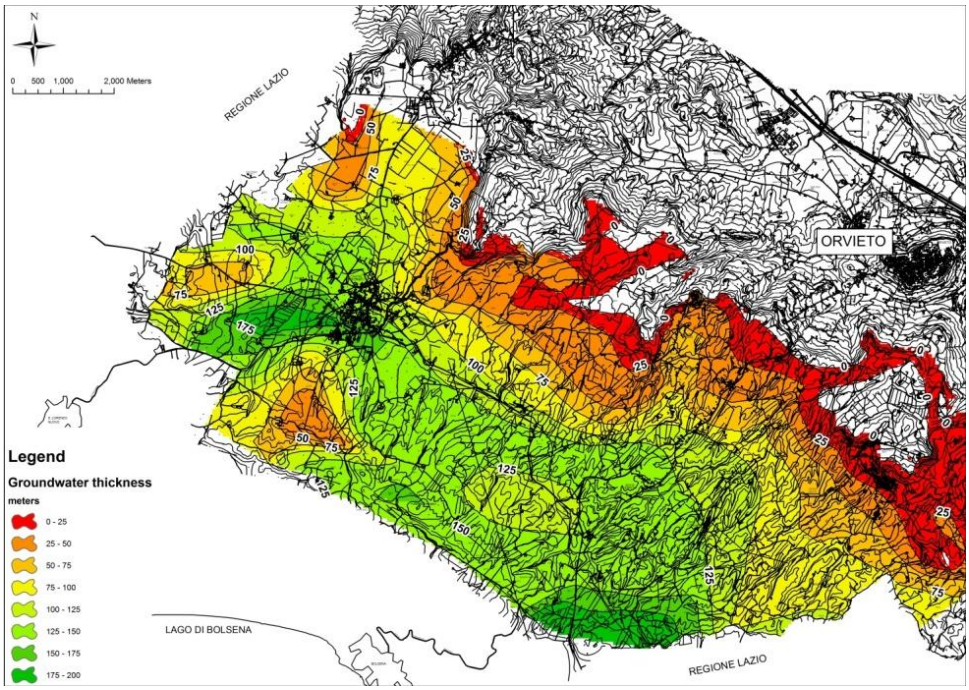

Figure 11Map of groundwater thickness of the basal volcanic aquifer

The map of groundwater depth evidences a progressive increase of the depth of the aquifer south-westward up to 250 meters (Fig. 12). The minor values correspond to the volcanic front where several springs were detected. This reconstruction is one of the most important parameters to determinate the vulnerability of the aquifer.

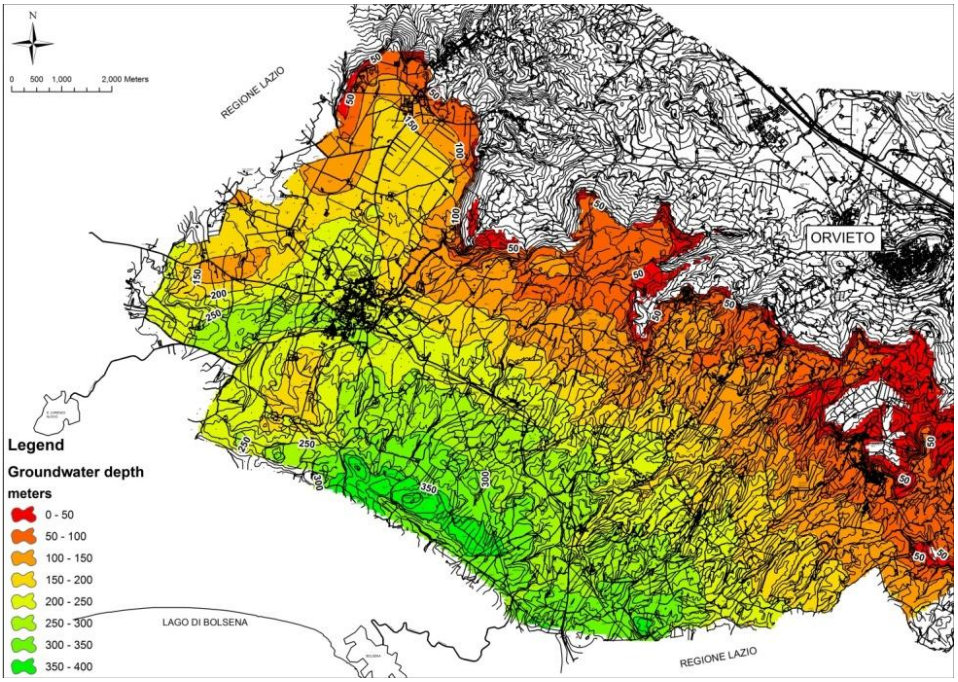

Figure 12 Map of groundwater depth of the basal volcanic aquifer

4. Roccamonfina Volcanic Complex

4.1. Geological settings

The Roccamonfina Volcano is part of the Ernici – Roccamonfina Volcanic Province located between the Roman (to the north) and the Campanian (to the south) magmatic provinces. The Ernici – Roccamonfina Province is a transitional zone between roman and campanian volcanoes (Fig 10) (Peccerillo 2005). These provinces belong to the volcanic belt of the Tyrrhenian margin.

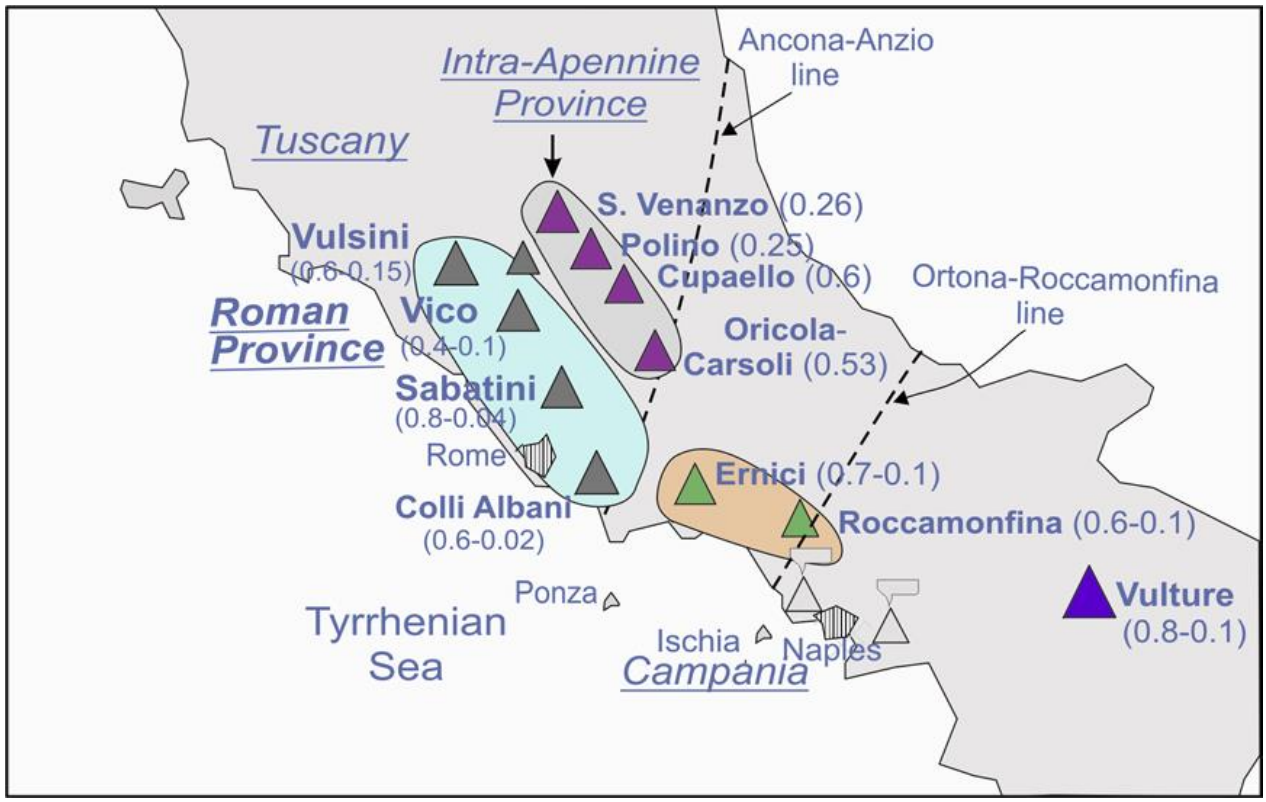

Figure 13 Perythirrenic Volcanism (Peccerillo 2005)

The origin of this magmatic activity is related to the eastern extensional structures of the Tyrrhenian basin, between the orogenic belt of the Apennines and the slow spreading center of the Tyrrhenian Sea. To the East of the Apennines, the Apulian micro-plate is subducted beneath the European plate, a convergent margin which is believed to be responsible for a classical arc-tectonic association of collision and extension, and onset of calcalkaline to ultra-potassic volcanism typical of the central-southern Italy (Peccerillo 2005).Roccamonfina lies at the intersection of a main NW – trending tectonic depression and the transverse, NE – oriented Garigliano Graben(De Rita and Giordano 1996). The main evolution of this graben during the Early Pleistocene was controlled by extensional Mount Massico fault at the northwestern border of Mount Massico structure (Nicotera and Civita 1969, Ippolito et al. 1973)

4.2. Geological evolution

The activity of the Roccamonfina began about 630 ka and ended around 53 ka (De Rita and Giordano 1996). Its activity is subdivided into three main epochs (Fig 14), corresponding to three different supersynthems (De Rita et al. 1997):
The first one (630-385 ka) is characterized by the growing of the stratovolcano and several small volcanic centers. During this epoch about 100 km^3 of mainly lava were erupted. The volcano edifice collapsed at the end of this phase.
The second activity epoch (385-230 ka) is characterized by a succession of highly explosive eruptions and about 10 km^3 of magma DRE were erupted
The last phase lasted until 53 ka. During this period minor freatomagmatic activity (1km^3 of magma DRE erupted) and lava domes occurred.
RVC evolution can be subdivided into two geochemical stages according to Appleton (1972). They correspond to two different magmatic series: the high-Kseries (HK), rich in leucite, and the low-K series (K), poor in leucite (Fig 15). The activity of the stage I characterized mostly the volcanic history of Roccamonfina, from 630 to 340 ka (Giannetti 1979; De Rita and Giordano 1996) with the emplacement of deposits characterized by the compositional interval from leucitic-tephrite to phonolite.

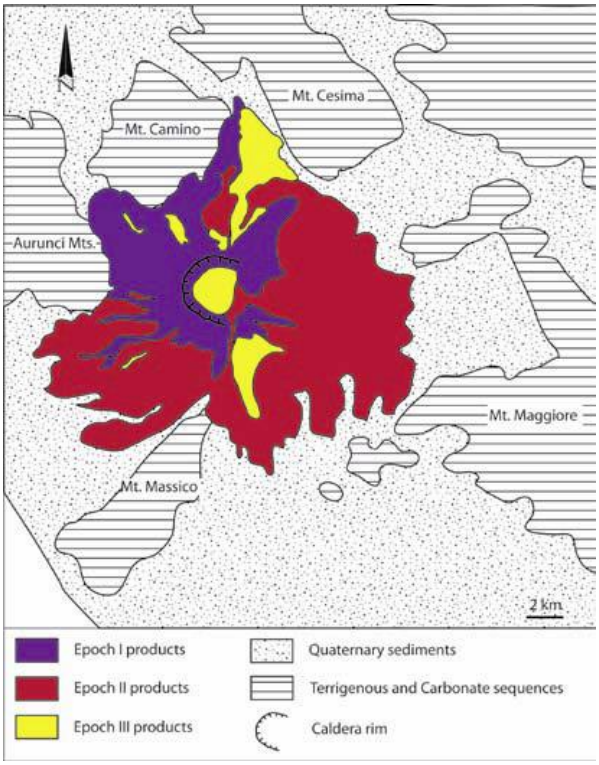

Figure 14Sketch of the distribution of the three different activity epochs products (modified from De Rita and Giordano 1996)

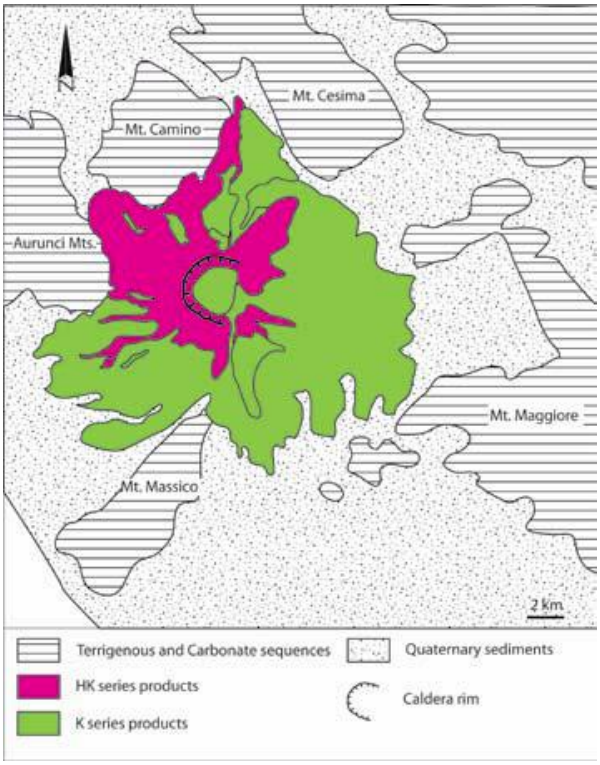

Figure 15The subdivision of the Roccamonfina volcanic products in HK and K magmatic series (modified from De Rita and Giordano 1996)

The First Epoch

The first epoch is mainly characterized by effusive activity with the emission of sub-saturated lava flows. A dating on lava deposits on the western flank of the volcano gave an

age of about 630 ka (Giannetti 1979), so the activity probably began before this data. Several parasitic centers were emplaced, such as Tuoro Piccolo and Mt. Capitolo (Cole et al. 1992; Rouchon et al., 2008). According to geochemical data of Appleton (1972), this epoch was characterized by the eruption of HK series magma having various parental melt compositions, differentiated dominantly at deep crustal levels.

The Second Epoch

At the end of Stage I a series of explosive eruptions emplaced a group of eight pyroclastic flow deposits (Santello 2010) called Brown Leucitic Tuff (BLT)(Luhr and Giannetti 1987). The onset of BLT (385- 325 ka) eruptions are marked by the upwelling of magmas derived from higher degrees of partial fusion, and less contaminated by subduction than the rest of HK series products. This may confirm the idea of Marra et al. (2004) about the existence of melt production cycles in the underlying lithospheric mantle. The BLT places itself between HK and K series products. Thus, it postdated the last HK series lavas, while the early K series lavas were erupted after the BLT. Actually the relationship between BLT and the main caldera has been highly debated during decades (Capuano et al. 1992, Cole et al. 1992, Chiesa et al. 1995, De Rita and Giordano 1996, Giannetti 2001). The formation of this crater by a caldera - forming event (e.g. deep reservoir collapse) was rejected by Watts (1987) and De Rita and Giordano (1996) after deep borehole investigation of the main crater, which did not indicate the presence of a disrupted or subsided basement. Alternatively, it has been suggested that the main caldera resulted from a lateral sector collapse linked to the eruption of the BLT (Watts, 1987; Chiesa et al. 1995) or to the instability of the eastern flank as a result of its continuous down throwing by the Mt. Massico fault (De Rita and Giordano 1996, Santello 2010). The K stage started at about 320 ka with the deposition of the White Trachytic Tuff (WTT) (Giannetti and De Casa 2000). The lower part of these deposits (LWTT) represents about 80% vol of the whole WTT succession. It contains frequent lithic accumulation zones of clasts derived from the demolition of the main cone, and dominantly from trachyandesite units in the main crater (Giannetti and De Casa 2000). Although the volume of the outcropping effusive products of the K stages is rather small in comparison with those of the HK stages. After LWTT activity, a number of trachybasaltic and shoshonitic parasitic centers erupted, (Rouchon et al. 2008). The main crater activity was also characterized by the emplacement of the shoshonitic basalts and by strombolian activity in the main crater dated 245-232 ka (Rouchon et al. 2008). Upper-WTT units represent limited erupted volumes related to localized explosions, emplaced 230 ka (Giannetti and De Casa 2000).

The Third Epoch

The end of the K series corresponds to the third and last supersynthem of the Roccamonfina volcano history (De Rita and Giordano 1996). The final stages consists of localized phreatomagmatic eruptions that led to the production and emplacement of the Yellow Trachytic Tuff (YTT) 227 ka from the N flank of the volcanic edifice, which result in the maar–shape of the northern crater (Giannetti 1996).

This epoch includes the building of Mt. S. Croce lava dome (dated about 150 ka) and Mt. Lattani lava dome (dated about 170 ka) and minor explosive eruption. They represent the most recent activity inside the caldera (Giannetti 1964).

4.3. Hydrogeological setting

Stratigraphic units can be combined into hydrogeological complexes having a similar hydraulic behavior according to their physical features. Within each complex may exist areas of non-homogeneity due to variable intensity of fracturing of lavas or limestone and to different primary porosity in stratified pyroclastic deposits. Eight hydrogeological complexes (Fig. 16) were defined using information from bibliographic works (Matta et al. 2013 and Capelli et al. 1999):

(Post volcanic units)

Detritic and alluvial deposits complex: this complex is composed by reworked sediments deposited at the base of slopes or in fluvial valley. These deposits could host restricted aquifers due to their high primary permeability

(Volcanic units)

Lava dome complex: this hydrogeological complex is composed by all lava dome of Roccamonfina activity and they are the preferential areas of effective infiltration on the volcanic edifice due to several cooling fractures that produce high secondary permeability
Pyroclastic complex: this complex is composed by pyroclastic flow deposits and pyroclastic fall deposits. These deposits have an average permeability due to their vertical heterogeneity.
Lava complex: this hydrogeological complex includes all lava flows emplaced during the Roccamonfina evolution. These lava are mainly characterized by secondary high hydraulic conductivity due to cooling fractures. They often lie over relative lower permeability deposits so lava flows could host superficial aquifers

(Pre volcanic units)

Flysch complex: this complex is composed by clay and calcarenite of miocenic flysch. These units are characterized by low relative permeability and sometimes they host unproductive aquifers in sandy layers characterized by relative higher primary porosity
Limestone and marly limestone complex: This complex is usually notably permeable with good transmissivity and storage due to its fractures and karst features; moreover it host a regional aquifer recharged by surrounding carbonate ridge.
Dolomite complex: this hydrogeological complex is composed by Triassic dolomite and dolomitic limestone and it's characterized by a relative lower permeability than calcareous and marly complex due to minor karst features. This complex is therefore considered an aquitard of the regional carbonate aquifer.

Another volcanic complex was described in Capelli et al. (1999) but this complex doesn't outcrop in the study area; it was only identified in some boreholes (Watts 1987) in Roccamonfina caldera
Volcanic breccia complex: This breccia is composed of fragments of lava deriving from the stratovolcano collapse during the second epoch of Roccamonfina evolution (De Rita

and Giordano 1996). The scarce presence of matrix gives a good hydraulic conductivity to this breccia

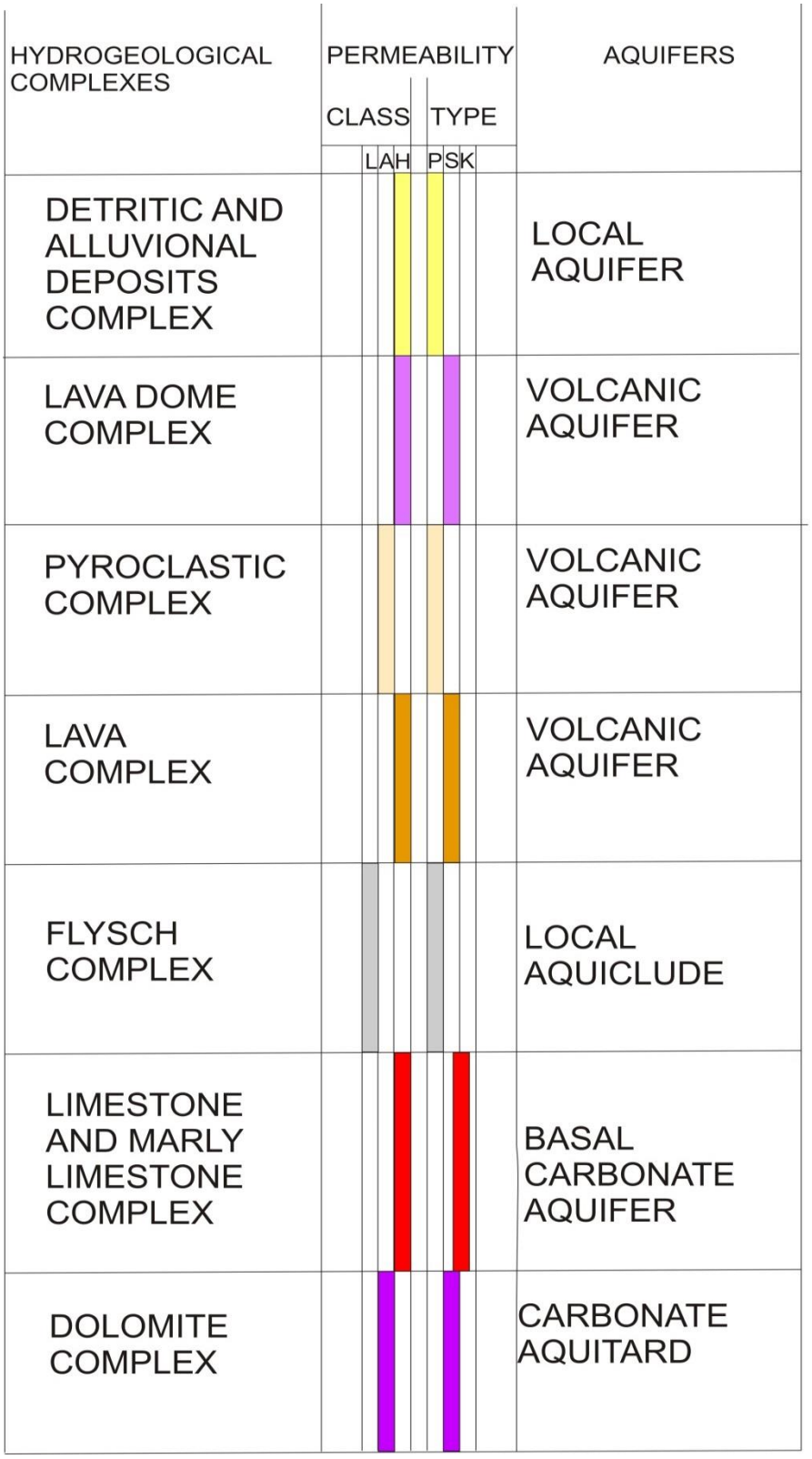

Figure 16 Summary of hydrogeological complexes (modified from Mazza et al. 2013). Classes of permeability: L (low), A (average) and H (high). Types of permeability: P (primary), S (secondary) and K (karst)

There aren't many previous hydrogeological works on Roccamonfina Volcano (Capelli et al. 1999, Allocca et al. 2007) because most of scientific articles and technical reports available in literature dealt especially with Riardo Plain and Ferrarelle Springs.
Capelli et al. (1999) identified 3 aquifers:

- **Carbonate aquifer**: it's the deepest aquifer of this area. The carbonate aquifer under the plain shows a southward drainage with the water table elevation included between 80 m a.s.l. and 40 m a.s.l.
- **Volcanic aquifer**: it's the main aim of this study. Two different areas can be distinguished by the piezometric pattern: the first area corresponds to the Roccamonfina volcanic edifice, the second one corresponds to the Riardo and Savone plains. Groundwater flows radially through Roccamonfina with a high gradient and it recharged the surrounding plains. The maximum groundwater level, over 600 m a.s.l., was detected in Roccamonfina Caldera while the minimum groundwater level was approximately 50 m a.s.l. in the southern area of this hydrogeological basin. The caldera is the preferential area of aquifer recharge since lava dome complex, characterized by high hydraulic conductivity, outcrops. The piezometric pattern shows the recharging role of the Roccamonfina Volcano eastward to Riardo Plain and southward to Savone Plain.
- **Shallow aquifer**: Alluvial deposits, reworked volcanic deposits and colluvium deposits host this shallow aquifer in Riardo Plain. The main drainage of this aquifer is north-eastward according to drainage area of Rio Pocciano. It shows water table elevation included between 150 and 100 m a.s.l..

Groundwater chemistry of the Roccamonfina volcano is characterized by a composite hydro-geologic dynamics and different mineralization processes related to different lithologies and CO2-gas-rich emissions in the deepest water tables. Chemical features can distinguish different groundwater within and outside the caldera (Cuoco et al. 2010):

a) K-rich waters flowing between the ultra-potassic basalts related to the first eruptive period of Roccamonfina volcano. The eastern deep aquifer shows low redox conditions, presence of Fe (II), and evidences of carbonates hydrolysis, which is explained with waters continuously interacting with both volcanic and carbonate facies. Several springs belonging to the eastern side of the volcano show high CO2-rich gas emissions at the vent site. The deep water after flowing through the K-rich basalts crosses into carbonate formations of the Riardo Plain. Conversely, the second aquifer (still belonging to the HKS series) is more superficial and is originated within the western side of the caldera and not influenced by carbonate hydrolysis.
b) Groundwater flowing through pyroclastic and/or lavas of the last eruptive period show different chemical features compared to aquifer (a). Also these low mineralized waters may (or may not) interact with carbonate rocks and/or waters; however, the process should occur superficially and it is limited on time.
c) The last type of groundwater, found in the area N-NE side of the volcano shows typical bicarbonate facies. These waters show only features from a carbonate aquifer without interactions with volcanic rocks and waters.

5. Hydrogeological survey of Roccamonfina Volcanic Complex

5.1. Materials and Methods

A hydrogeological survey was performed during the summer of 2012 to examine the non - homogeneous hydrogeological setting of this system. This survey focus especially on the eastern slope of Roccamonfina volcanic edifice, on Riardo and Presenzano Plains. The discharge of springs and streams, the piezometric levels in wells and piezometers were measured during this survey.
Water table elevation was detected in over 100 wells using both traditional gauges and sonic level meter. Technical information (depth of boreholes, presence of filters etc) was collected for each surveyed point. The discharge in many springs was measured by means of the traditional volumetric method at the sink. Flow measurements were performed using a magnetic current meter and by analyzing the flow velocity along every section. Several flow measurements were performed along each stream to identify springs in riverbed using a SEBA Hydrometrie M1 mini current meter and by analyzing the flow velocity along every discharge section (velocity area distribution of International Standards 2007).Basic physic-chemical parameters (temperature, electric conductivity and pH) of the groundwater were measured using portable probes. All these data are essential to distinguish the surveyed point between the overlapping aquifers in the Riardo Plain as previously described.
Hydrogeological survey data were used to realize potentiometric surface of the volcanic aquifer by the triangulation method with 5 meters of contour interval, then it was digitalized and elaborated in a GIS system. It is possible evaluate the thickness and the depth of basal aquifer starting from the realized hydrogeological map as already described in materials and methods chapter of the hydrogeological survey of Vulsini.

5.2. Results

During this work a deep regional volcanic aquifer and some shallow aquifers were distinguished through a detailed hydrogeological survey. The basal volcanic aquifer was detected through several measurements of water table elevation in wells placed especially in surrounding plains at the base of Roccamonfina and minor on the east slope of volcano. Water table elevation map of the regional volcanic aquifer (Fig. 17) was realized with 5 meters contour interval through the triangulation method removing data related to other aquifers. Groundwater morphology is more detailed in plain sector than on Roccamonfina slope; because there are only few deep wells on the volcano edifice since springs supply placed in Roccamonfina Caldera satisfy domestic and drinkable requirements. Therefore the lack of boreholes in the upper Roccamonfina volcano does not allow a complete knowledge of groundwater at water table elevation higher than 120 meters a.s.l.. Water

table morphology in the upper Roccamonfina Volcano is uncertain due to lack of deep monitoring wells but the bibliographic radial drainage pattern is still confirmed.

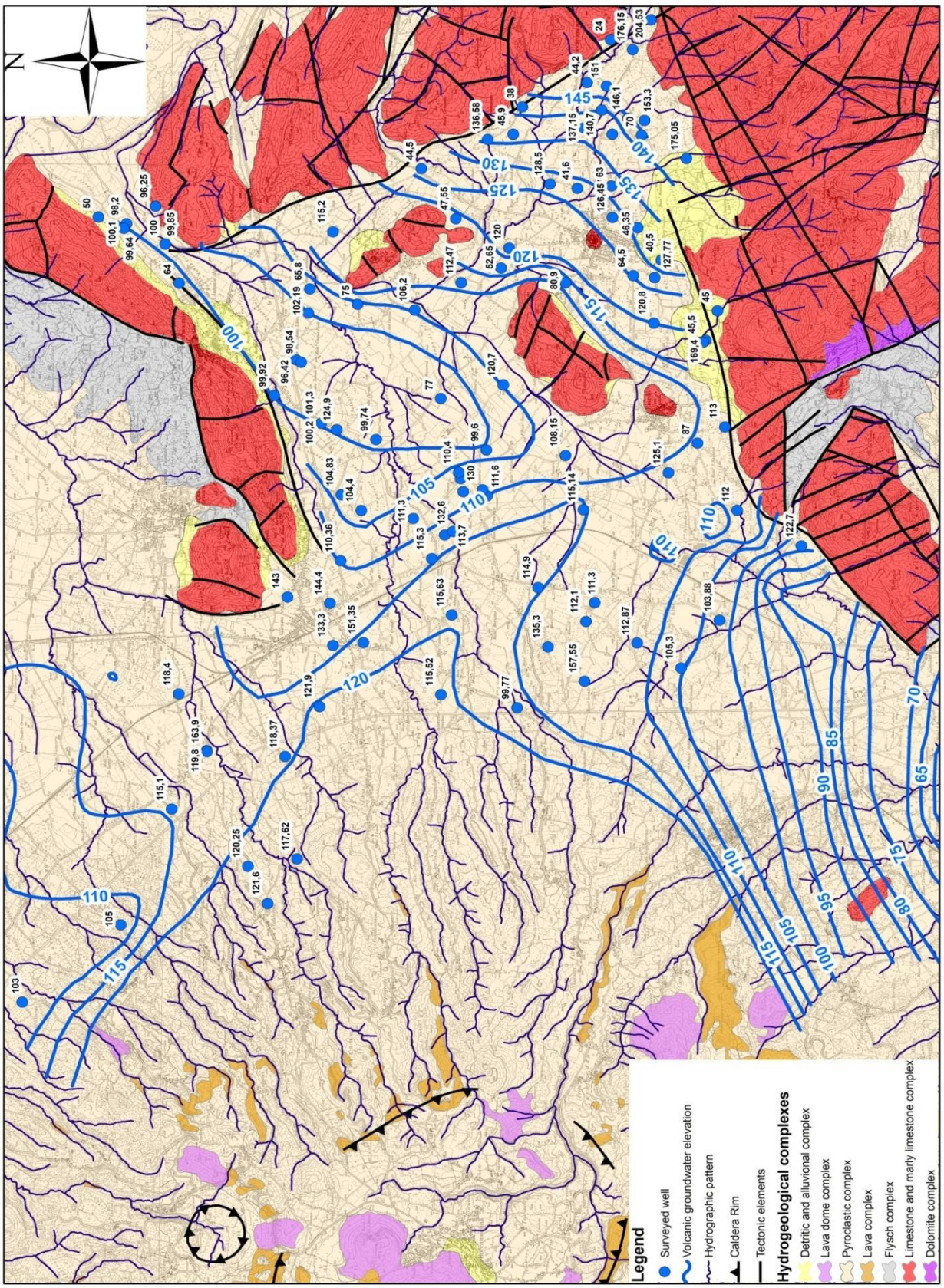

Figure 17 Hydrogeological map of Roccamonfina

Groundwater flows radially from Roccamonfina volcano to the surrounding plains. Two hydrogeological basins are defined by a dynamic groundwater divide with a W – E direction. The southern basin corresponds to the Riardo plain whereas the northern basin corresponds to the Presenzano Plain. The main recharge area of basal aquifer corresponds to Roccamonfina Caldera where hydrogeological complexes characterized by high permeability (lava dome complex and lava complex) outcrop.
The experimental water table surface map shows some differences from previous works (Capelli et al. 1999, Allocca et al. 2007).A NW – SE dynamic groundwater divide was identified in the Riardo Plain through the realization of water table elevation map. It divides groundwater into an eastern sector and a western one. The principal drainage axes of these sectors correspond southwestward to the Savone River and northeastward to Rio delle Starze. The hydrogeological basin of Savone River is recharged from Roccamonfina Volcano aquifer. Groundwater coming from the volcano passes through both volcanic deposits than the carbonate bedrock. This conceptual model is supported by data of water table elevation detected in wells filtrated in volcanic deposits and in wells catching water only from carbonate formations. In the eastern sector of the Riardo Plain a shallow and a deep aquifer can be distinguish. Volcanic deposits host the shallow aquifer whereas carbonate formations host the basal aquifer (Fig 18). Differences up to 100 meters in water table elevation between the two aquifers were detected in several wells different to as previously seen in the western area of the plain. The two aquifers seem to be separate by a still indeterminate aquitard. Different drainage patterns were detected as additional difference for these aquifers: volcanic aquifer is characterized by a NE drainage pattern according to Rio Pisciarello, whereas the carbonate aquifer flows southward trough Maggiore Mount Ridge with a higher hydraulic gradient.

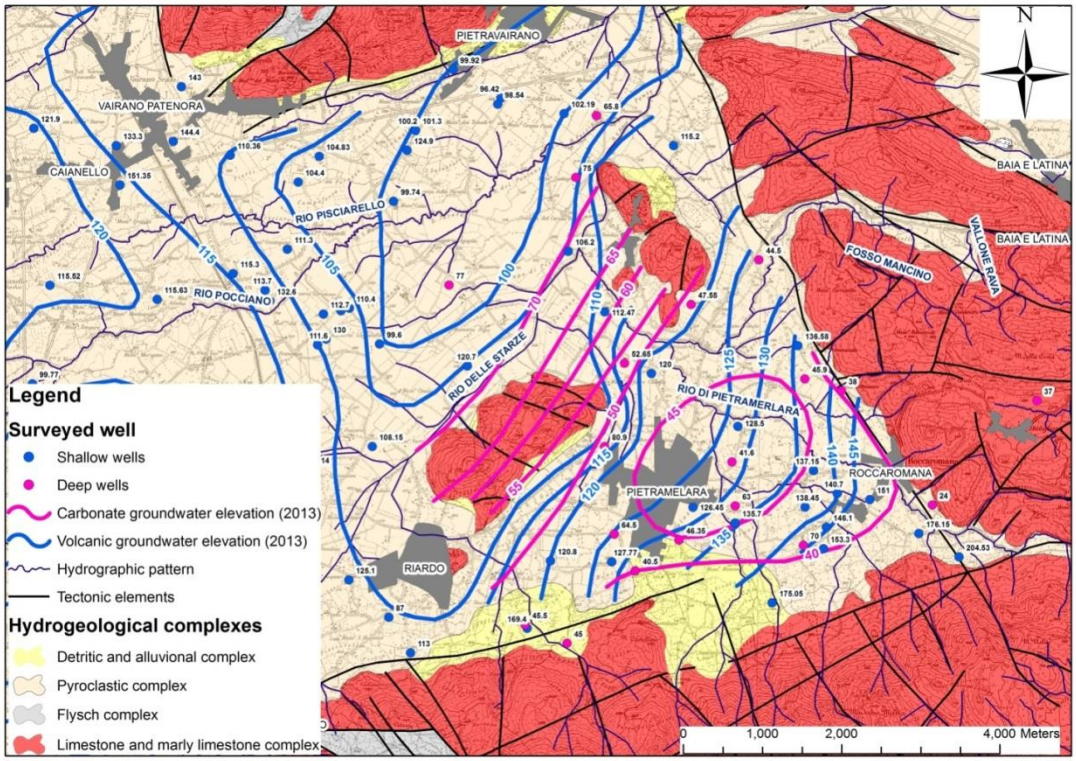

Figure 18 Hydrogeological schemes of carbonate and volcanic aquifers detected in the eastern sector of Riardo Plain

Furthermore there is a difference of several meters from the experimental water table elevation in Roccamonfina Volcano compared to previous works (Capelli et al. 1999, Allocca et al. 2007). This difference is due to a different hydrogeological conceptual model of Roccamonfina (Fig 19). According to Capelli et al. (1999) the volcano edifice hosts only one aquifer and the authors realized the water table surface map correlating the elevation of several springs on the east slope of Roccamonfina to piezometric data measured in wells placed in surrounding plains.

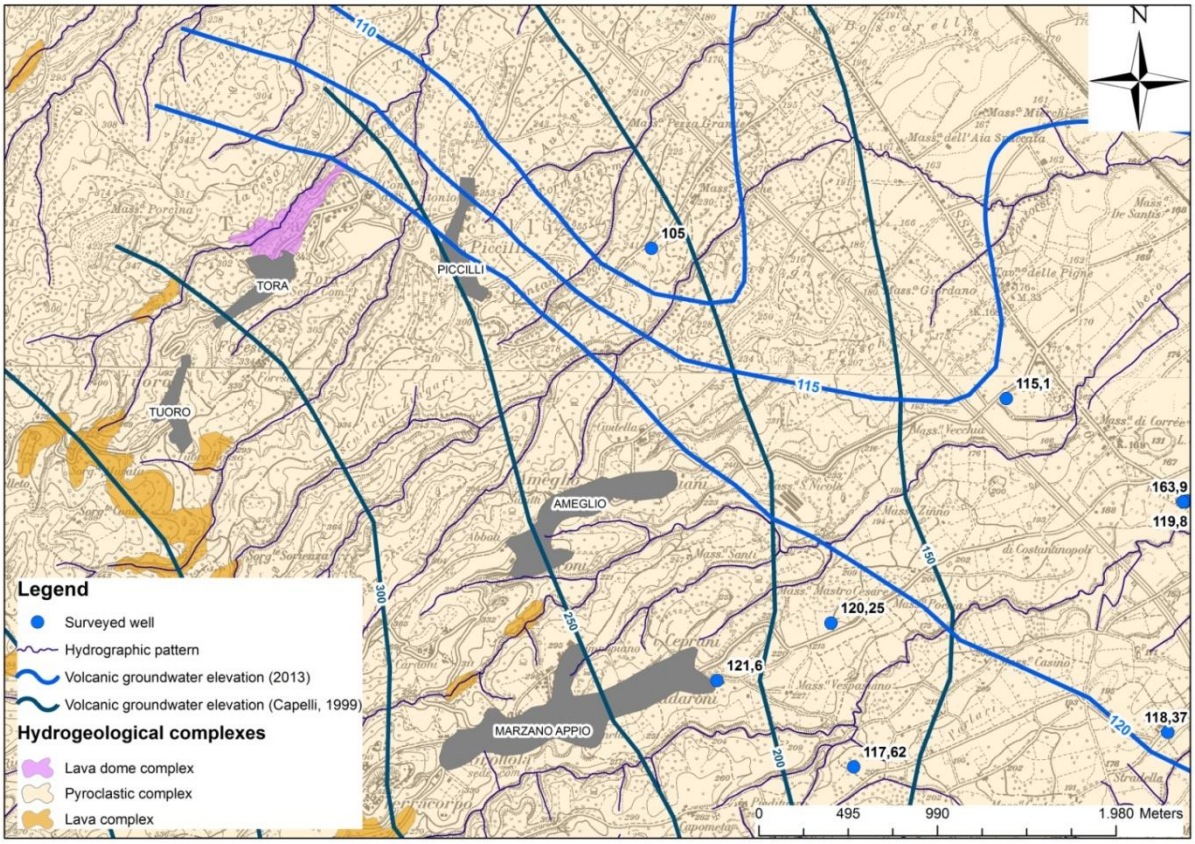

Figure 19 Comparison between bibliographic data and experimental data 2012

During the hydrogeological survey several springs detected on the east flank of Roccamonfina were related to shallow aquifers. In fact volcanic deposits outcropping in east slope of Roccamonfina volcano are characterized by different primary and secondary permeability. These difference could determinate the development of shallow aquifers characterized by scarce water yield on Roccamonfina slope. Shallow aquifers emerge as punctual or linear springs characterized by low variable flow rate during the hydrological year. For example some springs near Tora e Piccilli Town were measured during the last seasons; their maximum discharge (about 50 l/s) was measured during the rainy season whereas they appeared dry in June. Pumice levels of pyroclastic formations of RVC can host other minor shallow aquifers too. It's very difficult distinguish the limits of these basins due to the temporary nature of aquifer and to lack of boreholes in which measure groundwater level.

Groundwater depth of the principal volcanic aquifer was calculated subtracting water elevation data (meters a.s.l.) from the digital elevation model (DEM). The results were reclassified in 9 classes (Fig. 20). The aquifer was detected near ground level in several

areas; most of them correspond to drainage sections of some streams: groundwater depth gradually decreases north-eastward up to intersect Rio Cerrito and Rio delle Starze riverbeds increasing streams flows. In the southern sector groundwater was detected at least at 10 meter under ground level correspond to the drainage sections of Savone delle Ferriere stream, Torrente Savone di Assano valley and Savone Stream that drain southward the volcanic aquifer in the Savone Basin. Groundwater was detected less than 10 meters under ground level in the eastern sector of Riardo Plain. These higher water table elevation data were related to the presence of a low permeability aquitard sustaining the volcanic aquifer e to lateral recharge from alluvial fans. The last detected area where groundwater level is similar to ground level corresponds to Ferrarelle and Santagata sparkling mineral water springs near Riardo Town. Groundwater depth increases in the western sector of the Riardo Plain up to 40 meters under ground level closeness Vairano Scalo, then water table depth values quickly reach over 80 meters in the area of Roccamonfina volcano due to the increase of volcano slope (> 30%). This area was not further detailed due to lack of groundwater elevation data of the principal aquifer.

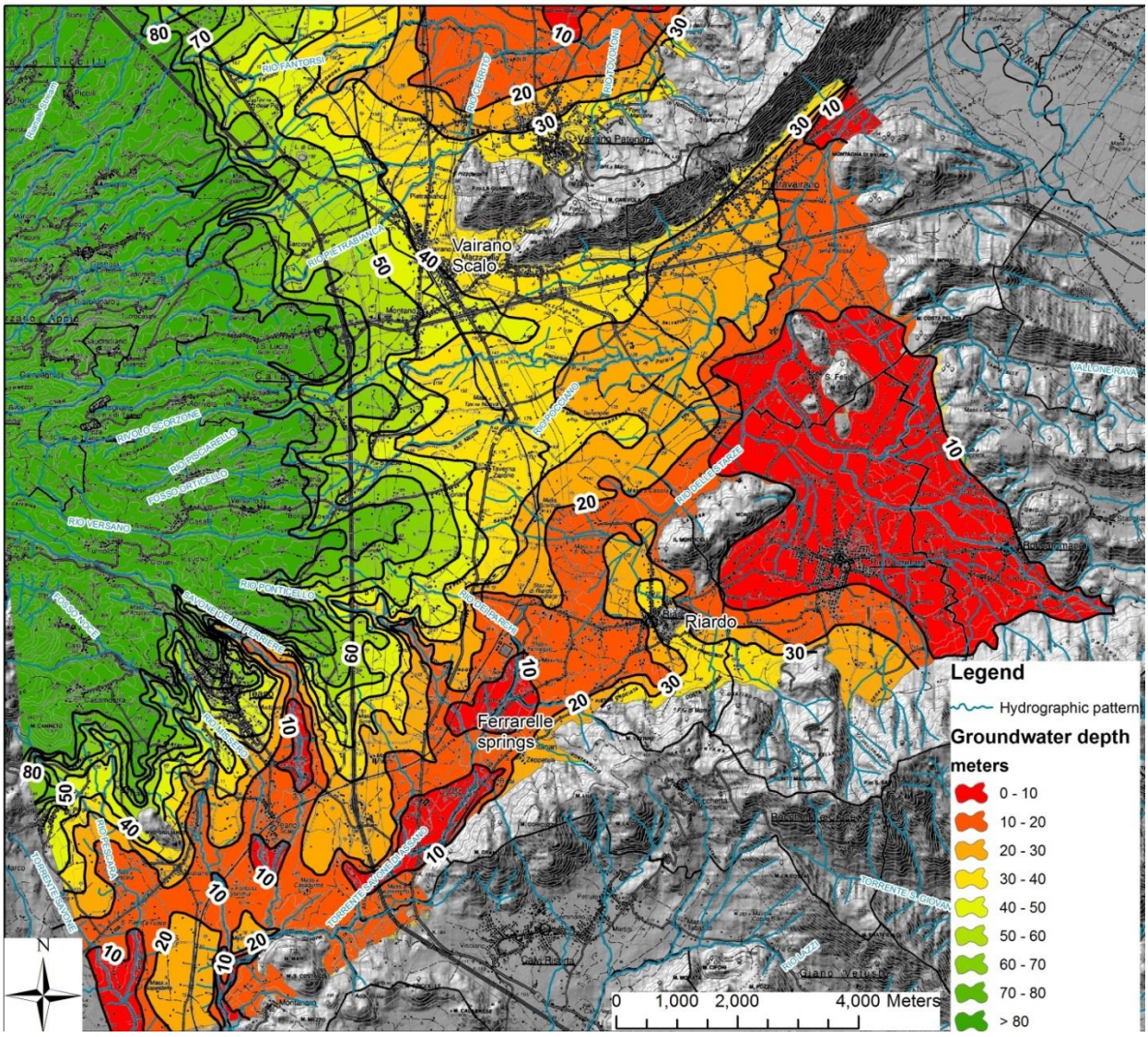

Figure 20Map of groundwater depth of the basal volcanic aquifer

The thickness of volcanic aquifer can not be calculated in this area differently from NE sector of Vulsini (Fig. 11). In fact here is not possible to identify a regional basal aquiclude of volcanic aquifer except in restricted areas like in the eastern sector of Riardo plain where flysch deposits separate the above volcanic deposits to the lower carbonate formations allowing the distinction between the volcanic and the carbonate aquifer. In other sectors volcanic deposits lying directly over carbonate permeable formations allowing the mixing between the two aquifers.

6. Colloids

Colloids are defined as particles less than 10 µm in diameter and include a variety of organic and inorganic materials in groundwater like layer silicates, sesquioxides (Fe – Al oxyhydroxides), mineral precipitates, weathering products and rock and mineral fragments organic macromolecules, bacteria and viruses.

Colloid transport in macroporous soils can be very rapid and deep due to the combination of high water flow rates and little sedimentation and sieving of colloids in large pores (Schelde et al. 2002).

Coarse – grained aquifer material can contain up to 5% clay sized materials (<2 µm) that may be detrial (contained in the original parent geological material) or authigenic (formed in situ through geochemical alteration of primary mineral solids in groundwater zones). Various layer silicates, as well as iron and aluminum oxides, can be detrial in subsurface sediments. Authigenic colloidal sized particles composed of secondary hydrous oxides, aluminosilicates, and silica as well as complex mixtures and solid solutions of these phases, also form on the surfaces of larger mineral grains as a result of the alteration of thermodynamically unstable primary minerals. The presence of a clay – sized fraction in many aquifer materials suggests that the colloidal fraction is not intrinsically mobile (Mc Carthy and Zachara 1989, Seta and Karathanasis 1996).

A first but essential step in the genesis of mobile colloids in groundwater is the formation of colloid suspension in the pore water. This step can involve a number of mechanisms including the homogeneous nucleation of inorganic solids in the fluid phase, the release of colloidal material from the geologic matrix and the translocation of inorganic and organic substances from the vadose or recharge zone (Mc Carthy and Zachara 1989)

To be mobile suspended colloidal material must be stable (resisting aggregation with other like particles) and must not be susceptible to the particle filtration in passing in through porous media. It depends on a complex combination of density, size, surface and water chemistry and water flow rates. The complicated interdependency of these factors makes it difficult to predict particle behavior (Mc Carthy and Zachara 1989, Seta and Karathanasis 1996).

Under favorable geochemical conditions, such colloid sized materials can remain suspended for a long time in soil pore waters without coagulation or precipitation and hence constitute another mobile phase in soil water system. (Deepagoda et al. 2011).

A variety of soils properties influence the dispersibility of colloids from aggregates. Besides the well documented effects of clay mineralogy, solution ionic strength and pH on colloid dispersion, total clay content, soil moisture conditions, soil management and interactions among these properties have also been shown to affect colloid dispersibility (De Jonge et al.2004, Guo et al. 2011). Furthermore, the amount of leached particles does not correlate well with either bulk density or clay content, as perhaps would be expected because soils with high clay contents contain more small particles. Thus, soil containing high concentrations of water dispersible colloidal particles does not necessarily exhibit high colloid leaching when a high water flow velocity in larger pores is combined with good mass transfer conditions. These results show that the soil structure and the related transport parameters were the most important factor for controlling colloid leaching,

whereas soil texture and the amount of water-dispersible colloids present in the soil were less important (Poulsen et al.2006)

Physical perturbation in the hydraulic system is known to be one of the primary causes of in situ colloid generation (Ryan and Elimelech 1996, Deepagoda et al. 2011). For example following a rapid rainfall event, the high raindrop impacts (on the ground surface) and hydrodynamic shear (on the pore walls by infiltrating rainwater) can cause extensive release of colloids from soil matrices.
Colloidal materials also can be released to groundwater as a result of geochemical and biological processes acting upon larger inorganic or organic particulate materials in the aquifer matrix. Permeability reductions in subsurface sediments and sandstone that accompany groundwater electrolyte changes have been ascribed to mobilization of colloids. Colloids also can move to groundwater from the vadose or root zone. Humic substances can be flushed from upper organic rich soil horizons to the vadose and saturated zone during major infiltration periods (Mc Carthy and Zachara 1989 Miller et al., 1990; Sumner, 1993; Levy et al., 1993).
Schelde et al. (2002) made several experiments of soil columns to identify the relationship between colloid mobilization and leaching simulations. Their results showed that there was a seemingly unlimited source of in situ colloids even after prolonged leaching and the peak concentration of colloids in the effluent after the flow interruption increased with increasing length of the preceding pause. The experimental results demonstrate that colloid mobilization a time-dependent process, meaning that shear is not important to in situ colloid mobilization (Schelde et al.2002) They found an initial high leaching of in situ particles, followed by a gradual decrease and a final low constant concentration of colloids in the effluent (Schelde et al. 2002)
Colloids have high sorptive capacity and can be effective sorbents of low solubility, strongly sorbing contaminants due to their high specific surface area. Transport of colloids through the vadose zone thus causes an increased risk of leaching of contaminants generally regarded as relatively immobile. (De Jonge et al. 2004) (Mc Carthy and Zachara 1989)
Layer silicate clays adsorb metallic and organic cations by ion exchange. Surfaces of iron, manganese, aluminum and silicon oxide particles strongly adsorb certain metallic cations and organic and inorganic acid ions. (Mc Carthy and Zachara 1989) (Schelde et al. 2002).
Preferential flow may accelerate the transport of externally applied colloid – contaminant complexes, or colloid – contaminant located to close to the preferential pathways (De Jonge et al. 2004).

7. Geochemical analyses

7.1. Materials and Methods

7.1.1. Field measurements and sampling

Water samples were collected from springs and in few cases from drilled wells for domestic use. Sample points coordinates have been registered with a Garmin eTrex GPS and using most detailed topographic maps available. Groundwater samples from wells were collected after standard purge procedure. This process involves removal of at least three well volumes of standing water until stable field parameters were recorded. Springs samples were collected after stabilization of the physical parameters of the groundwater. Field measurements consisted of unstable parameters like temperature, electrical conductivity (EC), pH and reduction potential (Eh). Temperature, pH, Eh and EC were measured in field during Roccamonfina hydrogeochemical survey, using a portable instrument Hanna model HI991300 with a model HI1332D probe. Geochemistry Laboratory of Environmental Sciences Department of 2nd University of Naples made these instruments available in Roccamonfina survey. The conductivity readings were checked in the field against freshly prepared KCL standards 1413 µS/cm for HI991300. The HI1332D probe glass electrode with a silver/silver chloride reference was used for the pH measurements. WTW portable pH/cond 340i with TetraCon 325 sensor and SenTix20 sensor were used for in situ measurements during Orvieto survey. It was not possible to measure Eh due to technical problems.
The total alkalinity (as HCO_3^-) was determined in situ after collection by tritation with 0.1 M HCl against methyl orange indicator (IRSA 2004). Water samples for chemical analyses of major ions were filtered in field using a 0.45 µm and 0,22 µm Minisart sterile cellulose acetate membrane filter. Water samples were collected from each motoring point:

- 0,20 µm filtered and un - acidified sample used for Ionic chromatographic analyses
- Unfiltered and acidified (HNO_3 60%Ultrapure MERK) in field sample used for ICP-MS analysis
- 0,45 µm filtered and acidified (HNO_3 60%Ultrapure MERK) in field sample used for ICP-MS analysis
- 0,20 µm filtered and acidified (HNO_3 60%Ultrapure MERK) in field sample used for ICP-MS analysis

Samples were stored in PE flacons, prewashed in MilliQ water.

7.1.2. Laboratory Analyses.

All laboratory analyses were performed in Environmental Sciences Department of 2nd University of Naples in Caserta. Anions were analyzed through ionic chromatography at Geochemistry Laboratory, while Microwave acid extractions and ICP-MS analysis was carried out in CRdC. A.M.R.A. Laboratory.

Ionic chromatography

Major elements were analyzed by ion chromatography (IC) (Dionex DX-120) on 0,22 μm filtered samples (Na^+, K^+, Mg^{2+}, Ca^{2+},F^-, Cl^-, NO_3^- and SO_4^-).

Figure 21Dionex DX-120 Ion Chromatograph

Detected concentrations have been reported in appendix. The Dionex DX-120 Ion Chromatograph (Fig 17) performs isocratic ion analysis applications using conductivity detection. This system allows switch between two sets of columns (column select mode) and between two eluents (eluent select mode). The used eluents are a buffer HCO_3^-/CO_3^{2-} 8mM for anions determinations and Methansulfonic acid (CH_4O_3S) 0.02 M for cations quantification. The columns system is subdivided into guard columns and analytical columns. Were used for anions line Ion Pac AS14A (AG14A guard column) and for cations Ion Pac CS14A (CG14A guard column) exchange resin paking columns. Self-regenerating suppressors are ASRS ultra 4mm and CSRS ultra 4mm respectely for HCO3/CO3 and CH_4O_3S eluents. The DX-120 uses as detector the models CDM-3 standard cell. The measured value is used for temperature compensation, the active volume is nominally 1,25 mL, and the detector cell constant has a nominal value of 160 cm-1. The DX-120 has been managed by operating commands from PeakNet 6 software via the DX-LAN interface. Instrument calibration has been performed with Dionex certificate standard solutions.

Microwave acid extraction

All samples, collected during this work, were pre-treat according to EPA Method 3015 before ICP-MS analysis. This method is applicable to the microwave acid extraction of

available metals in aqueous samples that contain suspended solids for the following elements:
*Aluminum (Al); Arsenic (As); *Barium (Ba); *Beryllium (Be); Boron (B); Cadmium (Cd); *Chromium (Cr); Cobalt (Co); Copper (Cu); *Iron (Fe); Manganese (Mn), Molybdenum (Mo); Nickel (Ni); Selenium (Se); Strontium (Sr); Thallium (Tl); *Vanadium (V) and Zinc (Zn).
*Elements which typically require the addition of HCl for optimum recoveries
The choice of an acid or acid mixture for digestion will depend on the analytes of interest and no single acid or acid mixture is universally applicable to all analyte groups. All acids are analytical grade to minimize blank metal contents. The reagent blank must be less than the lower limit of quantification in order to be used:

- Concentrated ultrapure MERK nitric acid (60% HNO_3) for trace analyses
- Ultrapure MERK hydrochloric acid (30% HCl)for trace analyses
- MilliQ water (18.2 MΩ) was used for sample preparation

All sample containers (plastic and glass) have been prewashed with acidified water (3% HNO_3).
Sample digestion procedure:
45 mL aliquot of a well-shaken, homogenized sample was taken using an appropriate volumetric measurement and transferred to a vessel equipped with a controlled pressure relief mechanism. Samples that are highly reactive or contaminated may require dilution. 4 ± 0.1 mL of concentrated nitric acid and 1 ± 0.1 mL of concentrated hydrochloric acid were added to the vessel in a fume hood (or fume exhausted enclosure). The addition of concentrated hydrochloric acid to the nitric acid is appropriate for the stabilization of certain analytes, such as Ag, Ba, and Sb and high concentrations of Fe and Al.
The vessel was placed in the Milestone ETHOS 1600 Microwave Digestion Labstation (Fig 22) and connected to temperature and pressure monitoring equipment to control the correct performance of digestion. This method is a performance-based method, designed to achieve or approach consistent leaching of the sample through achieving specific reaction conditions. The temperature of each sample rises to 170 ± 5°C in approximately 10 min and remains at 170 ± 5°C for 10 min.

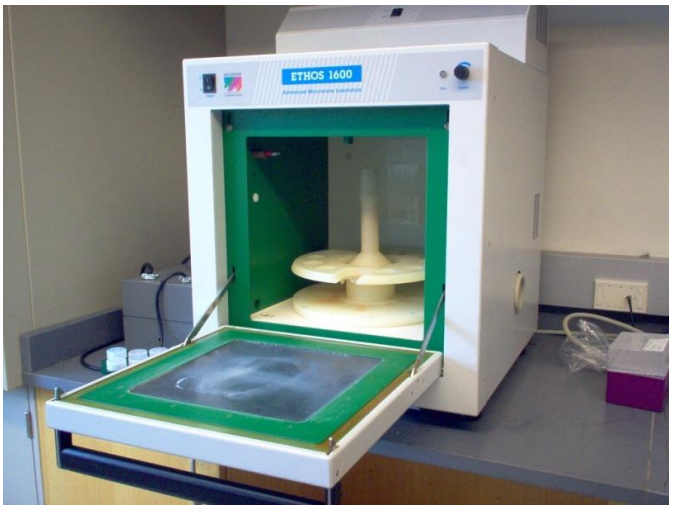

Figure 22Milestone ETHOS 1600 Microwave Digestion Labstation

Inductively Coupled Plasma Mass Spectrometry (ICP-MS)

Trace element analyses were carried out with an Agilent 7500 ce ICP-MS ORS technology (using collision cell technology). Li, Be, B, Al, Si, V, Cr, Mn, Fe, Co, Ni, Cu, Zn, As, Se, Rb, Sr, Mo, Cd, Ba, Tl, Pb and U were analyzed according to Wilbur and Soffey (2004). All determinations were performed with an external standard calibration method, using Y and Tb as internal standards. ICP-MS Agilent. The 7500ce ICP-MS uses an Octopole Reaction System (ORS) to eliminate interferences arising from the plasma and sample matrix. The ORS works in three ways:

- "No gas" (or norm) when cell's use is not required for one specific element which doesn't suffer spectral interference;
- "H2 gas"
- "He gas".

The octopole ion guide is contained within the ORS cell, which can be pressurized with helium or hydrogen gas. The ORS is positioned between the ion lens assembly and the quadrupole mass filter. As ions from the sample enter the cell, they interact with the gas, resulting in the reduction of the molecular interference by processes described below.

Helium mode:

1 collisional induced dissociation (CID) the polyatomic interference bond energies are lower than the collision Energy between the He atom and interference. CID is limited to polyatomic species with low bond energies such as $ArNa^+$ and ArO^+

2 Kinetic Energy Discrimination (KED) the larger polyatomic species (greater ionic radii) collide more frequently with the cell gas, they lose more Energy than the smaller analyte species, and can be prevented from entering the quadrupole by a positive potential step at the cell exit, effectively the cell acts as a molecular filter by resolving low Energy (polyatomic) and higher Energy (analyte) ions from each other in the ion beam.

3 the Agilent Shield Torch System produces ions with narrow Energy spread, which makes interference removal by KED very efficient. This allows for effective operation in He collision mode.

Hydrogen mode

1 Charge Transfer an electron is transferred from neutral hydrogen to interfering ion, resulting in a charged H ion and a neutral interfering species, which is system not focused through the analyzer and so disappears from the mass spectrum

2 Proton Transfer a proton is transferred to or from the interfering species, removing it from the analyte mass. Typically the new species has low Energy and is lost through Energy Discrimination processes.

Hydrogen reaction processes are quite specific and mostly target argon-based polyatomic species, such as Ar^+, Ar/Ar^+ and ArO^+, but are also effective in removing backgrounds due to other species, such as N_2.

ICP-MS mode for each element measured is reported in annex.

7.1.3. Rainfall

Amount of daily rainfall was collected to evaluate recharge rate of aquifers in study areas.

Three meteorological stations were detected near Roccamonfina Volcano:

- Weather station placed in ENEL pumped – storage hydroelectricity station in Presenzano Town
- Weather station placed in Ferrarelle mining area near Riardo Town
- Weather station placed south Presenzano Town managed by Agriculture department of Campania Region.

Figure 23 Ubication of detected weather stations.

Significant anomalies came from the comparison of collected data. In fact there were differences on distinction of rainy days and on quantification of daily rainfall also between nearby weather station. Therefore a weather station was installed on the roof of a house in Tora Town (Fig 19) according to World Meteorological Organization (WMO) guideline. This station is composed by a Hellmann type rain gauge Siap TP – 500 with a cylindrical body shape with a 500 cm^2 funnel area, an internal data logger and a digital thermometer

Figure 24 Rain gauge installed in Tora Town

On the contrary, several weather stations were detected in the northern sector of Vulsini Mount. Meteorological data were collected from three databases:

- Data of Proceno and Bagnoregio Towns weather stations were taken from Hydrographic Service of Latium Region database (Regione Lazio 2013)
- Data of Allerona Town and Orvieto Town weather stations were taken from Consorzio di Bonifica Val di Chiana Romana e Val di Paglia database
- Data of Allerona Town, Orvieto Town and Orvieto Scalo Town weather stations were taken from Hydrographic Service of Latium Umbria database (Regione Umbria 2013).

Rainfall data recorded (Fig 20) in these dataset do not show significant differences, especially data about Orvieto Town show great homogeneity then great reliability, hence there was no need to install a station.

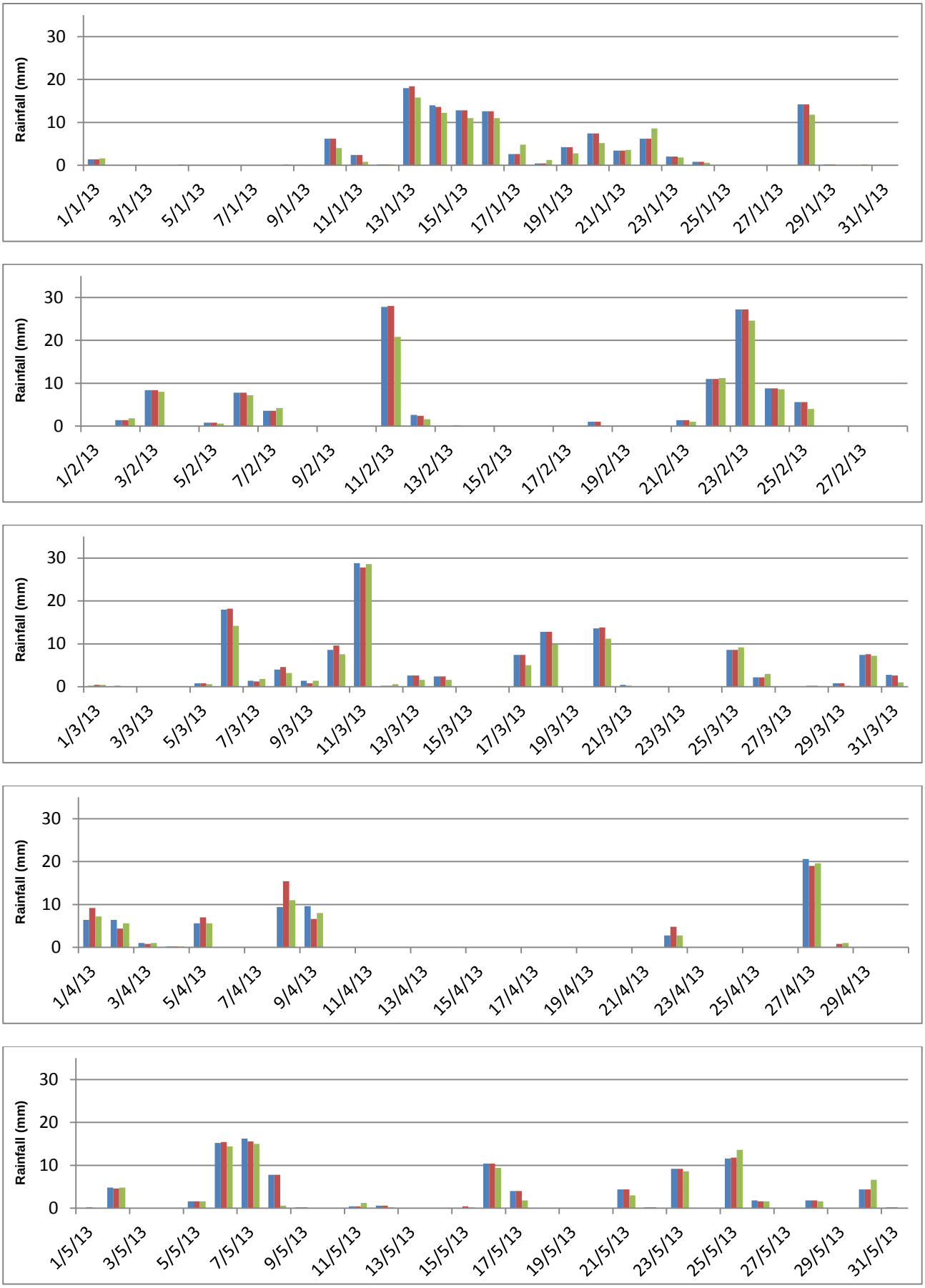

Figure 25 Rainfall data about Orvieto Town Weather Station (Consorzio di Bonifica Valdichiana e Val Romana) in blue, Orvieto Town (Regione Umbria 2013) in red and Orvieto Scalo (Regione Umbria 2013) in green.

7.2. Discussion

7.2.1. Discussion on Vulsini monitoring area

A restricted area was selected to realize a detailed hydrogeochemistry monitoring in Umbrian sector of Vulsini. Some considerations have been made to choose the most significant monitoring area. At first wells or boreholes were discard as possible monitoring point because they are a possible way of water mixing from different aquifers, then some springs ascribable to the basal aquifer cannot be used as survey points too. In fact some mixes at the front of volcanic plateau with shallow aquifers can contaminate basal springs. Therefore the promontory west to Rocca Ripesena Village was chosen as study area. At the front of this promontory there are four springs (RR1, RR2, RR3 and RR4) located at an altitude of about 400 meters a.s.l. corresponding to the outcropping of a shallow aquifer. The basal aquifer flows through a fountain (RR5) 60 meters under the shallow springs at an altitude of about 340 meters a.s.l. (Fig 26).

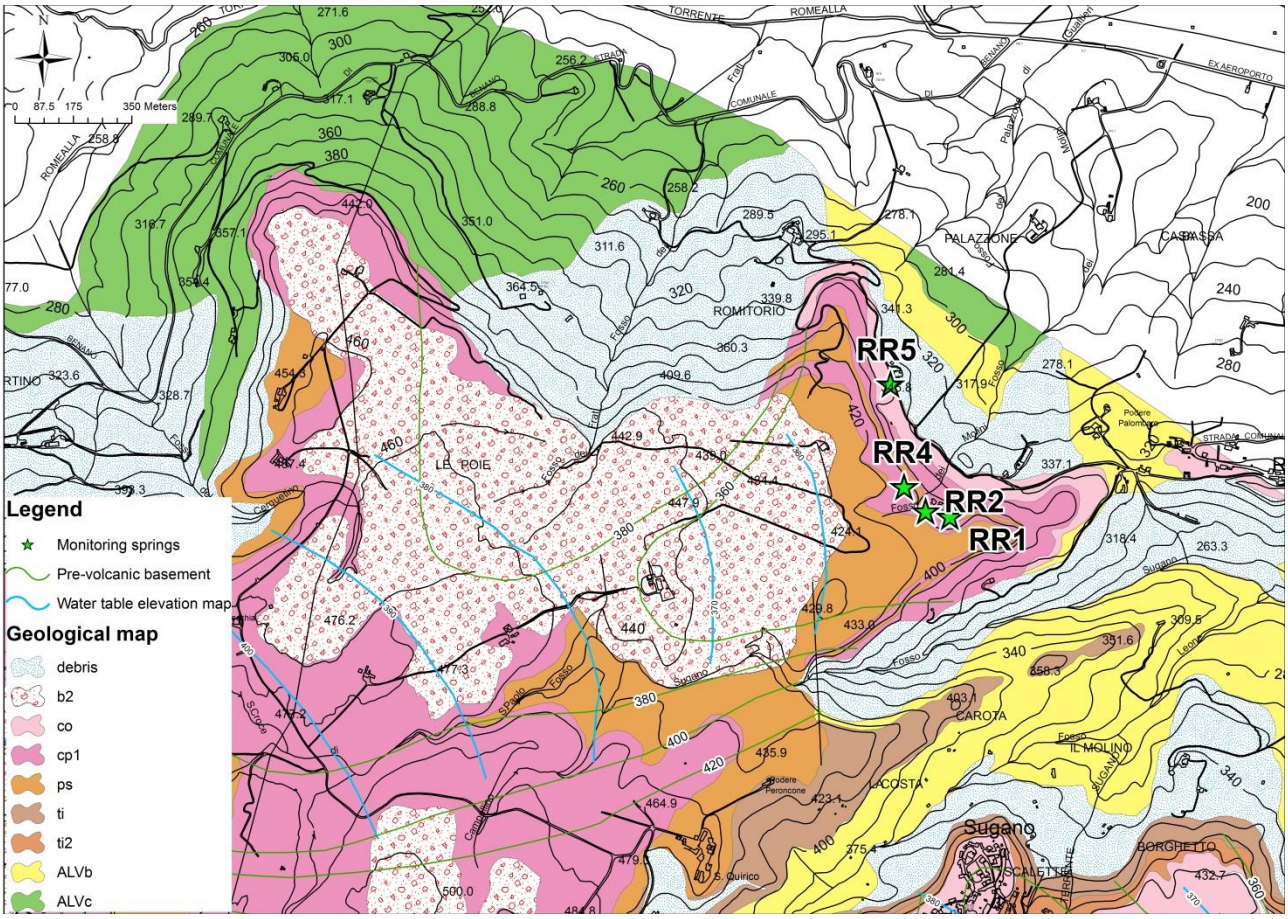

Figure 26 Location of monitoring springs. Legend: marine sand, silt and clay (ALVb, ALVc) Chiani –Tevere Syntem; Tione Formation: pyroclastic deposits (ti) and lava (ti2); Corsica Formation: pyroclastic layered deposits (co); Podere Sambuco Formation: pyroclastic layered deposits (ps); Case Perazza lava (cp1); Colluvium (b2); debris deposits (debris).

In this area the intermediate aquiclude is probably intact; in fact the shallow springs appear turbid, meanwhile clear uncontaminated water flows from the fountain. This

hydrogeological setting allows the monitoring of the two overlapping aquifers and their relationship in a restricted area.
The study area was investigated by means of 10 weekly springs discharge measurements, chemical-physical parameterization and water sampling, in the period March - September 2013 (Tab. 1).

Sampling letter	**Date**
A	28/03/2013
B	04/04/2013
C	11/04/2013
D	18/04/2013
E	30/04/2013
F	10/05/2013
G	16/05/2013
H	28/05/2013
L	28/06/2013
M	13/09/2013

Tab 1 Monitoring dates

Monitoring point RR3 was collected during the first four samples, and then it was left since it flows into RR4 sampling point.
Electrical conductivity, pH and temperature were collected. During this monitoring it was not possible measure Eh data due to problems with Eh probe. We can consider the Eh value for these samples greater than 0 because the monitoring points are located some meters far from the springs. This hypothesis is confirmed by bibliographic analysis with Eh detected value higher than 160 mV (Sii – ATI4, 2011).

Figure 27 Sampled springs: A) RR1; B) RR2; C) RR4

It was not possible to measure RR1 and RR2 flows separately because the thickness of the discharge channel was insufficient for used current meter; so flow measurements were made after the confluence of the two channels (Tab. 2).

Sampling letter	RR1 + RR2 (l/s)	RR4 (l/s)
A	23.4	15,65
B	22	18.5
C	25	20
D	23.5	18.3
E	25	19.17
F	23.7	24.9
G	n/a	n/a
H	24.3	25
L	21.2	11.1
M	11.21	10.9

Tab 2 Discharge rates of RR1, RR2 and RR4 springs

Flow measurements show fairly constant values in the first part of the monitoring (March – May) whereas the discharge of the shallow aquifer clearly decreases only during the dry season (June – September) when springs are recharged only by a perennial shallow aquifer.

Discharge of RR5 fountain were measured using volumetric method due to its low and concentrate flux; the results are report in Tab. 3.

Sampling letter	A	B	C	D	E	F	G	H	L	M
Q (L/s)	n/a	0.17	0.25	0.2	0.15	0.25	n/a	0.3	0.05	0.16

Tab 3 Discharge rate of RR5 spring

There are no significant differences between shallow springs discharge measured in September 2013 (about 22 L/s) compared with the bibliographic data (19 L/s) about a hydrogeological survey realized during 2011(ATI4-Sii 2011). The discharge rate of RR5 spring still remains at about 0,1 L/s

These data confirm a general conservation of groundwater settings, according to the water table elevation model already described in Hydrogeological survey 2013 chapter (page 13)

A spring related to a different shallow aquifer was added as sampling point (CAN) starting from the monitoring date “E”. Water has been collected in an ancient public laundry in Canonica Village. This external point allows comparing the variability in chemical composition of dissolved ions and suspended solids in waters of similar aquifers.

Data of chemical composition of all filtered and unfiltered samples are reported in Tab. XX in annex. Ion concentration less than 1 µg/L were report as “n/a”. Negligible differences in metal concentration were detected from the comparison between data obtained from 0,45 µm filtered samples and from 0,20 µm filtered samples, as confirmation of their ionic behavior. Whereas quantities of aluminum, iron, barium and manganese vary depending on filtered and unfiltered samples, in fact their concentration strictly decrease in relationship with the pores size of filters.

Some metals (Cu, Ni and Zn) were detected only in some unfiltered samples; the sources of these contaminations are still uncertain likely related to solids collected during the sampling. Therefore these data have not been taken in consideration for this research.
It was possible to determine the hydrogeochemistry facies of groundwater in the surveyed area from March 2013 to June 2013. Plotting the data in a Ludwig - Langelier Diagram, based on the relative proportion of major ions
The Ludwig Langelier Diagram (Fig 28) shows how all water samples are characterized by an intermediate facies between alkali bicarbonate and alkali – earth bicarbonate composition with a relative Ca^{2+} - Mg^{2+} increasing. RR5 and CAN samples show different results from Rocca Ripesena shallow aquifer (RR1, RR2, RR3, RR4), therefore seems to be confirmed the belonging of three different aquifers. The composition of these waters shows a relative higher concentration in Mg^{2+} and in Ca^{2+} compared to the characteristic facies of volcanic groundwater related to aquifer rock composition. Measured springs show low variations in chemical composition then it's confirmed that study hydrogeological systems belong to Vulsini volcanic deposits and there aren't water input from external systems.

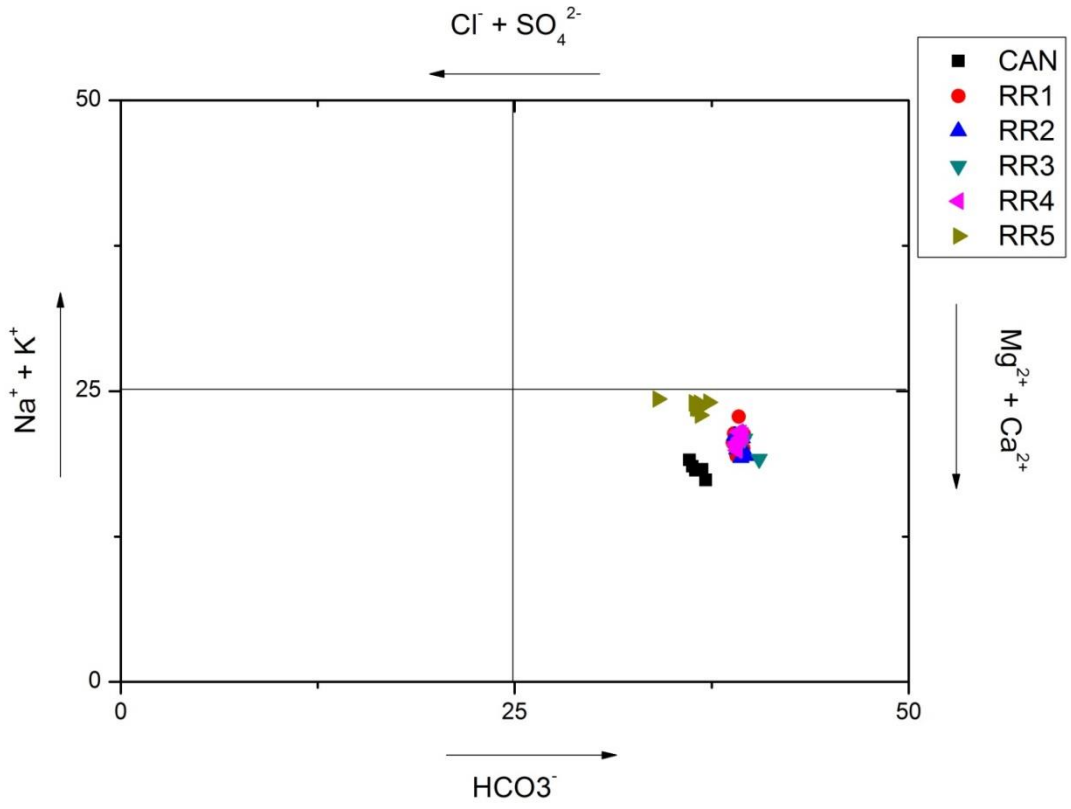

Figure 28 Ludwig Langelier diagram

Another important observation is about Na and K concentration in the sampled aquifers. In fact, the Na/K ratio close to 1 is typical of groundwater mineralization processes in silicate–volcanic rocks of the Campania-Lazio volcanic areas (Fig 25) (Chiodini and Frondini 2001).

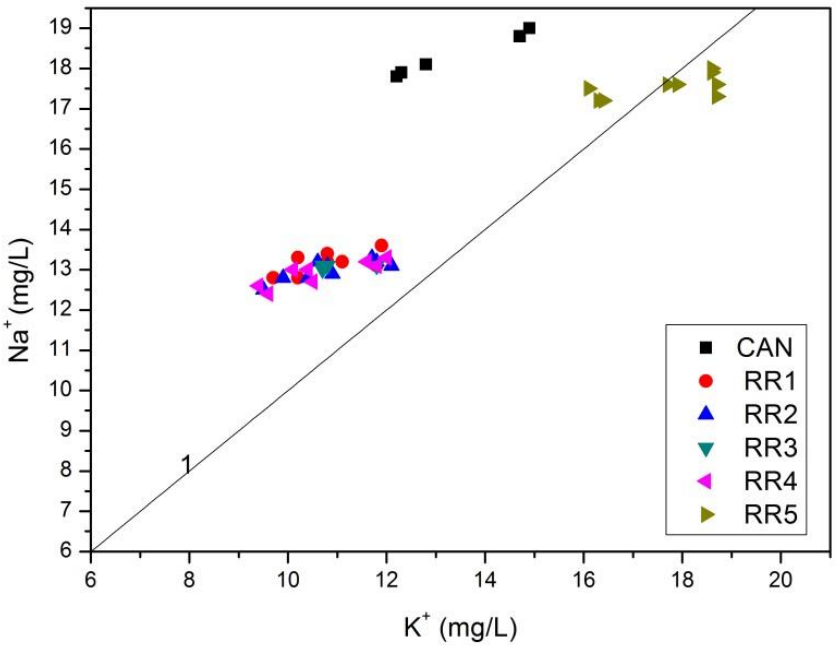

Figure 29 Na – K graph

This graph, according to Ludwig Langelier diagram, confirms the absence of mixing between volcanic aquifers and groundwater coming from external systems (i.e. sedimentary one). It evidences some small geochemical differences between the three sampled aquifers (Rocca Ripesena shallow aquifer, Canonica shallow aquifer and basal aquifer) constant in time. Detected Na^+ and K^+ fluctuations in the time are about in the order of magnitude of 2 mg/L, more likely related to solute concentrations in less rainy periods. Detected R^2 between Na^+ and K^+ is 0.6, and then their enrichment in circulating waters is depending on interaction with host rock. Temporal fluctuations of Na^+ and K^+ concentrations and rainfall amount are reported in diagrams (Fig. 30) where the increasing of alkali ions can be observed in low rainy periods. This figure shows the same mineralization processes for RR1, RR2 and RR4, while RR5 has a different behavior and different Na/K ratio due to its different alimentation basin if compared to shallow aquifer in the same area. In the Fig .30 alkali ions concentration are compared to rainfall data. K is more sensible to water rock interaction than Na, in fact sodium concentration depending on several enrichment factors as rain chemical composition and soil leaching whereas potassium concentration depends especially on water-rock interactions. In fact in the Fig.30 could be observed a general decreasing trend in alkali ions concentrations with rain increasing absolute concentrations of alkali ions tend to decrease, potassium concentration is characterized by higher variability due to dilution effect of rain and to lower residence time of water in the aquifer. On the contrary the higher K concentrations have been detected in less rainy period. Sodium and potassium concentration slight change in the RR5 samples because the chemical composition deeper aquifer was not quickly affected to the rainfall than the shallow aquifers. Na concentration in slightly higher if compared to K^+ due to its original quantity in fresh rainwater and then the Na/K ratio becomes slightly higher in rainy periods. Volcanic rocks-water interaction brings alkali ions,

in particular K+, in solution Described process drives all natural mineralization processes, and then salinity (i.e. electric conductivity and consequently, the ionic strength) of studied groundwater depends on rainfall quantity.

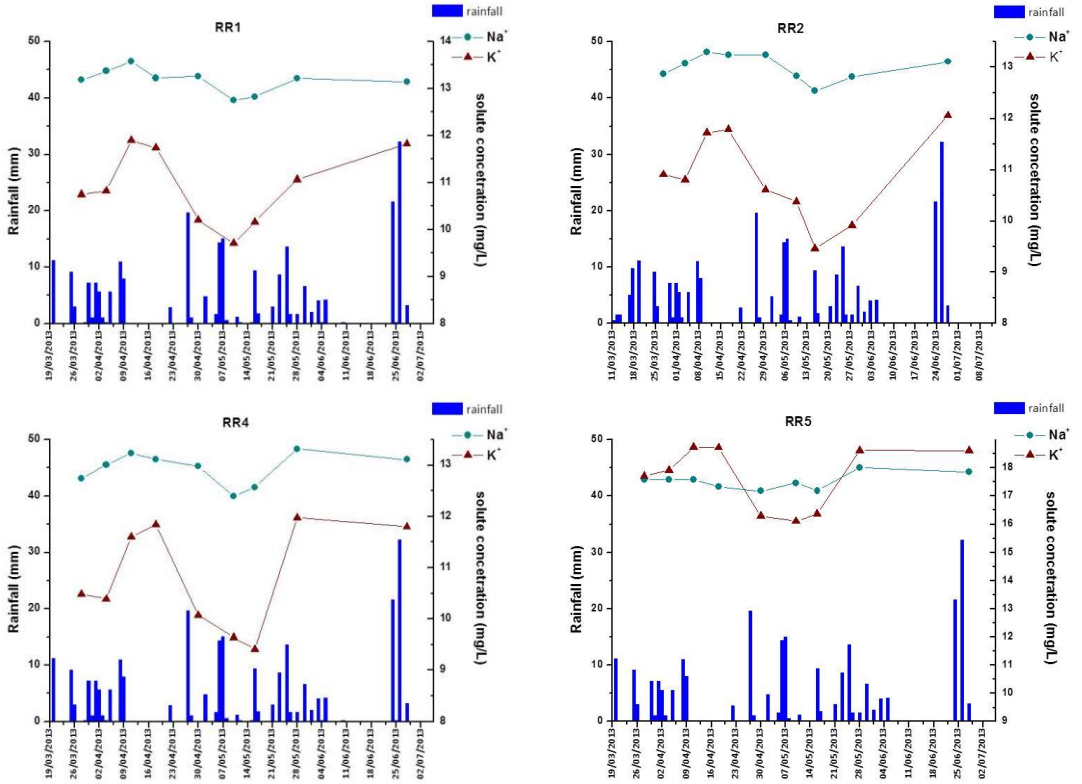

Figure 30 Na and K concentration in RR1, RR2, RR4 and RR5 samples

Correlation between the normalized electric conductivity (E.C.) and chlorine in Fig 26 is indicative of groundwater residence time then water – rocks interactions. Chloride concentration, as suggested by Celico (1988), should be the element to estimate the residence time of waters due its conservative behavior in solution.

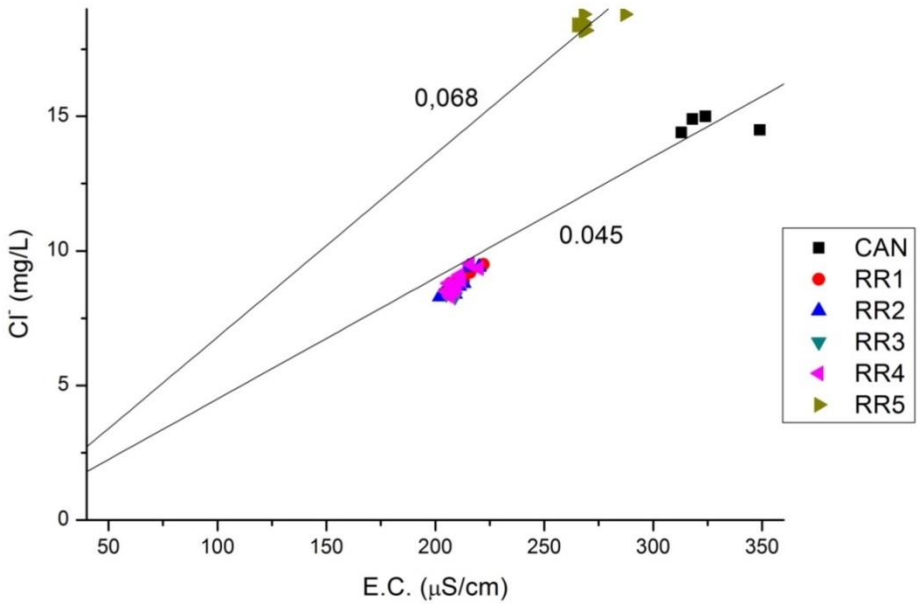

Figure 31 Electric conductivity – Cl graph

Here again may be observed the chemical evidence of RR5 belonging to a different, deep aquifer. All samples collected from a shallow aquifer have a Cl/EC ratio of about 0.045, while the deep aquifer (RR5) attains a value of 0.068. In fact these samples are characterized by higher concentration of chloride related to longer residence time of groundwater and a lower quantity of human contaminants than shallow springs. Samples collected in Canonica (CAN) show higher value of mineralization than Rocca Ripesena shallow springs (RR1, RR2, RR3, RR4 and CAN), probably due to a more extended hydrogeological basin and to a significant contribution of NO_3^- and SO_4^{2-} pollution. Moreover higher alkali earth ions and bicarbonate concentration has been detected in CAN samples. These results have been related to a different lithology of CAN hydrogeological basin compared to shallow Rocca Ripesena one.

Cl/EC ratio of basal aquifer collected in Rocca Ripesena (RR5) is higher (0,068) than shallow aquifers one. In fact these samples are characterized by higher concentration of chloride related to longer residence time of groundwater.

High concentrations in aluminum and iron were detected in unfiltered samples of shallow aquifers. These elements are not in solution according to pH and to the oxidant conditions detected in field and they are the cause of the turbidity of water. A strong linear relationship correlates Al and Fe (Fig 27) then the enrichment in these two elements probably depends to the same natural process.

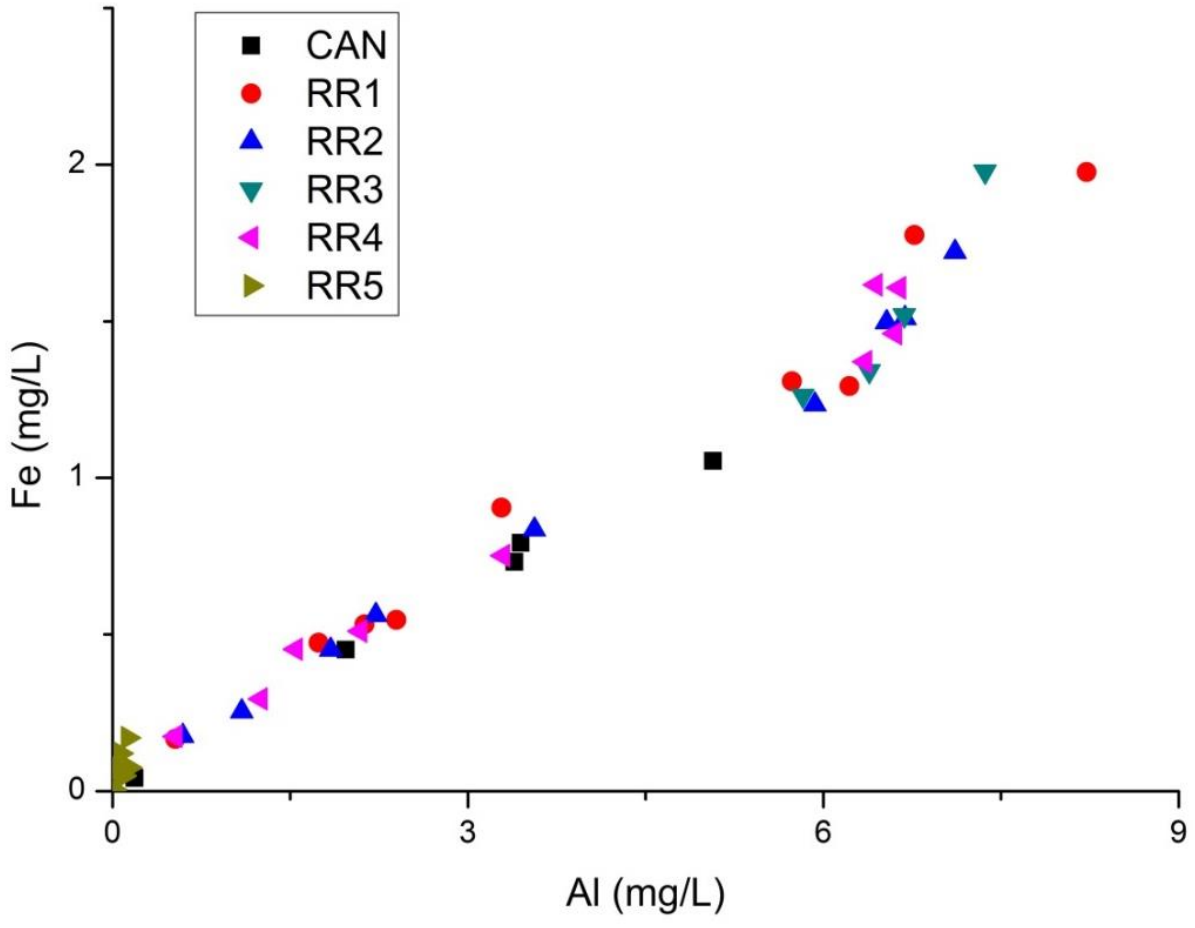

Figure 32 Relationships between Al and Fe

Aluminum and Iron cannot be mobile at measured pH values (Stumm and Morgan 1996). This observation together with their correlation suggests that Al and Fe concentration in the samples are related to suspended solids.
The histogram in Fig. 33 represents Al concentration in unfiltered samples (blue bars), in 0,45 μm filtered samples (red bars) and in 0,20 μm filtered samples (green bars), collected during the monitoring. The percentage of filtration efficiency allow to evaluate colloids size; in fact 80 – 90 % of aluminum particles were hold by 0,45 μm filters, whereas 0,20 μm filters usually hold almost the entire colloids. Therefore particle size between 0,45 and 0,20 μm were approximately between 10 and 20%.
There are not significant variations in colloids size classes during the monitoring and the scarce differences in filtration efficiency could be ascribe to analytical or sampling procedures.

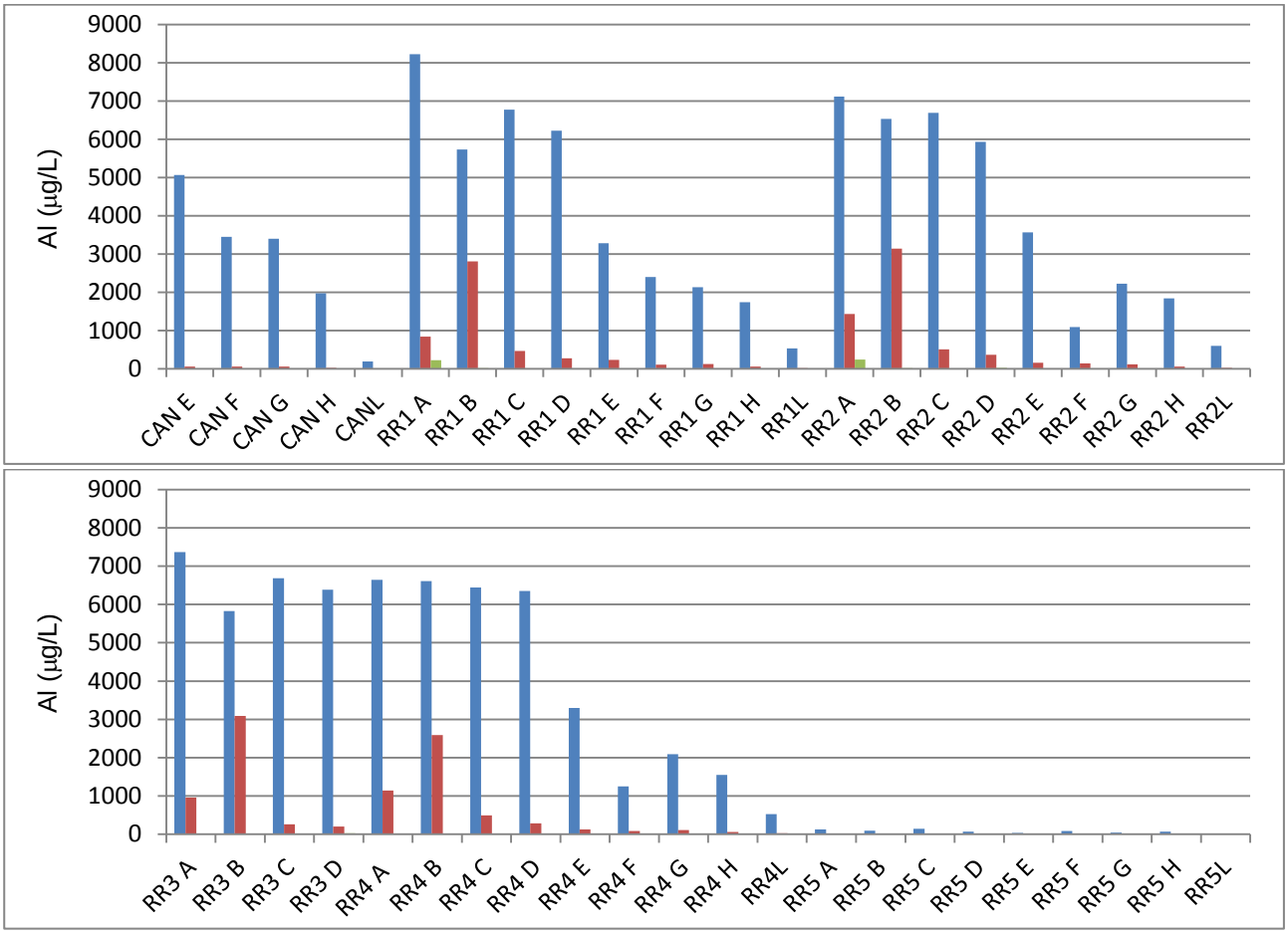

Figure 33 Al concentration in unfiltered samples (blue), in 0,45 μm filtered samples (red) and in 0,2 μm filtered samples (green)

The variability of Iron and aluminum concentration is similar with a constant ratio Al/Fe about 4,2. Iron detected in water samples is in colloidal phase as suggest by Eh-pH stability diagrams (Stumm and Morgan 1996). The linear correlation between Al and Fe concentration in unfiltered samples is confirmed in filtered samples too. Filtration efficiency on Fe is the same as calculated for Al concentration data (about 80 – 90 % using 0,45 μm filters and about 100% using 0,20 μm filters)(Fig. 34). The similarity in aluminum and iron behavior to filtration confirms that these elements constitute the same solid phase.

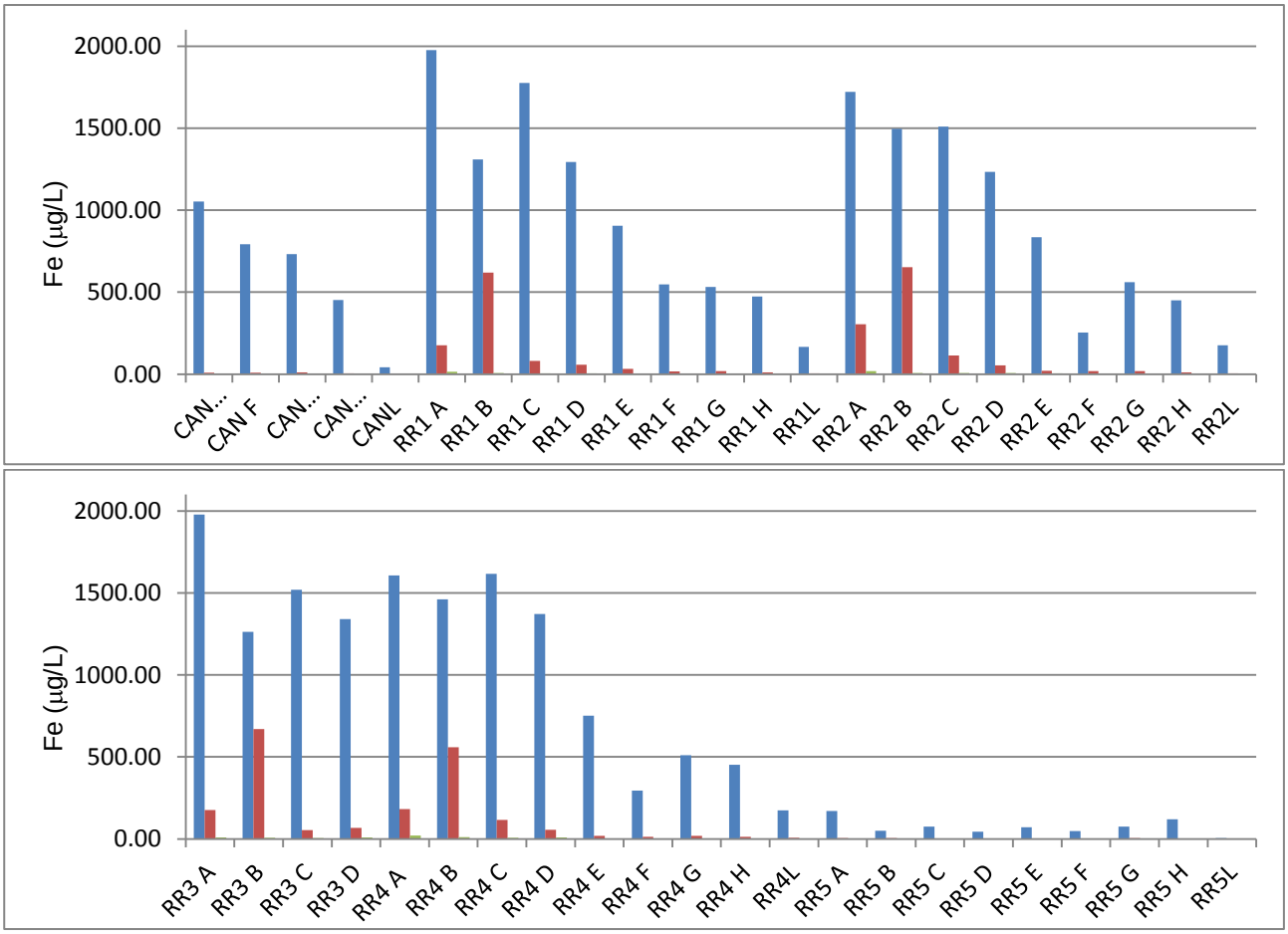

Figure 34Fe concentration in unfiltered samples (blue), in 0,45 µm filtered samples (red) and in 0,2 µm filtered samples (green)

Figure 35 shows variability in aluminum concentration during monitoring period.
Shallow springs are characterized by high concentration in Al (> 5000 µg/L) in the first four monitoring corresponding to the wettest period of the year (5 March – 9 April). This interval is characterized by 27 rainy days with a mean height of daily rainfall of 4,7 mm/d (Regione Umbria 2013). A pronounced reduction in aluminum concentration was detected from “E” monitoring depending on the rainfall occurrence and intensity. In fact from April to June mean rainfall data is about 2.2 mm/d in 27 rainy days in three months.
RR5 samples contain a lower concentration in aluminum which could be ascribed to water rich in colloids percolation from shallow to basal aquifer due to the presence of several not isolated wells and/or natural aquiclude discontinuities. For this reason variability of aluminum concentration in the basal aquifer is not related to rainfall data.

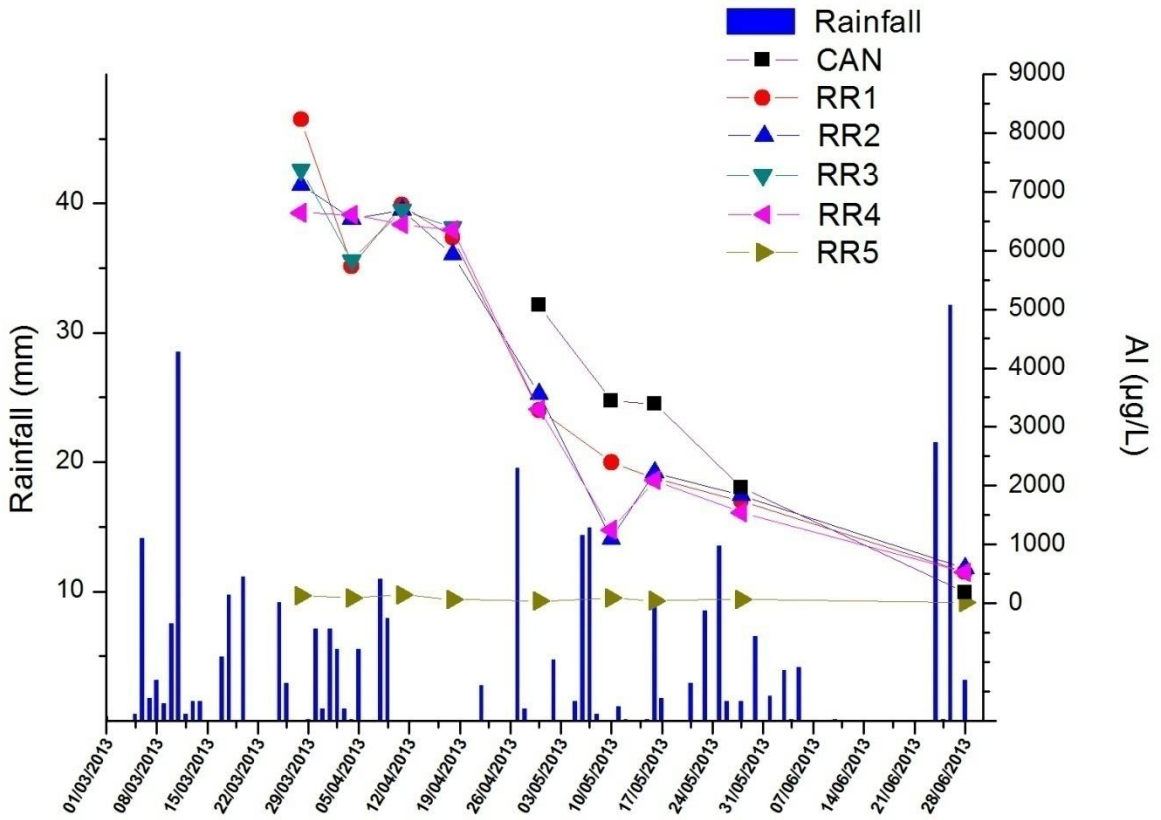

Figure 35 Aluminum concentration compared to rainfall data

Several authors (Ryan and Elimelech 1995, Schelde et al. 2002, Poulsen et al. 2006, Galvez et al. 2008, Deepagoda et al. 2011) described the relationship between rainfall rate and colloids mobilization realizing mathematics leaching models. These models could not be applied to the present study due to a different scale approach. In fact cited bibliographic works used experimental data obtained by leaching analyses on small size soil samples. Whereas springs recharged in a 6km^2 basin were analyzed in this research. Therefore different residence time of groundwater do not allows detailed relationship between daily rain amount and colloids concentration in water.

Concentrations of trace metals in solution are affected by adsorption onto solid particulate (Drever 1997). Adsorption occurs when a dissolved ion or molecule becomes attached to the surface of a preexisting solid. Most colloids possess amphoteric surface charge. The surface charge is strongly dependent on solution pH, because the minerals surface exchange protons with the solution. In general amphoteric minerals are positively charged at lower pH and negatively charged at higher pH values (Ryan and Elimelech1996). Therefore aluminum and iron colloids influence concentrations of trace metals deriving from rock leaching. This dynamics is depending on specific adsorption equilibrium. Barium and Manganese are strongly affected by adsorption on suspended solids, and then they have been chosen as representative of this geochemical process.

Barium is an element strictly correlate to Al and Fe behavior ($R^2 = 0.87$) in shallow aquifers but with lower concentrations. Barium concentration depends on filtration in fact it's lower in filtered samples than in unfiltered ones; whereas no significant differences were detected in barium concentration in 0,45 µm to 0,2 µm filtered samples (Fig 36). Barium is

always in ionic form at oxidant conditions according to pH – Eh graph different to Al and Fe, so the decreasing in concentration through the filter probably depends on adsorption phenomena on colloid particles.

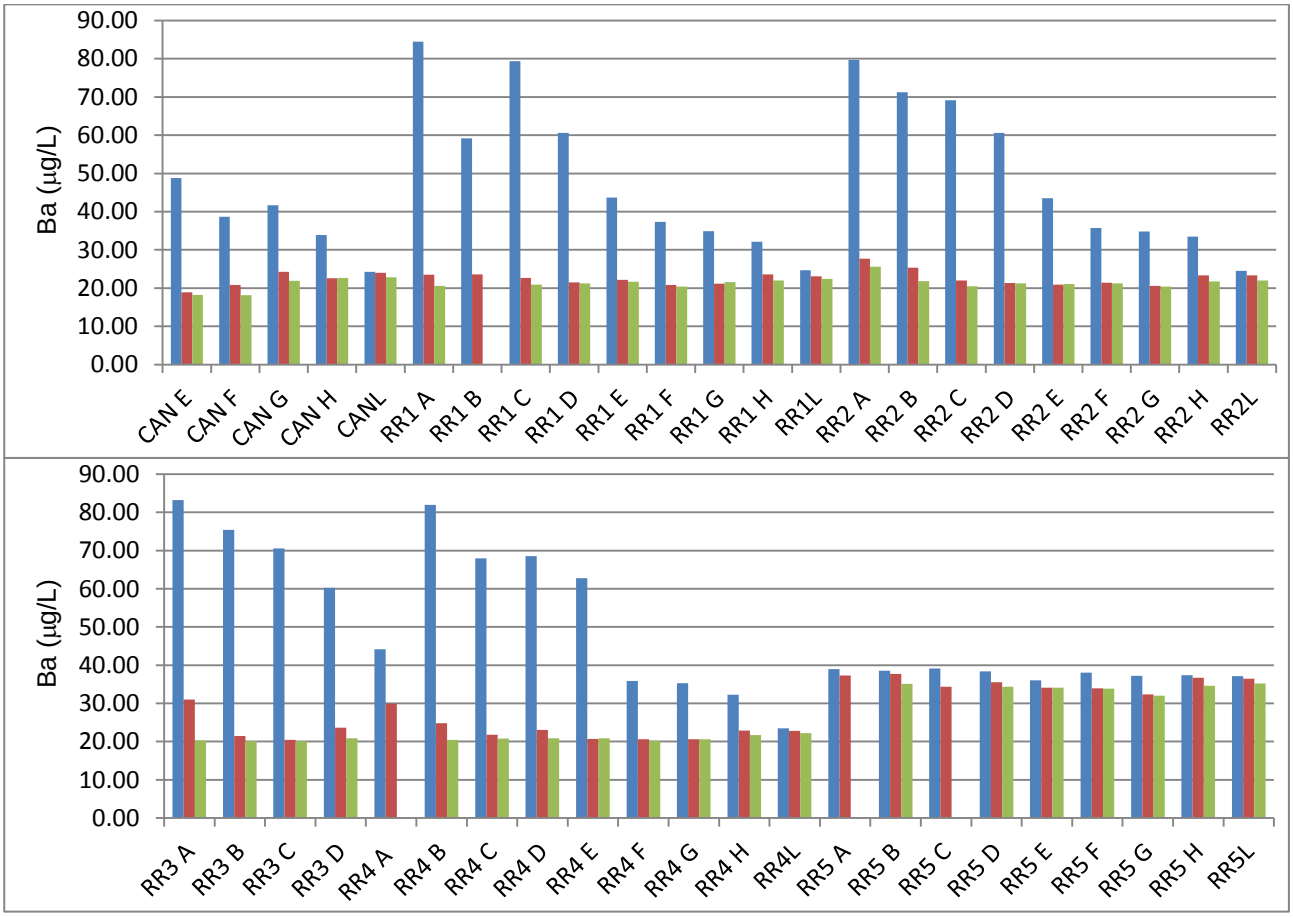

Figure 36 Ba concentration in unfiltered samples (blue), in 0,45 µm filtered samples (red) and in 0,2 µm filtered samples (green)

The same process affected the Manganese concentration too (Fig 37), in fact manganese in unfiltered samples is stricltly correlate with Aluminum and Iron concentration (mean R^2 = 0.96) whereas Mn concentration was reduce up to zero in filtered samples.

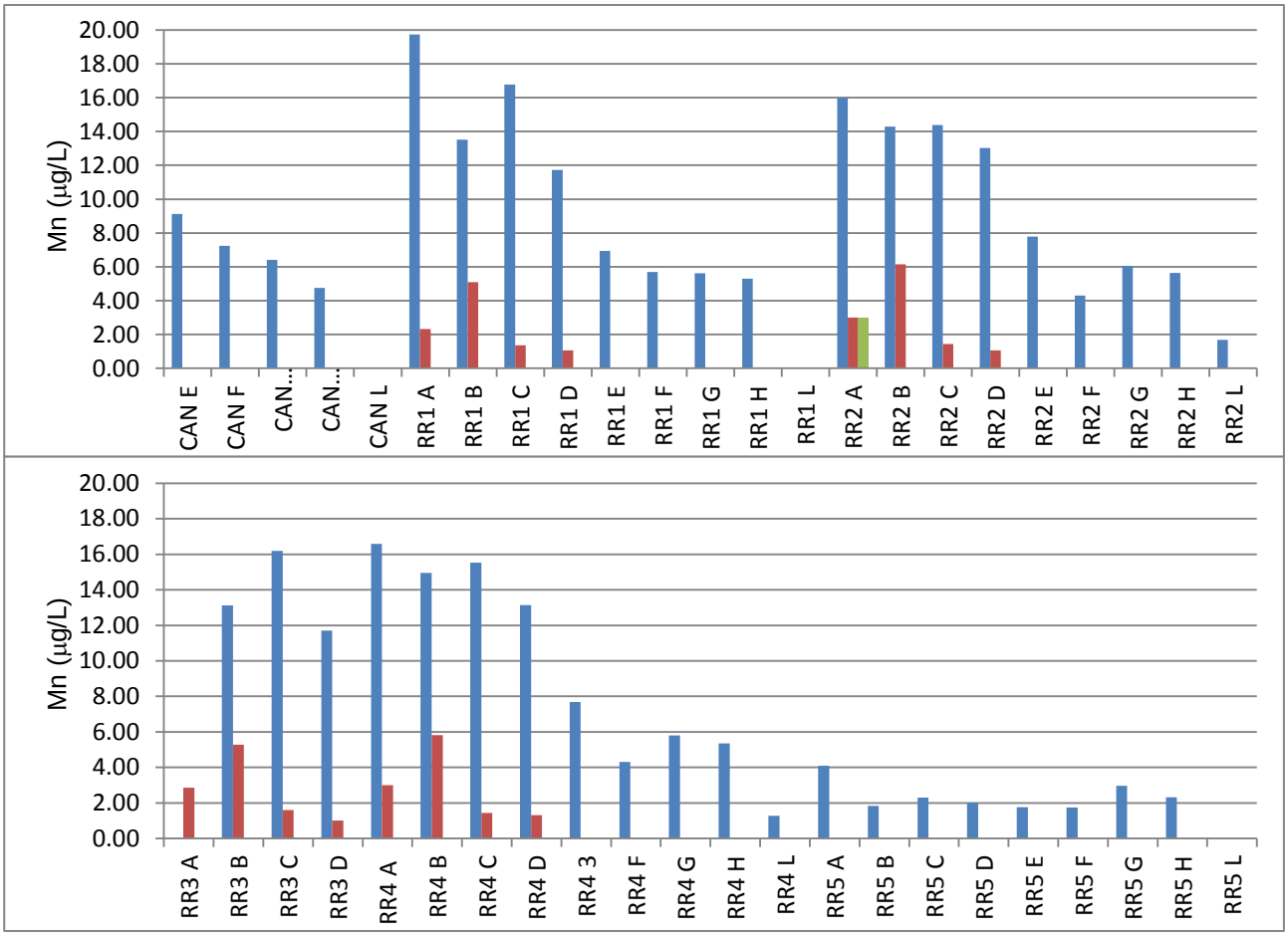

Figure 37 Mn concentration in unfiltered samples (blue) in 0,45 µm filtered samples (red) and in 0,2 µm filtered samples (green)

Manganese should be in ionic phase like Barium according to pH – Eh stability graphs so its occurrence could be related to adsorbion processes on colloidal particles (Aiuppa et al. 2000).The basal aquifer is characterized by higher mineralization and absence of suspended colloids so barium in RR5 samples is always in solution (no significant differences between filtered and unfiltered samples) and its concentration is higher than in shallow aquifers.

Principal Component Analysis

Principal Component Analysis (PCA) was carried out to point out the relationship between the water parameters and their variability. Multivariate statistical analysis is typically used to identify the various sources of components and their chemical behavior in studied water system. Factor analysis is used on the variance matrix of multivariate data, as a geochemical dataset, allowing analysis within a set of variables (Davis 1986).Chemical variables (analyzed parameters) governed by the same geochemical processes fall within the same factor. The extraction of several independent factors allows identification and separation of the various processes controlling the geochemical composition of the controlled waters (Cuoco et al. 2013)

The number of components to keep was based on the Kaiser criterion, for which only the components with eigenvalues greater than 1 are retained. As a result, all components that contain a greater variance than the original standardized variables are kept (Davis, 1986). The first three components extracted from the whole dataset have eigenvalues greater

than 1, and account for 91% of the total variance in the dataset. To maximize the variance of the first five principal axes, the Varimax normalized rotation was applied
Tab.4 presents the principal component loadings for these three components. Loadings, that represent the importance of the variables for the components, are in bold for values greater than 0.7

Parameters	Component 1	Component 2	Component 3
T	0,50	-0,07	**0,69**
EC	0,38	**0,88**	0,21
pH	0,42	-0,52	0,27
HCO3	0,46	**0,77**	0,33
F	**0,89**	-0,13	0,37
Cl	**0,82**	0,44	0,32
NO3	-0,59	**0,77**	-0,19
SO4	-0,16	**0,98**	0,05
Na	0,65	**0,73**	0,17
K	**0,90**	0,29	0,25
Mg	-0,01	**0,97**	0,09
Ca	0,06	**0,95**	0,16
Al	-0,33	-0,20	**-0,90**
Fe	-0,30	-0,23	**-0,91**
Rb	**0,80**	-0,27	0,51
Ba	**0,87**	-0,04	0,16
B	**0,96**	0,01	0,14
Si	**0,89**	-0,07	0,25
Sr	0,06	**0,95**	0,21
V	**0,84**	0,44	0,23
Mn	-0,18	-0,26	**-0,91**
Var. Sp.	7,92	7,23	4,01
Prp.Tot.	0,38	0,34	0,19
Eigenvalues	10,86	6,49	1,81
Explained variance (%)	51,7	30,9	8,6
Cumulative % of variance	51,7	82,6	91,2

Tab 4 Principal components loadings calculated from the entire geochemical database

The first two components explain about 52% and 31% of the variance, respectively, whereas component 3 explains about 9% amount of variance. The distribution of significant parameters in components 1 and 2 is affected by the presence of different aquifers data. In fact significant parameters detected in the component 1 are related to basal aquifer mineralization whereas significant parameters of the second component are related to shallow aquifers dynamics. The aim of this analysis is the identification of the processes affecting the shallow aquifers of this area, therefore geochemical data related to

the basal aquifer were removed and a new multivariate statistical analysis was carried out using only data of shallow aquifers. Two important components were detected in this new analysis according with Kaiser criterion (tab. 5).

Parameters	Component 1	Component 2
T	-0,06	**0,79**
EC	**0,99**	0,09
pH	-0,62	0,13
HCO3	**0,94**	0,25
F	-0,61	0,49
Cl	**0,98**	0,09
NO3	**0,99**	-0,01
SO4	**0,98**	0,09
Na	**0,99**	-0,06
K	**0,76**	0,02
Mg	**0,97**	0,14
Ca	**0,95**	0,17
Al	-0,25	**-0,93**
Fe	-0,28	**-0,93**
Rb	-0,53	0,62
Ba	-0,32	**-0,87**
B	0,06	-0,41
Si	-0,15	0,15
Sr	**0,95**	0,21
V	**0,91**	0,05
Mn	-0,29	**-0,87**
Var. Sp.	11,33	4,90
Prp.Tot.	0,54	0,23
Eigenvalues	11,55	4,68
Explained variance (%)	54,99	22,32
Cumulative % of variance	54,99	77,31

Tab 5 Principal component loadings calculated from geochemical data of shallow aquifer

The two components calculated in this new analysis explain about 51% and 30% of the variance. Fig 32summarizes this information by showing the position of the loadings of chemical parameters in the plane defined by the axes of components 1 and 2 that explain the 81% of total variance. A descriptive term is defined for each of the first two components based on their characteristic loadings.

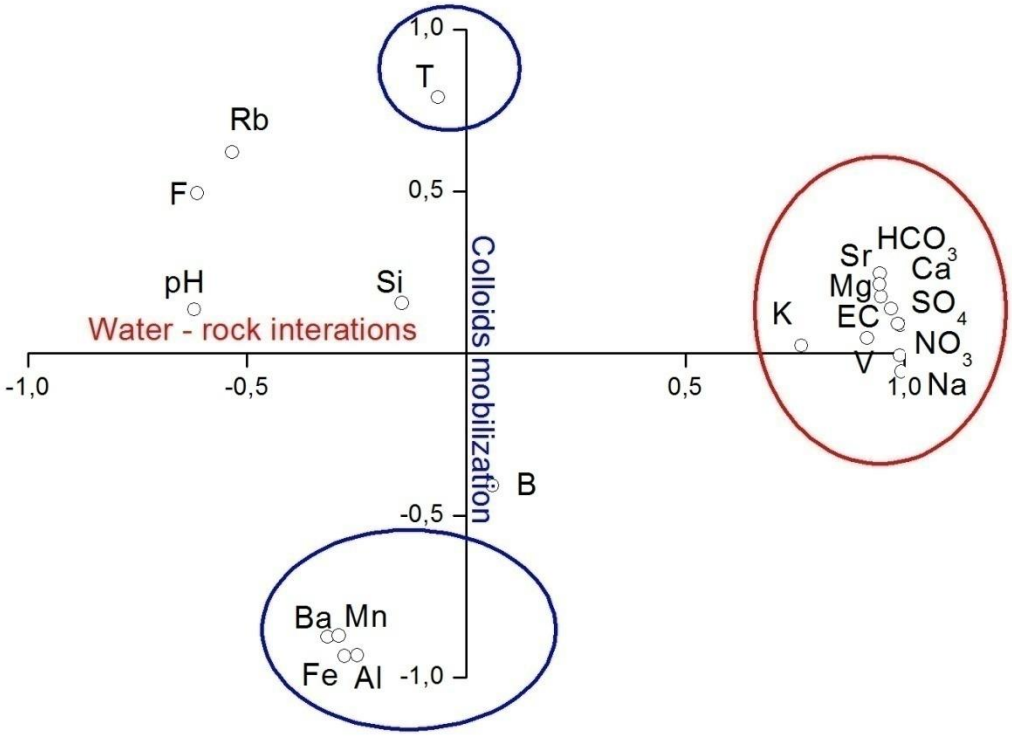

Figure 38 Display of first two components

Component 1 explains the greatest amount of the variance, and is characterized by highly positive loadings in EC, HCO_3^-, Cl^-, NO^{3-}, SO_4^{2-}, Na^+, K^+, Mg^{2+}, Ca^{2+}, Sr and V (Table). This component explains the enrichment of major ions in solution related to water – rock iteration processes.

Component 2 is characterized by highly positive loading in Temperature and negative loadings in total Ba, total Mn, total Al and total Fe. This component explains the colloid mobilization occurrence. Al, Fe, Mn and Ba concentrations were detected in unfiltered acidified samples in order to quantify the concentration of suspended elements and to evaluate their variability in time.

7.2.2. Discussion on Roccamonfina monitoring area

The second monitoring area of this work is the Rianale Stream Valley, near Tora and Piccilli towns on the NE slope of Roccamonfina Volcano. Rianale Stream is recharged during the rainy seasons by several springs along its channel characterized by white murky water with a lot of suspended solids. The first sampling site is nearby Tuoro Village at about 350 meters a.s.l.; where two sampled springs (S4 and S6) recharging Rianale Stream are detected. Their discharge was detected after their confluence (I5) (Fig 39).

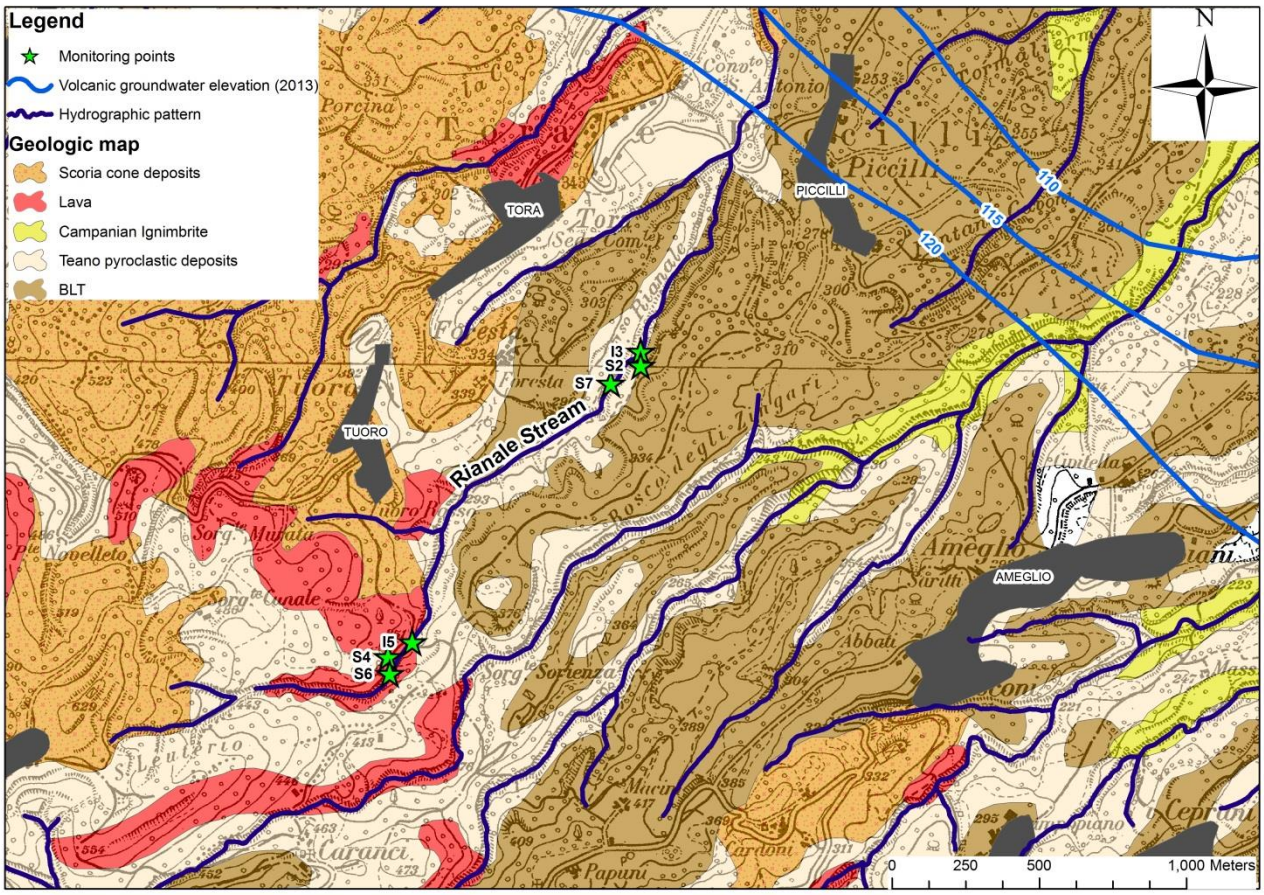

Figure 39 Sampled springs location, Geologic map modified from Servizio Geologico d'Italia (1971a, 1971b)

The second sampling site is downstream, 600 meters far from Tuoro and it's placed near Foresta Village at an altitude of 275 meters a.s.l. closeness to the paleontological site named "Devil's footprints" (Ciampate del Diavolo). A small spring (S2) was analyzed during the entire monitoring while S7 spring was detected only in the last survey because it was not visible since placed behind Rianale Stream waterfall. It was possible to identify it only when Rianale Stream went dry. Twenty meters downstream from the waterfall a surveyed point (I3) was defined to evaluate the Rianale flow rate and the chemical characteristics of stream water in the downstream sector of the study area. All sampled waters appeared murky (Fig. 40) during the entering sampling with a progressive decreasing in white visible suspended solid concentrations. The study area was investigated by means of 8 weekly measurements, identify by a letter (Tab. 6) from March 2013 to May 2013.

Survey letter	A	B	C	D	E	F	G	H
Date	08/3/13	15/3/13	08/4/13	17/4/13	23/4/13	02/5/13	08/5/13	24/5/13

Tab 6 Monitoring date on Rianale Stream Valley

Figure 40 Sampled springs A) S6; B) S4; C) S2 and D) I3

All monitoring points and their features were report in Tab. 7.

Name	Place	Elevation (m a.s.l.)	Type of measurements
S2	Foresta	275	IF + S + FM
I3	Foresta	270	IF + S + FM
S4	Forma	350	IF + S
I5	Forma	345	FM
S6	Forma	350	IF + S
S7	Foresta	275	IF + S

Tab. 7 Monitoring points in Rianale Stream Valley. Legend. IF: Temperature, electric conductivity, pH and Eh; S: Sampled; FM: flow measurements

All detected spring are recharged by restricted seasonal aquifers, in fact all spring discharge rate decrease to zero during the monitoring. Flow measurements were realized to determinate the discharge of S4 and S6 springs in Rianale Stream (I5) and the flow variance along the valley (I3) (Tab. 8).

Sampling letter	Q I5 (S4 + S6) L/s	Q I3 L/s
A	22,5	38,34
B	28,62	46,68
C	12,6	21,8
D	10,7	10
E	8,5	6,6
F	4,7	2
G	4,1	2,6
H	2 (estimated value)	2 (estimated value)

Tab. 8 Flow measurements along Rianale Stream

It's possible distinguish two different behaviors of Rianale flows (Fig 35): during the early surveys an increase in stream flow was detected from I5 to downstream I3. The increase of the flow is related to several rainy days before measurement dates. Part of the increased flow derived from some passing springs along the Rianale Valley or from runoff that occurs when the rate of rainfall on the ground exceeds the rate at which water can infiltrate the soil, and any storage has already been filled.
The second part of the monitoring in characterized by lower flows and Q I5 ≥ Q I3. These data demonstrate that Rianale Stream is recharged only by the springs detected near Forma (S4 and S6) and there aren't significant contributions from other aquifers.

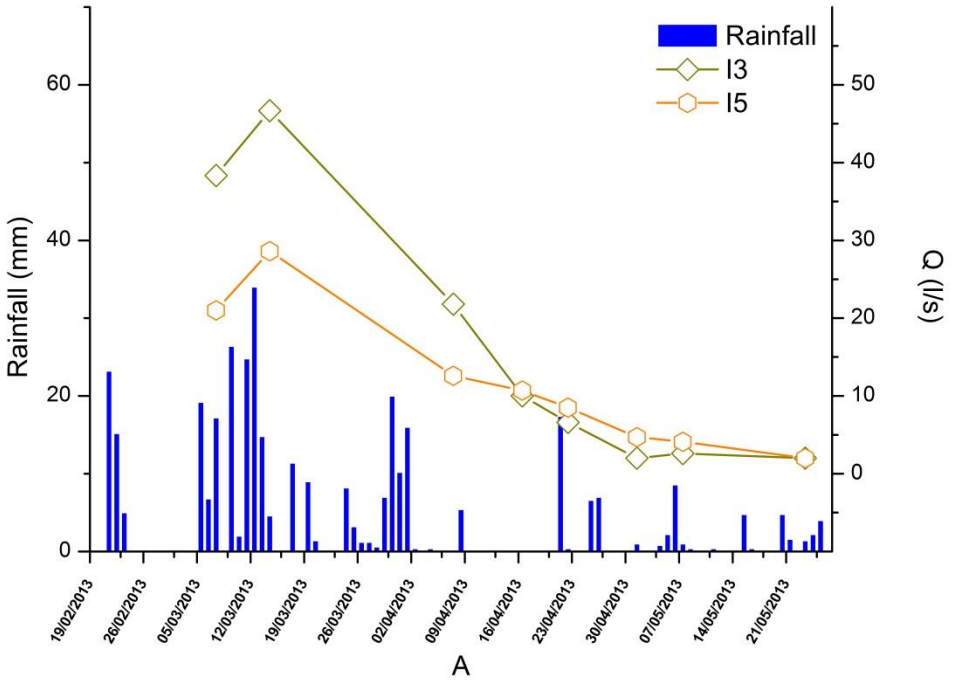

Figure 41 Flow discharge in Rianale Stream

S2 spring is characterized by low discharge (Q < 0,2 L/s) and it flows into Rianale Stream downstream to I3 monitoring point. This spring is recharged by an aquifer hosted in fractures of BLT lithic formation. The S2 discharge was measured using a volumetric method and the results are reported in Tab.9

Sampling letter	A	B	C	D	E	F	G	H
Q S2 (L/s)	0.14	0.17	0.05	0.04	0.02	0.016	0.015	0.012

Tab. 9 S2 spring discharge rate

Data of chemical composition of all samples are reported in Tab. XX in annex. Ion concentration less than 1 µg/L was report as “n/a”.
Some metals (Cu, Ni and Zn) were detected only in unfiltered samples in some monitoring; the sources of these contaminations are still uncertain probably related to solids picked up during the sampling. Therefore these data have not been taken in consideration for this research as occurred during the analyses of Orvieto samples.
Plotting the data in a Ludwig Langelier Diagram, based on the relative proportion of major ions, it was possible to determine the hydrogeochemistry facies (Fig 36) of groundwater in the study area surveyed from March 2013 and May 2013. Detected values show a slight variability in concentrations during the monitoring period.

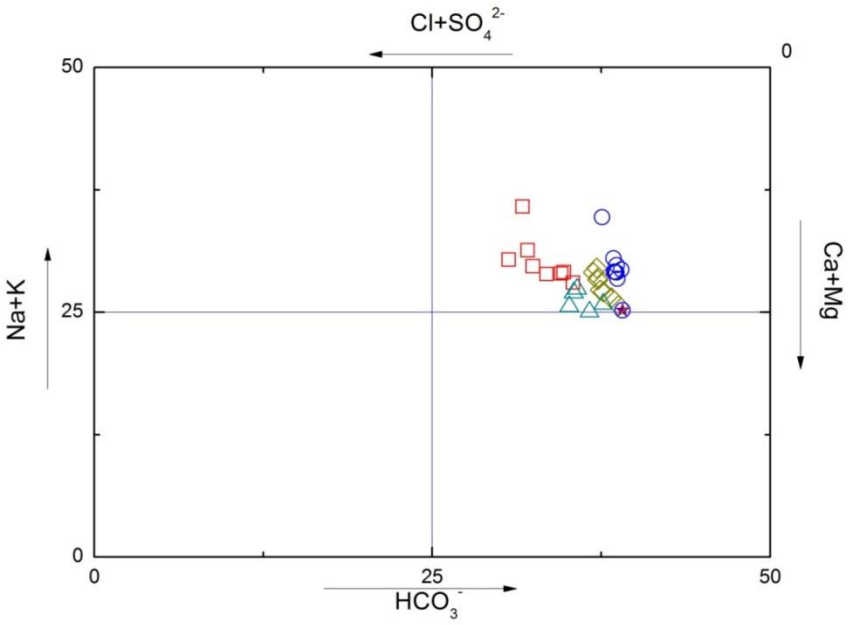

Figure 42 Langelier graph

The ternary diagram in Fig. 43shows the relative concentration of major cations (Ca^{2+}, Mg^{2+} and $Na^{+}+K^{+}$). The position of sample points on the plot indicates water–rock interaction processes. These data could be integrated with bibliographic analyses (Cuoco et al. 2010) of springs sampled in Roccamonfina Caldera and on NE slope of Roccamonfina Volcano. The caldera groundwater shows a Ca-enrichment as a probable consequence of latite domes influence on water chemical composition. Latite domes belong to the last eruptive period of the RVC and they are originated from the most

differentiated magma, with the highest CaO and MgO Wt% and the smallest K_2O Wt% compared to trachytic and tephritic products belonging to first and second Roccamonfina eruptive periods (Paone 2004). Therefore the recharge basin of the aquifer detected in the Roccamonfina Caldera is different to sampled Rianale Stream Valley one. In fact samples collected in Rianale Stream basin show a different relative composition of metals with an increase of alkali ion percentage (Fig.43), due to different volcanic formations involved in water mineralization.
Moreover, the monitoring springs show a similar low grade of mineralization (E.C. less than 300 µS/cm) but a different relative concentration in Ca^{2+} and $Na^{+}+K^{+}$ than the springs collected in the caldera. Therefore we can suppose that the recharge of the aquifer in Rianale Stream valley depends exclusively on local rainfall and there isn't a groundwater recharge from aquifer hosted in the Roccamonfina Caldera.

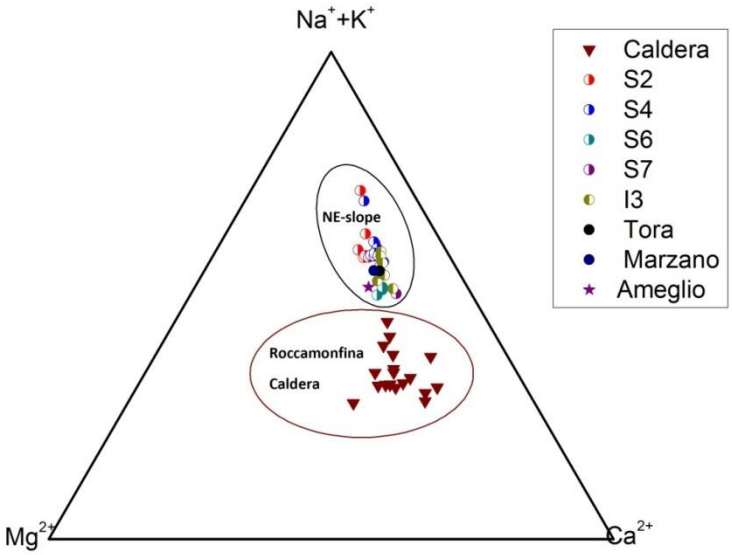

Figure 43 Ternary diagram; Caldara data from Cuoco et al. 2010

Quantitative analysis on spring discharge allows identifying the hydrogeological basin recharging S4 spring. The bibliographic value of effective infiltration on Roccamonfina Hydrogeological Structure is 368 mm/yr and it was detected from the map of Hydrogeological balances and groundwater resources, contained in Hydrogeological scheme of Central Italy (Boniet al. 1986). Dividing the base discharge flow of S4 spring and the effective infiltration value, the recharging area about 0,5 km^2 is calculated. It corresponds to a small relief composed by scoria cone deposits (Servizio Geologico d'Italia 1971a, 1971b) and Teano pyroclastic deposits (Giordano 1996) lying on lava flows of Roccamonfina Stratovolcano phase characterized by low permeability (Fig 44).This analysis confirm the limited extension of this basin and the absence of groundwater contribution from the upstream shallow aquifers of Roccamonfina Caldera.

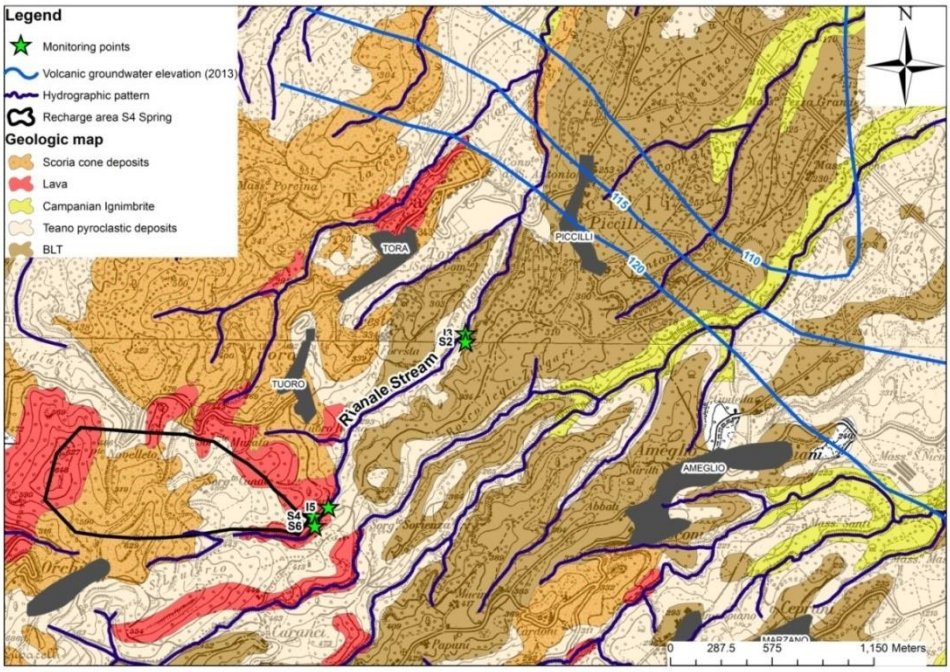

Figure 44 Recharge basin of S4 spring

The variability of parameters in the time shows interesting results about dynamics of mineralization of sampled springs.

Correlation between the electric conductivity (EC) and chloride in Fig 45 is indicative of groundwater residence time, water – rocks interactions and rainfall dilutions. In fact groundwater mineralization increases with the rising distance from the infiltration area to sampling area. chloride concentration, as suggested by Celico (1988), should be the element to estimate the residence time of waters due its conservative behavior in solution.

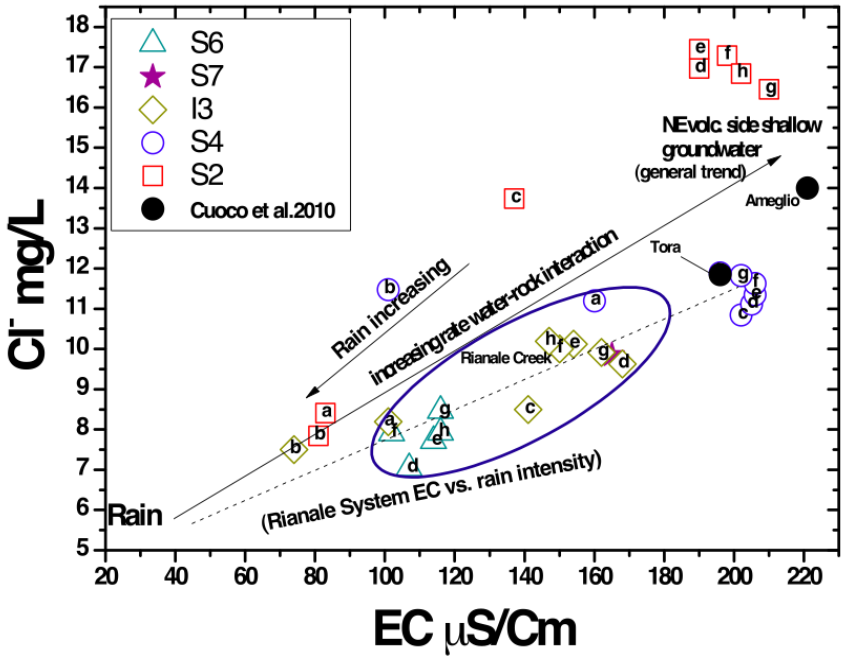

Figure 45EC – Cl graph

This limited circulation involves a lower mineralization of the sampled waters (EC 80-200 µS / cm) if compared to bibliographic data (EC 300-500 µS/cm) (Cuoco et al. 2010) of

aquifers characterized by more extended hydrogeological basins on the Roccamonfina Volcano. The increase of EC related to water – rock interaction during the observation period in sampled points is visible in Fig 45. Starting from the rain water (i.e. the starting endmember in water – rocks interaction processes) different mineralization occurred in two systems. The first hydrogeochemical system identified the S2 spring behavior: EC and Cl^- detected in the first three samples (A, B and C) are lower than later ones probably due to rainfall contribution. This dilution can occur easily in the rainy periods when the rainwater can seep through BLT fractures and change water chemistry close to the spring. Another parameter influencing the system is time of rock – water interaction. In fact increasing in water recharge produces faster and higher discharge in shallow aquifer therefore a lower amount of ions in solution (Celico 1988). Comparison in Cl^- / EC concentration between S2 and S4 springs suggests different dynamic of mineralization of these two systems. In fact at the same values of EC S2 samples contain higher concentration of Cl^- ion than S4 spring. This difference in chemical composition is probably related to different groundwater basin. The second system corresponds to Rianale Stream. This system is well defined in Fig 45 and it's the result of mixing of water from S4 spring and the lower mineralized S6 spring that generate I3 sample. This system suffers of the same dilution by rain water as S2 spring during the rainy days. In fact during the first weeks of monitoring it is characterized by abundant presence of runoff waters in Rianale basin (Fig 45). Also S7 spring is represent on Fig 45 too. Its composition is similar to I3, in fact more likely it isn't the outflow of a different aquifer; but it corresponds to under river bed flow of Rianale Stream coming out at the base of a little scarp.

Another distinctive geochemical diagram (Fig 46) represents the concentrations of two of the most mobile elements (Na and Cl) and their variability in time. Rainwater has an equimolar concentration of Na^+ and Cl^- (Berner and Berner, 1996), and then its Cl/Na ratio value is 1. Interaction of seeping rainwater with volcanic rocks brings Na^+ in solution which are not equilibrated by Cl^-, then the Na+/Cl- ratio increases. The linear trend on the Fig 46 shows the mineralization system of Rianale creek. Relative percentages in the mixing of i) rainfall and ii) mineralized groundwater from S4 spring define the chemical composition of Rianale creek in a specific sampling date. As it can be observed in Fig 46, in less rainy period Rianale creek (I3 and S7) has a Na/Cl ratio close to S4 spring. When rainfall increase (periods from "A" to "C") Na/Cl ratio decreases toward rain endmember. The linear trend on Fig 46 show the mixing between S4 spring and water deriving from rain and, consequential, superficial water circulation. In fact S6 (sampled upstream of S4) represents a typical contribution to Rianale creek deriving from superficial waters. On the graph in Fig 46samples collected from S2 falls in high diluted (from rain) waters (low mineralized springs in the graphs). Such water has low mineralization due its low residence time in BLT fractures. Low residence time in samples of rainy periods is attributed to the arising of hydraulic gradient in the springs basin due to the pressure operated by seeping waters. In fact with decreasing of rainfall (period from d to h) S2 attains its natural background separated from Rianale system. Interestingly, the S2 sampled in the "c" period shows an intermediate composition between the dilute and natural background of S2 water, allowing individuation of a mixing trend also for S2. From the observations deriving from Fig 46, it can be state that rainfall amounts influence the

chemistry of investigated water system and, in particular, springs at Tora and Piccili undergo chemical and quantitative changing after a short lapse of time from increase and/or decrease of rainy events. As can be confirmed by other samples collected in the area (Tora and Ameglio, Cuoco et al. 2010) this hydrogeological characteristics occur for whole SE side of Roccamonfina Volcano. Then the degree of mineralization of the sampled waters is strongly dependent on their residence time in the recharging basins. This residence time is lower during the rainy periods when greater amount of effective infiltration occurred.

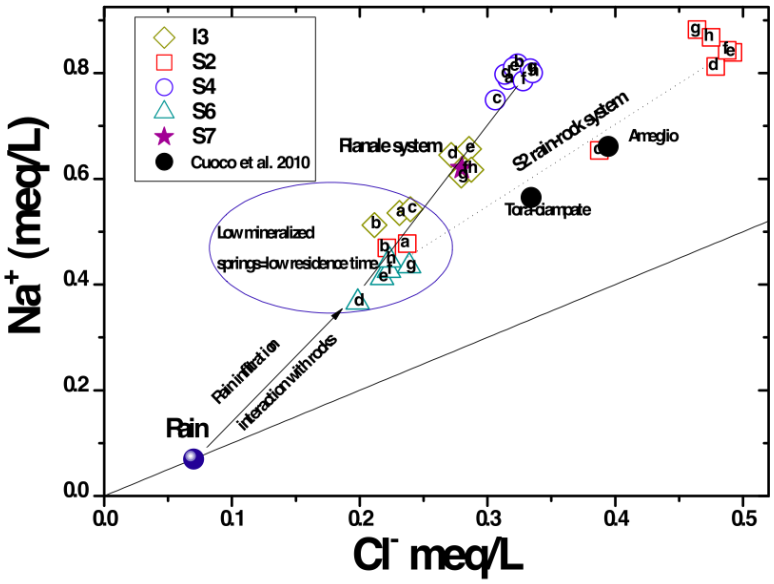

Figure 46 Na/Cl graph

Behavior of all elements in solution is similar to Cl^- one; in fact their concentration increases during the dry periods due to longer residence time of water in shallow aquifers. High concentrations in aluminum and iron were detected in unfiltered samples of shallow aquifers. A strictly linear relationship correlate Al and Fe (Fig 47) then the enrichment in these two elements probably depends to the same natural process.

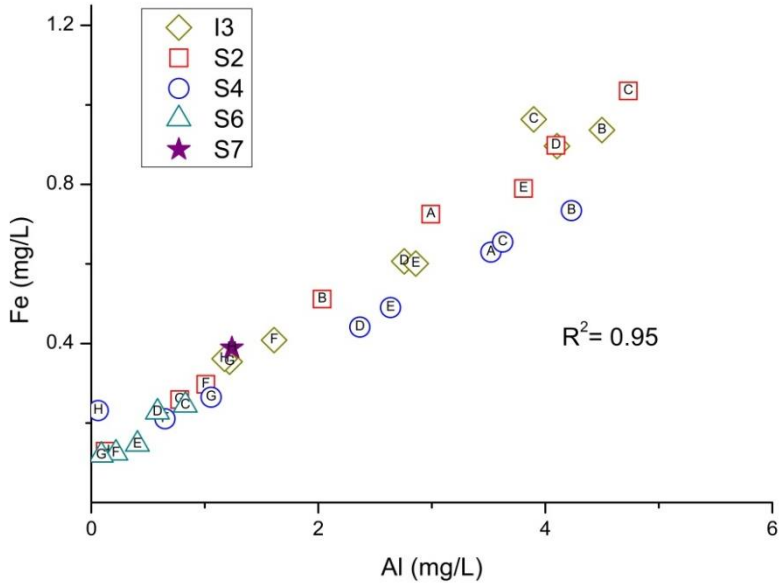

Figure 47 Al and Fe quantity

Results regarding Al and Fe in Rianale System samples match Orvieto presented in previous section. In fact high Al-Fe correlation (R^2= 0.94, Fig.47) and the decrease in aluminum and iron concentrations in 0,45 μm and 0,20 μm filtered samples (Fig. 48)have been detected as well as observed Rocca Ripesena shallow aquifer.

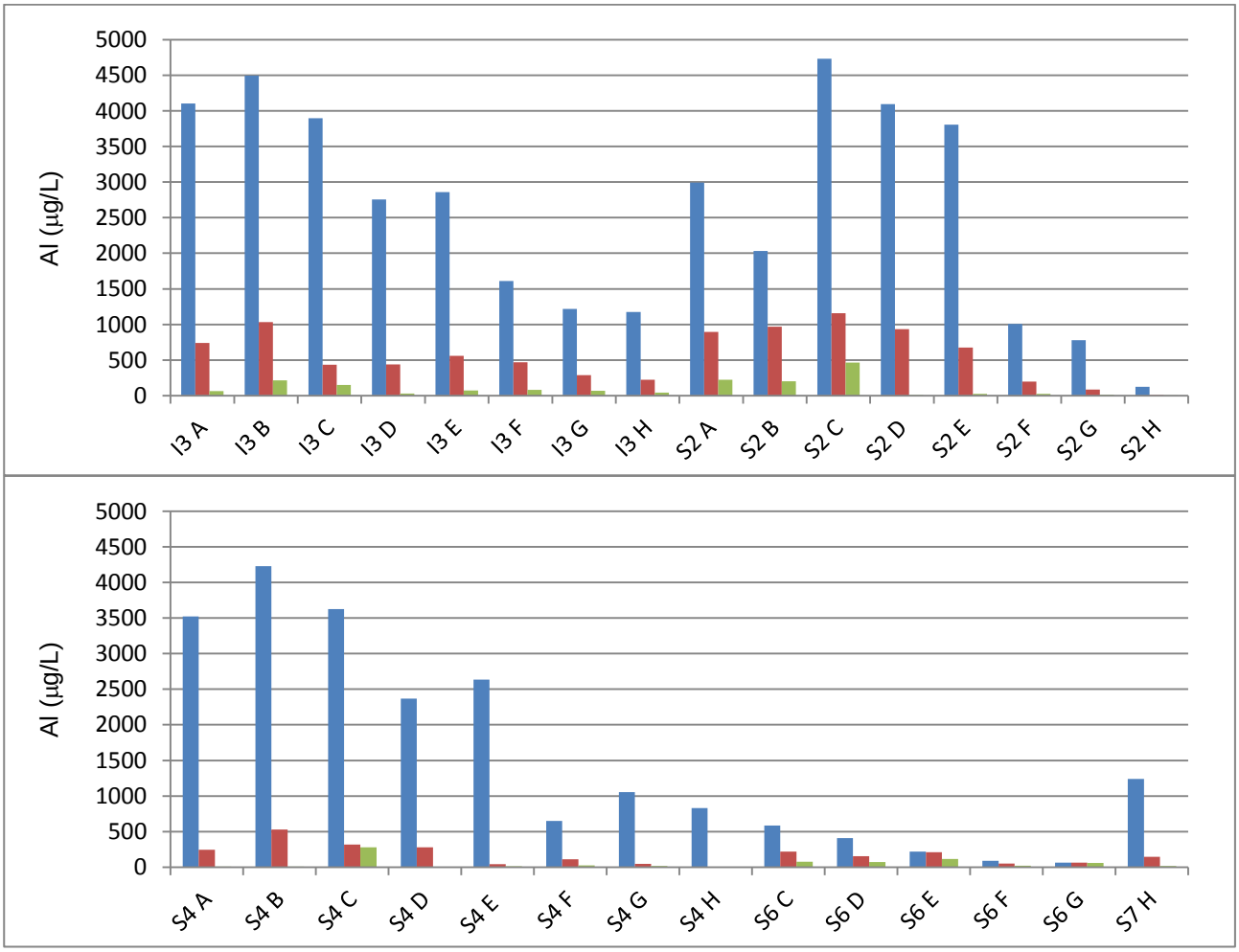

Figure 48Al concentration in unfiltered samples (blue), in 0,45 μm filtered samples (red) and in 0,2 μm filtered samples (green)

The percentage of filtration efficiency allow to evaluate colloids size; about 70 % of aluminum particles were hold by 0,45 μm filters, whereas 0,20 μm filters allow to remove almost the entire colloids. Therefore colloids with particle size included between 0,45 and 0,20 μm were approximately 30%. There are not significant variations in colloids size classes during the monitoring and the scarce differences in filtration efficiency could be ascribe to analytical or sampling procedures. Iron concentration data (Fig. 49) show the same filtration efficiency as much as on aluminum data.

These results confirm the similarities of colloids contamination observed in the Umbrian sector of Vulsini and in Rianale Stream Valley, therefore the geochemical features detected in the study areas could be probably detected in other areas characterized by similar volcanological and hydrogeological

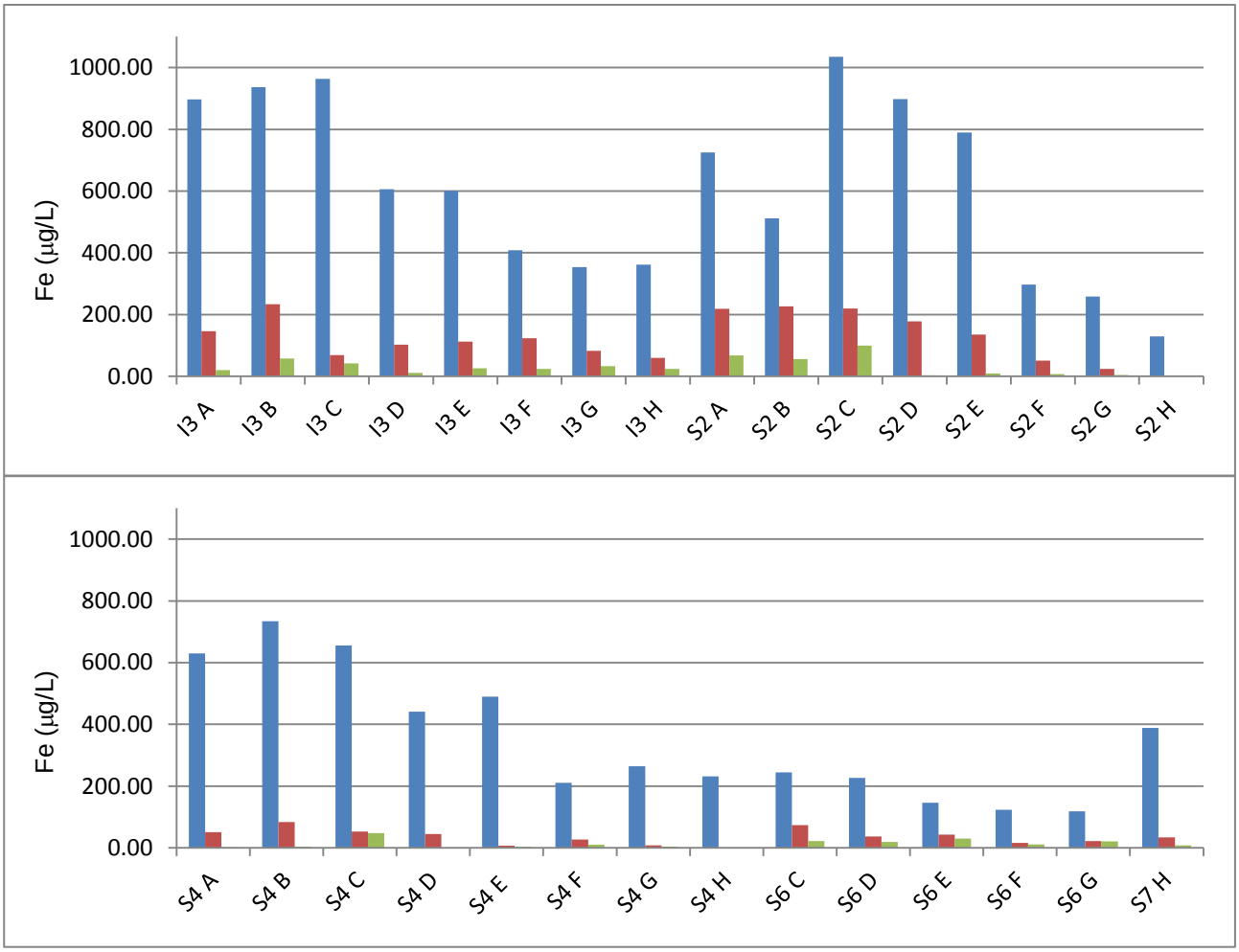

Figure 49Fe concentration in unfiltered samples (blue), in 0,45 m filtered samples (red) and in 0,2 µm filtered samples (green)

Analysis on correlation degree among iron and aluminum with other metals could be computed only on S4 because it's the most mineralized spring; being the others monitoring points characterized by low mineralized waters with no appreciable trace metal concentrations. This difference is likely related to permanence time of water in aquifers discharging at sampled points. Low permanence time means a low mineralization.

Barium and manganese are elements strictly correlate to Al and Fe concentration (R^2 = 0.97) in S4 samples. Barium and manganese concentration depends on filtration; in fact they were detected only in unfiltered samples because they are affected by adsorption phenomena onto colloids as well as Rocca Ripesena.

Principal Component Analysis (PCA) was carried out to point out the relationship between the water parameters and their variability using the same methodology already applied in discussion on Orvieto monitoring data on page 61.

Table below presents the principal component loadings for these three components, as well as their respective explained variance. Loadings, that represent the importance of the variables for the components, are in bold for values greater than 0.7 (Tab. 10).

Parameters	Component 1	Component 2	Component 3
T	-0,06	**-0,80**	-0,27
pH	-0,53	-0,36	**-0,63**
EC	**0,85**	-0,21	0,24
Eh	0,06	**0,78**	0,31
HCO3	**0,98**	0,01	-0,04
F	**0,73**	0,56	0,18
Cl	0,55	-0,09	**0,69**
NO3	0,26	-0,09	0,26
SO4	**0,92**	0,02	0,22
Na	**0,87**	0,10	0,44
K	**0,87**	0,23	0,04
Mg	**0,87**	-0,20	0,21
Ca	**0,94**	-0,11	-0,09
Al	-0,05	**0,91**	0,09
Fe	-0,13	**0,91**	0,09
Rb	-0,24	-0,38	**-0,85**
Ba	-0,50	-0,33	**-0,75**
B	**0,91**	-0,13	0,02
Si	**0,79**	0,08	0,41
Sr	0,30	-0,18	**-0,82**
V	**0,87**	0,12	0,36
Mn	-0,13	**0,63**	-0,40
Eigenvalues	10,60	4,54	2,21
Explained variance (%)	48,19	20,66	10,05
Cumulative % of	48,19	68,85	78,90

Tab 10 Principal components loadings calculated from the geochemical dataset of Rianale Stream Valley

The first two components explain about 49% and 21% of the variance, respectively, and thus, account for the majority of the variance in the original dataset. Component 3 is not so important in fact it explains about 10% amount of variance indicating that this component is related to more local effects than the first two components.

Fig 42summarizes this information by showing the position of the loadings of chemical parameters in the plane defined by the axes of components 1 and 2 that explain the 71% of total variance. A descriptive term is defined for each of the first two components based on their characteristic loadings.

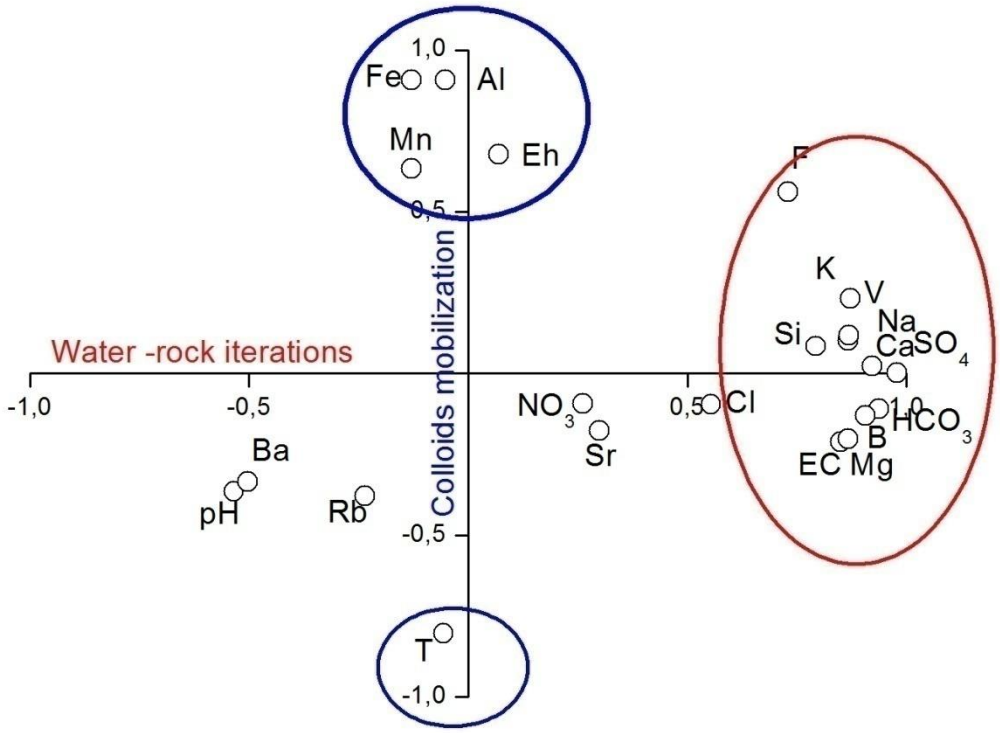

Figure 50 Displayed first two components

Component 1 explains the greatest amount of the variance, and is characterized by highly positive loadings in EC, HCO_3^-, SO_4^{2-}, Na^+, K^+, Mg^{2+}, Ca^{2+}, B, Si and V. This component explains the enrichment of major ions in solution related to water – rock iteration processes.

Component 2 is characterized by highly negative loading in Temperature and positive loadings in Eh, Mn, total Al and total Fe. This component explains the colloid mobilization occurrence. Al and Fe concentrations were detected in unfiltered acidified samples in order to quantify the concentration of suspended elements and to evaluate their variability in time. Eh value is related to rainwater contribution; its starting value is between +400 and +600 mV, then after the infiltration Eh value of water gradually decreases due to presence of organic matter, biological activity or to water – rock interaction processes (Appelo and Postma 2005). During rainy periods higher recharge produces faster discharge in shallow aquifers reducing time of iterations, then the oxygen consumption (Eh lowering) and increasing of mineralization (EC increasing). Therefore higher value of Eh corresponds to rainy periods, and to higher concentration of total Al and Fe in water. Manganese is included in this component because it is detected only in unfiltered samples so it is related to the solid phase in suspension even if it's characterized by a lower loading caused by interferences in superficial water samples.

Positive loading in Cl^- and negative loadings in Rb and Sr characterize component 3.

A graphic summary of relationship between suspend solid in water and principal elements of these systems is report in Fig 51. Temporal variation in the concentration of Cl, Al, Eh

and pH were also reported in the diagrams. As already described, Cl occurrence is related to residence time of waters in the aquifer, then to water- rocks iterations intensity; whereas Al detected in samples is representative of suspended solids quantity. Higher Eh values could be related to rainy periods due to the oxygen saturation of fresh rainwater. A greater amount of rainfall increases the recharge and the velocity of the discharge of analyzed shallow aquifers.

In all these graphs (representing all monitoring points S2 – I3 – S4 – S6) is clearly visible the inverse relationship between the mineralization of water (Cl) and suspended solids occurrence. Aluminum concentration increases in samples collected during first monitoring; they are also characterized by higher values of Eh and lower Cl- in solution, both elements related to rainy periods. In fact with residence time increasing, Eh value of infiltrate waters decrease because geochemical and biological processes consume dissolved oxygen in water and simultaneously increasing water – rocks iterations mineralization of water increases too.

The reciprocal relationship between these elements corresponds to principal component analysis results. Looking at the Fig 51 is known as the pH value behaves differently in surface waters (I3 and S6) and in groundwater (S2, S4).

In the first case pH decreases during the dry and hot periods since enhancement of biologic respiration increases CO_2 in solution (Drever 1997). Velocity of water in stream is higher than groundwater therefore the iteration time is not enough to buffer the pH of the solution. In springs samples pH value weakly increases during the monitoring due to the buffering effect of water – rock interaction processes

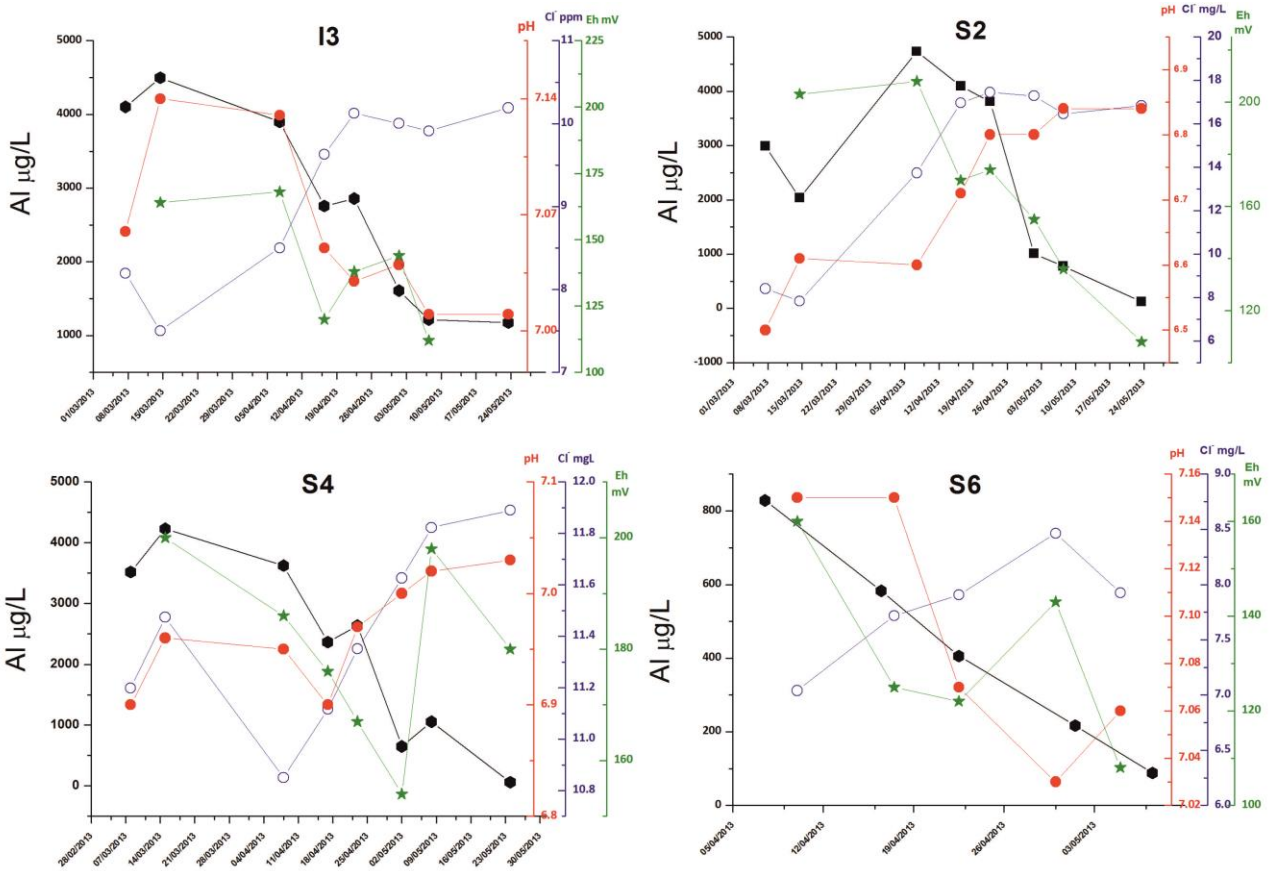

Figure 51 Al, Cl, pH and Eh variability

8. Pedological analyses

8.1. Sampling areas

8.1.1. Roccamonfina sampling area

The chemistry of most surface waters and groundwater is the result of interaction between rain and soils (Drever 1997). Several authors identified soils as principal source of colloids (Mc Carthy and Zachara1989, Ryan and Elimelech1996, De Jonge et al.2004, Poulsen et al. 2006, Laegdsmand2007, Deepagoda et al. 2011) which are mobilized by chemical and physical perturbations. The tendency of soil colloids to disperse in response to infiltration of water is a natural phenomenon (De Jonge et al. 2004).
Soil survey was conducted with the aim to identify the possible source of colloids in Rianale Valley and to determine some physical and chemical characteristics.
Different soils, formed in different tephra deposits can be identified on Roccamonfina volcano (Lulli et al. 1983, Vacca at al. 2003). Soils detected in the Rianale Valley could be distinguished in three main formations according to their parent material:

•soils developed from lava flows, which appear as thin mineral layers under an organic layer; these soils are often discontinuous, due to the erosion induced by runoff of rainfall over the low permeability parent material;

• soils derived from the weathering of BLT deposits, about 20 cm deep, occurring over lithified tufaceous rock, with very abundant roots of castanea sativa (chestnut trees) and of some species of quercus (oak trees) (Croce and Nazzaro 2012), pervading the entire soil profile;

• well developed soils from Teano pyroclastic deposits. This low consolidated volcanic formation is characterized by a good primary permeability which reasonably highly contributes to the development of the weathering of the source rock. A pedological survey station was placed near “Ciampate del Diavolo” paleontological site at an elevation of about 280 m a.s.l., where a complete section of pyroclastic flow deposit of Teano pyroclastic unit outcrops on the right bank of Rianale Stream. This pyroclastic flow was emplaced about 385 – 300 ka ago (De Rita and Giordano 1996) in a paleomorphological depression on NE flank of Roccamonfina Volcano, with a sub horizontal attitude that facilitates the development of thick evolved soil. A significant discharge of water rich in colloids was detected through this saturated deposit during the monitoring in 15 March 2013.On 22 July 2013 a pedological survey was performed on this soil section.

8.1.2. Orvieto sampling area

A second survey was performed on 12 August 2013 in Vulsini Volcanic complex deposits. A soil profile was detected about 600 meters upstream far from the monitoring springs near Rocca Ripesena at an elevation of 430 m a.s.l. Soil profile was placed on the left

bank of an affluent of Fosso Sugano. On the geological map in this area pyroclastic and lava deposits outcrop. Thin and irregular soils were detected on lava whereas more evolved soils derived from alteration of pyroclastic deposits. The most developed soils are placed in morphological depressions where reworked deposits stacked up or on the volcanic plateau of Vulsini Mounts. These deposits are part of Podere Sambuco Formation (ps) and Casa Perazza lava flows (cp1) emplaced about 230 ka.

8.2. Material and methods

8.2.1. Pedological survey

The outcropping section was cleaned, scraping off sufficient material to expose the fresh soil, and deepened about 60 cm under ground level in order to have a significant outcrop (2 meters length and 2 meters height). The main soil characteristics were provided for each soil horizon. Dry color, as Munsell's soil colors chart, texture, kind and nature of rock fragments (Φ< 2 mm), roots, soil redox conditions and soil horizon boundary were described. Thick layers showing low vertical variability were sampled with 15 cm depth interval. Sixteen samples were collected from Ciampate del Diavolo pedological profile and ten samples were collected from Rocca Ripesena soil profile (Fig. 52).

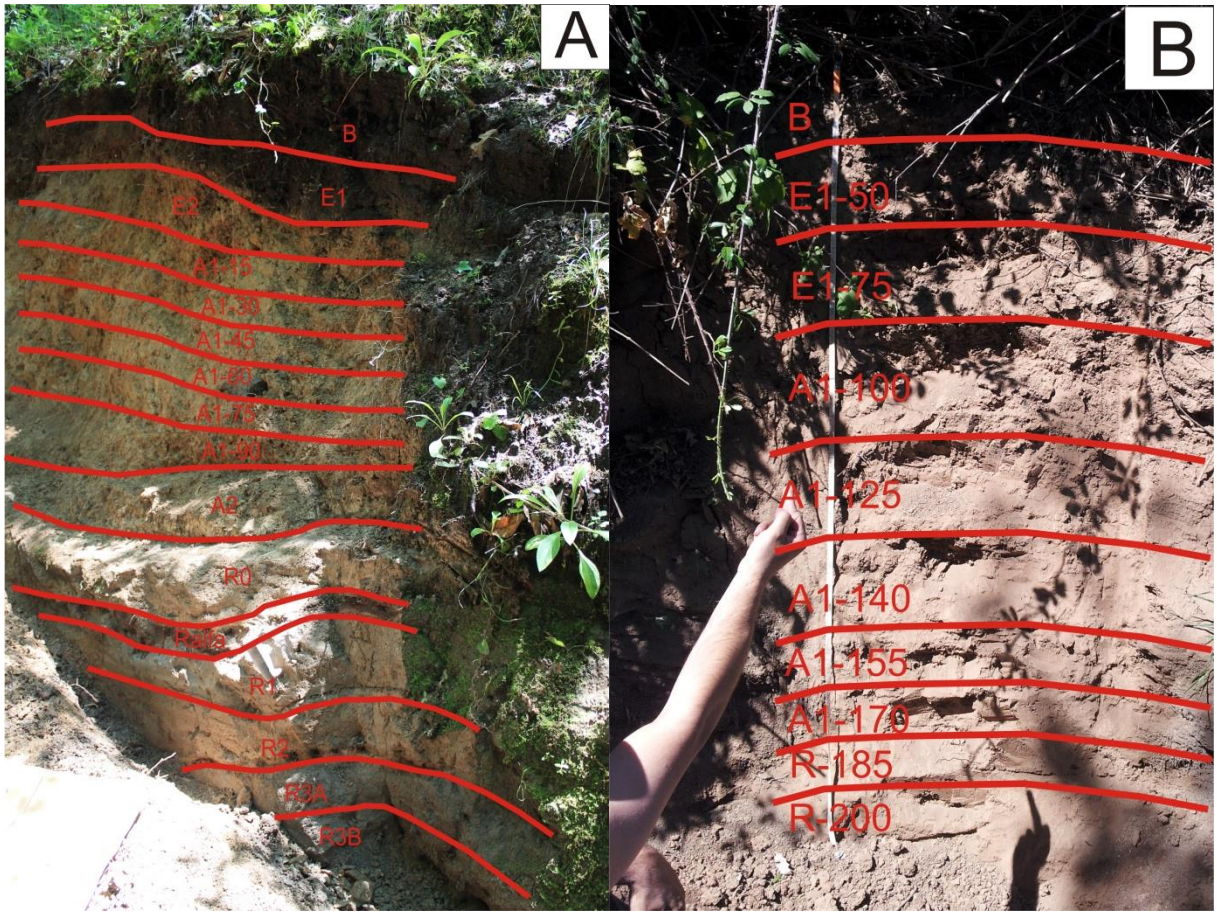

Figure 52 Ciampate del Diavolo (A) and Rocca Ripesena (B) soil profiles

About 1 kg of each layer was collected, air dried (Fig. 53) and then sieved to obtain a homogeneous earth fine sample (Φ< 2 mm) for laboratory analyses.

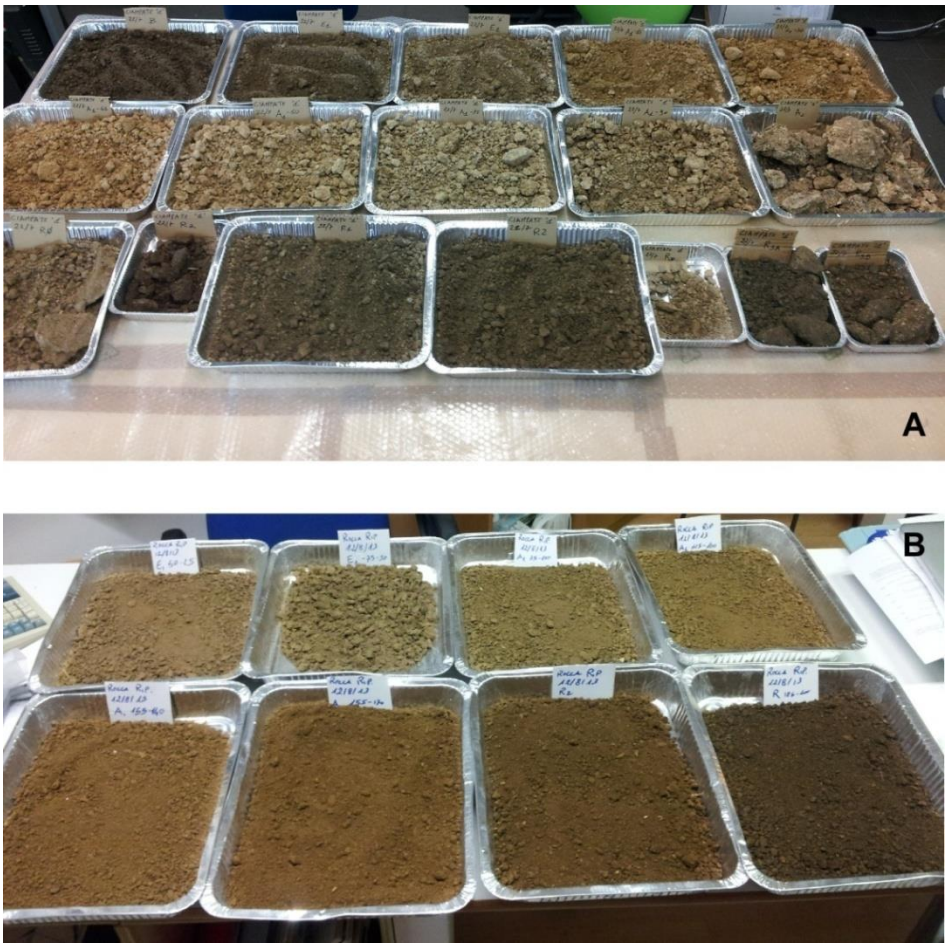

Figure 53 Samples collected in Roccamonfina (A) and Orvieto (B) sampling areas

8.2.2. Laboratory analyses

pH (H2O)

Soil reaction is expressed in terms of pH and is a measure of the acidity or alkalinity of the soil. It depends on:

•Ions exchange on the clay mineral surface and on humic compound

•Hydrolysis of Al^{3+} ions ($Al^{3+} + 3H_2O \leftrightarrow Al(OH)_3 + 3H^+$)

•Solubilization of CO_2 in liquid phase ($CO_2 + H_2O \leftrightarrow H^+ + HCO_3^-$)

In high rainfall areas, soils tend to acidity, as the basic cations are forced off the soil colloids, so that high rainfall rates can remove the nutrients, determining possible dystrophic conditions. When the colloids are saturated with H^+, the addition of any more hydrogen ions or aluminum hydroxyl cations tend to lower the soil.

Procedure

A common method of measuring soil pH is performed by placing a glass electrode in a mixture of soil and deionized water. 10 g of fine earth fraction (< 2 mm) sample are placed in a glass with 25 mL of H_2O and stirred for 2 hours.

pH (NaF)

This analysis is designed as a relative quick measurement of the content of the noncrystalline minerals (e.g., allophane, imogolite) in a soil (Fieldes and Perrott 1966). The initial pH (NaF) is 7.2 - 8.1. When mixed with soil, the fluoride anion reacts with the soil minerals (especially poorly crystalline materials), displacing hydroxyl ions and complexing Al. The pH (NaF) of the soil suspension increases as effect of OH ions released into solution.

Procedure

1 g of fine earth sample is mixed with 50 mL of 1 N NaF and stirred for 60 s. Sample is allowed to stand for 30 s. Soil pH is measured by placing a pH electrode in the solution.

Interferences

Soil organic matter is a positive source of error in this test, i.e., surface horizons or other layers high in organic matter may inflate NaF pH, due to extraction of OH ions from the organic matter rather than from inorganic sources.

Particle-size distribution

Due to the unreliability of silt and clay determination in volcanic soils (Mizota and van Reeuwijk 1989), the particle size analysis was not carried out by dispersed with Na hexametaphosphate. For this study, a partial grain size analysis on fine earth samples was carried out to separate the sand fraction (2-0.05 mm fraction) from the remaining particle, such as silt and clay (< 0.05 mm fraction) which are expressed by difference as sum of the particles in question.

Procedure

About 20 g of fine earth sample were placed in a baker with 25 mL of deionized water and 5 mL of hydrogen peroxide to break up the available organic matter and the organic bonds. Hydrogen peroxide was gradually added to the solution until no evident reactions were visible. Samples were dried and wet sieved using a 0.05 mm sieve. Weight of the sand fraction was recorded, while the silt and clay weight was assessed by difference.

Organic carbon

The Walkley-Black method (Walkley and Black 1934) was used for determining soil organic carbon utilizes a specified volume of acidic dichromate solution reacting with a determined amount of soil in order to oxidize the organic matter:

$2Cr_2O_7^{2-} + 3CO + 16H^+ \leftrightarrow 4Cr^{3+} + 3CO_2 + 8H_2O$.

The oxidation step is then followed by titration of the excess dichromate solution with ferrous sulfate which gives a volume of ferrous sulfate in mL.

$6\ Fe^{2+} + Cr_2O_7^{2-} + 14H^+ \leftrightarrow 2Cr^{3+} + 6Fe^{3+} + 7H_2O$

The organic carbon is calculated using the difference between the total volume of dichromate added and the volume titrated after reaction.

Procedure

- 0.16M Potassium dichromate ($K_2Cr_2O_7$): Dissolve 98.08 g of desiccated Potassium dichromate in approximately 1500 mL of pure water and dilute to 2 L
- 1.0M Ferrous Sulfate ($FeSO4 \cdot 7H_2O$): Dissolve 139 g of Ferrous Sulfate in approximately 1000 mL of pure water. Carefully add 20 mL of concentrated Sulfuric Acid, mix, cool, and dilute to 1 L. The tubing, stopcock, and attachments to the burette should be rinsed three times with new Ferrous Sulfate solution before titrating any blanks or samples.
- Weigh 1.0 g of soil filtered at 0,5 mm into a 250-mL wide mouth graduated Erlenmeyer flask.
- Titrate one blank sample (no soil) before proceeding with any unknown samples in order to standardize the Ferrous Sulfate solution.
- Pipet 10.0 mL of the Potassium dichromate solution into each flask containing unknown soil and mix by carefully rotating the flask to wet all of the soil.
- Under a fume hood, carefully add 20 mL of concentrated Sulfuric Acid to each flask and mix gently.
- Allow flasks to stand for 30 min under the fume hood.
- Add 200 mL pure water to each flask to stop the reaction. Mix by swirling gently.
- Add 0,5 mL of diphenylaminesulfate complex and 10 mL of Phosphoric acid, then immediately titrate with the Ferrous Sulfate solution.
- Record each volumetric reading when color of solution change from blue to a brillant green.

X-ray Diffraction analyses

X ray diffraction (XRD) analyses were performed using a Scintag X1 diffractometer. The Scintag X1 is a theta-theta diffractometer equipped with a Cu X-ray source, fixed silts, and a solid state Peltier cooled detector. Analyses were realized with 0,05° 2Θ in a scan range is 2°-150° 2Θ.

Ten earth fine samples collected from each soil profile were analyzed in order to characterize the mineralogical composition of soil layers distinguish on primary and weathered minerals.

A water sample collected in each monitoring area was analyzed in order to identify the crystalline or amorphous structure of suspended solid transported by groundwater. About 2,5 L of each water sample were evaporated in an oven at 70°C constant temperature. Precipitated salts and suspended solids were then collected and put on a slide when the sample was totally dried.

All diffractograms were elaborated and then reported in appendix.

8.3. Discussion

8.3.1. Roccamonfina sampling area

Particle-size distribution

Data of particle size distribution analysis are report in Fig 54. During these analysis sand fraction was distinguished to the sum of silt and clay fractions on earth fine samples and to available organic matter disaggregated by peroxide hydrogen. In these samples a mean value of 7,2% of organic matter was detected with a standard deviation of 2,4%. These quantities are related to the oxidation of bigger and more easily dissolved organic fragments like roots sections. B horizon is coarser in texture, having lost some of the finer materials by translocation to lower horizons and by erosion. E1 sample is characterized by a higher content in small size particles probably derived from the upper B layer. Increasing in fine elements is generally visible from A1-15 sample down to A1–90 sample (from 35% to 58%).

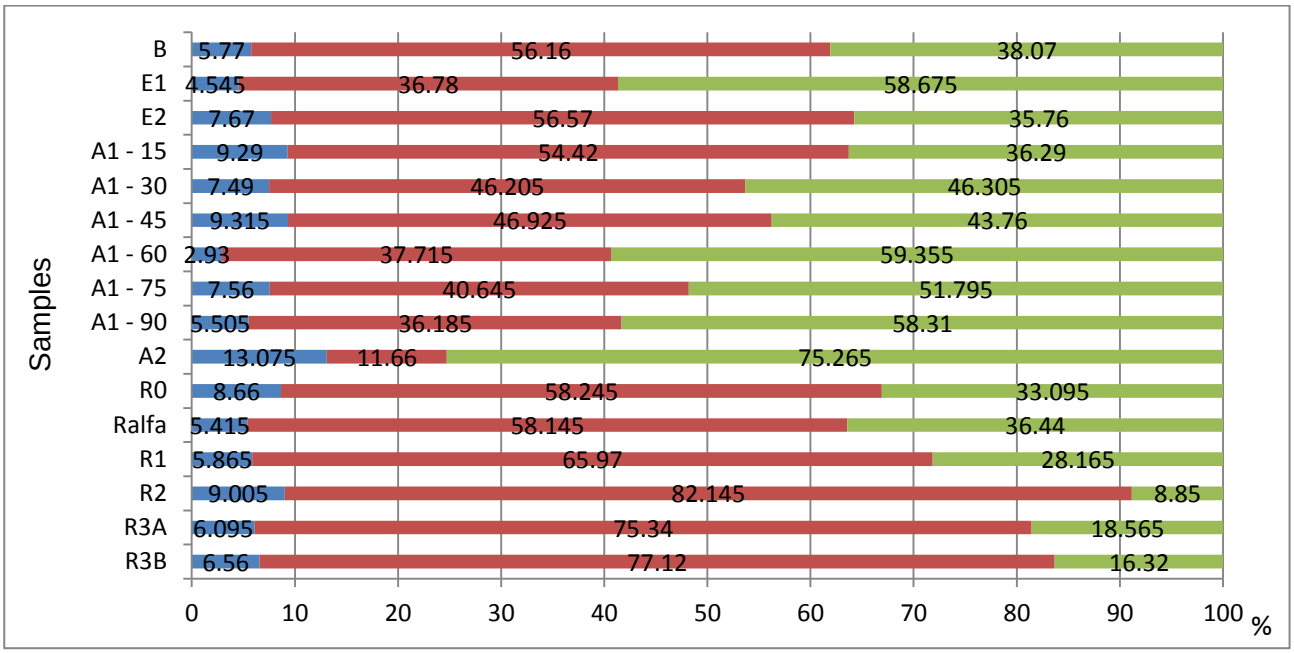

Figure 54Percentage of particle size distribution: silt and clay fraction (green), sand fraction (red) and organic matter (blue)

These samples correspond to the homogeneous and poorly sorted body of pyroclastic flow. The increasing in silt and clay size elements is probably related to a progressive alteration of the deeper layers related to the saturated layers occurrence. A2 sample is the most clayey layer of this deposit because it corresponds to the fine graded basal part of a pyroclastic flow unit (Sparks 1973) and the abundance of fine elements derived from the weathering of volcanic glass. The last six samples (R0, Ralfa, R1, R2, R3A and R3B) belong to a different pyroclastic flow deposit and they are characterized by higher quantity of sand fraction than the upper samples.

Organic Carbon

Results of organic carbon analysis were reported in Fig 55. There is a clear decreasing in organic carbon (OC) contents in analyzed samples: the topmost brown layer (B) contains a

significant amount of organic carbon (almost 20 g/kg). derived from partially decomposed (humified) organic matter that give to the soil a darker color than the lower horizons. This layer is the zone where the most biological activities occur. Organic carbon quantity quickly decrease related to the depth of the sample. The E1 sample, under the B layer, contains scarce quantity of OC (about 2,6 g/kg) derived from the organic materials gradually washed in from the overlying horizon especially during periods of major infiltration. This mobility is enhanced by formation of organic colloids in fact surface of iron, manganese, aluminum and silicon oxide particles strongly adsorb organic and inorganic acid anions (McCarthy and Zachora1989, Guo et al. 2011). The magnitude of this illuviation process decreases in the underlying layers (E2, A1–15, A1–30) until 85 cm under ground level where the detected OC is near zero. A1–45, A1–60, A1–75, A1–90, A2 and R0 samples are characterized by small amount or absence of OC. Vertical dispersion of organic matter depends on the soil texture and on its permeability. As already described, silt and clay fraction downward increases up to A2 layer so decreasing of permeability reduces the dispersion of OC in the underlying layers. R-alfa buried layer at about 176 cm under the ground level shows a higher concentration of OC (1 g/kg) than the surrounding horizons. This brown layer probably corresponds to a thin paleo soil developed during an intra-volcanic period. OC was not detected in the deepest samples (R1, R2, R3A and R3B).

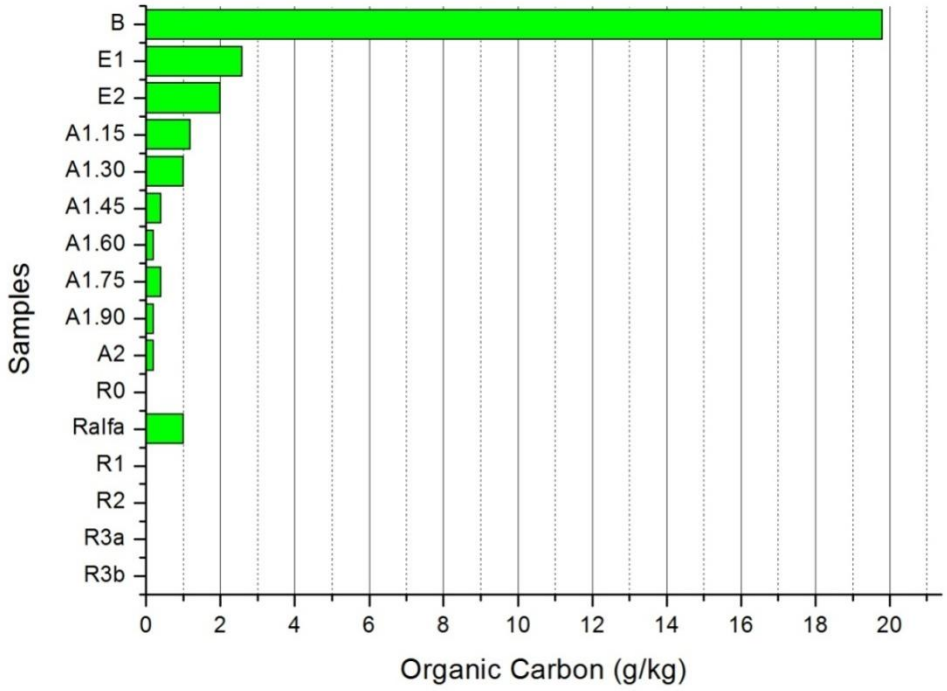

Figure 55 Organic Carbon

pH H_2O

Results of pH in H_2O analysis are report in Fig 56. All values correspond to neutral pH range (6,5–6,7) as detected in other soils derived from volcanic deposits of Roccamonfina volcano (Lulli et al. 1983, Vacca et al. 2003). No significant variations or trends are visible along the soil profile, so probably this is a homogeneous deposit without a more reactive (acid or basic) layer.

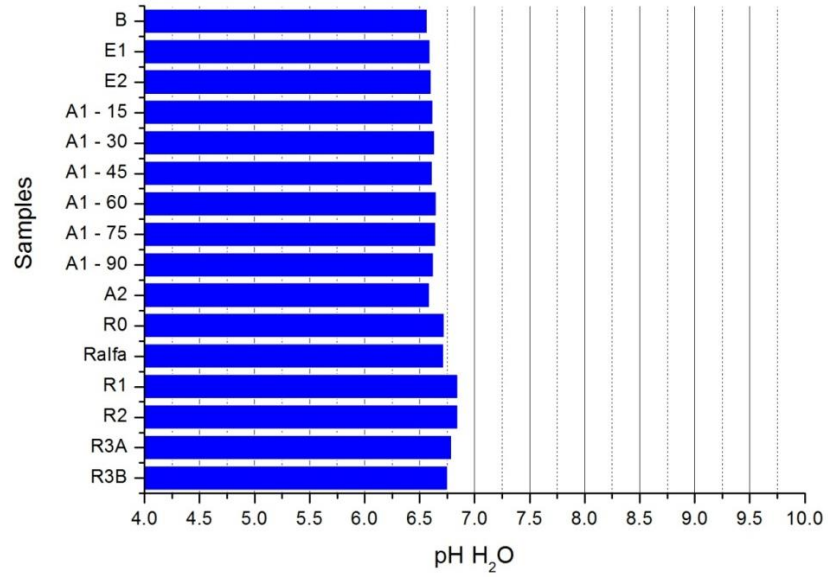

Figure 56 pH in H_2O

pH NaF

pH values detected in 1M NaF solution are report in Fig 57. These data are higher (more alkaline) compared to the pH-H_2O of the same soil; this is an indicator of the presence of short-range order minerals of free aluminum (oxyhydroxide forms) in soils deriving from volcanic deposits. When sample reacts with the NaF solution, fluoride ions create a stronger bond with the Al ions than the Al $(OH)_3$ one. This reaction releasing OH^- ions that determinate the increased values of pH.

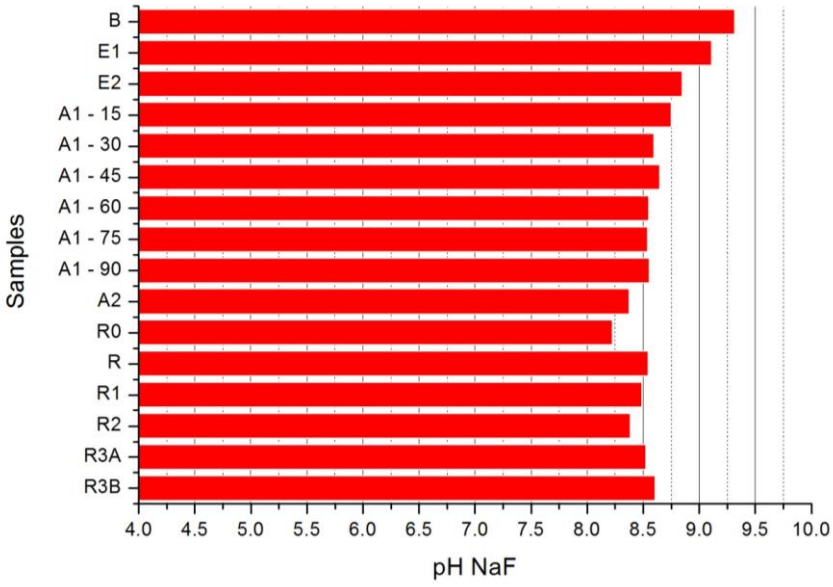

Figure 57 pH NaF

This type of reaction affects the organic compounds too. It's visible in the soil results a decreasing of pH NaF values according to the presence of the measured organic carbon.

XRD analyses

X ray diffraction (XRD) analyses were performed on 10 earth fine samples (B, E1, E2, A1–15, A1–30, A1–45, A1–75, A2, R0 and R – alfa) of Ciampate del Diavolo soil profile and on a dried water sample of S4 spring collected on 15 March 2013.
All diffractograms were elaborated and then reported in appendix
The presence of primary volcanic minerals like mica, sanidine, plagioclase and clino pyroxene was detected in all samples. Halloysite was detected in A1 – 15, A1 – 75 and A2 samples related to higher alteration processes of volcanic glass (Aomine and Wada 1962, Quantin et al 1988). Halloysite is not clear detectable in the analyzed samples because its characteristic peak is covered by the presence of 1 nm mica reflections. The collapse to 0,7 nm of the Halloysite main peak from 1 nm following heating at 105°C allowed to distinguish the two mineral phases (Adamo et al. 2001). Quartz and apatite characteristic peaks are detected in R–alfa sample. Diffuse, broad reflections at about 0,41 and 0,25 nm characterized all the XRD patterns. They might reflect contributions from pyroclastic glass and/or secondary disordered low crystalline fragments.
The diffractogram of dried water sample shows only few significant peaks related to two crystalline phases: in the sample Calcite ($CaCO_3$) and Halte (NaCl) were distinguished. These two minerals derived from the precipitation of salts during the evaporation of the sample. The non-crystalline structure of suspended solids in water is confirmed in the diffractogram where a serie of close undefined peaks were detected at the interval from 0,44 to 0,3 nm distinctive of abundant presence of amorphous particles.

Hypothesis on weathering evolution

The evolution of the surveyed section started when a first pyroclastic deposits were emplaced (R1, R2, R3A and R3B samples). A sequent intra – volcanic period allowed the development of a thin dark paleo soil (R – alfa sample) highlighted by the presence of organic carbon in this layer. Afterwards R0 deposit covered the paleo soil and shortly after a new pyroclastic flow deposit was emplaced (from A1 – 15 to A2 samples) preventing the development of a paleo soil on top of R0 horizon.
The infiltrated rain waters fluxed downward through the deposit to the base of the pyroclastic flow deposit, constituted by fine elements (Sparks 1973) then characterized by very low permeability. This is a local aquiclude that support a shallow periodic aquifer in the upper deposits. The lower part of pyroclastic flux is more weather due to more frequent saturation than the central body of the deposit. The basal layers are characterized by a major quantity of aluminum oxyhydroxide forms derived from alteration of fine glass matrix of volcanic deposit.
At the same time intense weathering processes affected the topmost layer. Below the topmost horizon there is a layer in which iron and aluminum have accumulated as fine grained, poorly, crystallized hydroxides or clay minerals (B horizon). The processes by which aluminum and iron are removed from the A horizon probably involve dissolution in form of organic complexes and transport of colloidal particles. Precipitation in the B horizon is caused by several processes, including the loss of organic complexing agents by bacterial decomposition and adsorption (Drever 1997)

8.3.2. Orvieto sampling area

Particle size distribution

Texture analysis carried out of 10 samples and the results are report on Fig 58. The samples were sifted using a 2 mm sieve but no rock fragments were detected. It was possible quantified available organic matter disaggregated by peroxide hydrogen. In these samples a mean value of 6% of organic matter was detected with a standard deviation of 1 %. These quantities are related to the oxidation and disaggregation of bigger and more easily dissolved organic fragments like roots sections Almost all samples are characterized by a high quantity in silt and clay fractions (from 56 to 78%). In this soil profile the absence of the organic level was already detected in field and these results confirm the absence of the “B” level which is usually characterized by coarser texture and black color. Only the R - 200 sample show a sandy texture with only 26 % in loam and clay content.

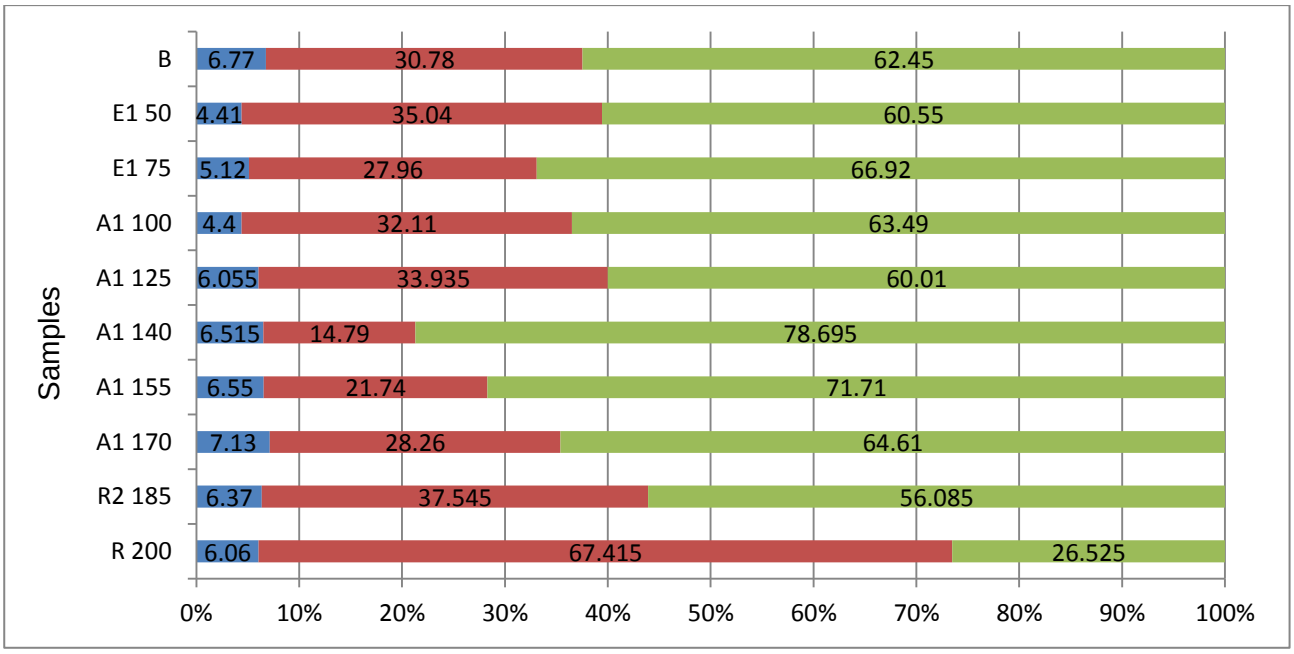

Figure 58Percentage of particle size distribution: silt and clay fraction (green), sand fraction (red) and organic matter (blue)

Organic Carbon

Results of organic carbon analysis are report on Fig. 59. Analyzed samples contain a high quantity of organic carbon along the entire profile decreasing downward from about 25 g/kg to 9 g/kg. These results can not be compared to Roccamonfina one because this section could not depict the real feature of Podere sanbuco (ps) volcanic deposits The presence of organic carbon in the deeper layers could be related to the agricultural land use of this area, in fact fertilization increases the OC concentration while plowing could mix the surface layers becoming an important component in the OC downstairs diffusion.

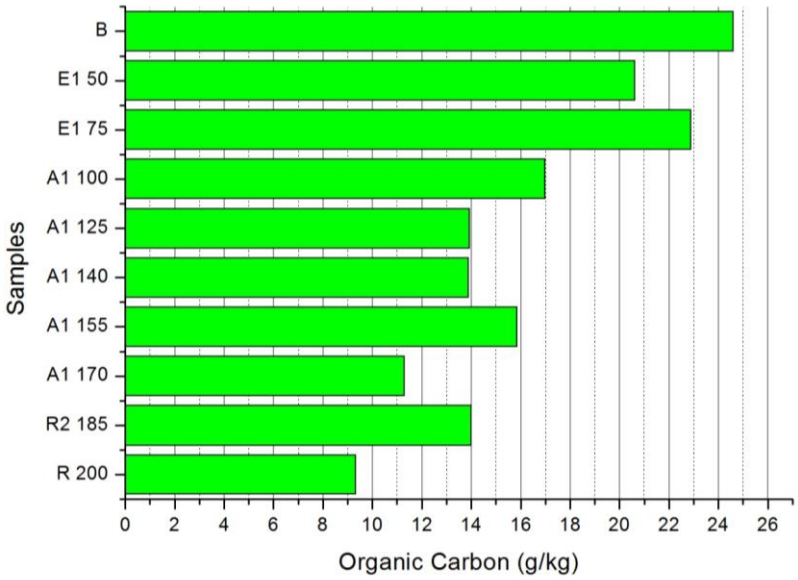

Figure 59 Organic Carbon

pH H_2O

The results of pH in H_2O are show in Fig 60. There aren't significant differences or trends between the samples along the soil profile, so probably this is a homogeneous deposit without a more reactive (acid or basic) layer. The three upper samples have a weak sub acid pH whereas from A1–100 sample neutral pH were detected. This little difference is probably related to the higher amount of organic matter in the three shallower layers.

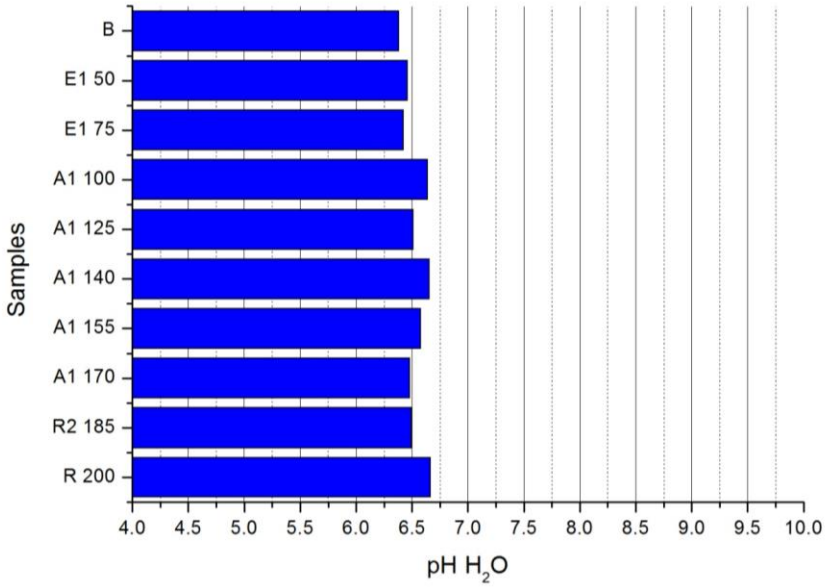

Figure 60 pH in H20

pH NaF

pH values detected in 1M NaF solution are report in Fig 61. These data are higher (more alkaline) compared to the pH-H2O of the same soil; this is an indicator of the presence of short-range order minerals of free (aluminum oxyhydroxide forms) in soils deriving from volcanic deposits. When sample reacts with the NaF solution, fluoride ions create a stronger bond with the Al ions than the $Al(OH)_3$ one. This reaction releasing OH^- ions that determinate the increased values of pH. These results are equivalent to Roccamonfina one, confirming the great abundance of oxyhydroxide forms.

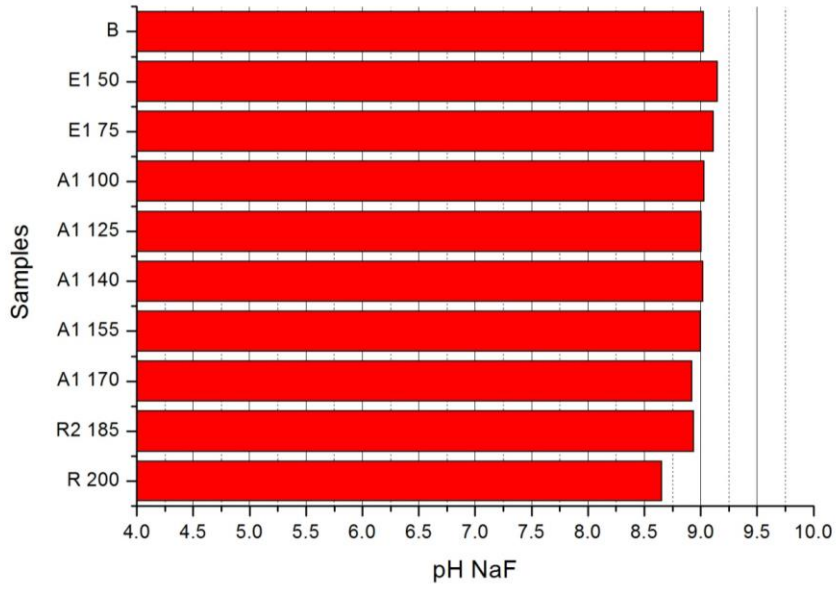

Figure 61 pH NaF

XRD analyses

X ray diffraction (XRD) analyses were performed on all ten earth fine samples of Rocca Ripesena soil profile and on a dried water sample of RR1 spring collected on 11 April 2013. All diffractograms were elaborated and then reported in appendix

The results of soil samples analyses show a great uniformity of mineral composition, in fact primary volcanic minerals like mica, sanidine, plagioclase, clino pyroxene and quartz was detected in all samples. Halloysite was detected in all samples related to a higher alteration processes developed along the entire sampled section. Halloysite is often detectable in the analyzed samples different to samples collected on Ciampate del Diavolo soil section because it was detected as 0,7 nm halloysite then there were not interferences between mica and 1nm Halloysite reflection peaks

The diffractogram of dried water sample shows only few significant peaks related to three crystalline phases: Calcite ($CaCO_3$), Halte (NaCl) and Sylvite (KCl). These three minerals derived from the precipitation of salts during the evaporation of the sample. The non-crystalline structure of suspended solids in water is confirmed in the diffractogram where a

serie of close undefined peaks were detected at the interval from 0,44 to 0,3 nm distinctive of abundant presence of amorphous particles.

9. Conclusions

In this study quantitative hydrogeological analyses of volcanic aquifers were support by geochemical and pedological surveys. The aim of this innovative study is the integration of different subjects to give a whole definition of quantitative fe
Hydrogeological settings of Umbrian VVD were carried out during this study. An updated water table elevation map of the basal aquifer was realized using experimental data form hydrogeological survey 2013. A NW–SE dynamic groundwater divide was identified, defining two major hydrogeological basins through the interpretation of experimental data. Several shallow aquifers, characterized by discrete discharge (from 50 L/s to 0,1 L/s), were identify, even if it was impossible create a complete water table elevation map due to lack of data and to un-continuity of these aquifers.
Another hydrogeological survey was performed in 2012 on the eastern sector of Roccamonfina Volcano and on Riardo Plain in order to improve the hydrogeological knowledge of the area and to evaluate the relationship between different overlying aquifers. A volcanic and a carbonate aquifer were distinguished In Riardo Plain pointing out different relationship between these two aquifers along the plain. Water table elevation map realized on the eastern flank of Roccamonfina Volcano, and then a new hydrogeological conceptual model for this area was realized. Previous scientific works (Capelli et al. 1999, Allocca et al. 2007) identified only one aquifer in the volcano system but during this research a basal aquifer (characterized by moderate gradient was detected in paleo – Roccamonfina fractured lava) and shallow aquifers(characterized by low productivity and limit extension were detected in porous pyroclastic deposits) were distinguished.
Shallow aquifers in both areas are characterized by murky waters due to abundant presence of colloids. A monitoring area was established in each volcanic domain: a promontory near Rocca Ripesena Village on VVD and a section of Rianale Stream Valley on the NE flank of Roccamonfina Volcano.
Shallow aquifers of both areas are characterized by low mineralized waters ascribable to volcanic hydrogeological facies. Major elements concentrations weakly change during the monitoring period, showing a progressive increase in electric conductivity during the dry season. Concentration above drinking water limits (200 μg/L) in aluminum and iron was detected in unfiltered samples in both monitoring areas; these concentrations strictly decrease through using 0,45μm (about 80% of filtration efficiency) and 0,22μm filters (about 100% of filtration efficiency). These differences between filtered and unfiltered samples highlight the colloidal form of Al and Fe according to their pH – Eh stability diagram. Manganese and barium concentration depends in part to colloids quantities too. These two elements at pH – Eh conditions detected in field must be in solution but comparing concentrations in filtered and unfiltered samples a part of Mn and Ba were keep from the filters. The strictly correlation between these elements with Al and Fe confirm their adsorption on colloid particles.
An contrary relationship was detected between rainfall and colloids concentration, it can be distinguish a first rainy period in which high concentrations of Fe and Al were detected and

a second period characterized by minor rainy days in which colloids concentration quickly decrease.
PCA analyses were performed on geochemical databases of the two monitoring areas. Both shallow systems are managed by two principal factors: the first component (explaining about 50 – 55 % of total variance) explains the enrichment of major ions in solution related to water – rocks iteration processes. The second component (explaining 22 -20 % of total variance) explains the colloids mobilization directly influenced by Eh values (only where it was possible to measure it) as identification parameter of rainfall.
XRD analyses were performed on dried unfiltered water samples of RR1 spring (Rocca Ripesena) and S4 spring (Roccamonfina). The results show only few crystalline elements deriving from salt precipitation from water: Calcite ($CaCO_3$), Halyte (NaCl) in S4 sample and furthermore Sylvite (KCl) and in RR1 sample. In both diffrattograms is visible a pronounced noise zone characteristic of the presence of amorphous elements as confirm of the absence of suspended crystalline elements that coul alterate the chemical analyses.
Soil surveys were carried out in monitoring areas to identify the source of these colloids. A complete soil profile on Teano pyroclastic deposits was analyzed in Rianale Valley whereas about upper two meters of soil were sampled in Colluvium – eluvium deposits near Rocca Ripesena springs.
Soil collected in Rianale Valley is characterized by neutral pH in H_2Ovalues (6,5 – 6,7) and alkaline pH in NaF (8,2 – 9,2) indicating the presence of short-range order minerals of free (aluminum oxyhydroxide forms) in soils deriving from volcanic deposits. Sampled soil is characterized by a high organic layer on topsoil whereas the organic carbon concentration quickly decreases to zero in the first 100 cm under the ground level. Under the topsoil layer the soil show a progressive downward increasing in clay and silt fraction up to A2 sample (145 – 165 cm under ground level)characterized by 75% of fine elements. This layer corresponds to the local aquiclude of shallow infiltration in weathered deposits.
Soil samples collected near Rocca Ripesena is characterized by neutral pH in H_2O values (6,4 – 6,7) and alkaline pH in NaF (8,7 – 9,1) indicating the presence of short-range order minerals of free (aluminum oxyhydroxide forms) in soils deriving from volcanic deposits. These samples didn't show significant variability along the profile neither in soil texture neither in organic carbon concentration (24 to 10 g/kg). these differences with soil profile analyzed in Rianale Valley depend on agricultural land use (fertilization and plowing) and the thickness of weathered deposits that rises up to several meters in Rocca Ripesena area. Then the sampled soil profile is not explicative of the characteristics of the whole weathered deposits so an excavating or a drilling should be done to have at disposal the complete soil layers.
After these analyses a clear relationship between the two study area was pointed out. Colloids in water are inorganic Al and Fe compounds with a un crystalline structure (oxyhydroxide forms). Their quantities directly depend on rainfall occurrence and infiltration in short time aquifers. Facilitated transport role of colloids was detected at least for Mn and Ba.
Identification background value of aluminum and iron in shallow volcanic aquifers is fundamental in a wise environmental management to discriminate natural contaminant processes to human pollution.

Furthermore study areas in Roccamonfina and in Orvieto shows a significant difference for local water management: the basal aquifer of VVD in characterized by a higher value of vulnerability than Roccamonfina one. The intermediate aquitard in Umbrian sector of VVD is constituted by lava deposits characterized by variable (from low to average) permeability and irregular distribution in the whole area. on the contrary on NE flank of Roccamonfina Volcano about 100 meters of low permeability BLT deposits protect the basal aquifer from the shallow contamination.
Not well done drilling or wells could be a factor of vulnerability increase, so shallow aquifers should be isolated from the basal one through a correct cementation in order to protect the water resource.
All detected contaminate springs both in Orvieto area and on Roccamonfina Volcano were referred to a unconsolidated weathered pyroclastic aquifer constituted by deposits emplaced in a similar period (about 330 ka). Then a detailed survey could be performed on the volcanic perithyrrenic domain to identify volcanic formations with the same characteristics in order evaluate if they show the same behavior.

References

Adamo P, Violante P, Wilson WJ (2001) *Tubular and spheroidal halloysite in pyroclastic deposits in the area of Roccamonfina volcano (Southern Italy).* Geoderma **99**: 295-316

Aiuppa A, Allard P, D'Alessandro W, Michel A, Parello F, Treuil M, Valenza M (2000) *Mobility and fluxes of major, minor and trace metals during basalt weathering and groundwater transport at Mt. Etna volcano (Sicily)*. Geochimica et Cosmochimica Acta **64** (11): 1827-1841

Allocca V, Celico F, Celico P, De Vita P, Fabbrocino S, Mattia C, Monacelli G, Musilli I, Piscopo V, Scalise AR, Summa G, Tranfaglia G (2007) *Carta idrogeologica dell'Italia Meridionale*. Istituto Poligrafico e Zecca dello Stato

Amodio M, De Rita D, Di Filippo M, Funiciello R, Galadini F, SposatoA (1987) *Evoluzione geologico-strutturale del bacino vulcano-tettonico di Bolsena (Complesso Vulcanico Vulsino)*. CNR Boll GNV: 21-36

Aomine S, Wada K (1962) *Differential weathering of volcanic ash and pumice, resulting in formation of hydrated halloysite*. The American Mineralogist **47**. 1024-1048

Appelo CAJ, Postma D (1995) *Geochemistry, Groundwater and Pollution*. Taylor & Francis, pp 668

Appleton JD (1972) *Petrogenesis of potassium-rich lavas from the Roccamonfina volcano, Roman region, Italy*. Journal of Petrology **13** (3): 425-456

ARPA Umbria (2013) *Dati monitoraggio acque superficiali, acque sotterranee e acque reflue*. http://www.arpa.umbria.it/pagine/elenco-monitoraggi

ATI4 (Ambito Territoriale Integrato), Sii Scpa (Servizio Idrico Integrato) (2011) *Indagini e studi idrogeologici dell'acquifero vulcanico vulsino nel territorio orvietano*. Relazione finale

Aurisicchio C, Nappi G, Renzulli A, Santi P (1992) *Mineral chemistry, glass composition and magma fractionation of the welded ignimbrite in the "Civitella d'Agliano Formation", Vulsini Volcanic District (Italy).*Mineralogica et Petrographica Acta **35**: 157-182

Baiocchi A, Lotti F, Piscopo V (2011) *Influence of hydrogeological setting on the arsenic occurrence in groundwater of the volcanic areas of central and southern Italy*. AQUA mundi Am04035: 131-142

Barberi F, Innocenti F, Landi P, Rossi U, Saitta M, Santacroce R (1984) *The evolution of Latera caldera (Central Italy) in the light of subsurface data*.Bull. Volcanol **47** (1): 125-141

Barberi F, Buonasorte G, Cioni R, Fiordelisi A, Foresi L, Iaccarino S, Laurenzi MA, Sbrana A, Vernia L, Villa IM (1994) *Plio-Pleistocene geological evolution of the geothermal area of Tuscany and Latium.*Mem. Descr. Carta Geol d'It. **49**: 77-134

Berner EK, Berner RA (1996) *Global environment*. Prentice Hall pp 376

Bertini M, D'Amico C, Deriu M, Girotti O, Tagliavini S, Vernia L (1971*) Note illustrative alla Carta Geologica d'Italia Foglio 137Viterbo*. Istituto Superiore per la Ricerca Ambientale. Roma

Boni CF, Bono P, Capelli G (1986) *Schema idrogeologico dell'Italia Centrale.*Mem. Soc. Geol. It. **35** (2) 991-1012

Buonasorte G, Fiordelisi A, Pandeli E, Rossi U, Sollevanti F (1987) *Stratigraphic correlations and structural setting of the pre-neoautochtonous sedimentary sequences of Nothern Latium*. Per Mineral **56**: 111-122

Buonasorte G, Pandelli E, Fiordelisi A, (1991) *The Alfina 15 well: deep geological data from Nothern Latium (Torre Alfina Geothermal Area)*. Boll. Soc. Geol. It. **110**: 823-831

Capaccioni B, Cinelli G, Mostacci D, Tositti L (2012) *Long-term risk in a recently active volcanic system: Evaluation of doses and indoor radiological risk in the quaternary Vulsini Volcanic District (Central Italy).*J. of Volcanol. And Geotherm. Res. **247**: 26-36

CapelliG, Mazza R, Trigari A, Catalani F (1999) *Le risorse idriche sotterranee strategiche nel distretto vulcanico di Roccamonfina (Campania nord-occidentale).* Atti del 3° convegno nazionale sulla protezione e gestione delle acque sotterranee per il III millennio. Quaderni di Geologia Applicata. Pitagora Ed. Bologna

Capelli G, Mazza R, GazzettiiC (2005) *Strumenti e strategie per la tutela e l'uso compatibile della risorsa idrica nel Lazio*. Quaderni di Tecniche di Protezione Ambientale vol **78**. Bologna

Capuano P, Continisio R, Gasparini P (1992) S*tructural setting of a typical alkali-potassic volcano: Roccamonfina, southern Italy*. J. of Volcanol. and Geotherm. Res. **53**: 355-369

Casentini B, Pettine M, Millero FJ (2010) *Release of Arsenic from volcanic rocks through interactions with inorganic anions and organic ligands*. Aquatic Geochemistry **16** (3): 373-393

Celico P (1988) *Prospezioni Idrogeologiche*. Liguori Ed. vol **1-2**: pp 1263

Chiesa S, Floris B, Gillot PY, Prosperi L, Vezzoli L (1995) *Il Vulcano di Roccamonfina*. In ENEA (Ed.), Lazio Meridionale. ENEA 128-150

Chiodini G, Frondini F (2001) *Carbon dioxide degassing from the Albani Hills volcanic region, Central Italy*. Chem. Geol. **177**: 67-83

Chiodini G, Giaquinto S, Zanzari AR (1982) *Caratteri idrochimici e analisi della distribuzione degli indicatori geotermici nelle acque del bacino del Fiume Paglia* in Bacino del Fiume Paglia (Umbria Toscana) studi strutturali, idrogeologici e geochimici. CNR – PFE – RF **16**: 56-90

Cioni R, Laurenzi MA, Sbrana A, Villa IM (1993) *$^{40}Ar/^{39}Ar$ chronostratigraphy of the initial activity in the Sabatini Volcanic Complex (Italy).*Boll. Soc. Geol. It. **112**: 251-263

Cole PD, Guest JE, Duncan AM, Chester DK, Bianchi R (1992) *Post collapse volcanic history of calderas on a composite volcano: an example from Roccamonfina volcano, southern Italy*. Bullettin of Volcanology **54**: 253-266

Cloutier V, Lefebvre R, Therrien R, Savard MM (2008) *Multivariate statistical analysis of geochemical data as indicative of hydrogeochemical evolution of groundwater in a sedimentary rock aquifer system*. Journal of Hydrology **353**: 294-313

Conticelli S, Peccerillo A (1992) *Petrology of final stage Latera lavas, Vulsini Mts.: mineralogical, geochemical and Sr-isotopic data and their bearing on the genesis of some potassic magmas in central Italy*. J. Volcanol. Geotherm. Res. **46**: 187-212

Cordeiro S, Coutinho R, Cruz JV (2012) *Fluoride content in drinking water supply in São Miguel volcanic island (Azores, Portugal)*. Science of the Total Environment **432**: 23-36

Croce A, Nazzaro R (2012) *The orchid flora of Roccamonfina – Foce Garigliano regional park (Campania, Italy)*. Journal of Europälscher orchideen **44** (3): 509-583

Cuoco E, Verrengia G, De Francesco S, Tedesco D (2010) *Hydrogeochemistry of Roccamonfina volcano (Southern Italy)*. Environ. Earth Sci. **61**: 525-538

Cuoco E, De Francesco S, Tedesco D (2013) *Hydrogeochemical dynamics affecting steamheated pools at El Chichon Crater (Chipas – Mexico)*. Geofluids **13** (3): 331-343

Custodio E, Llamas MR (2005) *Idrologia sotterranea*. Flaccovio Ed. vol **1-2**: pp 2200

Davis JC (1986) *Statistics and Data analysis in Geology*. John Wiley & Sons pp 656

De Jonge LW, Kjaergaard C, Moldrup P (2004) *Colloids and colloid-facilitated transport of contaminants in soils: an introduction*. Vadose Zone Journal **3**: 321-325

De Rita D, Giordano G (1996) *Volcanological and structural evolution of Roccamonfina Volcano (Southern Italy)*. In McGuire WJ, Jones AP, Neuberg J; Volcano Instability on the Earth and other planets. Geol. Soc. Lond. Spec. Publ. **110**: 209-224

De Rita D, Giordano G, Milli S (1997) *Forestepping-backstepping stacking pattern of volcanoclastic successions: Roccamonfina Volcano,Italy*. J. of Volcanol. And Geotherm. Res. **78**: 267-288

Deepagoda TKKC, Kawamoto K, Saito H, De Jonge LW, Moldrup P, Komatsu T (2011) *Mobilization and leaching of natural and water dispersible colloids in aggregated volcanic ash soil columns*. Soils and Foundations **51** (1): 123-132

Di Filippo M, Lombardi S, Nappi G, Reimer M, Renzulli A, Toro B (1999) *Volcano-tectonic structures, gravity and helium in geothermal areas of Tuscany and Latium (Vulsini Volcanic District), Italy*. Geothermics **28**: 377-393

Di Matteo L, Dragoni W (2006) *Rapporto sull'idrogeologia dell'area vulsina umbra e note illustrative della carta idrogeologica di sintesi in scala 1:25.000*. Progetto Emergenza Idrica O.P.G.R. n° 48/04 Analisi delle risorse idriche sotterranee nell'Umbria nord-occidentale e sud-occidentale. Relazione inedita pp 127

Di Matteo L, Dragoni W, Giontella C, Melillo M (2010) *Impact of climatic change on the management of complex systems: the case of Bolsena Lake and its aquifer (Central Italy).* Global Groundwater Resources and Management. Paliwal B.S. ed. **5**. 91-106

Dong-Chan K, Gi-Tak C, Yoon-Yeol Y, Bong-Rae K, Gi-Won K, Ki-Hwa P (2009) *Baseline geochemical characteristics of groundwater in the mountainous area of Jeju Island, South Korea: Implications for degree of mineralization and nitrate contamination*. Journal of Hydrology **376**: 81-93

Drever JI (1997) *The Geochemistry of natural waters*. Second edition. Pearson Education pp 437

Ducci D, Sellerino M (2012) *Natural background levels for some ions in groundwater of the Campania region (southern Italy)*. Environmental Earth Sciences **67** (3): 689-693

EPA Method 3015a *Microwave assisted acid digestion of aqueous samples and extracts*

Fieldes M, Perrott KW (1966) *The nature of allophone in soils. Part 3. Rapid field and laboratory test for allophone*. New Zealand J. Sci. **9**: 623-629

Faraone d, Stroppa F (1988) *Il tufo di Orvieto nel quadro dell'evoluzione vulcano tettonica della caldera di Bolsena, Monti Vulsini*. Boll. Soc. Geol. It. **107**. 383-397

Fornasieri M (1985) *Geochronology of volcanic rocks from Latium (Italy).*Rend SIMP **40**: 73-106

Frondini F, Francesconi F, Fratini S, Checcucci R (2013) *Geochimica delle acque sotterranee nel settore settentrionale dei Monti Vulsini.* Atti delle giornate itineranti SoGel 2012: "La valutazione del rischio geochimico: nuovi strumenti per una gestione sostenibile del territorio" e "Il ruolo della geochimica nel monitoraggio ambientale". 27 - 32

Galvez JF, Barahona E, Mingorance MD (2008) *Measurement of infiltration in a small field plots by a portable rainfall simulator: application to trace-element mobility*. Water, Air and Soil Pollution **191**: 257-264

Giannetti B (1964) *Contributo alla conoscenza del vulcano di Roccamonfina. Nota I: le ultime manifestazioni eruttive della caldera*. Boll. Soc. Geol. It. **83** (3): 87-133

Giannetti B (1979) *The geology of Roccamonfina caldera (Campanian Province, Italy).* Giornale Geologia ser 2, 43: 187-206

Giannetti B (1996) *The geology of the Yellow Trachytic Tuff, Roccamonfina volcano, Italy*. J Volcanol. Geotherm. Res. **71**: 53-72

Giannetti B (2001) *Origin of the calderas and evolution of Roccamonfina volcano (Roman region, Italy)*. J. Volanol. Geotherm. Res. **106**: 301-319

Giannetti B, De Casa G (2000*) Stratigraphy, chronology and sedimentology of ignimbrites from the white trachytic tuff, Roccamonfina Volcano, Italy*. J. Volcanol. Geotherm. Res. **96**: 243-295

Gillot PY, Nappi G, Santi P, Renzulli A (1991) *Space-time evolution of the Vulsini Volcanic Complexes, central Italy*. Abstract EUG VI Strasburg 24-28 March 1991: 446

Giordano G (1996) *Carta geologica del settore SW del vulcano di Roccamonfina*. Phd Thesis pp 171

Gray CW, McLaren (2006) *Soil factors affecting heavy metal solubility in some New Zealand soils*. Water, Air and Soil Pollution **175**: 3-14

Guo H, Zhang B, Zhang Y (2011) *Control of organic and iron colloids on arsenic partition and transport in high arsenic groundwaters in the Hetao basin, Inner Mongolia.* Applied Geochemistry **26**. 360-370

Haan CT (1977) *Statistical Methods in Hydrology*. Iowa State University Press, Ames, USA.

International Standard (2007) ISO 748:2007, *Hydrometry, Measurement of liquid flow in open channels using current-meters or floats*. International Organization for Standardization

Ippolito F, Ortolani F, Russo M (1973) *Struttura marginale tirrenica dell'Appennino campano: reinterpretazioni dei dati di antiche ricerche di idrocarburi*. Mem. Soc. Geol. It. **12**: 227-250

IRSA (2004) *Metodi analitici per le acque*. pp 1153

Laaksoharju M, Skårman C, Skårman E (1999) *Multivariate mixing and Mass-balance (M3) calculation, a new tool for decoding hydrogeochemical information*. Applied Geochemistry **14** (7): 861-871

Laegdsmand M, Moldrup P, De Jonge LW (2007) *Modelling of colloid leaching from unsaturated, aggregated soil.*European Journal of Soil Science **58** (3): 692-703

LINQ (2013) *Archivio dati geologico-idrogeologico del Laboratorio di Idrogeologia*. Università degli Studi Roma Tre

Luhr JF, Giannetti B (1987) *The Brown Leucitic Tuff of Roccamonfina volcano (Roman Region, Italy)*. Contrib. Miner. Petrol. **95**: 420-436

Lulli L, Bidini D, Dabin B, Quantin P (1983) *Étude de deux sols andique dérivés de roches volcaniques d'Italie du Sud (Monts Roccamonfina et Vulture) à caractère cryptopodzolique*. Environnement, morphologie et caractères des constituants minéraux. Cah Pedol. **XX** (1): 27-44

Marra F, Taddeucci J, Freda C, Marzocchi W, Scarlato P (2004) *Recurrence of volcanic along the Roman Comagmatic Province (Thyrennian margin of Italy) and its tectonic significance*. Tectonics **23**: 1-15

Mazza R, Pietrosante A, Taviani S, Viaroli S (2013) *A preliminary understanding of groundwater exchanges between the Riardo Plain and Mount Maggiore ridge (Campania, Italy).*IX Convegno Nazionale Giovani Ricercatori Napoli 14-15 Febbraio 2013

Mc Carthy JF, Zachara JM (1989) *Subsurface transport of contaminants*. Environ. Sci. Technol. **23**: 496-502

Metzelin S, Vezzoli L (1983) *Contributi alla geologia del Vulcano di Latera (Monti Vulsini, Toscana meridionale-Lazio settentrionale).*Mem. Soc. Geol. It. **25**: 247-271

Mizota C, van Reeuwijk LP (1989) *Clay mineralogy and chemistry of soils formed in volcanic material in diverse climatic regions*. Soil Monograph 2, ISRIC pp 185

Nappi G (1969) *Stratigrafia e petrografia dei Vulsini sud-occidentali (Caldera di Latera).* Boll. Soc. Geol. It. **88**: 171-181

Nappi G, Chiodi M, Rossi S, Volponi E (1982) *L'ignimbrite di Orvieto nel quadro dell'evoluzione volcano-tettonica dei Vulsini orientali. Caratteristiche geologiche e tecniche*. Boll. Soc. Geol. Ital. **101**: 327-342

Nappi G, Renzulli A, Santi P (1991*) Evidence of incremental growth in the vulsinian calderas (Central Italy)*. J. Volcanol. Geotherm. Res. **47**: 13-31

Nappi G, Capaccioni B, Renzulli A, Santi P, Valentini L (1994) *Stratigraphy of the Orvieto-Bagnoregio ignimbrite eruption (eastern Vulsini District Central Italy)*. Mem Descr. Carta Geol. D'It. **49**: 241-254

Nappi G, Renzulli A, Santi P, Gillot PY (1995) *Geological evolution and geochronology of the Vulsini Volcanic District (Central Italy)*. Bull. Soc. Geol. Ital. **114**: 599-613

Nappi G, Antonelli F, Coltorti M, Milani L, Renzulli A, Siena F (1998) *Volcanological and petrological evolution of the Eastern Vulsini District, Central Italy*. J. of Volcanol. And Geotherm. Res. **87**: 211-232

Nappi G, Renzulli A, Santi P, Gillot PY (2005) *Geological evolution and geochronology of the Vulsini Volcanic District (Central Italy)*. Bull. Soc. Geol. Ital. **114**: 599-613

Nicotera P, Civita M (1969) *Idrogeologia della piana del basso Garigliano (Italia meridionale).* Memorie e Note dell'Ist. Di Geol. Appl. dell'Università di Napoli 11 parte 2

Pagano G, Menghini A, Floris S (2000) *Bilancio idrogeologico del bacino vulsino*. Geologia Tecnica & Applicata vol **3**

Palladino DM, Valentine GA (1995) *Coarse-tail vertical and lateral grading in pyroclastic flow deposits of the Latera Volcanic Complex (Vulsini Central Italy): origin and implications for flow dynamics*. J. Volcanol. Geotherm. Res. **69** (3-4): 343-364

Palladino DM, Agosta E (1997) *Pumice fall deposits of the Western Vulsini Volcanoes (Central Italy)*. J. Volcanol. Geotherm. Res. **78** (1-2): 77-102

Palladino DM, Simei S (2005) *Eruptive dynamics and caldera-collapse during the Onano eruption, Vulsini, Italy*. Bull. Volcanol. **67**: 423-440

Paone A (2004) *Evidence of crustal contamination, sediment and fluid components in the companion volcanic rocks*. J. Volcanol. Geotherm. Res. **138**: 1-26

Peccerillo A (2005) Plio-Quaternary volcanism in Italy. Springer XIV: pp 365

Poulsen TG, Moldrup P, De Jonge LW, Komatsu T (2006)*Colloid and Bromide transport in undisturbed soil columns: application of two-regional model*. Vadose Zone Journal **5:** 649-656

Preziosi E, Giuliano G, Vivona R (2010) *Natural background levels and threshold values derivation for naturally As, V and F rich groundwater bodies: a methodological case study in Central Italy.*Environmental Earth Sciences **61** (5): 885-897

Quantin P, Gautheyrou J, Lorenzoni P (1988) *Halloysite formation through in situ weathering of volcanic glass from trachytic pumices, Vico's Volcano, Italy*. Clay Minerals **23**. 423-437

Regione Lazio (2013) Dati termo-pluviometrici servizio idrografico regionale http://www.idrografico.roma.it/annali/

Regione Umbria (1991) *Piano ottimale di utilizzazione delle risorse idriche della regione (I stralcio) – I fase operativa. Indagini geoidrologiche preliminari – area vulcanica di Orvieto*. Assessorato Difesa del Suolo, Ambiente e Infrastrutture, Perugia

Regione Umbria (2013) Dati termo-pluviometrici servizio idrografico regionale http://www.idrografico.regione.umbria.it/annali/Default.aspx

Rouchon V, Gillot PY, Quidelleur X, Chiesa S, Floris B (2008) *Temporal evolution of the Roccamonfina volcanic complex (Pleistocene), Central Italy*. J. of Volcanol. And Geotherm. Res. **177**: 500-514

Ryan JN, Elimelech M (1996) *Colloid mobilization and transport in groundwater*. Colloids and surfaces, A: Physiochemical and Engineering Aspects **107**: 1-56

Santello L (2010) *Analysis of a trampled formation: the Brown Leucitic Tuff (Roccamonfina volcano, Southern Italy).* PhD Thesis pp154

Santi P (1990) *New geochronological data of the Vulsini Volcanic District (central Italy).*Proceedings of SIMP Congress on "Genesi e differenziazione del magmatismo potassico del bordo tirrenico", Ischia 15-18 October 1990

Schelde K, Moldrup P, Jacobsen OH, De Jonge H, De Jonge LW, Komatsu T (2002) *Diffusion-limited mobilization and transport of natural colloids in macroporous soil*. Vadose Zone Journal **1**: 125-136

Sequaris JM, Klumpp E, Vereecken H (2013) *Colloidal properties and potential release of water-dispersible colloids in an agricultural soil depth profile*. GEODERMA **193**: 94-101

Servizio Geologico d'Italia (1971a) Carta Geologica d'Italia alla scala 1:100.000 – Foglio 161 "Isernia"

Servizio Geologico d'Italia (1971b) Carta Geologica d'Italia alla scala 1:100.000 – Foglio 172"Caserta"

Seta AK, Karathanasis AD (1996) *Water dispersible colloids and factors influencing thei dispersibility from soil aggregates*. Geoderma **74:** 255-266

Sparks RSJ (1973) *Products of ignimbrite eruptions*. Geology **1**: 115-118

Sparks RSJ (1975) *Stratigraphy and geology of the ignimbrites of Vulsini Volcano Central Italy*. Geol. Rundsch. **64**: 497-523

Stumm W, Morgan JJ (1996) *Aquatic chemistry: chemical equilibria and rates in natural waters*. Third edition. Wiley –Interscience Publication. pp 1005

Toro B (1978) *Anomalie residue di gravità e strutture profonde nelle aree vulcaniche del Lazio settentrionale*. Geol. Romana **17**: 35-44

Vacca A, Adamo P, Pigna M, Violante P (2003) *Genesis of Tephra-derived soils from the Roccamonfina Volcano, South Central Italy*. Soil Sci. Soc. Am. J. **67**: 198-207

Varekamp JC (1980) *The geology of the Vulsinian area Latium Italy*. Bull. Volcanol. **43** (3): 487-503

Vezzoli L, Conticelli S, Innocenti F, Landi P, Manetti P, Palladino DM, Triglia R (1987) *Stratigraphy of the Latera Volcanic Complex: proposal for a new nomenclature*. Per Mineral. **56**: 89-110

Walkley A, Black IA (1934) *An examination of the Degtjareff method for determining soil organic matter and proposed modification of the chromic acid tritation method*. Soil Science **37**: 29-38

Watts MD (1987) *Geothermal exploration of the Roccamonfina volcano, Italy*. Geothermics **16** (5/6): 517-528

Wilbur S, Soffey E (2004) In: McCurdy (ed) *Real world analysis of trace metals in drinking water using Agilent 7500cd ICP-MS with ORS Technology*

A.Surveyed wells data

Code	Longitude	Latitude	Ground elevation	Water depth	Water table elevation (2013)	Water table elevation (2011)
			meters	meters	meters a.s.l.	meters a.s.l.
P19	258440	4727695	578	-149.9	428.1	426.7
P35 OV3	253662	4732083	546	-109.7	436.3	438.1
P44	258697	4732239	462	-69.1	392.9	397.5
P47	259527	4732426	465	-80.7	384.3	384.4
P28	251204	4734472	534	-66.45	467.55	467
P74	254625	4733551	515	-78.13	436.87	436.2
P41	255534	4733834	503	-71.9	431.1	431.8
P80	253500	4733015	535	-87.07	447.93	447.9
P18	252996	4730199	616	-189.96	426.04	428.1
P77	249374	4733953	547	-113.6	460.4	460.4
P63 OV4	252696	4730685	580	-39.43	540.57	n/a
P64 OV1	258349	4729131	489	-59.97	429.03	428.4
P65 OV6	255241	4730631	555	-121.07	433.93	435.1
P126	259876	4727175	550	-124.85	425.15	424.3
P85 OV8	261376	4731649	440	-81.2	358.8	358.8
P515	257411	4729452	580	-149.2	430.8	n/a
P40	258844	4729310	489	-57.4	431.6	n/a

Tab 11 Data collected during the hydrogeological survey of Roccamonfina Volcanic Compelx (2012). Projected coordinate system UTM Zone 33N ED 50

Code	Longitude	Latitude	Ground elevation	Well depth	Water depth	Water table elevation
			m a.s.l.	meters	meters	m a.s.l.
VP417052P1	421314	4574886	220	n/a	99.8	120.3
VP417052P2	423182	4574280	182	75.0	63.6	118.4
VP417052P3	421440	4574088	205	n/a	87.4	117.6
VP417062P2	427636	4573363	140	50.0	35.2	104.8
VP417062P3	428745	4573439	130	8.0	5.1	124.9
VP417062P4	428852	4573692	128	100.0	27.8	100.2
VP417062P5	428576	4572797	128	110.0	28.3	99.7
VP417062P6	429327	4574459	118	n/a	18.1	99.9
VP417062P7	429933	4574099	123	100.0	26.1	96.4
VP417063P1	425896	4574242	145	6.0	2.0	143.0
VP417063P2	424031	4573717	168	75.0	46.1	121.9
VP417063P3	425792	4573551	152	10.0	7.6	144.4
VP417063P4	426514	4573377	144	120.0	33.7	110.4
VP417063P5	425121	4573004	159	60.0	7.7	151.4
VP417063P6	425073	4573500	156	70.0	22.7	133.3
VP417064P2	423284	4575562	170	100.0	50.2	119.8
VP417064P3	423267	4575558	170	8.0	6.1	163.9
VP417064P6	424247	4576017	164	60.0	45.6	118.4
VP417073P1	430729	4573904	115	100.0	12.8	102.2
VP417074P2	431900	4576237	105	n/a	5.0	100.0
VP417074P3	432170	4576913	105	11.0	5.4	99.6
VP417074P4	432248	4576868	105	70.0	6.8	98.2
VP417101P1	429276	4571739	127	150.0	50.0	77.0
VP417101P2	427616	4570984	140	n/a	28.4	111.6
VP417101P4	428306	4569705	123	100.0	14.9	108.2
VP417101P5	429508	4570719	125	10.0	4.3	120.7
VP417101P6	427911	4571417	135	n/a	14.7	120.4
VP417101P7	426952	4571676	139	60.0	25.3	113.7
VP417102P1	428790	4567103	161	70.0	48.0	113.0
VP417102P2	427372	4566903	125	41.0	13.0	112.0
VP417102P5	427382	4569413	132	62.0	16.9	115.1
VP417102P6	428012	4568023	129	9.0	3.9	125.1
VP417103P1	424462	4569392	180	n/a	22.5	157.6
VP417103P2	424688	4567818	153	100.0	47.7	105.3
VP417103P3	425502	4567192	122	75.0	18.1	103.9
VP417103P4	425801	4569229	158	n/a	46.7	111.3
VP417103P5	425478	4569372	165	n/a	52.9	112.1
VP417103P6	425114	4568536	149	95.0	36.1	112.9
VP417104P1	425589	4571561	160	60.0	44.4	115.6
VP417104P2	424236	4571737	186	140.0	70.5	115.5
VP417104P3	424013	4570496	185	110.0	85.2	99.8
VP417104P4	425047	4569991	185	80.0	49.7	135.3

Code	Longitude	Latitude	Ground elevation	Well depth	Water depth	Water table elevation
			m a.s.l.	meters	meters	m a.s.l.
VP417104P5	426056	4570151	155	106.0	39.6	114.9
VP417112P1	435718	4568311	211	n/a	6.5	204.5
VP417112P2	433752	4568461	150	150.0	80.0	70.0
VP417113P1	430264	4567413	175	13.0	5.6	169.4
VP417113P2	432181	4568525	145	150.0	98.7	46.4
VP417113P3	433358	4567733	185	17.0	10.0	175.1
VP417113P4	431363	4568598	130	90.0	65.5	64.5
VP417113P5	431332	4568251	135	8.0	7.2	127.8
VP417113P6	430559	4568261	142	32.0	21.2	120.8
VP417113P9	430768	4567223	215	250.0	170.0	45.0
VP417114P1	430781	4572165	118	30.0	11.8	106.2
VP417141P1	426767	4565855	125	n/a	2.3	122.7
VP417074P1	431237	4576010	113	66.0	49.0	64.0
VP417074P2	431900	4576237	105	n/a	5.2	99.9
VP417074P3	432170	4576913	105	11.0	4.9	100.1
VP417074P23	432363	4577331	120	n/a	70.0	50.0
VP417074P24	432547	4576397	103	n/a	6.8	96.3
VP417073P9	430879	4573098	120	110.0	45.0	75.0
VP417073P52	431139	4573877	112	114.0	46.2	65.8
VP417113P42	432356	4568938	135	65.0	8.6	126.5
VP417113P43	432891	4568956	133	150.0	70.0	63.0
VP417113P44	432889	4568739	138	15.0	2.3	135.7
VP417101P11	427721	4571058	136	n/a	6.0	130.0
VP417101P3	428399	4570997	131	104.0	31.4	99.6
VP417101P43	427690	4571374	137	n/a	24.3	112.7
VP417101P10	428017	4571449	134	100.0	23.6	110.4
VP417101P45	427014	4571539	139	n/a	6.4	132.6
VP417101P47	427233	4572192	140	n/a	28.7	111.3
VP417104P32	426549	4571886	150	100.0	34.7	115.3
VP417112P19	434181	4569112	145	7.0	4.3	140.7
VP417112P20	433772	4568941	142	n/a	3.6	138.5
VP417112P21	434042	4568686	149	20.0	2.9	146.1
VP417112P22	434007	4568416	157	n/a	3.7	153.3
VP417112P23	435380	4568967	164	180.0	140.0	24.0
VP417112P25	434650	4569353	153	140.0	108.8	44.2
VP417112P6	433879	4569402	143	40.0	5.9	137.2
VP417112P26	435211	4568607	180	7.0	3.9	176.2
VP417111P10	433682	4570976	139	n/a	2.4	136.6
VP417112P27	434591	4569034	154	30.0	3.0	151.0
VP417111P13	433771	4570557	142	117.0	96.1	45.9
VP417114P16	432333	4571496	142	128.0	94.5	47.6
VP417111P11	434234	4570408	148	150.0	110.0	38.0

Code	Longitude	Latitude	Ground elevation	Well depth	Water depth	Water table elevation
			m a.s.l.	meters	meters	m a.s.l.
VP417114P62	433188	4572058	143	180.0	98.5	44.5
VP417114P64	431833	4570624	124	60.0	4.0	120.0
VP417073P53	432111	4573500	118	8.0	2.8	115.2
VP417114P65	431493	4570754	123	208.0	70.4	52.7
VP417114P67	432925	4569957	132	8.0	3.5	128.5
VP417114P68	432851	4569509	130	n/a	88.4	41.6
VP417113P45	430235	4567456	174	153.0	128.5	45.5
VP417113P7	431630	4568138	142	155.0	101.5	40.5
VP417114P69	431243	4569705	123	120.0	42.1	80.9
VP417102P74	428515	4567550	143	80.0	56.0	87.0
VP417062P1	427370	4573039	138	100.0	33.6	104.4
VP417062P8	429890	4574020	123	100.0	24.0	98.5
VP417062P4	428852	4573692	128	100.0	26.7	101.3
VP417114P82	431243	4571405	120	20.0	7.5	112.5
VP417111P3	436703	4570284	282	275.0	245.0	37.0

Tab 12 Data collected during the hydrogeological survey of Roccamonfina Volcanic Compelx (2012). Projected coordinate system UTM Zone 33N WGS 84

B. Chemical analyses

ICP-MS statement: suffered interference, ORS mode and integration time for each element

Element	Suffered Interferences	Chosen isotope	ORS mode	Itegration time
Li	Does not suffer from any interferences	7	norm	0.3
Be	Does not suffer from any interferences	9	norm	0.3
B	Does not suffer from any interferences in aqueous solutions	11	Norm	0.3
Al	High level of Mg may lead to 26MgH interference. It can also suffer from a CN interference in high C matrices	27	He	1.5
Si	29Si is often preferred for the determination of Si a sit has the least interferences, however 29Si is <5% abundant and therefore limits of detection will be poor. The main interference on 28Si is N_2	28	H2	1.5
V	Only 31V should be used (50V is both low abundance and subject to interference from Cr and Ti isotopes.) V readily suffers interference from ClO and SOH species.	51	He	1.5
Cr	The main Cr isotopes can suffer interference from Ar, C, Cl and S based species	52	He	1.5
Mn	Manganese can suffer from KO_2, ArN and CaN interferences	55	norm	0.3
Fe	Iron suffers from several plasma based interferences (e.g. ArO) and also from CaO interference	56	H2	1.5
Co	Cobalt can suffer from CaO, SO2 and ArF interferences	59	norm	0.3
Ni	60Ni is preferred for analysis as the major isotope, 58Ni suffers interference from both Fe and ArO. The presence of Ca compounds in the sample can also lead to interferences from CaO	60	He	1.5
Cu	Both isotopes of Cu can suffer from interferences by Ca, Ti and S species and 63Cu is notably subject to interferences from NaAr and P species.	63	He	1.5

Zn	The presence of S compounds in the sample can lead to interferences from S2 and SO2	66	norm	0.3
As	May be Subject to interference from rare earth element 2+ ions. Chlorine matrices readily lead to ArCl interferences on As	75	He	1.5
Se	Does not suffer from any interferences	78	He	0.3
Rb	Rb suffers from few interferences except from some rare earth elements 2+ ions	85	He	0.3
Sr	Sr can form doubly charged species which are coincident with Ca isotopes. Sr may be subject to interference from rare earth element 2+ ions.	88	norm	0.3
Mo	Some isotopes may be subject to interference from ZrH	95	norm	0.3
Cd	In presence of high concentration of Mo, all isotopes except 106Cd are subject to interference from MoO.	111	norm	0.3
Ba	Ba forms 2+ ions which can interfere with Ga and Zn isotopes	138	norm	0.3
Tl	Does not suffer from any interferences	205	norm	0.3
Pb	Does not suffer from any interferences	208	norm	0.3
U	Does not suffer from any interferences	238	norm	0.3

Vulsini monitoring area – In field parameters and IC analysis

ID		Date	T	E.C.	pH	HCO_3	F	Cl	NO_3	SO_4	Na	K	Mg	Ca
			°C	*µS/cm*		*mg/L*	*mg/L*	*mg/L*	*mg/L*	*mg/L*	*mg/L*	*mg/L*	*mg/L*	*mg/L*
CAN	**E**	30/04/13	n/a	n/a	n/a	109,8	0,1	14,2	33,4	14,0	17,8	12,2	8,1	21,9
CAN	**F**	10/05/13	13,4	313	6,75	114,7	0,1	14,4	34,5	14,6	17,9	12,3	8,6	23,0
CAN	**G**	16/05/13	13,5	318	6,93	122,0	0,1	14,9	35,6	15,3	18,1	12,8	8,9	24,2
CAN	**H**	28/05/13	13,7	324	6,58	125,7	0,1	15,0	35,2	14,8	19,0	14,9	10,0	25,4
CAN	**L**	28/06/13	13,8	349	6,7	126,3	0,2	14,5	35,0	14,8	18,8	14,7	10,4	27,7
RR1	**A**	28/03/13	13,4	205	7,06	81,8	0,2	8,5	17,2	6,2	13,2	10,8	4,7	12,5
RR1	**B**	04/04/13	13,4	207	7,2	81,8	0,2	8,8	17,3	6,4	13,4	10,8	5,3	14,4
RR1	**C**	11/04/13	13,5	207	6,76	85,4	0,3	8,6	15,2	6,1	13,6	11,9	5,6	15,0
RR1	**D**	18/04/13	13,5	209	6,72	85,4	0,3	8,6	15,9	6,8	13,2	11,7	5,6	14,9
RR1	**E**	30/04/13	13,6	211	6,92	88,5	0,3	9,0	16,2	6,8	13,3	10,2	5,1	14,4
RR1	**F**	10/05/13	13,6	211	6,57	85,4	0,3	9,0	16,9	7,1	12,8	9,7	5,1	14,5
RR1	**G**	16/05/13	13,8	213	6,78	87,9	0,2	8,9	16,8	6,7	12,8	10,2	5,3	14,8
RR1	**H**	28/05/13	14	216	6,7	90,3	0,5	9,2	17,6	7,4	13,2	11,1	6,1	16,9
RR1	**L**	28/06/13	14,8	222	6,8	97,0	0,4	9,5	17,6	7,4	13,1	11,8	5,9	16,3
RR2	**A**	28/03/13	13,1	202	7,28	83,6	0,2	8,3	17,4	6,2	12,9	10,9	4,9	14,3
RR2	**B**	04/04/13	13,3	206	7,17	81,8	0,2	8,7	17,0	6,4	13,1	10,8	5,2	14,5
RR2	**C**	11/04/13	13,3	207	7,15	83,8	0,3	8,5	15,7	6,5	13,3	11,7	5,5	14,7
RR2	**D**	18/04/13	13,5	209	7,35	85,4	0,4	8,4	15,8	6,7	13,2	11,8	5,6	15,0
RR2	**E**	30/04/13	13,7	211	7,04	92,8	0,3	8,9	16,7	6,7	13,2	10,6	5,1	18,1
RR2	**F**	10/05/13	13,7	211	6,85	88,5	0,3	8,7	16,6	6,8	12,8	10,4	5,1	14,5
RR2	**G**	16/05/13	13,6	213	7	86,6	0,2	8,8	16,6	6,8	12,5	9,5	5,2	15,0
RR2	**H**	28/05/13	13,6	215	6,68	94,0	0,4	9,4	17,6	7,3	12,8	9,9	6,0	16,0
RR2	**L**	28/06/13	14,8	220	7,2	92,8	0,4	9,4	17,3	7,6	13,1	12,1	6,0	16,5
RR3	**A**	28/03/13	13,3	205	7,21	81,8	0,2	8,4	17,5	6,2	13,1	10,7	5,1	14,4
RR3	**B**	04/04/13	13,4	207	6,81	97,6	0,4	8,5	17,7	6,5	13,1	10,8	5,4	18,4
RR3	**C**	11/04/13	13,4	207	7,21	84,2	0,3	8,6	15,5	6,3	13,0	10,7	5,5	14,9
RR3	**D**	18/04/13	13,5	209	7,34	85,4	0,3	8,3	16,0	6,4	13,1	11,8	5,6	15,0
RR4	**A**	28/03/13	13,5	205	7,25	81,8	0,2	8,5	17,1	6,2	12,7	10,5	4,9	13,8
RR4	**B**	04/04/13	13,1	206	7,3	85,4	0,4	8,8	15,8	6,4	13,0	10,4	5,3	14,5
RR4	**C**	11/04/13	13,3	207	7,3	83,0	0,3	8,3	16,9	6,4	13,2	11,6	5,4	14,4
RR4	**D**	18/04/13	13,7	209	7,36	85,4	0,4	8,5	15,6	6,4	13,1	11,8	5,5	14,8
RR4	**E**	30/04/13	13,8	210	6,9	87,9	0,3	8,7	16,1	7,0	13,0	10,1	5,1	14,5
RR4	**F**	10/05/13	13,8	211	7,03	87,3	0,3	9,1	16,6	7,0	12,4	9,6	5,1	14,5
RR4	**G**	16/05/13	13,5	212	7,02	88,5	0,3	8,9	17,1	7,3	12,6	9,4	5,2	15,2
RR4	**H**	28/05/13	13,4	216	6,66	92,1	0,4	9,5	17,4	7,3	13,3	12,0	5,9	15,5
RR4	**L**	28/06/13	15	220	7,4	91,53	0,4	9,35	17,3	7,29	13,1	11,8	5,9	16,5
RR5	**A**	28/03/13	14,5	267	6,85	113,5	1,1	18,4	8,2	6,8	17,6	17,7	6,0	17,1
RR5	**B**	04/04/13	14,6	266	6,78	112,3	1,5	18,4	7,8	6,8	17,6	17,9	6,2	18,8
RR5	**C**	11/04/13	13,3	268	7	109,8	1,2	18,2	7,2	6,9	17,6	18,7	6,3	17,6
RR5	**D**	18/04/13	14,6	268	6,77	109,8	1,2	18,5	7,5	7,1	17,3	18,7	6,3	17,4
RR5	**E**	30/04/13	14,8	287	6,86	88,1	1,1	18,8	7,7	7,0	17,2	16,3	5,2	15,9
RR5	**F**	10/05/13	14,8	268	6,59	109,8	1,1	18,8	8,0	6,9	17,5	16,1	5,5	16,3
RR5	**G**	16/05/13	14,9	265	6,52	111,7	1,1	18,4	8,6	6,8	17,2	16,4	5,6	16,4
RR5	**H**	28/05/13	14,9	268	6,65	119,6	1,5	18,4	8,7	7,2	18,0	18,6	6,2	17,0
RR5	**L**	28/06/13	15,7	269	6,67	111,23	1,1	18,2	8,5	7,1	17,9	18,6	6,0	17,4

Vulsini monitoring area – ICP-MS analysis on unfiltered samples

ID		Date	B	Al	Si	V	Mn	Fe	Rb	Sr	Ba
			µg/L	*µg/L*	*mg/L*	*µg/L*	*µg/L*	*µg/L*	*µg/L*	*µg/L*	*µg/L*
CAN	**E**	30/04/13	27.8	5068.4	20.1	20.5	9.1	1053.8	16.1	294.6	46.7
CAN	**F**	10/05/13	30.6	3445.2	19.8	18.7	7.2	792.1	14.6	324.5	39.8
CAN	**G**	16/05/13	28.8	3394.1	20.4	20.7	6.4	732.0	16.0	337.1	37.6
CAN	**H**	28/05/13	32.0	1968.7	18.4	19.6	4.8	451.4	14.9	372.6	32.9
CAN	**L**	28/06/13	31.5	187.4	17.5	15.9	n/a	41.9	14.1	371.4	16.4
RR1	**A**	28/03/13	40.1	8223.6	24.2	17.1	19.7	1976.5	20.5	158.8	74.2
RR1	**B**	04/04/13	31.7	5735.0	22.6	15.8	13.5	1308.8	17.6	179.1	60.0
RR1	**C**	11/04/13	31.3	6770.4	23.6	16.9	16.8	1775.4	19.4	178.8	72.9
RR1	**D**	18/04/13	31.2	6219.4	21.6	17.0	11.7	1293.2	19.0	182.9	56.6
RR1	**E**	30/04/13	31.7	3281.9	24.1	16.0	6.9	904.8	16.5	204.8	42.0
RR1	**F**	10/05/13	31.1	2395.3	18.5	15.8	5.7	546.8	15.8	212.9	36.4
RR1	**G**	16/05/13	30.2	2126.5	18.9	15.7	5.6	532.3	16.1	217.1	33.5
RR1	**H**	28/05/13	34.6	1738.7	18.5	15.6	5.3	473.7	16.1	227.9	31.5
RR1	**L**	28/06/13	38.1	529.7	17.9	13.2	n/a	166.5	15.6	214.4	18.3
RR2	**A**	28/03/13	33.4	7112.6	22.9	16.7	16.0	1720.9	20.2	160.2	68.6
RR2	**B**	04/04/13	29.9	6533.8	24.3	17.1	14.3	1496.5	20.0	175.3	61.8
RR2	**C**	11/04/13	28.5	6689.3	22.8	17.2	14.4	1509.9	20.2	177.0	61.1
RR2	**D**	18/04/13	39.1	5930.5	21.2	17.4	13.0	1234.3	19.9	188.4	57.2
RR2	**E**	30/04/13	30.1	3561.9	20.1	16.2	7.8	835.0	17.4	204.2	42.0
RR2	**F**	10/05/13	31.0	1090.8	17.5	15.3	4.3	254.2	15.2	209.3	33.3
RR2	**G**	16/05/13	29.8	2223.1	18.9	15.5	6.1	561.9	16.6	216.2	33.5
RR2	**H**	28/05/13	36.9	1840.9	17.4	16.2	5.6	451.2	17.2	223.5	31.3
RR2	**L**	28/06/13	53.7	592.7	16.9	12.7	1.7	176.7	15.9	218.5	19.3
RR3	**A**	28/03/13	40.5	7364.8	23.8	16.7	36.1	1977.6	19.8	164.9	75.2
RR3	**B**	04/04/13	319.9	5828.3	21.8	16.9	13.1	1262.1	18.8	177.1	64.8
RR3	**C**	11/04/13	27.9	6683.8	21.6	17.0	16.2	1518.7	19.3	183.0	60.9
RR3	**D**	18/04/13	32.6	6388.3	21.9	17.5	11.7	1341.0	19.7	183.5	54.9
RR4	**A**	28/03/13	29.8	6641.6	21.9	16.5	16.6	1606.5	19.4	159.4	71.1
RR4	**B**	04/04/13	31.3	6606.0	21.9	17.2	15.0	1461.0	20.2	177.1	59.4
RR4	**C**	11/04/13	29.4	6441.6	21.5	16.9	15.5	1616.5	19.9	179.3	63.2
RR4	**D**	18/04/13	29.3	6352.7	21.1	17.0	13.1	1371.0	19.8	185.0	57.0
RR4	**E**	30/04/13	29.6	3295.2	19.6	16.0	7.7	751.6	17.3	204.0	42.7
RR4	**F**	10/05/13	34.1	1249.9	17.7	15.3	4.3	294.0	15.5	213.1	34.6
RR4	**G**	16/05/13	30.5	2089.8	18.4	15.4	5.8	510.3	16.8	220.4	34.0
RR4	**H**	28/05/13	37.4	1547.6	18.6	15.3	5.4	452.7	16.4	225.9	31.0
RR4	**L**	28/06/13	33.1	529.5	16.5	12.5	1.3	174.8	15.8	213.1	17.9
RR5	**A**	28/03/13	69.5	129.7	32.0	21.1	4.1	170.8	19.0	278.0	39.2
RR5	**B**	04/04/13	62.8	92.2	24.4	21.6	1.8	49.9	19.1	259.9	35.6
RR5	**C**	11/04/13	52.6	142.0	23.9	21.1	2.3	75.4	19.1	264.4	37.7
RR5	**D**	18/04/13	55.9	68.6	23.6	21.8	2.0	44.5	19.5	267.6	37.3
RR5	**E**	30/04/13	49.1	37.2	28.0	20.3	1.8	70.2	18.3	255.6	35.0
RR5	**F**	10/05/13	58.2	88.9	22.8	21.2	1.7	47.1	19.2	260.4	35.9
RR5	**G**	16/05/13	54.1	47.5	22.5	21.5	3.0	75.2	19.6	263.3	35.4
RR5	**H**	28/05/13	51.8	68.5	21.5	20.9	2.3	120.3	19.0	262.9	36.0
RR5	**L**	28/06/13	46.2	13.0	20.6	18.7	n/a	5.5	19.9	241.1	29.7

Vulsini monitoring area – ICP-MS analysis on 0.45 μm filtered samples

ID		Date	B	Al	Si	V	Mn	Fe	Rb	Sr	Ba
			μg/L	*μg/L*	mg/L	*μg/L*	*μg/L*	*μg/L*	*μg/L*	*μg/L*	*μg/L*
CAN	**E**	30/04/13	25.8	51.3		16.9	n/a	9.1	12.3	287.0	21.2
CAN	**F**	10/05/13	24.0	58.8		16.8	n/a	8.7	12.7	297.9	22.8
CAN	**G**	16/05/13	45.3	55.3	24.2	20.2	n/a	10.8	14.5	313.9	23.9
CAN	**H**	28/05/13	38.9	19.1	24.7	18.5	n/a	5.6	13.9	342.4	25.4
CAN	**L**	28/06/13	35.3	7.2	24.8	18.9	n/a	2.1	14.4	347.0	24.5
RR1	**A**	28/03/13	43.0	835.7	21.1	14.7	2.3	176.1	13.7	182.5	26.7
RR1	**B**	04/04/13	25.2	2804.0	21.8	13.5	5.1	619.3	13.2	155.5	47.8
RR1	**C**	11/04/13	30.9	464.8	21.4	15.1	1.4	80.0	14.6	192.3	24.0
RR1	**D**	18/04/13	29.1	275.7	22.6	14.2	1.1	56.8	14.1	196.6	23.7
RR1	**E**	30/04/13	25.8	230.5	22.8	13.9	n/a	31.6	14.2	195.9	24.1
RR1	**F**	10/05/13	28.0	108.4	21.6	13.6	n/a	16.0	14.2	216.3	24.6
RR1	**G**	16/05/13	25.4	125.2	21.5	13.5	n/a	17.8	14.4	202.5	23.1
RR1	**H**	28/05/13	41.3	52.9	25.3	16.4	n/a	11.3	15.9	205.4	22.0
RR1	**L**	28/06/13	38.6	11.7	24.9	16.1	n/a	4.3	16.2	228.3	23.9
RR2	**A**	28/03/13	34.0	1430.0	23.3	14.3	3.0	304.0	14.3	174.5	30.5
RR2	**B**	04/04/13	22.7	3138.0	20.9	13.4	6.1	653.0	13.9	154.1	59.8
RR2	**C**	11/04/13	28.6	504.7	23.4	14.4	1.4	114.2	14.6	189.2	23.9
RR2	**D**	18/04/13	27.4	365.4	20.1	14.0	1.1	53.1	14.6	194.9	23.6
RR2	**E**	30/04/13	26.2	152.7	23.0	14.2	n/a	21.4	15.1	197.7	22.3
RR2	**F**	10/05/13	24.6	140.2	22.2	13.7	n/a	18.6	14.9	199.5	22.9
RR2	**G**	16/05/13	25.6	111.2	21.6	13.3	n/a	18.4	14.8	207.0	22.9
RR2	**H**	28/05/13	42.4	56.3	25.5	16.4	n/a	11.4	16.7	224.0	23.9
RR2	**L**	28/06/13	38.2	19.2	25.1	16.0	n/a	5.5	16.7	230.1	23.7
RR3	**A**	28/03/13	31.1	961.8	21.0	13.6	2.9	176.9	12.7	177.1	37.4
RR3	**B**	04/04/13	23.0	3091.0	22.1	13.8	5.3	669.6	13.9	154.6	45.6
RR3	**C**	11/04/13	28.6	257.1	23.1	14.4	1.6	54.3	14.1	192.7	22.0
RR3	**D**	18/04/13	25.4	201.0	37.1	16.3	1.0	67.6	15.7	185.5	22.0
RR4	**A**	28/03/13	28.6	1146.0	21.4	16.0	3.0	181.8	15.3	170.3	36.7
RR4	**B**	04/04/13	21.0	2588.0	19.8	13.4	15.8	558.3	13.4	148.4	64.7
RR4	**C**	11/04/13	27.3	495.5	38.7	14.5	1.4	116.7	14.4	188.0	23.8
RR4	**D**	18/04/13	27.2	281.2	37.8	14.8	1.3	55.8	15.0	198.2	25.7
RR4	**E**	30/04/13	25.9	128.6	22.5	14.0	n/a	19.3	15.0	199.0	22.4
RR4	**F**	10/05/13	23.9	86.0	22.3	13.7	n/a	13.1	15.1	195.7	21.2
RR4	**G**	16/05/13	24.7	107.9	21.0	13.4	n/a	17.9	15.1	202.3	22.3
RR4	**H**	28/05/13	39.8	62.9	25.4	16.0	n/a	12.8	16.2	220.0	23.6
RR4	**L**	28/06/13	37.8	27.4	25.4	16.0	n/a	7.0	16.7	226.9	23.4
RR5	**A**	28/03/13	53.0	14.3	29.2	20.2	n/a	5.5	18.4	226.5	41.6
RR5	**B**	04/04/13	43.9	8.4	27.2	19.3	4.9	4.3	17.8	211.4	44.0
RR5	**C**	11/04/13	48.7	5.0	28.1	19.6	n/a	2.8	18.6	227.8	38.1
RR5	**D**	18/04/13	44.2	2.	28.1	19.1	n/a	1.3	18.4	222.3	38.9
RR5	**E**	30/04/13	45.4	1.6	27.0	19.3	n/d	1.7	18.6	226.9	38.0
RR5	**F**	10/05/13	43.4	n/a	26.3	18.8	n/a	n/a	18.4	226.8	38.3
RR5	**G**	16/05/13	42.4	n/a	25.6	18.6	n/a	4.1	18.2	242.6	36.3
RR5	**H**	28/05/13	59.4	7.3	30.1	22.0	n/a	3.4	20.2	236.7	38.6
RR5	**L**	28/06/13	56.8	3.9	31.3	21.8	n/a	1.9	19.8	241.0	39.6

Vulsini monitoring area – ICP-MS analysis on 0.20 μm filtered samples

ID		Date	B	Al	Si	V	Mn	Fe	Rb	Sr	Ba
			μg/L	*μg/L*	*mg/L*	*μg/L*	*μg/L*	*μg/L*	*μg/L*	*μg/L*	*μg/L*
CAN	**E**	30/04/13	26.8	n/a	20.7	19.5	n/a	2.6	12.5	323.4	19.9
CAN	**F**	10/05/13	27.2	n/a	21.1	19.8	n/a	2.5	13.1	340.6	21.7
CAN	**G**	16/05/13	26.7	n/a	20.4	19.4	n/a	2.6	13.1	346.6	21.5
CAN	**H**	28/05/13	26.4	n/a	20.3	19.0	n/a	2.9	13.2	357.3	22.2
CAN	**L**	28/06/13	25.7	n/a	20.5	18.4	n/a	1.3	12.8	372.8	22.9
RR1	**A**	28/03/13	34.1	23.0	24.3	16.7	n/a	15.3	14.1	221.3	21.9
RR1	**B**	04/04/13	17.8	14.1	15.3	13.7	n/a	7.2	10.8	137.5	58.5
RR1	**C**	11/04/13	31.4	2.8	24.0	16.9	n/a	4.3	14.5	214.6	20.4
RR1	**D**	18/04/13	28.6	7.4	23.4	16.8	n/a	5.9	14.6	211.2	20.2
RR1	**E**	30/04/13	28.7	5.9	22.5	16.9	n/a	2.8	14.9	222.6	21.4
RR1	**F**	10/05/13	27.8	6.5	22.0	16.6	n/a	3.2	14.6	219.7	21.3
RR1	**G**	16/05/13	26.4	5.3	21.6	16.2	n/a	3.1	14.5	212.1	20.6
RR1	**H**	28/05/13	26.2	3.2	21.0	16.3	n/a	2.9	14.8	215.1	20.8
RR1	**L**	28/06/13	27.7	2.3	20.8	16.2	n/a	2.2	15.1	232.1	22.4
RR2	**A**	28/03/13	31.9	24.6	24.6	17.0	3.4	18.1	15.2	222.7	27.3
RR2	**B**	04/04/13	30.5	15.0	25.7	17.2	n/a	7.5	15.4	235.3	22.5
RR2	**C**	11/04/13	30.8	6.0	24.0	17.1	n/a	6.5	15.4	218.9	20.0
RR2	**D**	18/04/13	28.5	23.2	23.5	17.2	n/a	6.9	15.6	213.5	20.0
RR2	**E**	30/04/13	27.4	4.8	25.1	16.7	n/a	4.4	15.3	215.8	20.0
RR2	**F**	10/05/13	25.3	4.4	22.0	16.5	n/a	3.4	15.3	206.2	19.6
RR2	**G**	16/05/13	27.7	3.0	21.9	16.3	n/a	3.2	15.4	223.0	21.0
RR2	**H**	28/05/13	27.5	3.2	21.2	16.1	n/a	3.2	15.3	224.6	21.5
RR2	**L**	28/06/13	28.0	2.2	20.8	15.8	n/a	2.9	15.1	235.1	22.7
RR3	**A**	28/03/13	30.9	17.5	24.8	17.5	n/a	9.4	14.8	218.6	19.8
RR3	**B**	04/04/13	31.6	18.8	22.2	16.3	n/a	7.3	15.2	231.5	20.3
RR3	**C**	11/04/13	29.6	7.3	23.7	16.6	n/a	4.9	14.4	216.3	19.8
RR3	**D**	18/04/13	27.4	26.3	22.7	16.1	n/a	8.1	13.9	214.0	21.8
RR4	**A**	28/03/13	22.4		17.9	14.4	16.7	19.8	11.9	145.8	72.9
RR4	**B**	04/04/13	30.5	14.8	24.0	17.2	n/a	10.0	15.3	218.9	20.0
RR4	**C**	11/04/13	29.3	8.8	22.9	16.0	n/a	6.1	14.3	214.1	21.4
RR4	**D**	18/04/13	28.1	20.3	22.6	16.9	n/a	9.8	15.4	216.6	20.6
RR4	**E**	30/04/13	28.3	7.3	22.5	16.1	n/a	3.1	14.8	224.6	21.2
RR4	**F**	10/05/13	27.6	5.1	22.1	16.5	n/d	2.6	15.3	221.7	21.0
RR4	**G**	16/05/13	25.2	4.8	21.8	16.2	n/a	3.3	15.3	205.9	19.4
RR4	**H**	28/05/13	27.1	3.0	21.0	16.0	n/a	2.7	15.2	226.1	21.6
RR4	**L**	28/06/13	27.5	4.0	20.6	15.9	n/a	3.3	15.2	231.6	22.1
RR5	**A**	28/03/13	n/a	n/a	n/a	n/a	n/a	n/a	n/a	n/a	n/a
RR5	**B**	04/04/13	46.7	2.0	27.9	22.0	n/d	1.6	18.8	234.6	35.3
RR5	**C**	11/04/13	50.8	n/a	45.2	29.1	n/d	n/d	26.1	280.0	43.6
RR5	**D**	18/04/13	49.7	n/a	26.8	20.7	n/d	n/a	17.7	258.2	39.3
RR5	**E**	30/04/13	47.3	n/a	25.4	21.4	n/d	1.5	18.4	252.1	37.8
RR5	**F**	10/05/13	46.2	n/a	26.0	21.4	n/d	n/a	18.4	236.6	36.2
RR5	**G**	16/05/13	46.1	n/a	25.0	21.4	n/d	3.0	18.4	234.1	34.6
RR5	**H**	28/05/13	43.9	n/a	24.2	21.0	n/d	1.5	18.1	227.0	35.2
RR5	**L**	28/06/13	45.8	n/a	23.7	21.4	n/d	2.7	18.4	237.7	37.1

Roccamonfina monitoring area – In field parameters and IC analysis

ID		Date	T	E.C.	pH	Eh	HCO_3	F	Cl	NO_3	SO_4	Na	K	Mg	Ca
			°C	*µS/cm*		*mV*	*mg/L*	*mg/*	*mg/L*	*mg/L*	*mg/L*	*mg/L*	*mg/L*	*mg/L*	*mg/L*
I3	A	08/03/13	11,1	101	7,48	n/a	67,1	0,3	8,2	n/a	5,1	12,3	8,1	2,6	8,9
I3	B	15/03/13	9	74	7,30	164	54,9	0,2	7,5	0,4	4,8	11,8	7,8	1,7	7,1
I3	C	08/04/13	12	141	7,46	168	64,1	0,2	8,5	0,2	5,6	12,5	7,8	2,0	7,9
I3	D	17/04/13	14	168	7,74	120	68,3	0,2	9,6	n/a	6,0	14,8	10,5	2,3	9,4
I3	E	23/04/13	12,4	154	7,48	138	73,2	0,2	10,1	n/a	6,0	15,1	10,4	2,5	10,0
I3	F	02/05/13	14,5	150	7,47	144	73,2	0,2	10,0	n/a	5,8	14,2	9,0	2,7	9,8
I3	G	08/05/13	13,8	162	7,57	112	73,2	0,2	9,9	0,8	5,4	13,9	8,3	2,5	9,8
I3	H	24/05/13	13	147	7,45	200	82,4	0,2	10,2	n/a	5,0	14,2	6,4	2,5	10,7
S2	A	08/03/13	11,6	83	6,79	n/a	45,2	0,2	8,4	n/a	3,2	11,0	5,6	1,8	6,8
S2	B	15/03/13	11,3	81	6,39	203	30,5	0,2	7,8	0,1	3,2	10,8	4,7	0,9	3,2
S2	C	08/04/13	12,3	137	6,54	208	48,8	0,2	13,7	0,3	5,6	15,0	6,7	2,0	7,5
S2	D	17/04/13	12,3	190	6,63	170	68,3	0,2	17,0	n/a	7,1	18,7	11,3	2,7	8,7
S2	E	23/04/13	13	190	6,48	174	73,2	0,2	17,4	n/a	7,5	19,3	10,3	3,5	9,3
S2	F	02/05/13	13	198	6,76	155	79,3	0,2	17,3	n/a	7,4	19,4	10,3	3,6	10,3
S2	G	08/05/13	13	210	6,77	136	85,4	0,2	16,5	1,3	7,2	20,3	10,8	3,6	10,7
S2	H	24/05/13	13	202	6,9	108	85,4	0,2	16,8	0,4	7,2	20,0	9,2	3,4	10,6
S4	A	08/03/13	12,9	160	6,21	n/a	93,1	0,3	11,2	0,2	6,8	18,1	16,9	3,5	11,7
S4	B	15/03/13	11	101	6,90	200	85,4	0,3	11,5	0,4	6,7	18,8	16,5	2,1	7,6
S4	C	08/04/13	13	202	6,48	186	91,5	0,3	10,9	0,4	7,0	17,2	14,7	2,7	10,0
S4	D	17/04/13	13	205	6,5	176	95,2	0,3	11,1	n/a	7,0	18,4	16,6	3,0	11,7
S4	E	23/04/13	13,4	206	6,42	167	97,6	0,3	11,4	n/a	7,2	18,6	16,9	3,5	12,3
S4	F	02/05/13	12,8	206	6,33	154	103,7	0,3	11,6	0,3	7,3	18,1	16,6	3,3	11,7
S4	G	08/05/13	13	202	6,36	198	100,7	0,3	11,8	0,7	7,6	18,6	16,2	3,2	12,3
S4	H	24/05/13	13	196	6,4	180	103,7	0,3	11,9	0,2	7,7	18,4	13,9	3,0	12,6
S6	C	08/04/13	13	107	7,51	160	42,7	0,1	7,0	n/a	4,7	8,4	4,3	1,7	6,2
S6	D	17/04/13	16	114	7,9	125	47,6	0,1	7,7	n/a	4,5	9,5	5,6	1,7	6,4
S6	E	23/04/13	15	102	7,84	122	47,6	0,1	7,9	n/a	4,6	9,8	5,9	1,9	6,8
S6	F	02/05/13	17,2	116	7,8	143	54,9	0,1	8,5	n/a	4,3	10,0	6,1	2,4	7,8
S6	G	08/05/13	16	116	7,96	108	58,0	0,1	7,9	0,2	4,2	10,3	6,2	2,1	7,8
S7	H	24/05/13	13	165	6,5	136	82,4	0,1	9,9	n/a	4,8	14,1	6,1	2,5	11,1

Roccamonfina monitoring area – ICP-MS analysis on unfiltered samples

ID		Date	B	Al	Si	V	Mn	Fe	Rb	Sr	Ba
			μg/L	*μg/L*	*mg/L*	*μg/L*	*μg/L*	*μg/L*	*μg/L*	*μg/L*	*μg/L*
I3	**A**	08/03/13	15.7	4102.9	12.4	2.9	12.2	896.5	39.5	110.9	31.0
I3	**B**	15/03/13	14.5	4498.4	11.1	2.9	14.1	936.5	33.1	95.0	42.8
I3	**C**	08/04/13	12.7	3897.4	7.8	2.9	36.8	963.5	26.4	71.4	96.9
I3	**D**	17/04/13	18.2	2757.5	12.9	3.0	8.5	606.3	53.2	130.1	18.3
I3	**E**	23/04/13	22.7	2858.6	12.0	3.0	10.7	600.8	56.8	137.0	19.6
I3	**F**	02/05/13	20.9	1609.8	13.1	2.1	10.5	408.3	63.9	135.5	21.4
I3	**G**	08/05/13	20.1	1217.7	13.0	1.8	12.7	354.0	65.5	138.3	20.2
I3	**H**	24/05/13	21.0	1174.3	13.1	1.5	6.9	361.3	64.6	114.9	17.0
S2	**A**	08/03/13	14.8	2990.8	10.4	1.9	7.2	725.0	7.1	6.5	7.1
S2	**B**	15/03/13	14.8	2034.2	9.5	1.3	4.5	511.7	6.7	5.5	3.9
S2	**C**	08/04/13	14.1	4731.8	14.4	2.9	7.9	1034.8	10.4	9.3	7.2
S2	**D**	17/04/13	17.9	4094.0	18.2	4.0	5.9	898.0	15.8	14.5	4.4
S2	**E**	23/04/13	19.7	3807.4	19.0	4.7	5.1	789.8	17.0	16.5	4.2
S2	**F**	02/05/13	26.0	1008.8	20.8	5.8	1.6	297.3	23.4	10.6	n/a
S2	**G**	08/05/13	23.6	778.7	20.1	5.8	1.3	258.8	23.4	10.5	n/a
S2	**H**	24/05/13	25.5	123.8	21.3	6.5	n/a	129.0	25.4	13.1	n/a
S4	**A**	08/03/13	18.7	3520.8	15.9	4.9	4.8	629.7	21.9	114.5	9.2
S4	**B**	15/03/13	15.7	4229.6	13.3	4.0	5.7	734.2	16.0	99.5	13.1
S4	**C**	08/04/13	18.1	3624.1	13.6	4.4	5.3	655.2	18.0	117.8	10.4
S4	**D**	17/04/13	19.1	2366.4	13.9	4.8	3.5	441.1	23.7	136.8	5.9
S4	**E**	23/04/13	19.7	2636.4	14.4	4.6	3.7	490.2	22.7	134.0	6.9
S4	**F**	02/05/13	25.3	649.4	16.5	5.3	n/a	210.8	31.5	214.5	2.8
S4	**G**	08/05/13	22.0	1055.9	15.5	4.9	1.6	264.9	29.9	186.0	3.3
S4	**H**	24/05/13	23.2	828.5	15.5	5.0	1.3	231.4	31.7	198.5	2.7
S6	**C**	08/04/13	18.7	582.8	7.5	n/a	2.9	244.5	63.8	162.7	16.0
S6	**D**	17/04/13	17.0	406.2	7.6	n/a	1.7	227.1	70.3	181.2	n/a
S6	**E**	23/04/13	18.2	217.1	7.3	n/a	n/a	146.5	68.9	191.0	n/a
S6	**F**	02/05/13	17.5	88.6	7.7	n/a	n/a	123.9	81.2	223.2	n/a
S6	**G**	08/05/13	18.2	61.7	7.9	n/a	n/a	118.7	85.7	242.4	n/a
S7	**H**	24/05/13	21.1	1238.8	13.1	1.6	5.4	388.7	64.9	121.5	n/a

Roccamonfina monitoring area – ICP-MS analysis on 0.45 μm filtered samples

ID		Date	B	Al	Si	V	Mn	Fe	Rb	Sr	Ba
			μg/L	μg/L	mg/L	μg/L	μg/L	μg/L	μg/L	μg/L	μg/L
I3	**A**	08/03/13	21.9	740.9	16.2	3.1	2.0	146.6	53.0	155.2	10.3
I3	**B**	15/03/13	18.8	1033.0	15.3	3.0	6.1	233.3	42.1	143.6	13.4
I3	**C**	08/04/13	21.4	432.3	17.6	3.7	16.0	68.9	57.3	161.4	10.8
I3	**D**	17/04/13	21.2	438.7	18.0	3.8	8.9	102.8	60.5	164.8	12.1
I3	**E**	23/04/13	28.7	556.8	20.6	3.3	1.1	113.0	66.4	243.5	15.7
I3	**F**	02/05/13	21.3	470.2	17.5	2.8	n/a	123.9	62.8	147.9	12.3
I3	**G**	08/05/13	23.9	286.6	17.9	2.5	n/a	82.9	64.9	167.2	13.4
I3	**H**	24/05/13	27.8	221.3	21.1	1.9	n/a	59.5	67.5	183.5	11.5
S2	**A**	08/03/13	6.8	895.9	13.2	2.3	2.6	219.1		5.4	n/a
S2	**B**	15/03/13	5.7	967.0	11.7	1.8	2.7	227.0		4.5	n/a
S2	**C**	08/04/13	9.9	1159.0	17.8	3.3	2.3	219.9	12.8	9.5	n/a
S2	**D**	17/04/13	21.2	934.3	23.5	5.2	1.3	178.0	18.1	15.3	n/a
S2	**E**	23/04/13	31.9	675.5	32.9	6.7	n/a	135.5	24.0	27.1	n/a
S2	**F**	02/05/13	25.7	197.6	27.3	6.9	n/a	50.7	22.8	21.1	n/a
S2	**G**	08/05/13	28.9	83.6	27.5	7.2	n/a	24.5	23.3	21.5	n/a
S2	**H**	24/05/13	35.0	5.7	37.0	7.5	n/a	n/d	23.9	31.7	n/a
S4	**A**	08/03/13	27.2	242.7	29.2	7.6	n/a	50.8	29.7	185.5	n/a
S4	**B**	15/03/13	25.2	529.8	24.6	8.0	n/a	83.6	28.6	170.7	n/a
S4	**C**	08/04/13	23.3	317.3	21.3	6.5	n/a	53.0	25.4	166.9	n/a
S4	**D**	17/04/13	24.0	276.8	21.7	6.4	n/a	44.9	26.9	179.8	n/a
S4	**E**	23/04/13	33.7	40.4		8.6	n/a	7.3	38.4	273.9	n/a
S4	**F**	02/05/13	25.0	110.4	21.1	6.3	n/a	26.9	29.1	194.0	n/a
S4	**G**	08/05/13	25.6	46.1	21.2	6.4	n/a	8.1	30.7	201.1	n/a
S4	**H**	24/05/13	36.8	2.9	29.3	8.0	n/a	n/d	39.9	310.4	n/a
S6	**C**	08/04/13	16.4	218.2	9.8	n/a	n/a	74.1	58.2	172.3	14.0
S6	**D**	17/04/13	17.6	152.5	10.1	n/a	n/a	37.3	66.2	188.0	14.1
S6	**E**	23/04/13	17.4	210.5	11.3	n/a	n/a	43.1	68.1	194.5	10.7
S6	**F**	02/05/13	18.2	48.9	10.5	n/a	n/a	16.5	78.0	216.1	15.5
S6	**G**	08/05/13	18.7	61.7	10.5	n/a	n/a	22.3	79.8	231.0	17.1
S7	**H**	24/05/13	26.7	146.8	20.8	n/a	n/a	33.7	66.4	175.3	13.1

Roccamonfina monitoring area – ICP-MS analysis on 0.20 μm filtered samples

ID		Date	B	Al	Si	V	Mn	Fe	Rb	Sr	Ba
			μg/L	*μg/L*	*mg/L*	*μg/L*	*μg/L*	*μg/L*	*μg/L*	*μg/L*	*μg/L*
I3	**A**	08/03/13	13.4	61.5	18.2	2.9	n/a	19.9	57.8	162.2	7.1
I3	**B**	15/03/13	12.0	215.4	18.0	3.2	n/a	57.9	53.8	150.5	6.8
I3	**C**	08/04/13	16.8	147.8	19.9	4.3	20.5	41.8	69.8	201.7	12.1
I3	**D**	17/04/13	16.0	29.9	18.7	3.9	n/a	11.5	67.2	197.9	9.9
I3	**E**	23/04/13	16.0	74.2	19.1	3.5	14.2	26.6	65.9	195.6	10.7
I3	**F**	02/05/13	17.2	79.5	18.7	3.0	34.0	24.4	70.3	171.0	10.7
I3	**G**	08/05/13	17.2	65.7	18.5	2.7	40.8	33.1	70.0	172.3	11.3
I3	**H**	24/05/13	20.0	41.7	24.9	2.4	13.0	24.0	74.8	182.6	11.7
S2	**A**	08/03/13	6.7	221.1	14.8	2.4	n/a	67.7	10.0	7.1	n/a
S2	**B**	15/03/13	6.4	202.8	14.4	2.0	n/a	55.7	8.8	5.9	n/a
S2	**C**	08/04/13	10.1	464.0	20.8	3.4	n/a	99.5	14.8	10.7	n/a
S2	**D**	17/04/13	15.6	7.7	27.0	5.4	n/a	3.7	20.4	17.3	n/a
S2	**E**	23/04/13	17.8	26.3	28.4	6.3	n/a	8.8	21.9	19.9	n/a
S2	**F**	02/05/13	19.9	22.8	28.3	7.2	n/a	7.6	24.2	22.3	n/a
S2	**G**	08/05/13	20.3	11.2	28.1	7.5	n/a	4.5	24.3	22.6	n/a
S2	**H**	24/05/13	26.4	3.7	36.2	11.0	n/a	n/a	32.1	30.3	n/a
S4	**A**	08/03/13	18.7	7.3	25.5	7.7	n/a	1.9	32.0	204.0	1.1
S4	**B**	15/03/13	18.6	6.0	25.5	7.9	n/a	3.9	30.3	202.8	1.1
S4	**C**	08/04/13	17.0	280.3	20.8	6.8	n/a	47.6	27.2	185.7	2.2
S4	**D**	17/04/13	17.9	n/d	23.1	6.8	n/a	n/a	29.4	204.3	n/a
S4	**E**	23/04/13	18.6	10.6	23.6	6.7	n/a	3.7	29.8	212.6	1.8
S4	**F**	02/05/13	19.0	23.9	20.8	6.9	4.6	10.1	31.3	216.3	4.4
S4	**G**	08/05/13	20.6	14.7	22.5	6.5	1.1	3.9	30.9	217.4	1.3
S4	**H**	24/05/13	29.8	n/d	35.6	10.9	n/a	n/a	52.1	363.2	2.0
S6	**C**	08/04/13	11.1	78.1	10.8	1.5	1.9	22.6	72.2	211.4	12.9
S6	**D**	17/04/13	9.8	70.9	10.6	1.4	n/d	19.4	66.1	202.2	13.2
S6	**E**	23/04/13	11.4	116.4	11.6	1.6	2.7	30.6	74.7	222.0	14.7
S6	**F**	02/05/13	11.3	21.0	11.4	1.2	2.4	10.8	80.8	242.9	16.3
S6	**G**	08/05/13	11.7	59.9	11.0	1.2	n/a	20.8	79.9	255.5	16.7
S7	**H**	24/05/13	20.1	14.7	23.1	2.5	1.5	7.9	75.9	181.4	13.4

C. XRD analyses

Roccamonfina sampling area

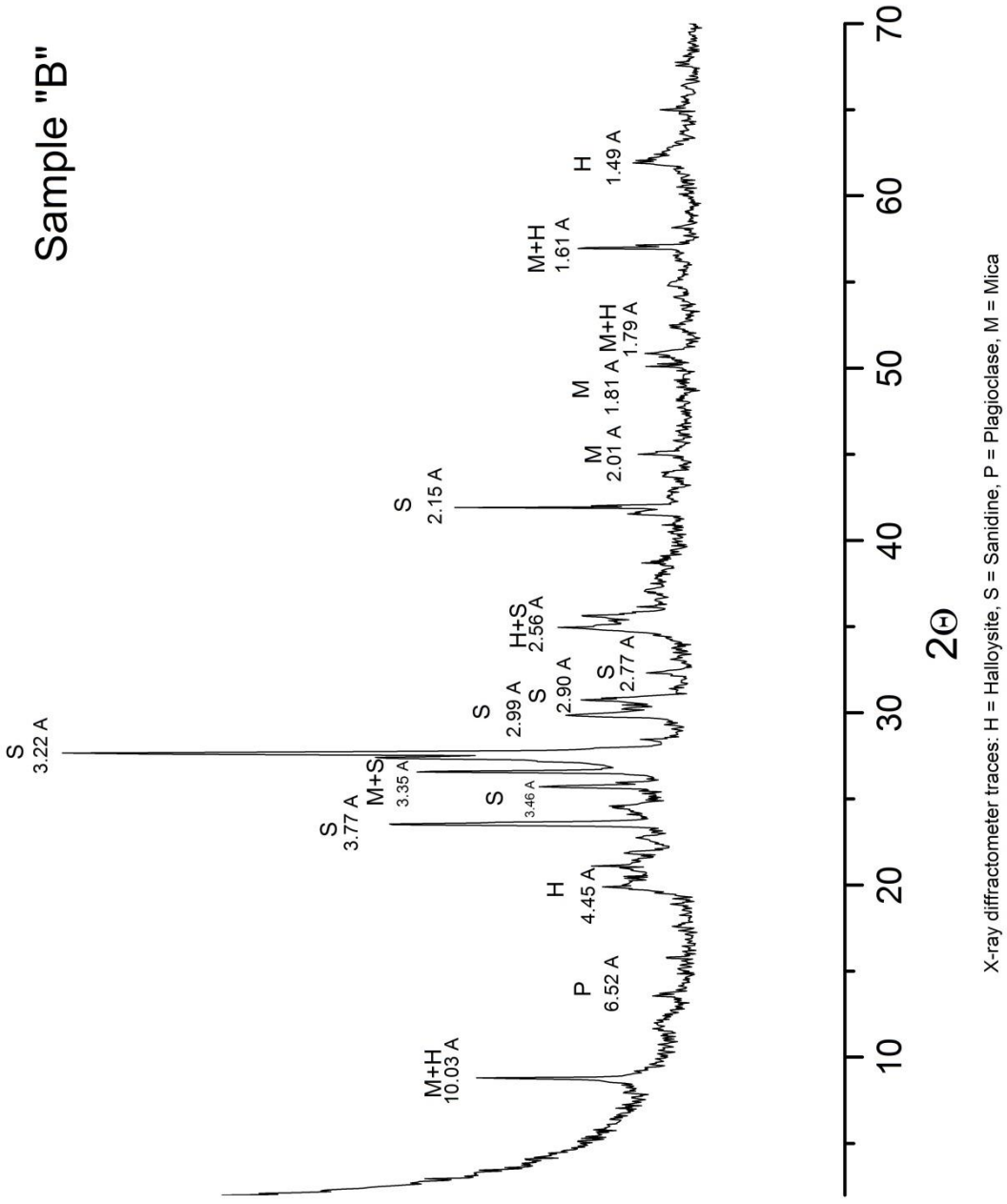

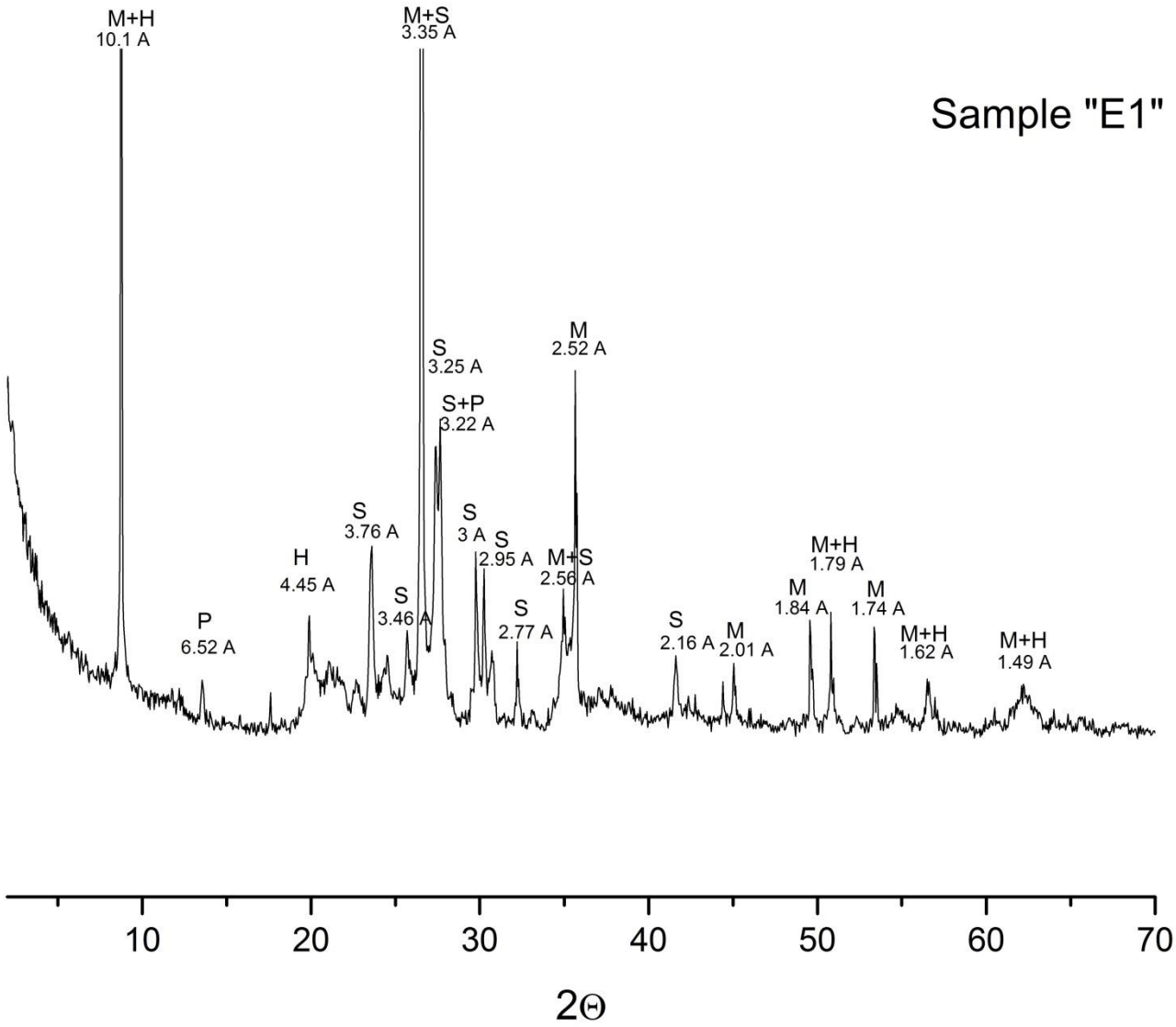

X-ray diffractometer traces: H = Halloysite, S = Sanidine, P = Plagioclase, M = Mica

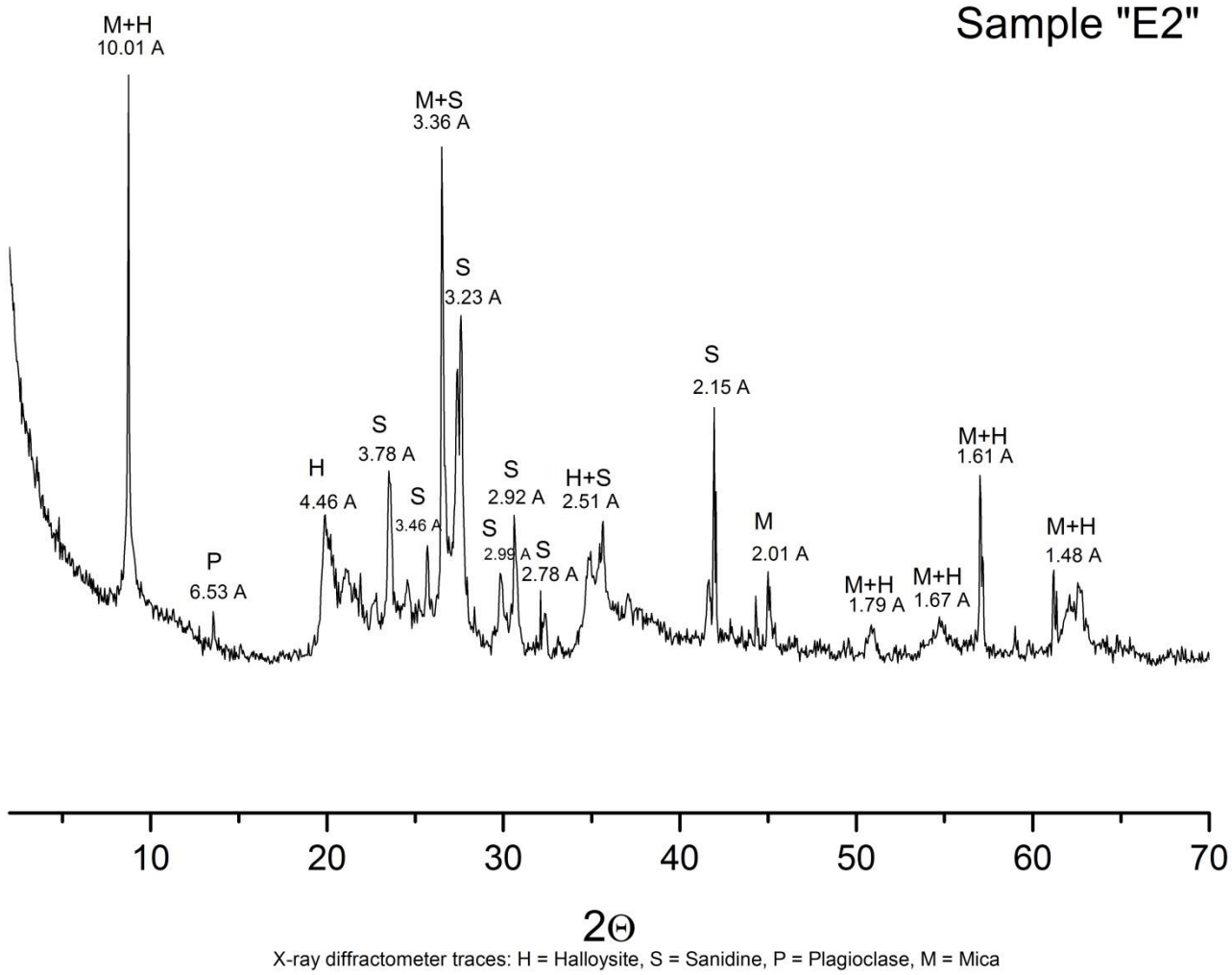

X-ray diffractometer traces: H = Halloysite, S = Sanidine, P = Plagioclase, M = Mica

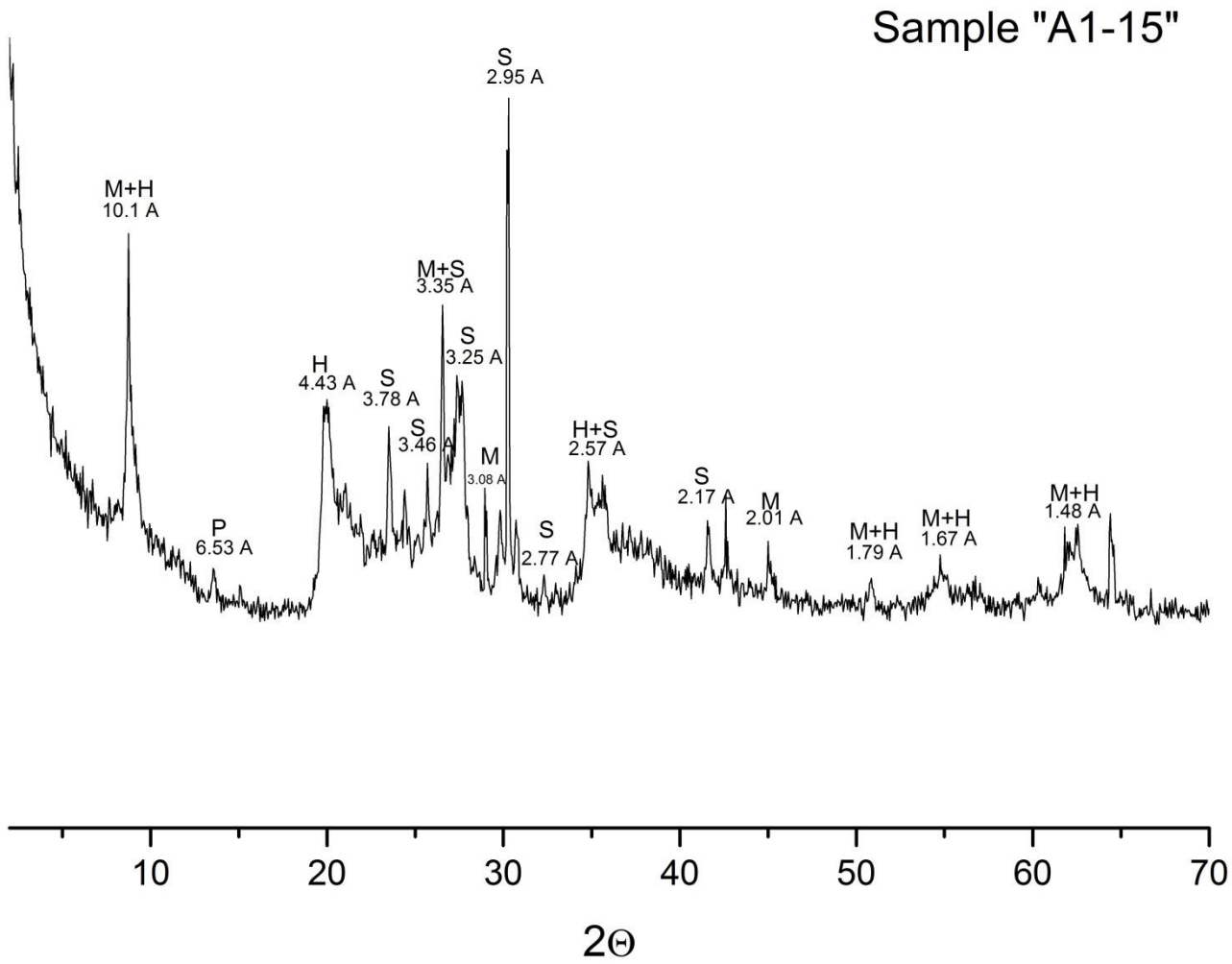

X-ray diffractometer traces: H = Halloysite, S = Sanidine, P = Plagioclase, M = Mica

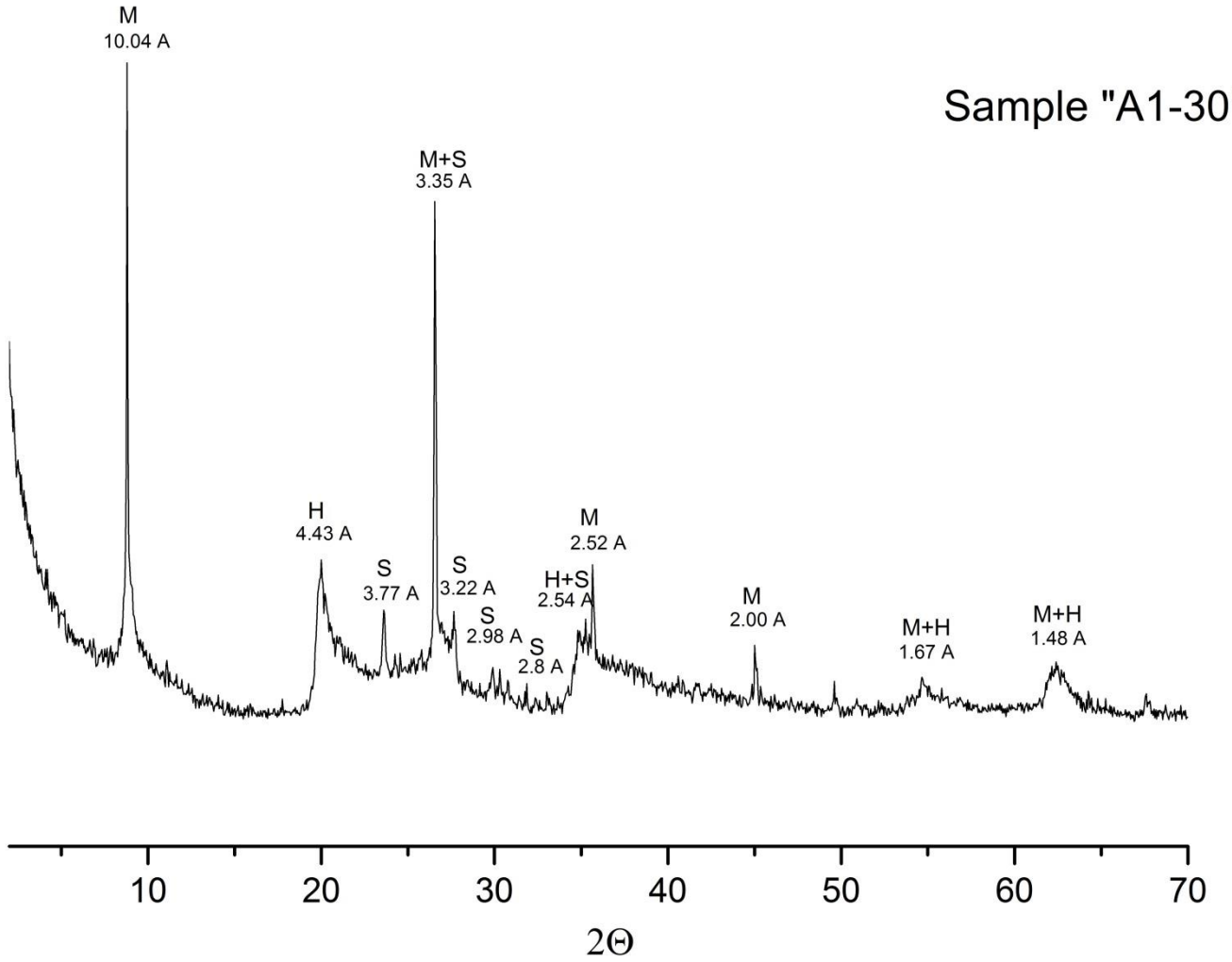

X-ray diffractometer traces: H = Halloysite, S = Sanidine, M = Mica

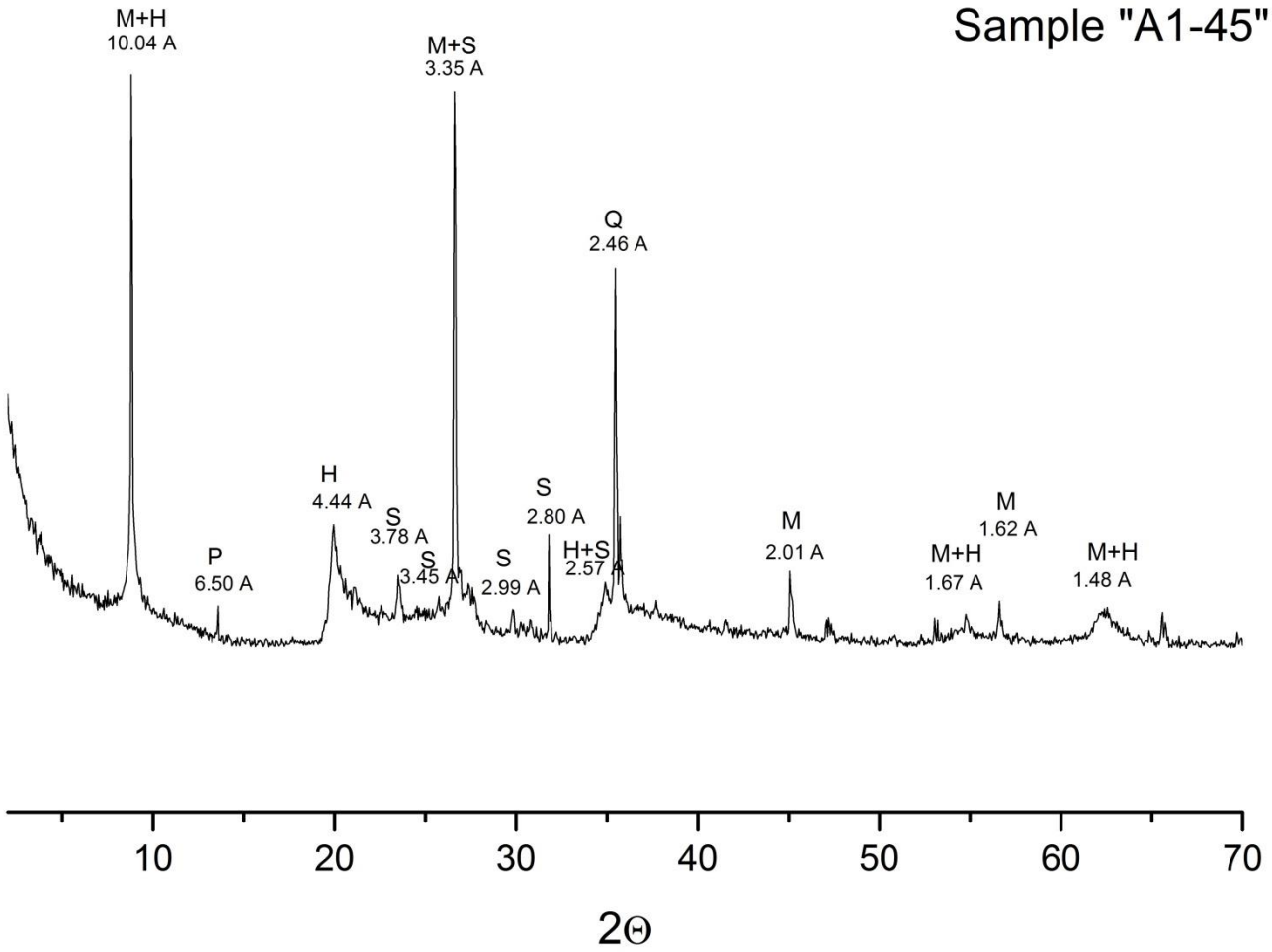

X-ray diffractometer traces: H = Halloysite, S = Sanidine, P = Plagioclase, M = Mica, Q = Quartz

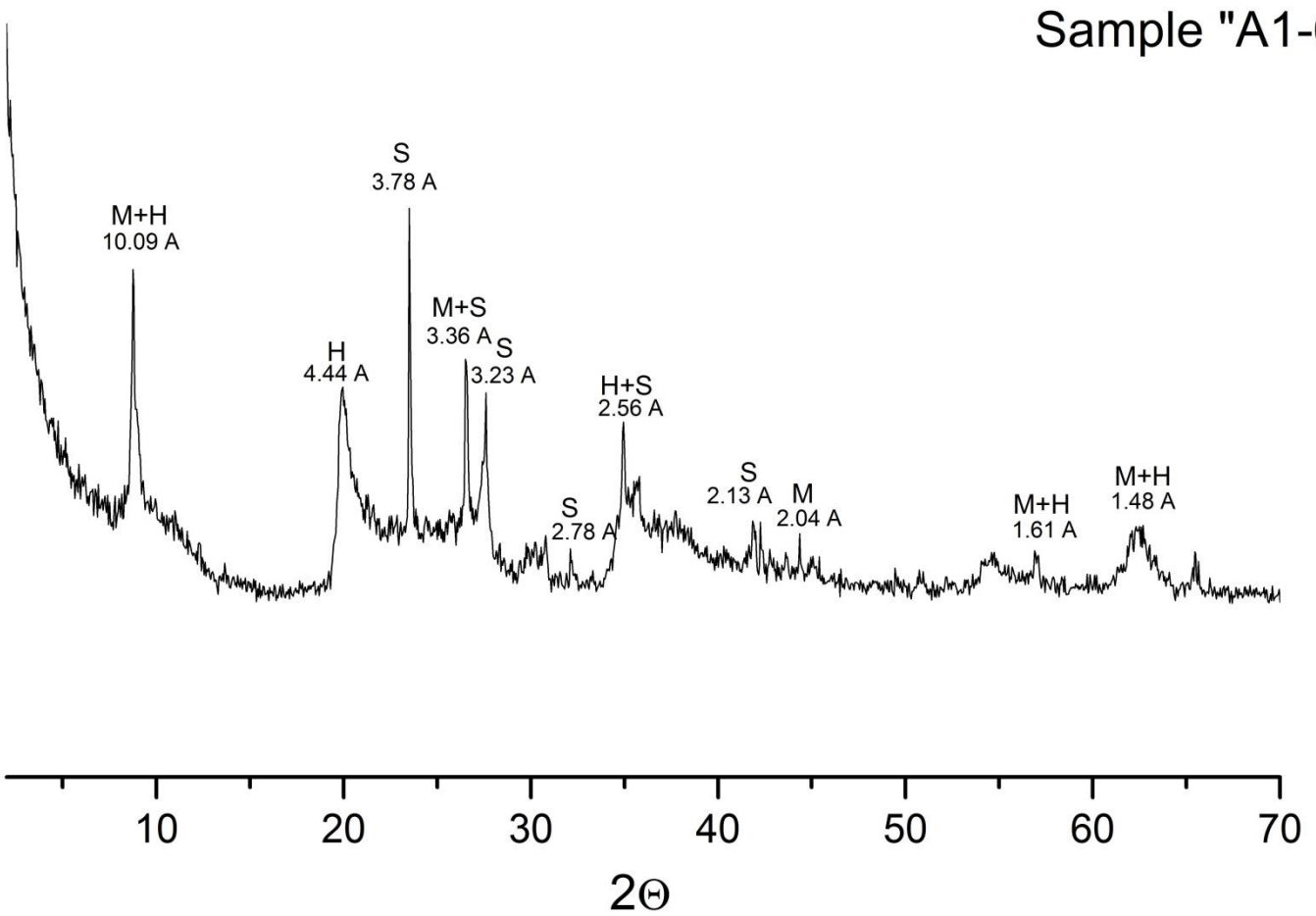

X-ray diffractometer traces: H = Halloysite, S = Sanidine, P = Plagioclase, M = Mica

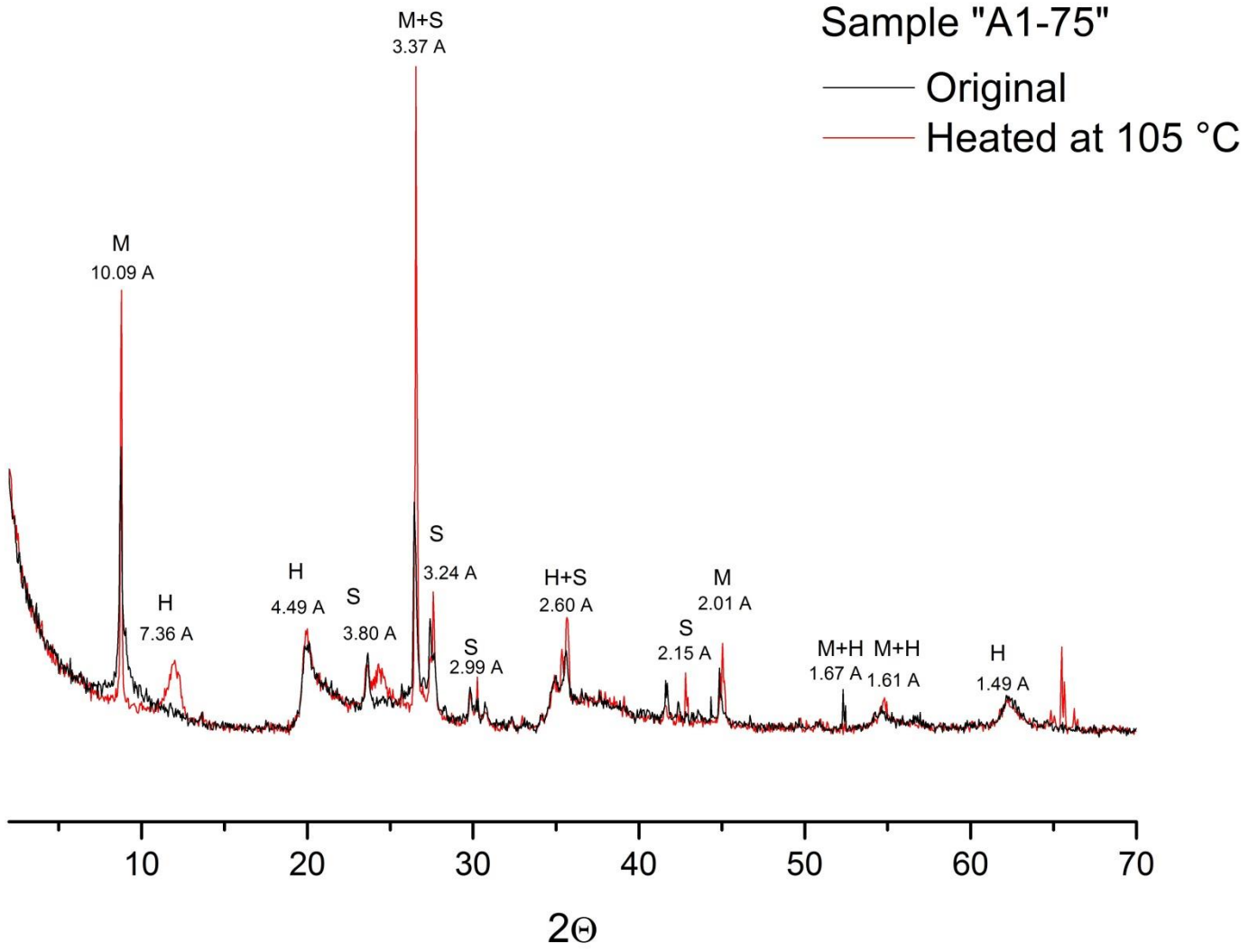

X-ray diffractometer traces: H = Halloysite, S = Sanidine, P = Plagioclase, M = Mica

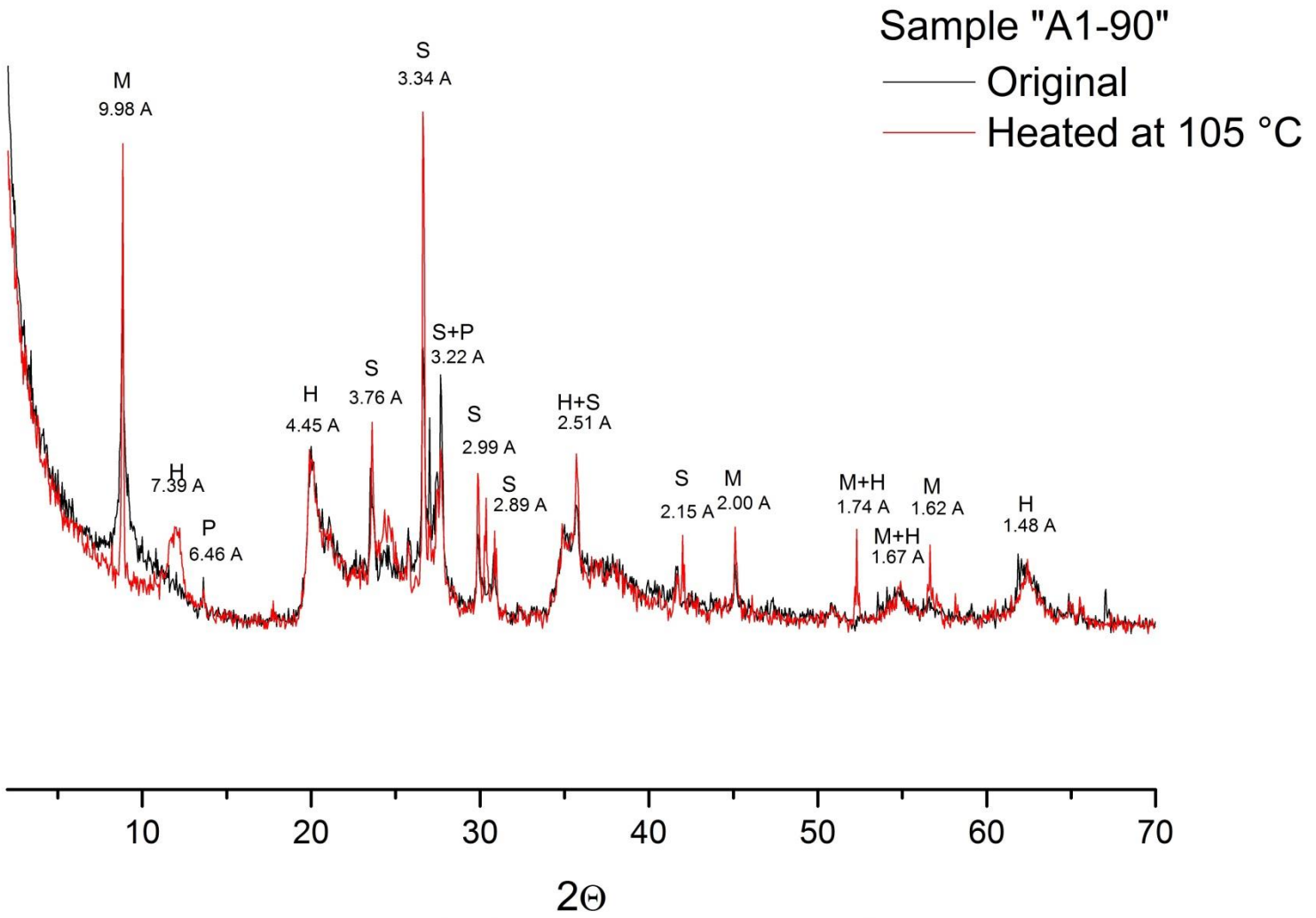

X-ray diffractometer traces: H = Halloysite, S = Sanidine, P = Plagioclase, M = Mica

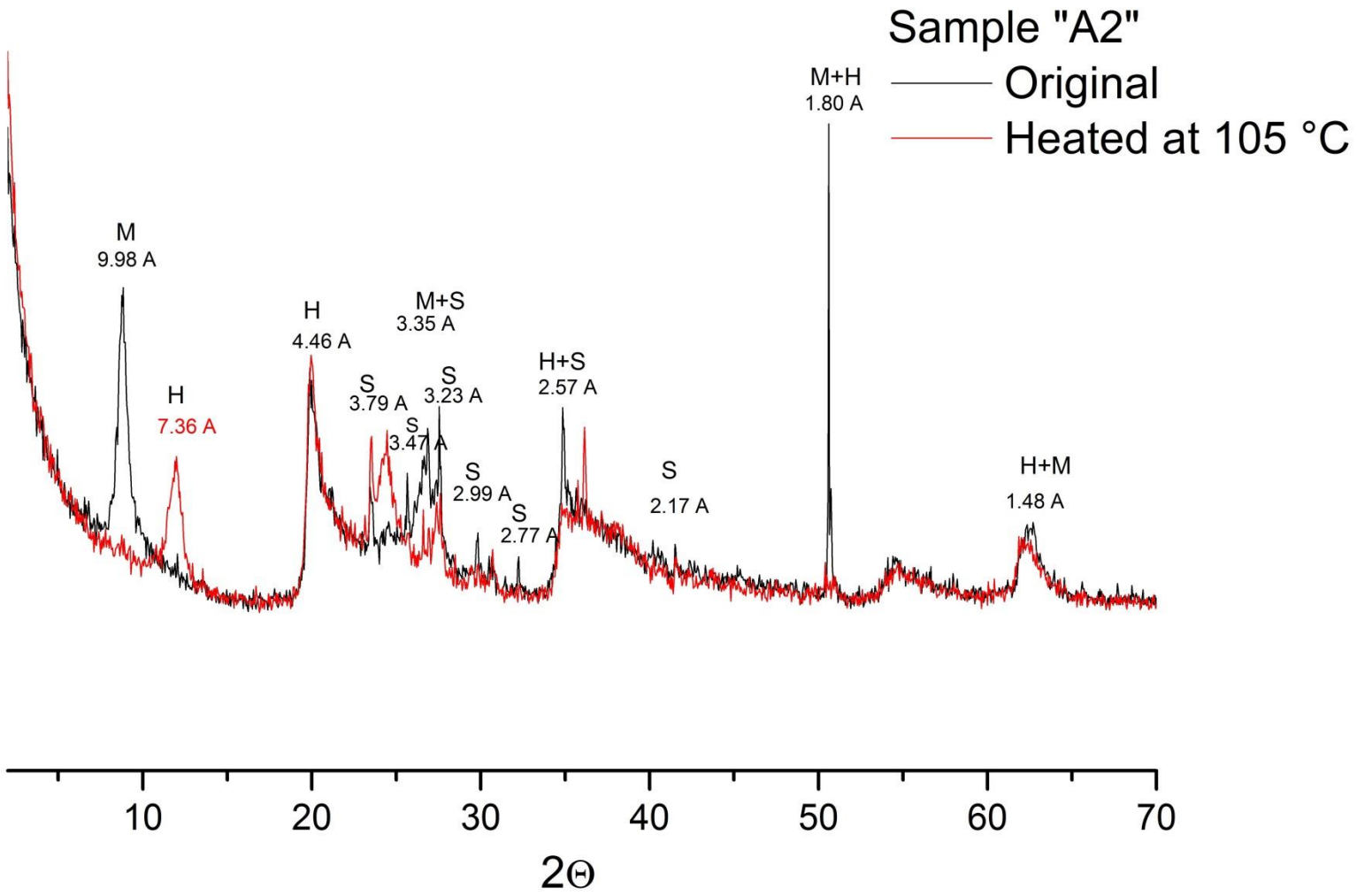

X-ray diffractometer traces: H = Halloysite, S = Sanidine, P = Plagioclase, M = Mica

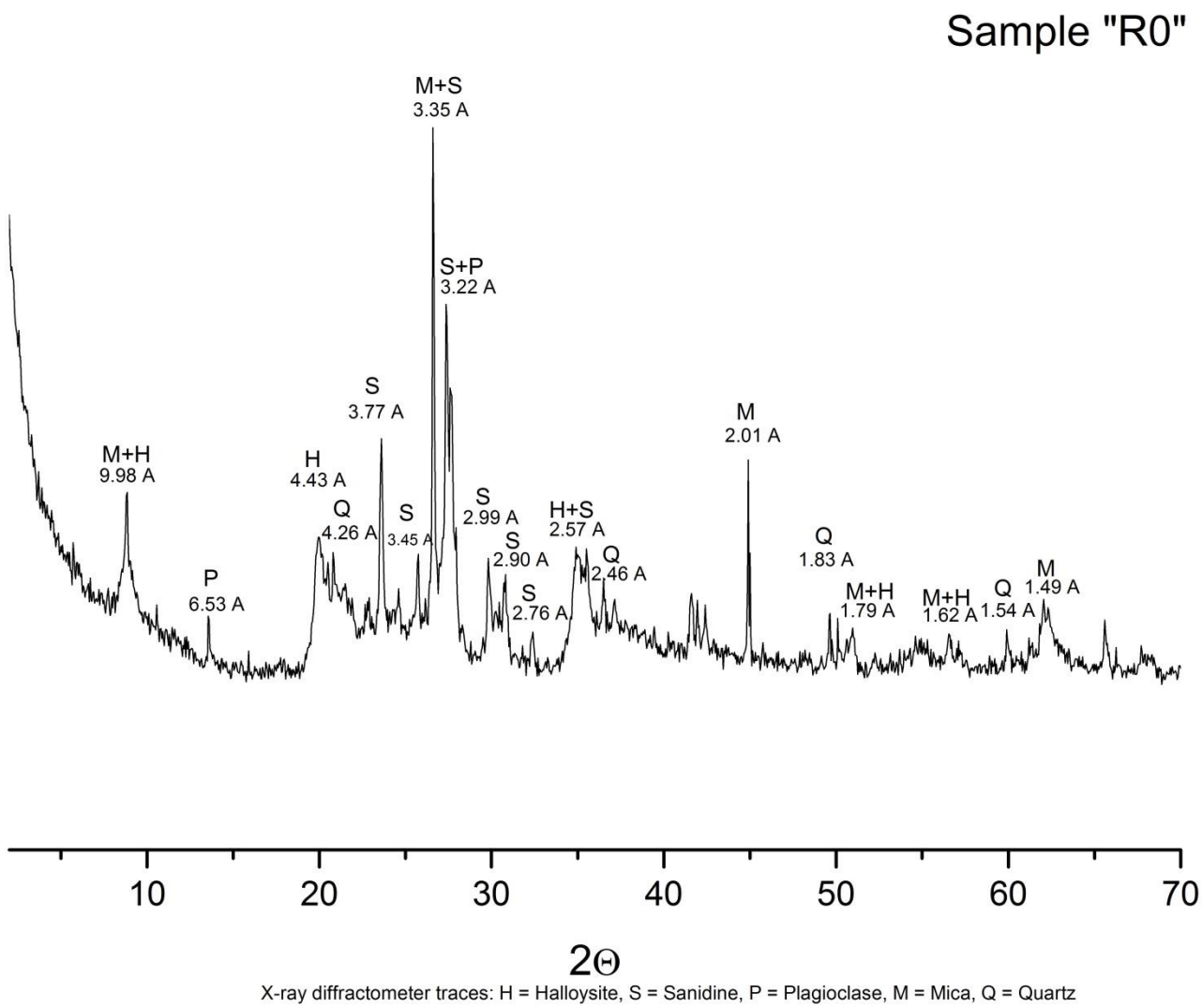

X-ray diffractometer traces: H = Halloysite, S = Sanidine, P = Plagioclase, M = Mica, Q = Quartz

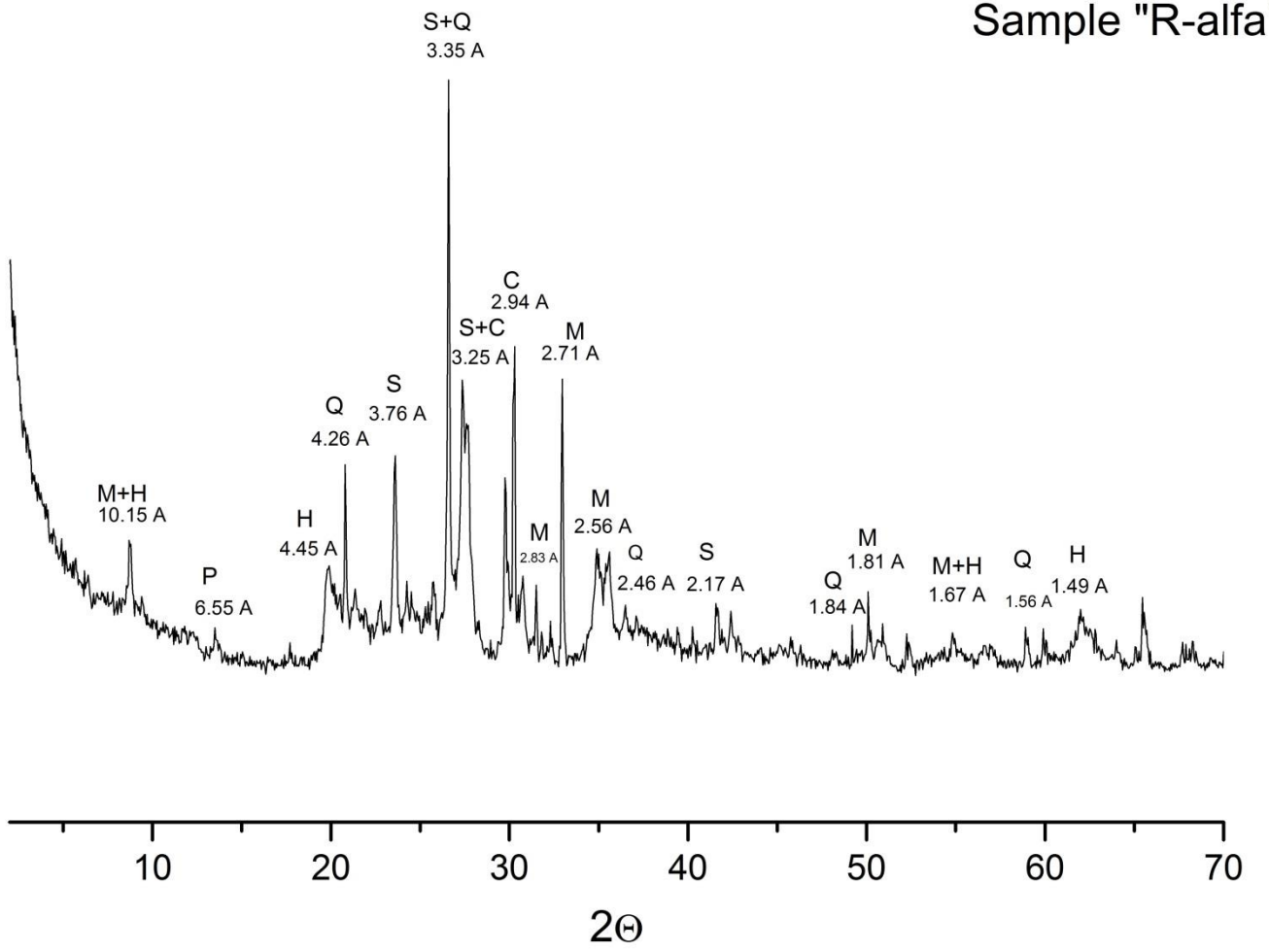

X-ray diffractometer traces: H = Halloysite, S = Sanidine, P = Plagioclase, M = Mica, Q = Quartz, C = Clinopiroxene

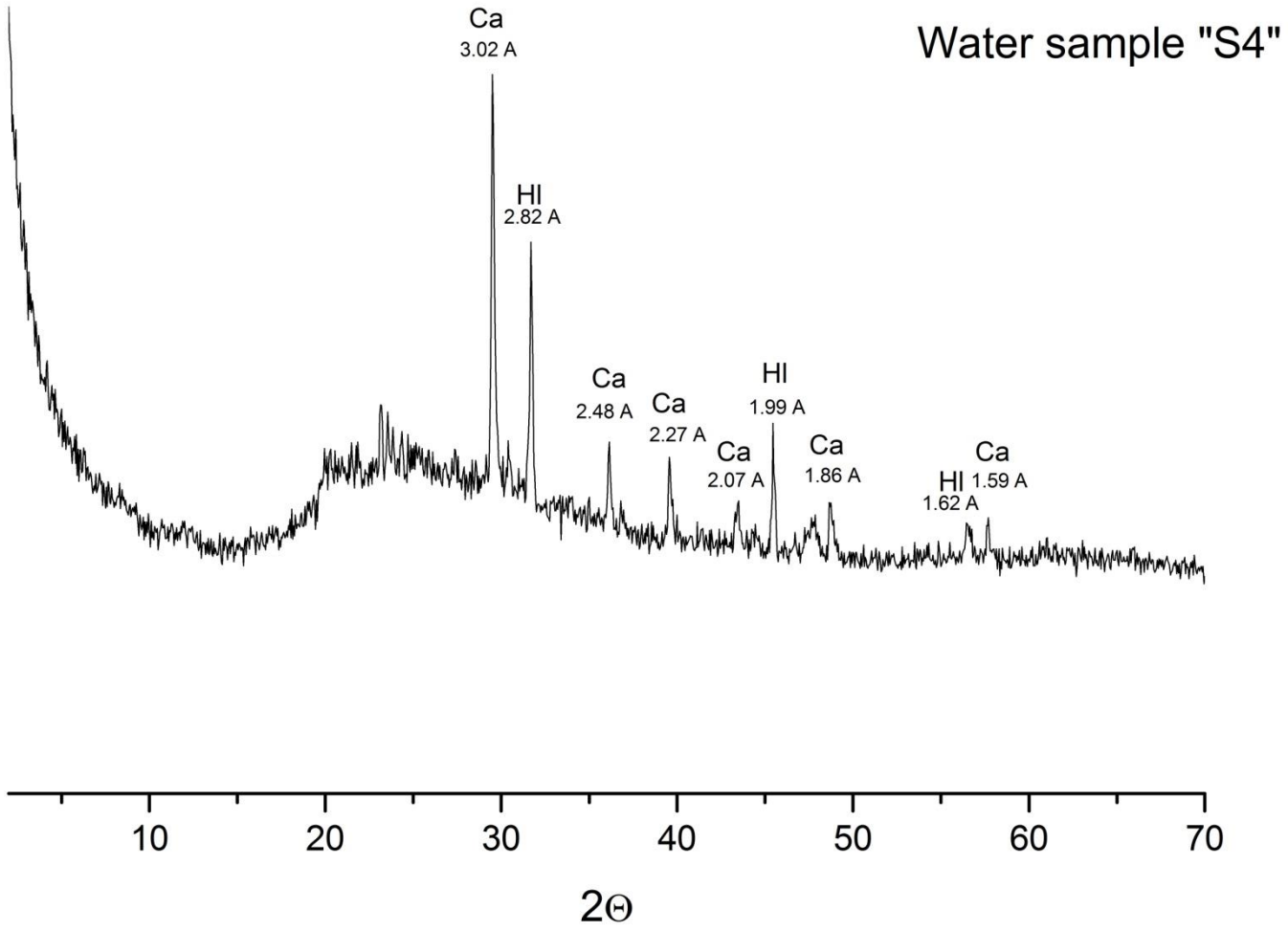

X-ray diffractometer traces: Hl = Halite, Ca = Calcite

Orvieto sampling area

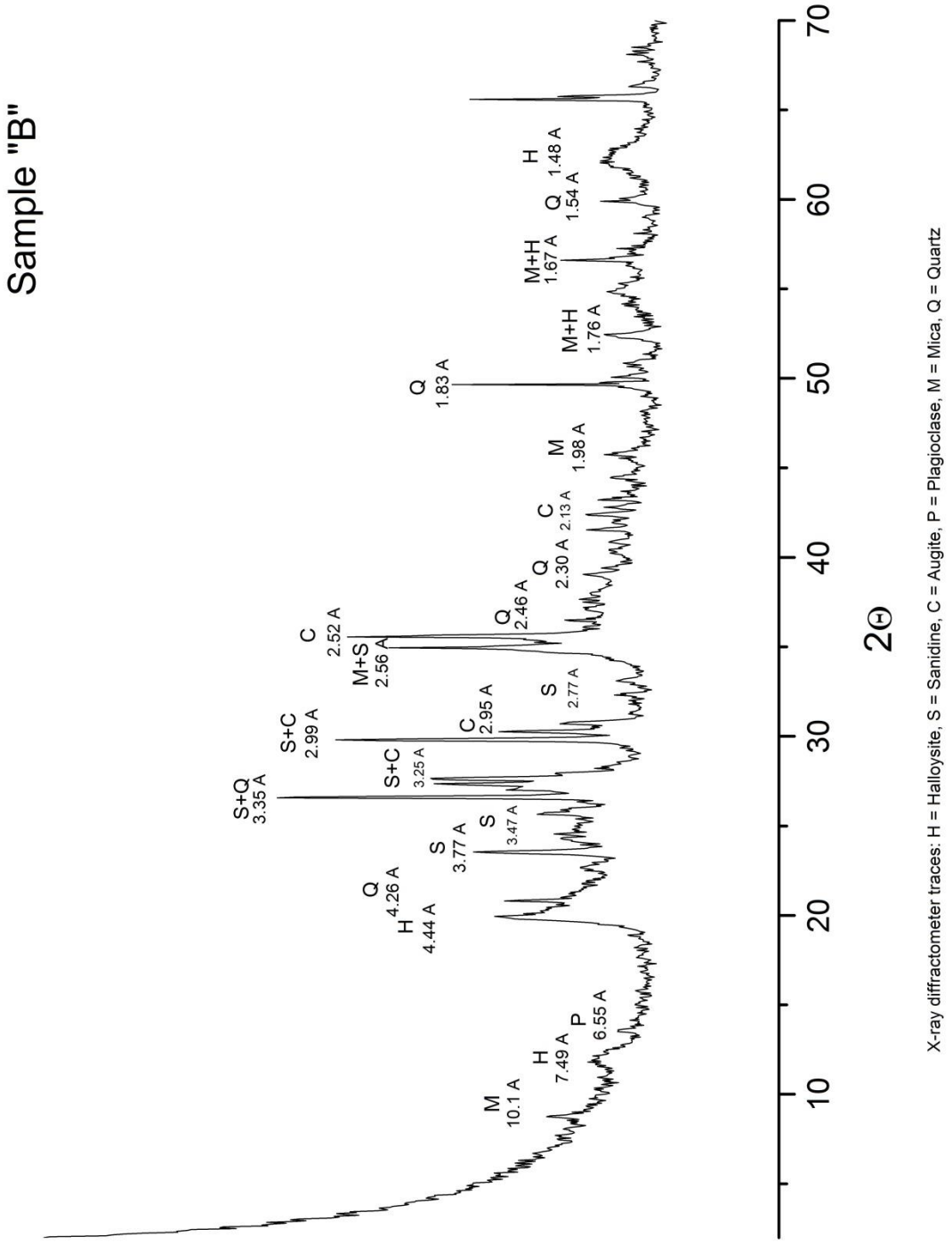

X-ray diffractometer traces: H = Halloysite, S = Sanidine, C = Augite, P = Plagioclase, M = Mica, Q = Quartz

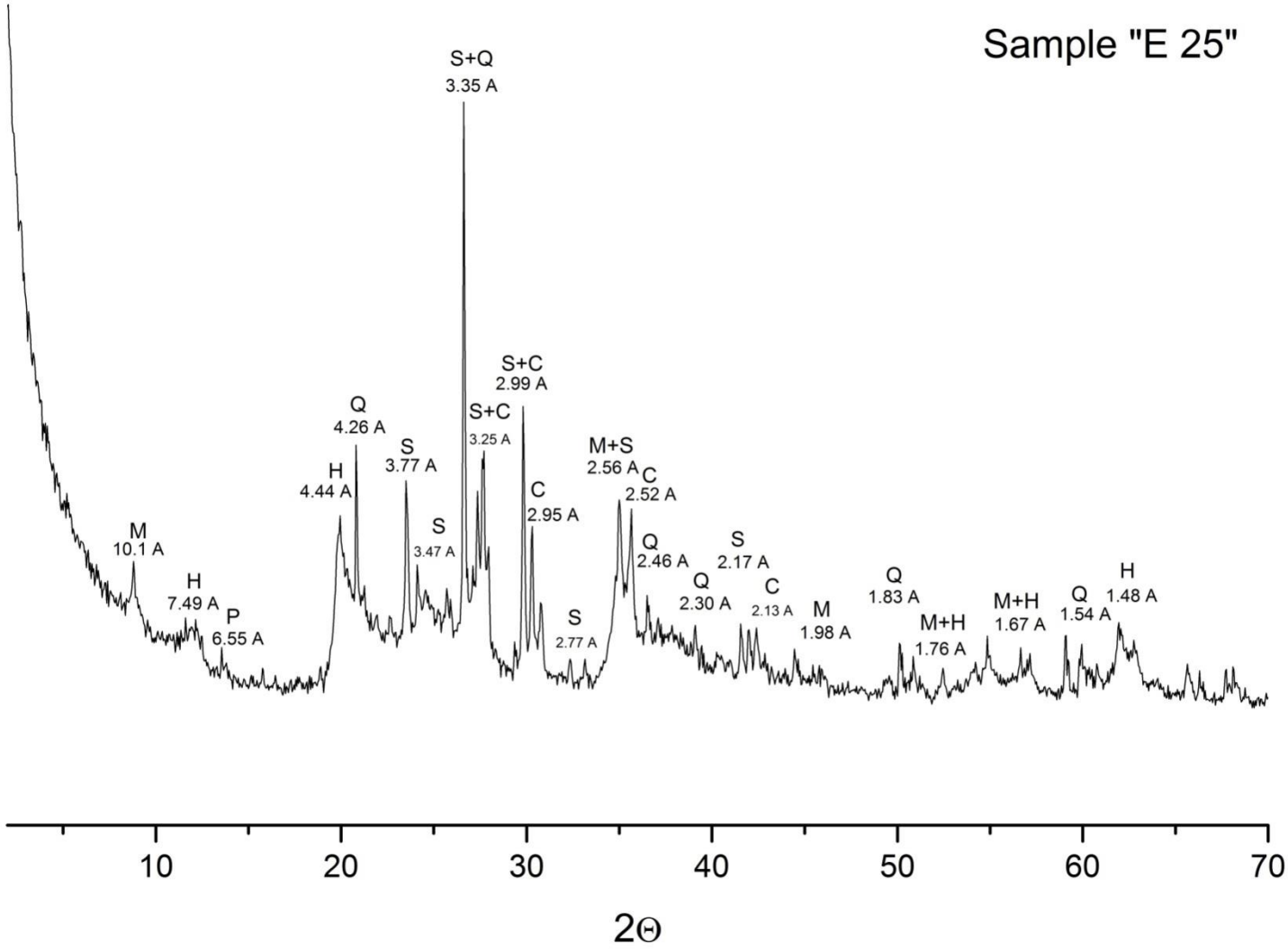

X-ray diffractometer traces: H = Halloysite, S = Sanidine, C = Augite, P = Plagioclase, M = Mica, Q = Quartz

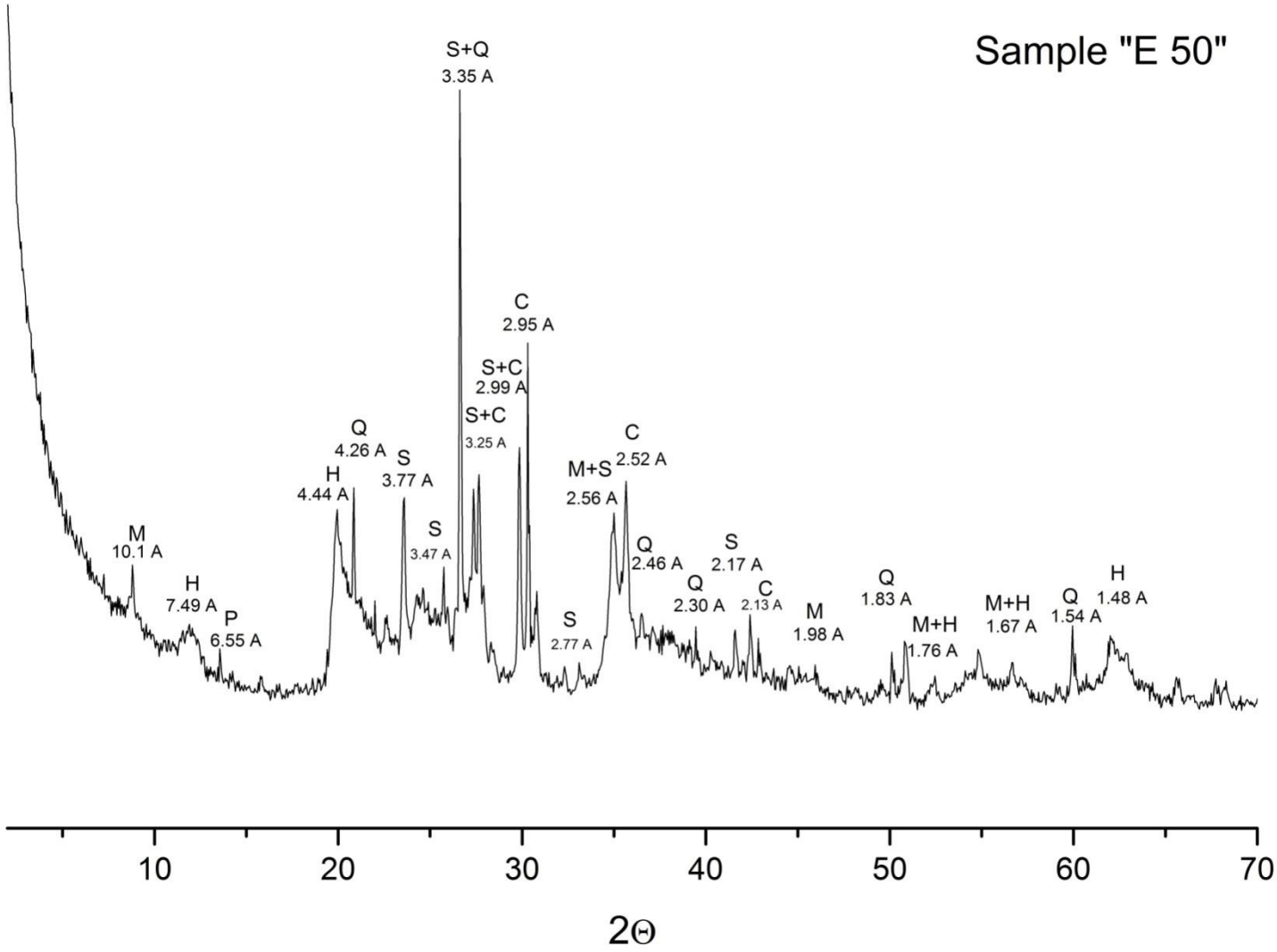

X-ray diffractometer traces: H = Halloysite, S = Sanidine, C = Augite, P = Plagioclase, M = Mica, Q = Quartz

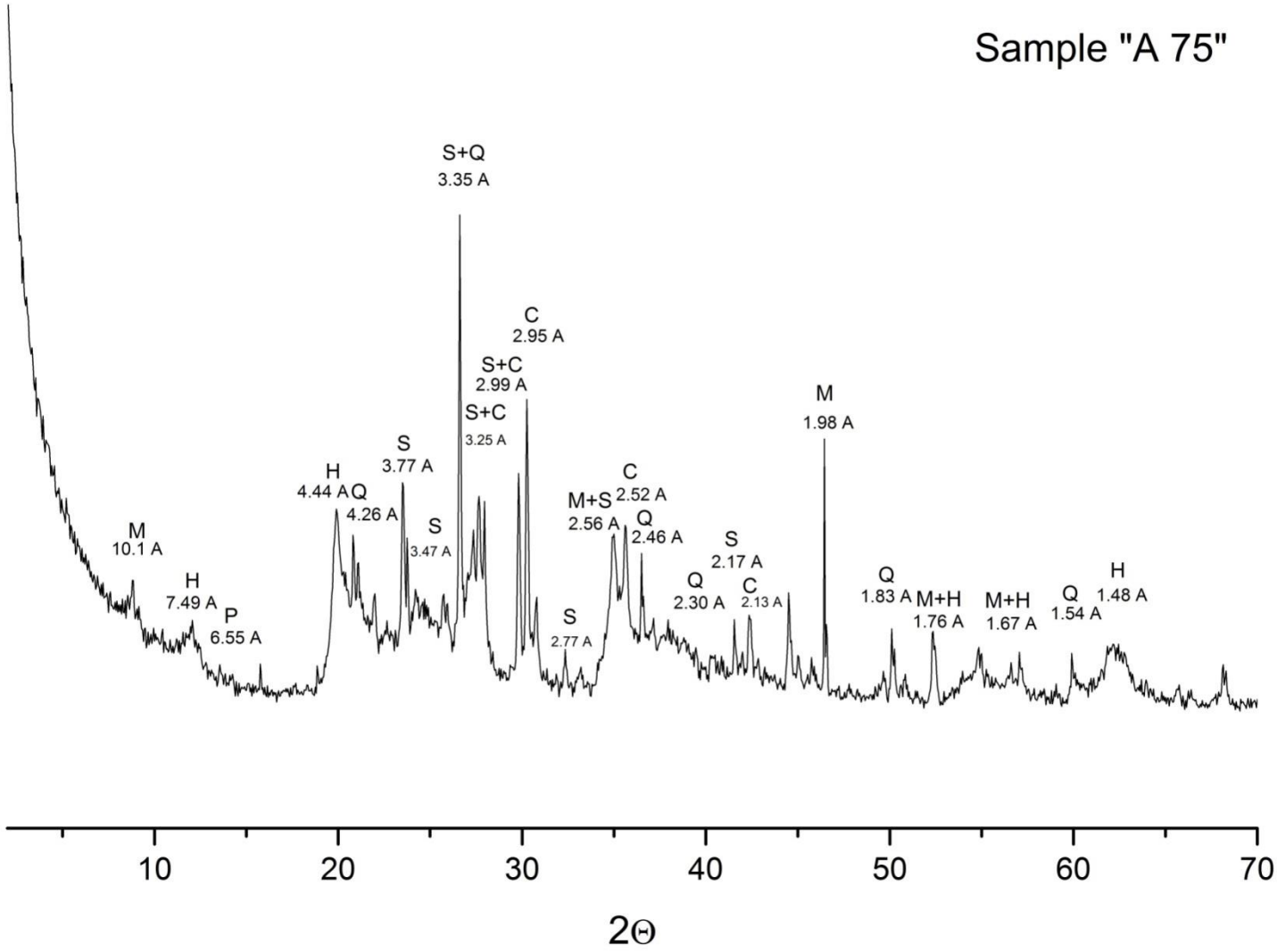

X-ray diffractometer traces: H = Halloysite, S = Sanidine, C = Augite, P = Plagioclase, M = Mica, Q = Quartz

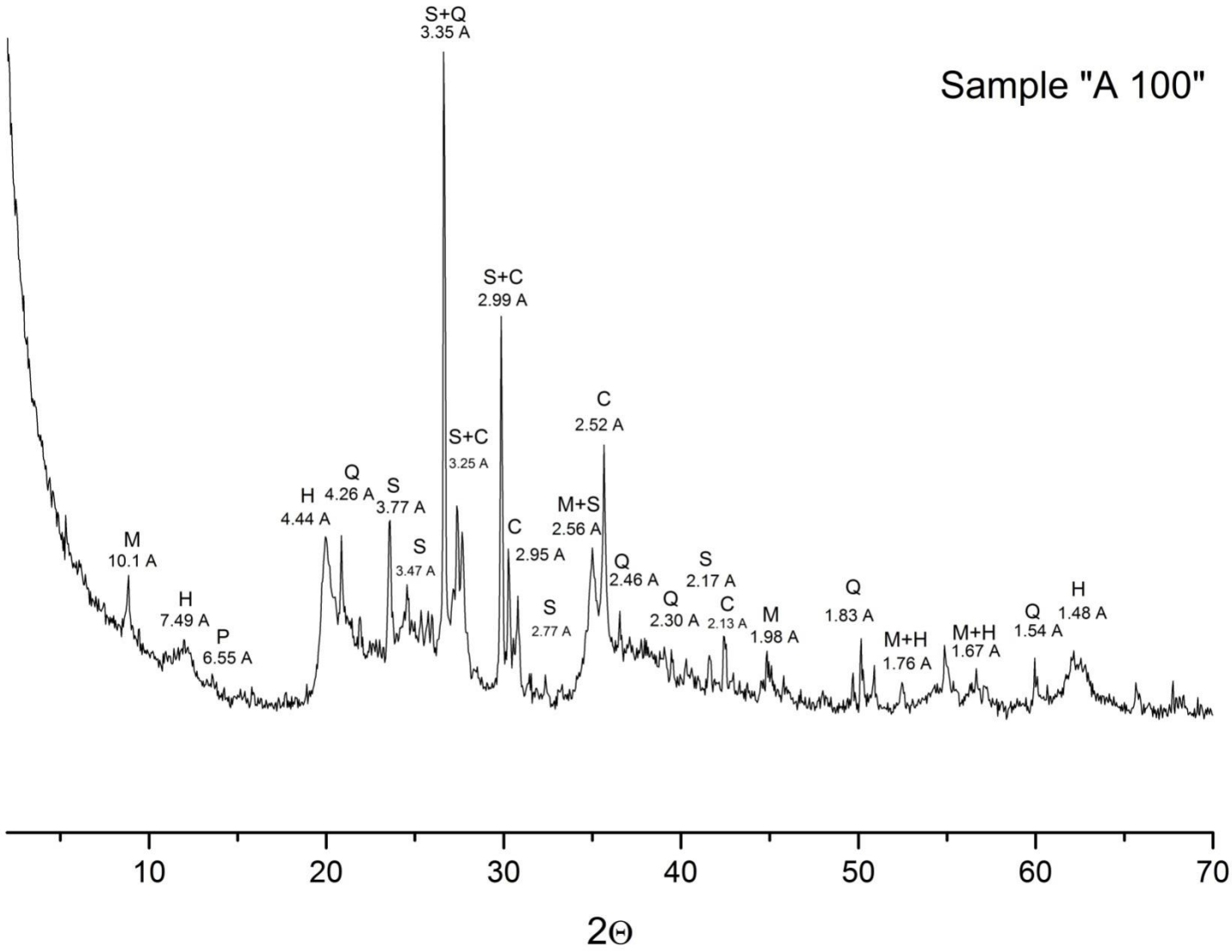

X-ray diffractometer traces: H = Halloysite, S = Sanidine, C = Augite, P = Plagioclase, M = Mica, Q = Quartz

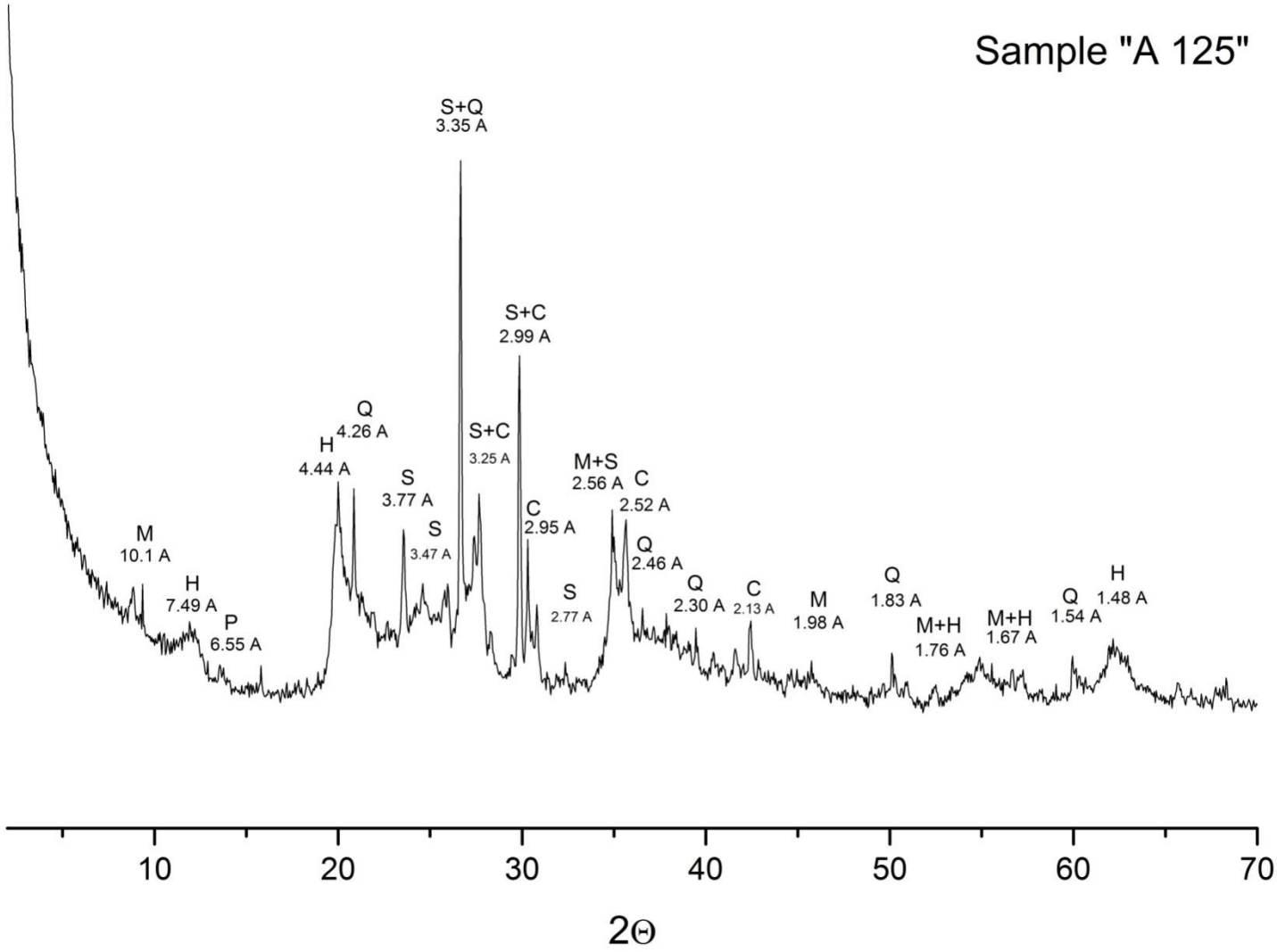

X-ray diffractometer traces: H = Halloysite, S = Sanidine, C = Augite, P = Plagioclase, M = Mica, Q = Quartz

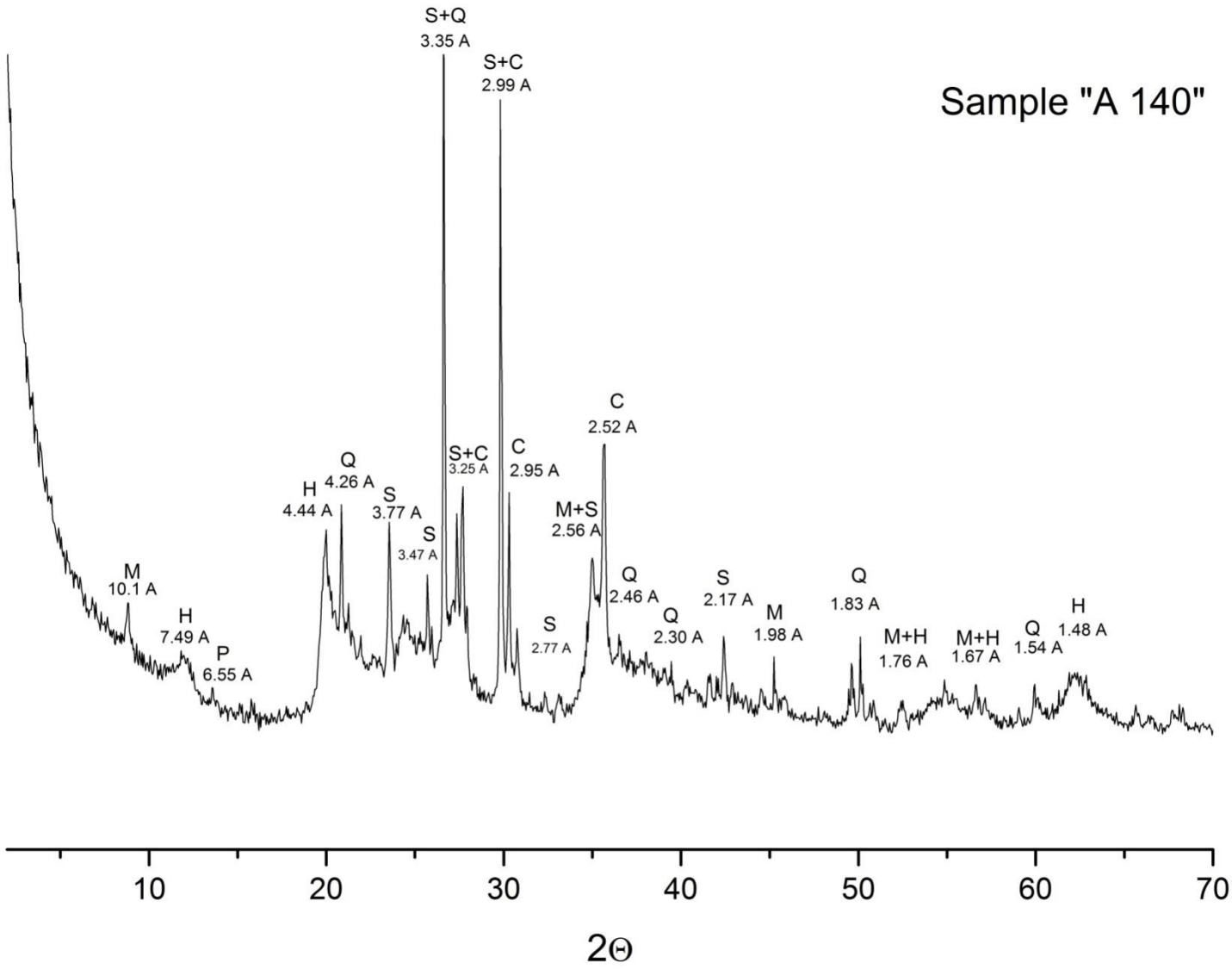

X-ray diffractometer traces: H = Halloysite, S = Sanidine, C = Augite, P = Plagioclase, M = Mica, Q = Quartz

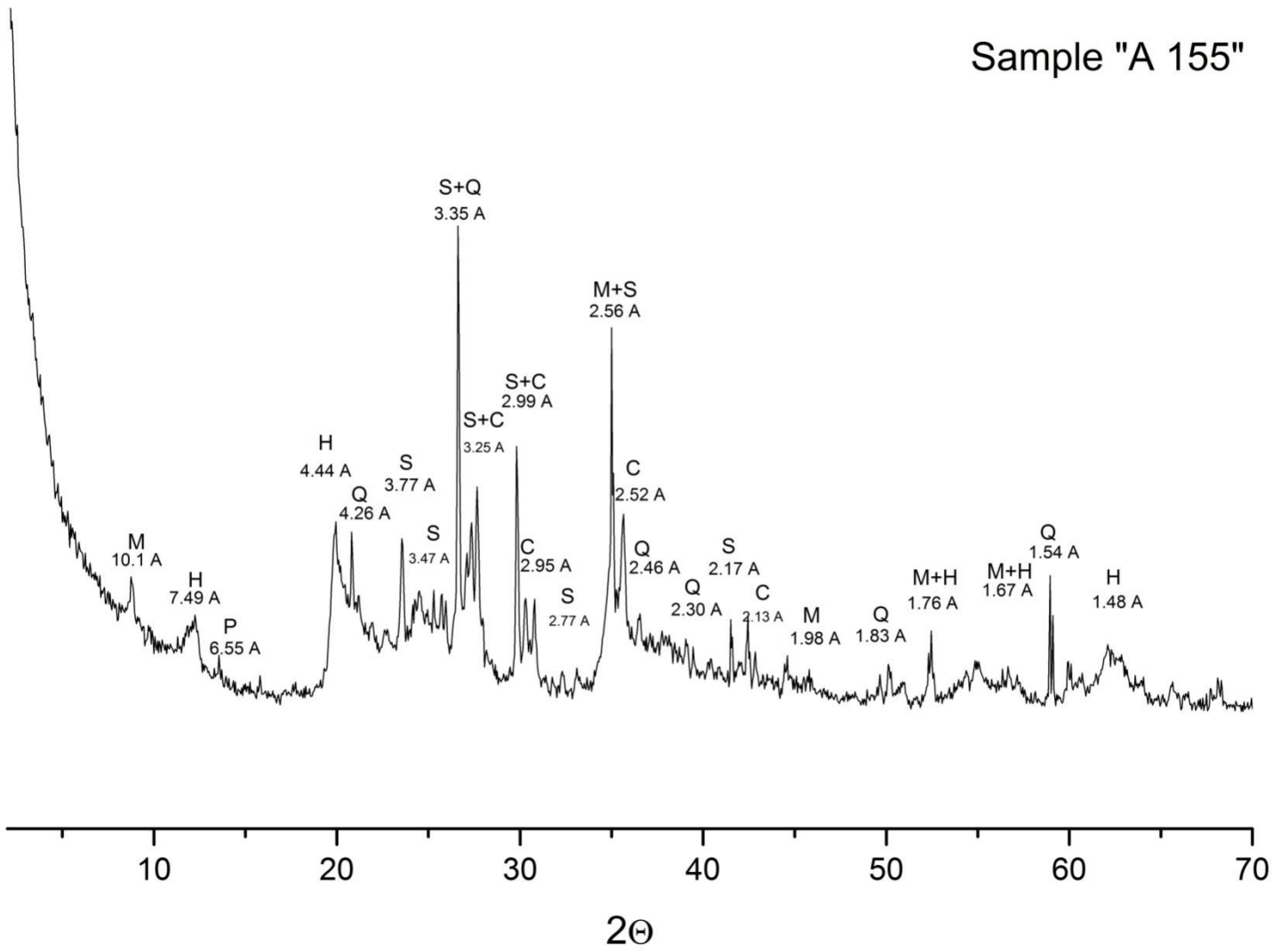

X-ray diffractometer traces: H = Halloysite, S = Sanidine, C = Augite, P = Plagioclase, M = Mica, Q = Quartz

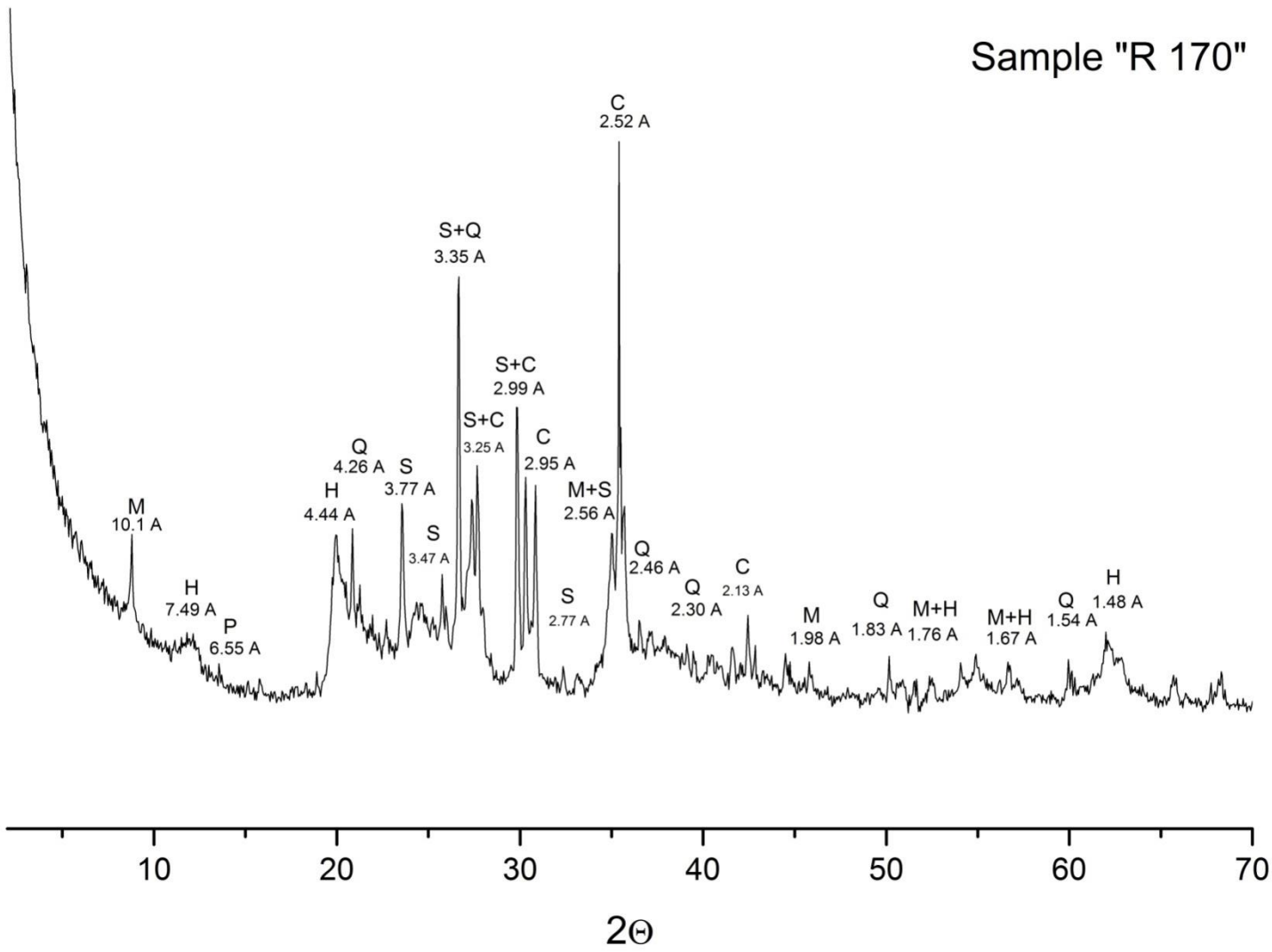

X-ray diffractometer traces: H = Halloysite, S = Sanidine, C = Augite, P = Plagioclase, M = Mica, Q = Quartz

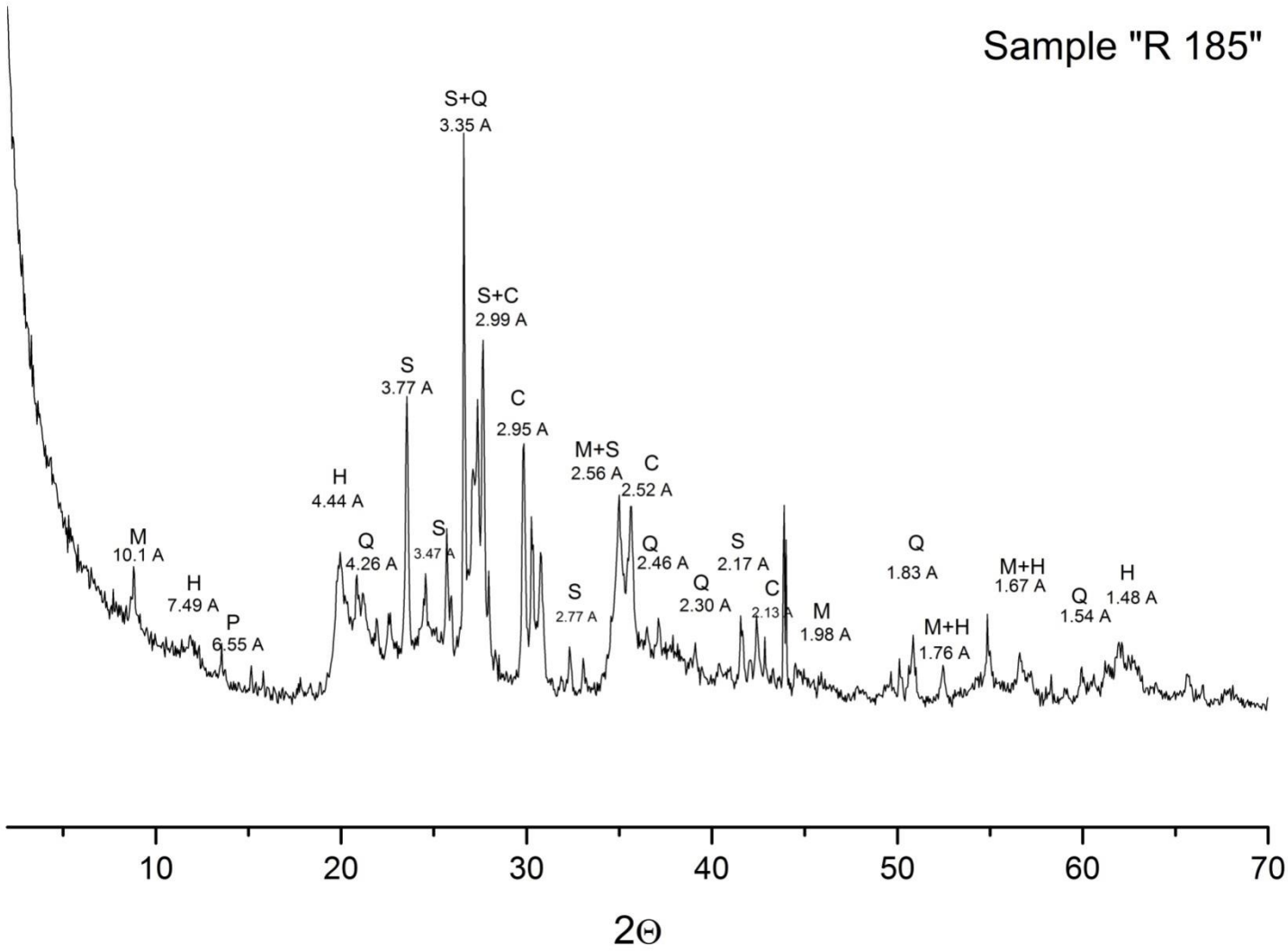

X-ray diffractometer traces: H = Halloysite, S = Sanidine, C = Augite, P = Plagioclase, M = Mica, Q = Quartz

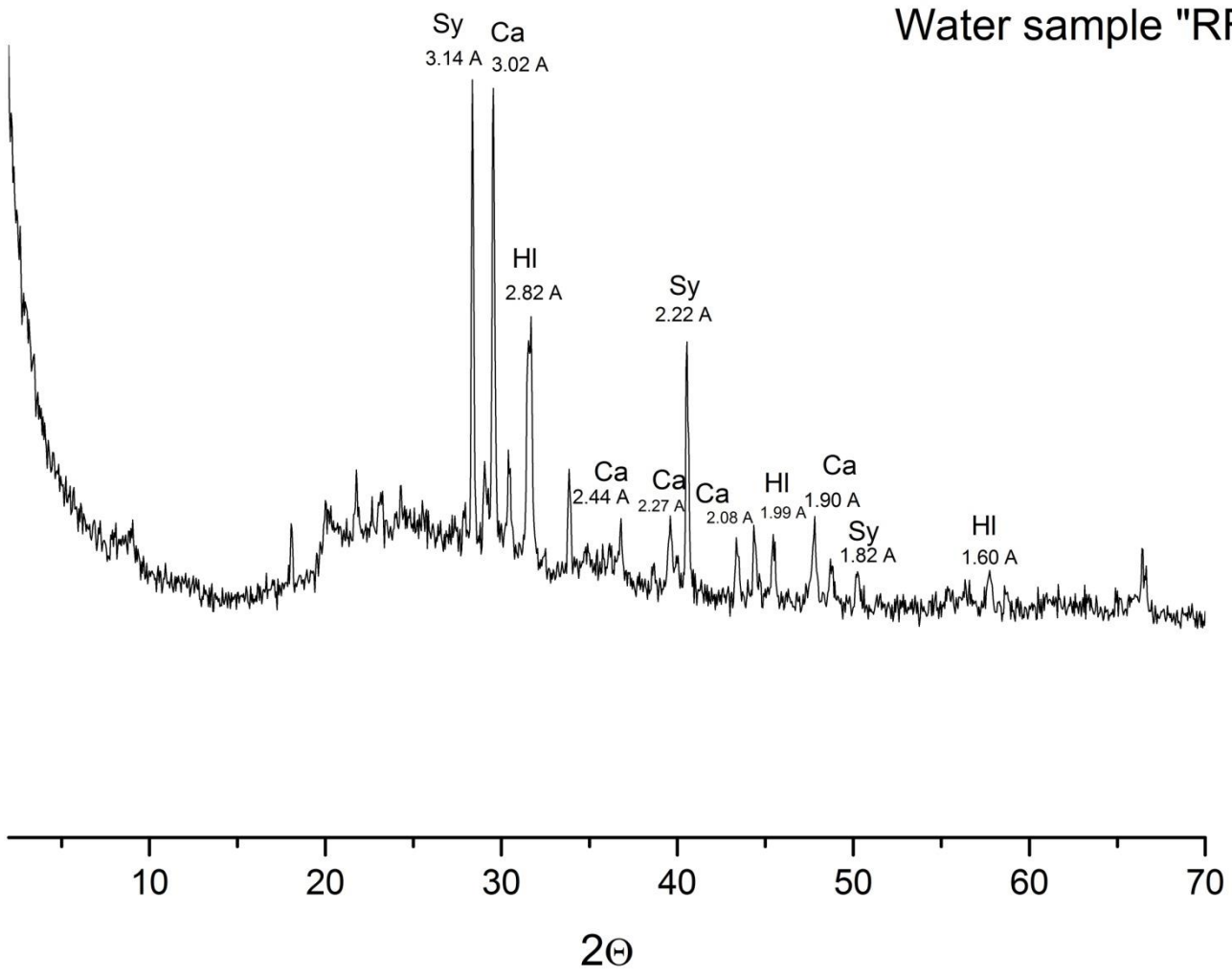

X-ray diffractometer traces: Hl = Halite, Ca = Calcite, Sy = Sylvite